VNIVERSITAT DE VALÈNCIA

VNIVERSITAT DE VALÈNCIA Facultat de Ciències Matemàtiques

DEPARTAMENTO DE ESTADÍSTICA E INVESTIGACIÓN OPERATIVA

PHD THESIS:

NESTING PROBLEMS: EXACT AND HEURISTIC ALGORITHMS

A Thesis submitted by Antonio Martínez Sykora for the degree of Doctor of Philosophy in the University of Valencia

---

Supervised by:
Ramón Álvarez-Valdés Olaguíbel
José Manuel Tamarit Goerlich

To the women of my life: Natalia and Olaya...

ACKNOWLEDGEMENTS

This thesis would not have been possible without the generous support of Ramón Álvarez-Valdés Olaguíbel and Jose Manuel Tamarit Goerlich who strongly supported me.

Special appreciation to professor Enrique Benavent, who spent a lot of time to introduce me into the Operational Research world.

I want to thank all the examiners, Enriqueta Vercher, José Fernando Oliveira, Maria Antonia Carravilla, Fran Parreño, Rubén Ruiz and Enrique Benavent for the great effort of reading the thesis carefully and their for all the observations and corrections.

Many thanks to professors José Fernando Oliveira, Maria Antónia Carravilla and António Miguel Gomes for supervising me in my research internship in Porto.

Special thanks to Julia Bennell, who spent a lot of her valuable time supervising me in my research internship in Southampton.

Special thanks to Jonathon Scandrett, who has corrected and improved the English redaction.

I warmly want to thank my family: Juan, Vera, Juanito and Verus.

Finally, very special thanks to Natalia and Olaya for their infinite patience.

Contents

Chapter 1

Introduction to *Nesting* problems

1.1 Introduction

Nesting problems are two-dimensional cutting and packing problems involving irregular shapes. This thesis is focused on real applications on *Nesting* problems such as the garment industry or the glass cutting. The aim is to study different mathematical methodologies to obtain good lower bounds by exact procedures and upper bounds by heuristic algorithms. The core of the thesis is a mathematical model, a Mixed Integer Programming model, which is adapted in each one of the parts of the thesis.

This study has three main parts: first, an exact algorithm for *Nesting problems* when rotation for the pieces is not allowed; second, an *Iterated Greedy* algorithm to deal with more complex *Nesting problems* when pieces can rotate at several angles; third, a constructive algorithm to solve the two-dimensional irregular bin packing problem with guillotine cuts. This thesis is organized as follows.

The first part is focused on developing exact algorithms. In Chapter 2 we present two Mixed Integer Programming (MIP) models, based on the Fischetti and Luzzi *MIP* model [27]. We consider horizontal lines in order to define the *horizontal slices* which are used to separate each pair of pieces. The second model, presented in Section 2.3, uses the structure of the *horizontal slices* in order to *lift* the bound constraints. Section 2.5 shows that if we solve these formulations with *CPLEX*, we obtain better results than the formulation proposed by Gomes and Oliveira [32]. The main objective is to design a *Branch and Cut* algorithm based on the MIP, but first a *Branch and Bound* algorithm is developed in Chapter 3. Therefore, we study different branching strategies and design an algorithm which updates the bounds on the coordinates of the reference point of the pieces in order to find incompatible variables which are fixed to 0 in the current branch of the tree. The resulting *Branch and Bound* produces an important improvement with respect to previous algorithms and is able to solve to optimality problems with up to 16 pieces in a reasonable time.

In order to develop the *Branch and Cut* algorithm we have found several classes of valid inequalities. Chapter 4 presents the different inequalities and in Chapter 5 we propose separation algorithms for some of these inequalities. However, our computational experience shows that although the number of nodes is reduced, the computational time increases considerably and the *Branch and Cut* algorithm becomes slower.

The second part is focused on building an *Iterated Greedy* algorithm for *Nesting problems*. In Chapter 6 a constructive algorithm based on the MIP model is proposed. We study different versions depending on the objective function and the number of pieces which are going to be considered in the initial MIP. A new

idea for the insertion is presented, *trunk insertion*, which allows certain movements of the pieces already placed. Chapter 7 contains different movements for the local search based on the reinsertion of a given number of pieces and compaction. In Chapter 8 we present a math-heuristic algorithm, which is an *Iterated Greedy* algorithm because we iterate over the constructive algorithm using a destructive algorithm. We have developed a local search based on the reinsertion of one and two pieces. In the constructive algorithm, for the reinsertion of the pieces after the destruction of the solution and the local search movements, we use several parameters that change along the algorithm, depending on the time required to prove optimality in the corresponding MIP models. That is, somehow we adjust the parameters, depending on the difficulty of the current MIP model. The computational results show that this algorithm is competitive with other algorithms and provides the best known results on several known instances.

The third part is included in Chapter 9. We present an efficient constructive algorithm for the two dimensional irregular bin packing problem with guillotine cuts. This problem arises in the glass cutting industry. We have used a similar MIP model with a new strategy to ensure a guillotine cut structure. The results obtained improve on the best known results. Furthermore, the algorithm is competitive with state of the art procedures for rectangular bin packing problems.

1.2 Types of *Nesting Problems*

There are several types of *Nesting* problems depending on the real application the problem comes from. We define the placement area as a *big item* and the pieces which have to be arranged into the big item as *small items* . There are several different objectives, but the most used one is focused on reducing the total waste produced.

The most studied problem is the strip packing problem where the width of the strip is fixed and the objective is based on reducing waste. As all the pieces have to be placed into the strip without overlapping, minimizing the waste is equivalent to minimizing the total required length. These problems arise in a wide variety of industries like garment manufacturing (see Figure 1.1), sheet-metal cutting, furniture making and shoe manufacturing.

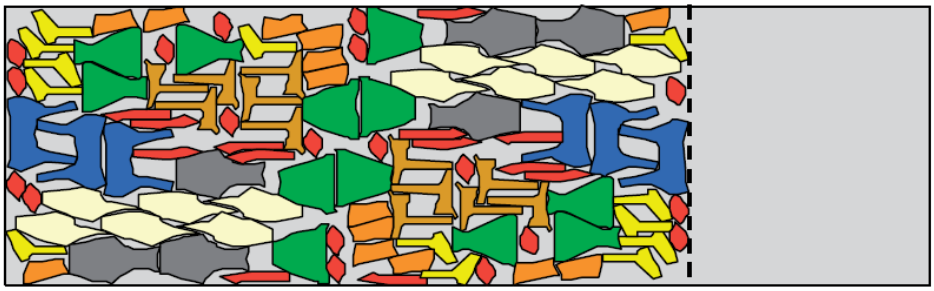

Figure 1.1: *An example from garment manufacturing (taken from Gomes and Oliveira [32])*

Two-dimensional Bin Packing Problems consist in placing a set of pieces into a finite number of bins in

such a way that the total number of bins is minimized. In some applications, the placement areas into which the pieces have to be packed or cut can have irregular shapes, as in the case of leather hides for making shoes. The placement area can have uniform or varying qualities depending on the region, sometimes including defective parts that cannot be used. In these cases the objective is based on reducing the number of *big items* needed to place all the pieces.

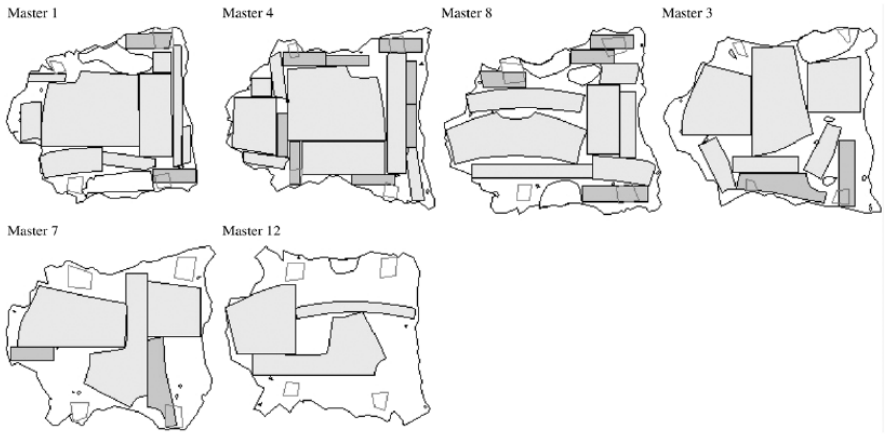

Figure 1.2: *An example of a leather cutting instance given by Baldacci et al. [7]*

The leather nesting problem (LNP) consists in finding the best layouts for a set of irregular pieces within large natural leather hides whose contours could be highly irregular and may include holes. According to the typology presented by Wäscher et al. [70], LNP can be classified as a two-dimensional residual cutting stock problem (2D-RCSP). Figure 1.2 shows an example of a leather nesting problem.

Heistermann et. al. [33] proposed a greedy algorithm for real instances in the automotive industry. They consider holes, defects and regions with different levels of quality (quality zones) in the leather hides. Recently, Alves et. al. [3] have proposed several constructive algorithms, reporting an extensive computational experiment using two real data sets.

Baldacci et al. [7] use the raster representation to design a heuristic algorithm. They propose an iterative algorithm based on three different constructive procedures for the *Irregular Single Knapsack Problem*. They compare their algorithms on instances defined for *two-dimensional strip packing problems*, *two-dimensional bin packing problems* and *real-world leather cutting instances*.

Crispin et. al. [21] propose two genetic algorithms using different coding methodologies for shoe manufacturing. They consider directional constraints for the pieces in given regions of the hides which reduce the solution space.

There are several publications on the leather nesting problem that do not take quality zones into account. We can find a heuristic algorithm based on placing the shapes one by one on multiple sheets in Lee et. al [39], and Yupins and Caijun [72] propose both genetic algorithms and simulated annealing.

Nevertheless, in the literature of *Nesting* problems the variant with more publications is the two-dimensional

strip packing problem where the width of the strip is fixed and minimizing the total required length is the common objective. This problem is categorized as the two-dimensional, irregular open dimensional problem in Wäscher et al. [70]. Fowler and Tanimoto [28] demonstrate that this problem is NP-complete and, as a result, solution methodologies predominantly utilize heuristics. In Sections 1.4 and 1.5 we can find a literature review on exact methods and heuristic algorithms, respectively. In this thesis we focus on that problem and both exact and heuristic algorithms are proposed.

One important characteristic of the pieces is their shape. In *Nesting problems* pieces are irregular and most frequently polygons. However, there are several publications that consider circular edges. Burke et. al. [18] propose a generalized bottom-left corner heuristic with hill climbing and tabu search algorithms for finding a good sequence of the given pieces. Scheithauer et al. [59] use ϕ-functions to deal with circular edges. In practice, circular edges of the pieces could be approximated by polygons, so most of the publications consider the pieces as polygons.

Another feature of the pieces is the allowed angles of rotation: rotation can be free; only specific angles can be allowed (90^o, 180^o,...) or rotation is not allowed at all. The angles of rotation can be fixed because pieces have to respect a given pattern in the stock sheet or due to the structural properties of the material being cut. In most of the published studies, rotation of the pieces is not allowed or is restricted to several fixed angles, though there are several studies dealing with free rotation. Xiao Liu and Jia-Wei Ye [41] propose a constructive heuristic algorithm and Stoyan et al. [63] use ϕ-functions.

The *periodic packing* of irregular shapes, also known as *regular packing* or *lattice packing*, consists in packing congruent copies of one shape. Costa et al. [20] propose heuristic algorithms for large-scale periodic packing. They allow pieces to be rotated freely on the condition that all the pieces must follow the same orientation (*single lattice*) or can be rotated 180^o (*double lattice*). According to the typology by Wäscher [70], this problem is a two-dimensional irregular IIPP (Identical Item Packing Problem).

Another application of *Nesting* problems arises in the glass cutting industry. In this case the cutting process divides the stock sheet (or the given part that is going to be cut) into two different parts. These cuts are known as guillotine cuts and a direct consequence is that pieces cannot have concavities. Pieces have to be placed into bins of a fixed width and length, so the objective is to use as few bins as possible to pack all the pieces.

Finally, we can find several publications on three-dimensional nesting problems. Scheithauer et al. [67] extend ϕ-functions to three dimensional objects and Egeblad et al. [26] propose a heuristic algorithm that can be applied on three-dimensional problems.

1.3 Geometry overview

The main difficulty of solving two-dimensional packing problems appears when we want to ensure that there is no overlap in the solution or, in the case that there is overlapping, we want to identify the pieces involved. In this section we review the strategies that can be found in the literature.

First we describe the *pixel/raster* method, which divides the stock sheet into pixels with each pixel ha-

ving a value to indicate if it is used by a piece. This approach has the disadvantage of losing precision when the problem has irregular pieces. The second method is based on direct trigonometry, using the known *D-functions*. The third method uses the *Non-Fit Polygons*, introduced by Art [5]. The *Non-Fit Polygon (NFP)* reduces the problem of identifying whether two polygons overlap to the problem of checking if one point satisfies any of a subset of linear inequalities. When pieces are allowed to be rotated, the *NFP*s can be used only by calculating the *NFP* of each pair of pieces for each combination of the allowed angles of rotation. Moreover, when the rotation of pieces is free, the *NFP* does not work. The *Phi-function*, introduced by Stoyan et al. [63], is a generalization of the *NFP* and gives a measure of the separation between a pair of pieces. The *Phi-function* tool is limited by the mathematical complexity needed for it to be defined. However, it considers the rotation of the pieces. A recent approach is the sentinel method proposed by Macarenhas and Birgin [47], which also works for a free rotation of the pieces but can be constructed for pieces only with simple (convex) shapes.

1.3.1 *Pixel/Raster* method

The idea is to use a matrix where the digits represent a codification of a given area. The stock sheet is divided into small squares called pixels, obtaining a grid in such a way that the position of each piece in the strip is given by a set of covered pixels. Each element of the matrix represents a pixel of the strip. Note that with this representation we lose precision because no pixel is allowed to be covered by two or more different pieces. Moreover, if we consider a thinner grid then the computational effort would increase considerably. The codification of the matrix is important, and basically there are three approaches.

Oliveira and Ferreira [50] use a simple codification where each pixel of the matrix takes the value $k = 0, 1, 2, \ldots$ if there are k pieces covering it. Note that if the matrix has a pixel which takes the value 0, there is no piece covering it. In the case where there is a pixel which takes a value greater than 1, there is overlapping in the given pixel. In Figure 1.3 we can see the codification of one piece. It is important to mention that there are pixels which are not completely covered by the piece, but we have to consider that it is covered in order to ensure that pieces have a non-overlapping configuration, so the corresponding value in the matrix takes the value 1.

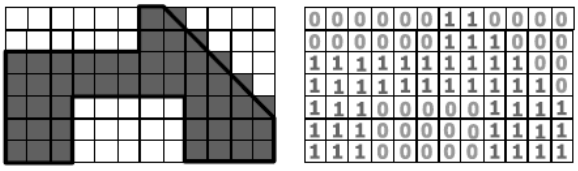

Figure 1.3: *Oliveira and Ferreira representation (taken from Bennell and Oliveira [12]).*

Segenreich and Braga [60] propose a codification which identifies not only overlapping, but also whether the pieces are in contact. Their codification uses a 1 for the boundary of the pieces and a 3 for the inner part. Then, in the pixel-matrix, a pixel with a value greater than 4 indicates that there is overlapping and a

pixel with value 2 means that two pieces are in contact but that they do not overlap. If the matrix has all the elements lower than or equal to 2, then the resulting solution is feasible. In Figure 1.4 we can see two pieces separately, and then their sum. Note that in the resulting sum we can observe some pixels with a value of 6, meaning that the pieces are in an overlapping position and pixels with the value 4 indicate that, in the respective pixels, pieces are in a non-feasible position (the boundary of one piece with the inner part of the other piece).

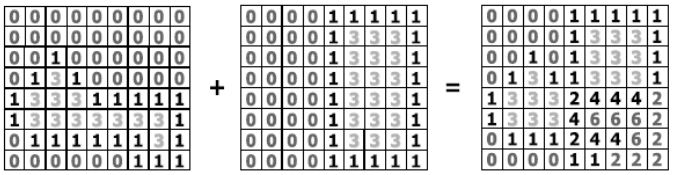

Figure 1.4: *Segenreich and Braga non boolean representation for irregular pieces (taken from Bennell and Oliveira [12]).*

Babu and Babu [6] propose a different idea. Oliveira and Ferreira's codification, as with Segenreich and Braga's, uses 0 for representing the absence of pieces, and a number greater than 0 for the presence of pieces. Babu and Babu use 0 for representing the inner part of the pieces and a number greater than 0 for the adjacent pixels. These adjacent pixels are enumerated from right to left in increasing order, starting with 1 at the right of the piece. In Figure 1.5 we can observe how they represent a piece with a hole. The two central pixels with values 1 and 2 represent the hole in the piece.

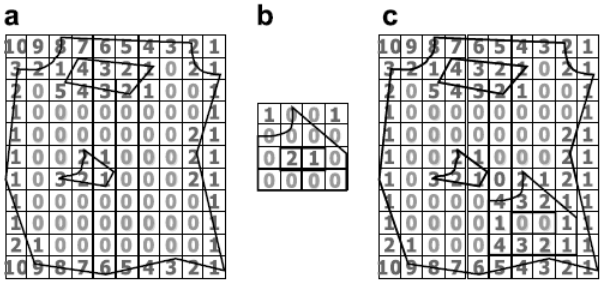

Figure 1.5: *Babu and Babu representation (taken from Bennell and Oliveira [12]).*

The Babu and Babu codification generalizes the shape of the stock sheet. The big item where we have to arrange the small items can be an irregular polygon and can also have holes which cannot be used by any piece. One advantage of this codification is that the code of each pixel represents the number of pixels needed to push the represented piece to the right in order to make the solution possible. In that way, in a given configuration it is easy to calculate the compaction of the pieces in the bottom-left corner of the strip. The

disadvantage of this approach is an increase in the computational effort needed to update the pixel matrix and its complexity.

1.3.2 Trigonometry and *D functions*.

This method considers the pieces as polygons. An important advantage when we use polygons for representing the pieces is the precision that we gain when we deal with irregular pieces. Note that in the pixel/raster method, precision depends on the accuracy used when defining the grid. However, when we use polygons we can approximate each piece as much as is necessary.

On the other hand, in the pixel/raster method the amount of required information depends on the area of the pieces. When the pieces are larger the pixel matrix is more complex and it is harder to update it. If we use polygons, the amount of required information increases with the number of vertices of the polygons used for representing the pieces.

The main problem of using polygons appears when we want to guarantee that pieces do not overlap. The first idea that comes to mind is based on direct trigonometry. There are known tools that allow us to identify when two segments intersect or if a given point is placed inside a given polygon. These tools are more complex compared with the pixel/raster method. In fact, the computational time of the pixel/raster method is quadratic on the size of the pixel matrix, and when we use direct trigonometry the computational time is exponential on the number of edges of the polygons.

In what follows we are going to present an approach using trigonometry to evaluate whether two polygons overlap. In Figure 1.6(a) we can observe that if two polygons overlap, then their respective enclosed rectangles also overlap. Figure 1.6(b) shows that if any two edges intersect, then the rectangles whose diagonal is one of these edges also overlap.

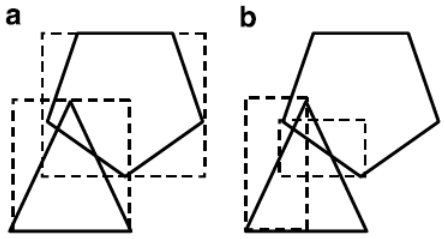

Figure 1.6: *(a) If two polygons overlap, then their respective enclosed rectangles also overlap. (b) If two edges intersect, then the rectangles whose diagonal is one of the edges also overlap (taken from Bennell and Oliveira [12]).*

If the enclosing rectangles of two given polygons do not overlap, then the polygons are not in a overlapping position. This is much easier to check than checking if two complex polygons overlap. Then, in order to know whether two pieces overlap or not, the first step is to check if the enclosed rectangles overlap. Ferreira et. al. [4] study the reduction of checking the feasibility of one given solution by first applying the

study of the enclosed rectangles of each pair of pieces, which ranges between 90.7% and 97.6% of the pairs. Furthermore, if we also analyze the edges, the reduction ranges between 96% and 99.4%. Obviously, the complexity of the polygons reduces the effectiveness of the study of the enclosing rectangles, but Ferreira et al. never obtain a reduction percentage lower than 90%.

In order to check if two polygons overlap, Bennell and Oliveira [12] give a set of hierarchical tests.

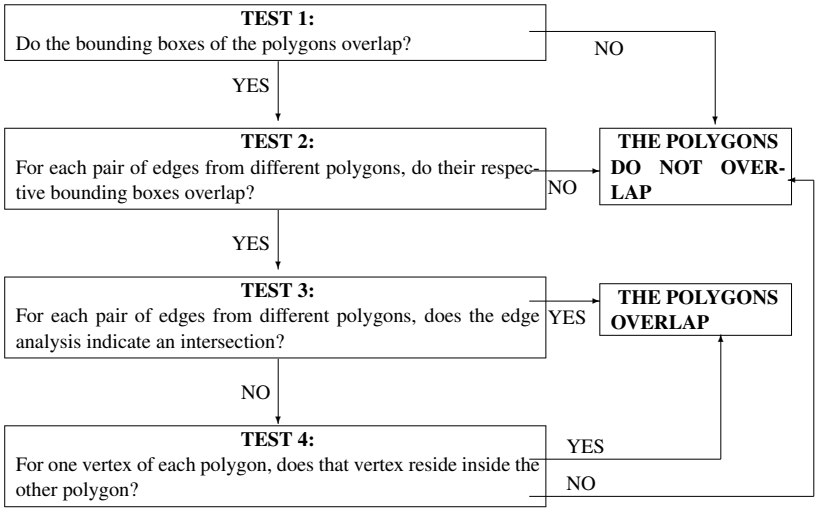

Figures 1.7 (a) and (b) show, respectively, negative answers for Tests 1 and 2. An example of an affirmative answer is shown in Figures 1.7 (c) and (d), and in Figure 1.7 (e) we can see both possibilities for Test 4.

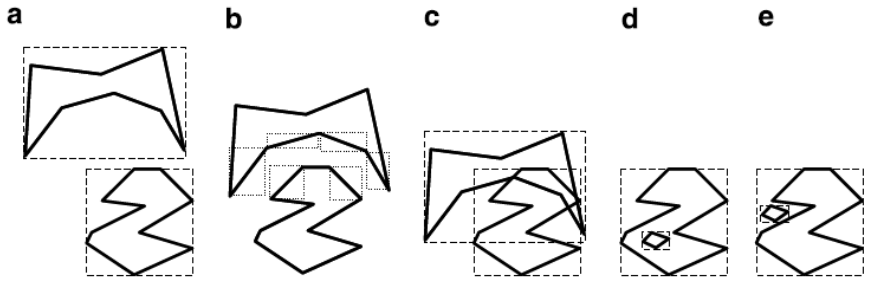

Figure 1.7: *Different cases of the relative position between two pieces (taken from Bennell and Oliveira [12]).*

Preparata and Shamos [54] propose a test to identify if a given point is inside a polygon. This test is useful to solve Test 4. In order to answer Test 3, we can use the known *D functions*, which are an efficient

tool to obtain the relative position between two edges.

$$D_{ABP} = ((X_A - X_B)(Y_A - Y_P) - (Y_A - Y_B)(X_A - X_P)) \tag{1.1}$$

D functions were introduced by Konopasek [38] and give the relative position between one point, P, with respect to an oriented edge, AB, see Figure 1.8.

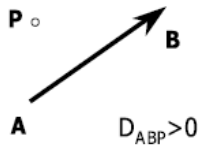

Figure 1.8: *Interpretation of the D functions (taken from Bennell and Oliveira [12]).*

These functions come from the equation of the distance from a point to a line. The interpretation is the following one:

- If $D_ABP > 0$, then point P is placed to the left of segment AB.
- If $D_ABP < 0$, then point P is placed to the right of segment AB.
- If $D_ABP = 0$, then point P is placed on the segment AB.

We have to consider the origin of the coordinate axis in the bottom-left corner, i.e. the X axis always increases to the right and the Y axis increases upward. It is possible to use these functions to study the relative position between two segments with given orientations. Mahadevan [43] gives a complete study for differentiating all the cases.

1.3.3 *Non-Fit polygons*

Nowadays, the *Non-Fit polygon (NFP)* is the most widely used and effective tool. The idea of the *NFP* is the study of the different relative positions between one polygon B, with respect to another polygon A, such that both polygons are in a touching position without overlapping, i.e. the *NFP* studies all the positions of polygon B in which it touches polygon A. This concept was introduced by Art [5].

We denote by P_A the reference point of polygon A and P_B denotes the reference point of polygon B. Let us consider that both reference points are in the bottom-left corner of the enclosing rectangle of their respective polygons. The *NFP* of pieces A and B, denoted by NFP_{AB}, is the region in which the reference point of polygon B cannot be placed because it would overlap polygon A. To build it, P_A is placed at the origin and P_B slides around polygon A in such a way that there is always a point of polygon B touching the border of polygon A. The left-hand side of Figure 1.9 shows several positions of polygon B (triangle) moving around polygon A (square). The right-hand side of the figure shows NFP_{AB}, the forbidden region for placing P_B, relative to P_A, if overlapping is not allowed. Note that NFP_{BA} matches NFP_{AB} with a rotation of 180^o.

Cuninghame-Green [22] proposes an algorithm to obtain the *NFP*s of convex pieces. In a first step, a different orientation is assigned to each polygon as is shown in Figure 1.10 (a). Then, fixing the position of polygon A at the origin in a counterclockwise orientation, all the edges of both polygons are sorted by

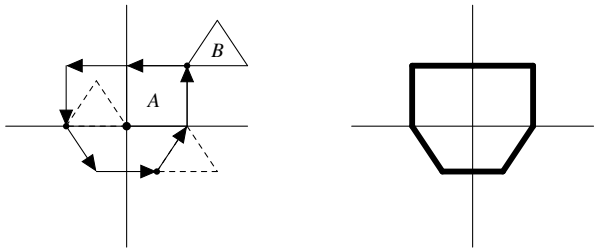

(a) Piece B moves around A (b) NFP_{AB}

Figure 1.9: *Building the NFP of pieces A and B*

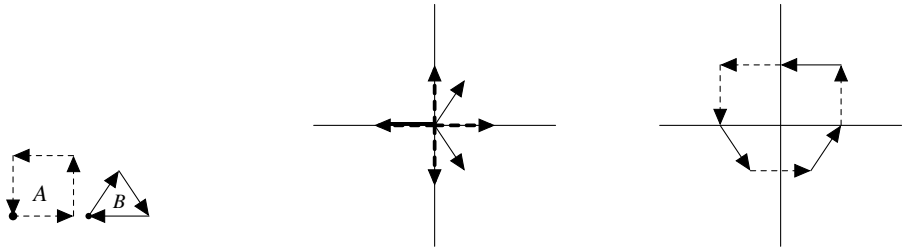

(a) Orientation of the polygons (b) Different slopes (c) NFP_{AB}

Figure 1.10: *Building NFP of convex pieces*

non-increasing slope, see Figure 1.10 (b). Finally, all the edges have to be drawn in the corresponding order, thus obtaining the NFP_{AB} (Figure 1.10 (c)).

When one or both polygons are non-convex, the construction of the *NFP* is more complex. Figure 1.11, taken from Bennell and Oliveira [12], shows complicated cases. In Figure 1.11(a), piece B has some feasible positions within the concavity of A and therefore NFP_{AB} includes a small triangle of feasible placements for the reference point of B. In Figure 1.11(b), the width of B fits exactly into the concavity of A and its feasible positions in the concavity produce a segment of feasible positions for the reference point of B in NFP_{AB}. In Figure 1.11(c), there is exactly one position in which B fits into the concavity of A and then NFP_{AB} includes a single feasible point for the reference point of B.

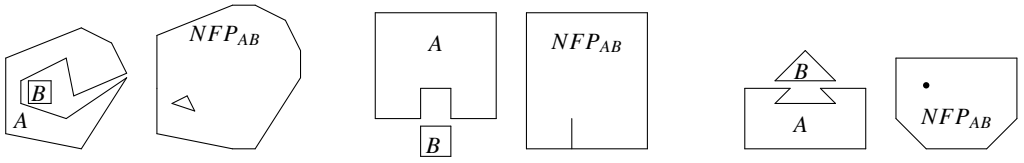

(a) (b) (c)

Figure 1.11: *Special cases of NFP when non-convex pieces are involved (taken from Bennell and Oliveira [12])*

In this thesis we assume that for each pair of pieces i, j, NFP_{ij} is given by a polygon and, if that is the case, by a set of points (as in Figure 1.11(c)), a set of segments (as in Figure 1.11(b)) or a set of enclosed polygons (as in Figure 1.11(a)).

Algorithms to calculate *NFP*s

Sliding Algorithm

Mahadevan [43] proposes a *sliding* algorithm in order to obtain the *NFP*. Let A and B be two pieces and P_A and P_B be their respective reference points. In order to obtain NFP_{AB}, we first need an initial position of the pieces that guarantees the touching position without overlapping. To ensure that, we match the maximum value of the Y coordinate of B with the minimum value of the Y coordinate of A. The reference point of B in this position is going to be the first vertex of NFP_{AB}. In the case that there is more than one position satisfying the previous condition, then the initial vertex will be the point located further to the left in order to ensure that the initial vertex is a vertex of NFP_{AB}.

Then, in Figure 1.12 we can see that there are three different possibilities for the first movement of B:

- Case (a): The slope of edge (a_j, a_{j+1}) is lower than the slope of edge (b_j, b_{j+1}). In that case, b_j slides over the edge (a_j, a_{j+1}).
- Case (b): The slope of edge (b_j, b_{j+1}) is lower than the slope of edge (a_j, a_{j+1}). In that case, a_j slides over the edge (b_j, b_{j+1}).
- Case (c): Both edges, (a_j, a_{j+1}) and (b_j, b_{j+1}), have the same slope. In that case, both glides of cases (a) and (b) are done.

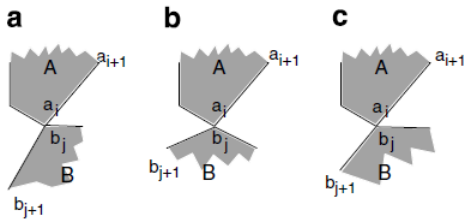

Figure 1.12: *Different cases to begin to slide piece B around piece A (taken from Bennell and Oliveira [12]).*

Mahadevan uses the *D functions* in order to know the inner part of the NFP_{AB} defined by the side of the segment which is obtained by sliding a complete combination of a vertex-edge of pieces A and B. In the event that any piece has a concavity, when one vertex slides completely over one edge, the polygons could be in an overlapping position, see Figure 1.13. In that case, the glide corresponds to the minimum distance from the starting point to the intersection point of both polygons, which matches with the maximum distance available for sliding B along the edge such that no overlaps exist with piece A.

The *sliding algorithm* only works for pairs of polygons that are relatively simple connected polygons. For example, in Figure 1.11 this algorithm does not find the hole in (a) or the point of (c)).

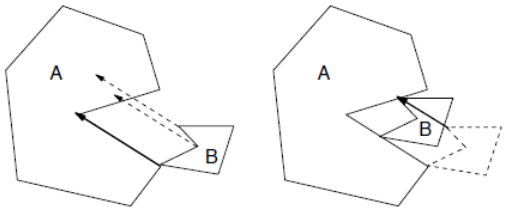

Figure 1.13: *Projection of B when it is moved over the edge of A (taken from Bennell and Oliveira [12]).*

Whitwell [71] proposes an extension of the *sliding algorithm* in order to identify the holes. He studies if there is any edge of any polygon which is not traveled over, i.e. the edge is not used for sliding any point in the Mahadevan algorithm. If there is any relative position for the non-visited edges such that non-overlapping is produced, then there is a hole in the NFP_{AB}. This hole can be obtained in a similar way, using a glide as above, whose result is the border of the hole. The Whitwell algorithm first applies the Mahadevan sliding algorithm, but the considered edges are flagged. If there is any non-flagged edge, we can suppose, without loss of generality, that it belongs to A and each vertex of B is checked to see if it can slide along this edge without producing an overlap. That can be studied by checking if the two edges whose intersection defines the given vertex of B are both to the left of the given edge of A. In the case that one or both of them are placed to the left of the edge of A, then there is no feasible glide between A and B such that the given vertex of B could touch the given edge of A, see Figure 1.14.

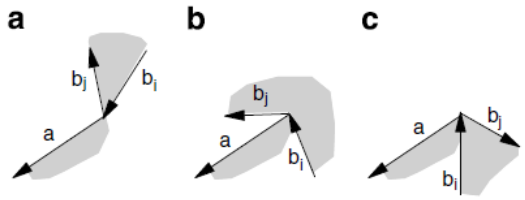

Figure 1.14: *(a) b_i and b_j are both on the right of edge a, (b) b_i is on the left and b_j is on the right of a, (c) b_i an b_j are both on the left of a (taken from Bennell and Oliveira [12]).*

Let us suppose that there is one vertex of B such that the two incident edges are both to the right of edge a, as shown in Figure 1.14 (a). In that case it is necessary to study whether there are some positions in which to place this vertex over the edge a which produce an overlap of pieces A and B. In order to check this, Whitwell uses a similar structure to the Mahadevan algorithm. Figure 1.15 shows an example of how the Whitwell algorithm works in order to find a feasible initial point starting from an overlapping position. Obviously, when the shapes of the pieces are more complex, having more edges and concavities, this approach will need more computational effort.

The Minkowski sum

The concept and theory of Minkowski operations comes from the more general field of morphology. The morphological operation that forms the basis of this technique for finding the NFP is termed dilation. Dilation grows the image set A through vector addition with set B, and is denoted as A/B. The dilation operator

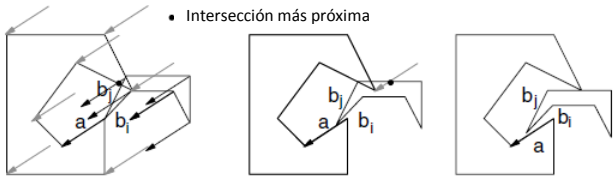

Figure 1.15: *The Whitwell method for finding feasible initial points (taken from Bennell and Oliveira [12]).*

may also be called the Minkowski sum, defined as follows.

Let A and B be two arbitrary closed sets of vector points in $\mathbb{R}^2$. S is the resulting sum of adding all the vector points in A to those in B. Then the Minkowski sum, S, is defined as

$$S = A \oplus B = \{a + b \mid a \in A,\ b \in B\}.$$

The union of geometric translations of sets can also define the Minkowski sum. If A_b denotes set A translated by vector b, then

$$S = A \oplus B = \bigcup_{b \in B} A_b.$$

Stoyan and Ponomarenko [64] first formalized the relationship between Minkowski sums and NFPs, providing a rigorous proof in their paper. They termed the NFP as the hodograph. Proof of this relationship is also discussed in Milenkovic et al. [48] and Bennell [8], who describe it as the Minkowski difference. In order to use the Minkowski sums and its relationship with the *NFP*, the realization of the above definition needs to be formulated into a procedure to obtain the NFP. Ghosh [30] develops a set of Boundary Addition Theorems for both the convex and non-convex cases that underpin his method of obtaining the Minkowski sum. That shows that there is sufficient information in the boundary of the polygons to obtain the boundary of the Minkowski sum. The theorems also support the use of slope diagrams, which form the basis of his approach, for representing the Minkowski sum. Ghosh [30] provides a detailed explanation of these theorems and Bennell [8] provides a discussion of the approach with respect to the NFP. In a Bennell et al. [12] tutorial we can find easy examples of Ghosh's idea. Recently, Bennell et al. [61] propose an efficient algorithm to calculate the NFPs using Minkowski sums based on the principles defined by Ghosh.

1.3.4 ϕ functions

The ϕ function is a topology concept. This tool can be viewed as a generalization of the *NFP*s, whose purpose is to represent all the mutual positions of two pieces, which can be polygons or pieces with curved lines. In Bennell et al. [14] an extensive tutorial on the ϕ functions and ϕ objects can be found.

The ϕ function is a mathematical expression which describes the interaction between two geometrical objects in such a way that the positions of the objects are the *input* and a real value is the *output*. This value can be viewed as the distance between the objects: if the value is 0, the pieces are touching each other; if the value is positive, the pieces are separated; and if the value is negative, the pieces overlap.

Stoyan et al.[63] use the ϕ functions to solve the non-overlapping problem for *Nesting* problems. They consider problems with several copies of one and two pieces. In Stoyan et al. [66] this idea is applied to

3-dimensional *Nesting* problems. In this case, they use the ϕ functions not only to know if a given solution is feasible, but also to define the mathematical model.

For basic pieces in two dimensions, a ϕ function class is already defined (see Stoyan et al. [68]). When dealing with more complex pieces, each piece can be decomposed into convex polygons or basic pieces, which correspond to a wide set of fixed-orientation bi-dimensional objects, see Stoyan et al. [65]. Scheithauer et al. [59] study the different combinations of basic pieces with circular segments. Stoyan et al. [67] and [66] apply this concept to the 3-dimensional case.

There is a close relation between the ϕ function and the *NFP* and the *Minkowski* sum. When the rotation of both pieces and the position of one of the pieces is fixed, the set of points such that the value of the ϕ function is 0 describes the *NFP*. However, the ϕ function has more information because it is not necessary to fix one of the pieces, and also gives an overlapping measure.

1.4 Exact algorithms

Since *Nesting* problems are harder than rectangular packing problems, which are already *NP-hard*, we find mostly heuristic algorithms in the literature. Gomes and Oliveira [32] propose a mixed integer programming model (*MIP* model) for pieces with a fixed orientation. They use that model to solve the *compaction* and the *separation* problems embedded into a heuristic algorithm. The *compaction* problem consists in finding a better layout from a feasible layout without changing the relative positions between the pieces. The *separation* problem tries to transform an unfeasible layout into a feasible solution by minimizing the increase in the required length. In Gomes and Oliveira [32], the non-overlapping constraints are modeled using binary variables and *big-M* constants. In each case the binary variables expressing the relative position of the pieces are fixed according to certain heuristic rules and the *MIP* model is transformed into a linear problem.

The only exact algorithm that can be found in the literature is proposed by Fischetti and Luzzi [27]. They develop a Mixed Integer Programming *MIP* model and a branching strategy which is used with *CPLEX*. The Fischetti and Luzzi *MIP* non-overlapping constraints use tighter coefficients instead of *big-M* constants. The branching strategy is based on separating pieces by blocks, that is, when a block of n pieces is already separated then the next piece which overlaps with it is separated from the pieces of the block. Their exact algorithm has been tested on three instances, *glass1*, *glass2* and *glass3* with 5, 7 and 9 pieces, respectively. These instances are broken glass problems, for which the optimal solution has 100% utilization. Fischetti and Luzzi [27] are able to prove optimality only for instances *glass1* and *glass2*.

1.5 Heuristic algorithms

Bennell and Oliveira [13] in their tutorial in irregular shape packing problems provide an introduction to heuristic solution methods. There are two ways of dealing with *nesting* problems: working with partial solutions and working with complete solutions. The first approach represents the construction of a layout piece by piece and in some cases can produce reasonable quality solutions at little computational cost. The second approach works with complete solutions and applies a local search, iteratively making small changes, to a

set of candidate solutions.

One of the first strategies to deal with the *Nesting problem* is based on the known placement rule BL (Bottom Left). This rule iteratively moves each piece to the left-most feasible position with respect to the set of already placed polygons. Albano and Sapuppo [1] propose this constructive algorithm where the ties are broken by preferring the lowest feasible position. In Blazewicz [16] we can find an extension which allows the polygons to be placed into a hole surrounded by already placed polygons. Dowsland and Dowsland [24] and Gomes and Oliveira [31] extend the constructive algorithm, considering the whole container instead of the envelope formed by the pieces which are already placed. Gomes and Oliveira [31] add a local search to find a good sequence of the given polygons using a random weighted length criterion. Finally, Burke et al. [18] propose an extension of the algorithm to deal with irregular pieces having circular edges. They propose searching from the left side of the layout through the unfeasible positions until a feasible position is found.

Oliveira et al. [51] develop the *TOPOS* algorithm with an alternative placement rule. The positions of the pieces on the stock sheet are not fixed and only the relative position between pieces which are already placed are fixed. They investigate different placement rules for growing the solution with the aim of keeping the layout as compact as possible while trying to avoid an increase in length.

The *JOSTLE* algorithm, proposed by Dowsland et al. [25], oscillates between packing from the left end of the stock sheet to packing from its right end, and the sequence of pieces is determined by the x-coordinate of each piece in the previous iteration.

On the other hand, there are many publications that use algorithms based on linear programming (LP) for *compaction* and *separation*. Milenkovic and Li [49] propose different algorithms for the *compaction* and *separation* of pieces, a physically-based simulated method for compaction and a position-based model that finds a local optimum for separation. Bennell and Dowsland [10] propose LP-based compaction and separation algorithms with a tabu search whose original version was proposed without the integration of LP in Bennell and Dowsland [9]. The tabu search is used to solve the *overlap minimization problem* (OMP), which minimizes the overlap penalty for all pairs of polygons under the constraint that they are placed into a container of a given width and length. The solution obtained by solving the OMP could be unfeasible.

Gomes and Oliveira [32] develop a simulated annealing algorithm and use an LP model for *compaction* and *separation*. This model is, initially, a Mixed Integer Programming (*MIP*) model where the relative position of each pair of polygons is determined by a set of binary variables. Then they fix the binary variables and the model is transformed into an LP model which is easy to solve and is used for *compaction* and *separation*. They use the constructive TOPOS heuristic presented in [51] to build the initial solution. Song and Bennell [62] use the TOPOS heuristic to design a heuristic algorithm based on the study of the permutations by adopting a beam search.

Egeblad et al. [26] propose a guided local search algorithm for OMP in which the neighborhood consists in moving the polygons in both vertical and horizontal directions from its current position. In this paper pieces cannot protrude from the stock sheet and they use the intersection area for each pair of polygons as the overlap penalty.

Imamichi et al. [35] propose an *iterated local search* (ILS) to solve an OMP algorithm which allows

pieces to protrude from the stock sheet. They use a measure of overlap that they call the *penetration depth*, which is the minimum translational distance to separate a given pair of polygons. They incorporate a nonlinear programming technique. Umetami et al. [69] propose a guided local search for a similar OMP which adds a direction to the pieces in order to calculate the measured overlap (*directional penetration depth*). They develop an algorithm which finds the position with a minimum overlap penalty for each polygon when it is translated in a specified direction.

Recently, Leung et al. [40] propose an extended local search based on the separation algorithm used in Imamichi et al. [35]. A tabu search algorithm is used to avoid local minima and a compact algorithm is used. Kubagawa et al. [58] propose a two-level algorithm in which an external level controls the value of the length (the open dimension) and an inner level controls the initial temperature used for simulated annealing, and the objective is to place all items inside the container. They use the *collision-free region* which indicates permitted placements for the insertion of the pieces.

1.6 Instances

In this section we are going to present the instances that we can find in the literature and a set of smaller instances that we have created in order to test the exact algorithm developed for *Nesting Problems*. In the first subsection the most known instances and their characteristics are presented. In the second subsection we introduce the set of smaller instances for testing the exact procedure. Finally, since in Chapter 9 we develop a constructive algorithm for the two dimensional irregular bin packing problem with guillotine cuts, the corresponding set of instances are presented in the third subsection.

1.6.1 Instances for *Nesting Problems*

There are a wide variety of *Nesting problems*, depending on the shape of the big item and the rotation of the pieces. In this thesis we consider the shape of the big item to be rectangular, with a fixed width and the objective is to minimize the total required length. If we look at the rotation of the small items, there are three kinds of problems:

- No rotation allowed.
- Several angles of rotation are allowed: 0^o, 90^o, 180^o and 270^o.
- Free rotation: pieces can be rotated at any angle.

Most of the known instances in the literature consider one of the first two types of instances. It is not common to allow free rotation for the pieces. In Table 1.1 we can see the set of instances that can be found in the literature, ordered by the non-decreasing number of pieces. Fischetti and Luzzi [27] use the first three instances, *glass1*, *glass2* and *glass3*, to test their exact algorithm. The remaining instances have been used only for heuristic algorithms due to the large number of pieces.

In what follows we present the pictures of the best results obtained using algorithms presented in the thesis. We use the notation L_{best} to denote that it is the best known solution for the current problem, but not necessarily the optimal solution.

Table 1.1: *Nesting instances from the literature*

Instances	Types of Pieces	Number of pieces	Average of vertices	Allowed rotation angles	Plate width	Problem type	Authors
glass1	5	5	6	0	45	Puzzle,convex	Fischetti and Luzzi [27]
glass2	7	7	5.42	0	45	Puzzle,convex	Fischetti and Luzzi [27]
glass3	9	9	5.44	0	45	Puzzle	Fischetti and Luzzi [27]
dighe2	10	10	4.7	0	100	Jigsaw puzzle	Dighe and Jakiela [23]
fu	12	12	3.58	0-90-180-270	38	Artificial, convex	Fujita et al. [29]
poly1a	15	15	4.6	0-90-180-270	40	Artificial	Hopper [34]
poly1a0	15	15	4.6	0	40	Artificial	Hopper [34]
dighe1	16	16	3.87	0	100	Jigsaw puzzle	Dighe and Jakiela [23]
mao	9	20	9.22	0-90-180-270	2550	Garment	Bounsaythip and Maouche [17]
blaz2	4	20	7.5	0-180	15	Artificial	Oliveira and Ferreira [50]
marques	8	24	7.37	0-90-180-270	104	Garment	Marques et al. [45]
albano	8	24	7.25	0-180	4900	Garment	Albano and Sapuppo [1]
jakobs1	25	25	5.6	0-90-180-270	40	Artificial	Jakobs [37]
jakobs2	25	25	5.36	0-90-180-270	70	Artificial	Jakobs [37]
shapes2	7	28	6.29	0-180	15	Artificial	Oliveira and Ferreira [50]
dagli	10	30	6.3	0-180	60	Garment	Ratanapan and Dagli [55]
poly2a	15	30	4.6	0-90-180-270	40	Artificial	Hopper [34]
poly2b	30	30	4.53	0-90-180-270	40	Artificial	Hopper [34]
shapes1	4	43	8.75	0-180	40	Artificial	Oliveira and Ferreira [50]
shapes0	4	43	8.75	0	40	Artificial	Oliveira and Ferreira [50]
poly3a	15	45	4.6	0-90-180-270	40	Artificial	Hopper [34]
poly3b	45	45	4.6	0-90-180-270	40	Artificial	Hopper [34]
swim	10	48	21.9	0-180	5752	Garment	Oliveira and Ferreira [50]
poly4a	15	60	4.6	0-90-180-270	40	Artificial	Hopper [34]
poly4b	60	60	4.6	0-90-180-270	40	Artificial	Hopper [34]
trousers	17	64	5.06	0-180	79	Garment	Oliveira and Ferreira [50]
poly5a	15	75	4.6	0-90-180-270	40	Artificial	Hopper [34]
poly5b	75	75	4.57	0-90-180-270	40	Artificial	Hopper [34]
shirts	8	99	6.63	0-180	5752	Garment	Dowsland et al. [25]

1.6.2 Smaller *Nesting* instances without rotation

In this section we include small instances with up to 16 pieces which we have used in our exact algorithms, listed in Table 1.2.

Instances *three*, *threep2*, *threep2w9*, *threep3* and *threep3w9* are constructed with copies of 3 pieces with simple shapes: a square, a triangle and a diamond.

Pieces from instances *shapes4* and *shapes8* are taken from instance *shapes0* in Table 1.1, which has pieces with very irregular shapes.

Instance fu in Table 1.1 has 12 pieces and 4 allowed angles of rotation. We create instance *fu12* by using the same pieces of instance fu but with a fixed orientation for the pieces. Furthermore, we have built instances *fu5*, *fu6*, *fu7*, *fu8*, *fu9* and *fu10* which consider, respectively, the first 5, 6, 7, 8, 9 and 10 pieces of instance fu.

Instances *glass1*, *glass2*, *glass3*, *dighe2* and *dighe1ok* are the *broken glass* instances used by Fischetti and Luzzi [27].

We have built 15 instances from instance *Jakobs1* by choosing 10, 12 and 14 pieces randomly. Analogously, we have built 15 instances from instance *Jakobs2*. We call these instances *Ja-b-c-d*, where *a* denotes the initial problem (*Jakobs1* or *Jakobs2*); *b* denotes the number of pieces; *c* represents the width of the strip and *d* the creation order, used to distinguish between the 5 instances of each type.

Finally, we consider the instance *poly*1*a* with 15 pieces.

In what follows, we present the pictures of the best results obtained with the exact algorithms. We use the notation L_{ub} to denote that it is an upper bound, that is, that no optimality is proved, and L if it is the optimal solution.

Table 1.2: *Small instances used to test the exact algorithms*

Instances	Types of pieces	Number of pieces	Average of vertices	Plate width	Type of problem	Upper bound
three	3	3	3.67	7	Artificial	7
shapes4	4	4	8.75	13	Artificial	24
fu5	5	5	3.60	38	First 5 pieces of fu	24
glass1	5	5	5.00	45	Artificial	45
fu6	6	6	3.67	38	First 6 pieces of fu	24
threep2	6	6	3.67	7	Artificial	11
threep2w9	6	6	3.67	9	Artificial	10
fu7	7	7	3.71	38	First 7 pieces of fu	28
glass2	7	7	5.43	45	Artificial	60
fu8	8	8	3.75	38	First 8 pieces of fu	32
shapes8	8	8	8.75	20	Artificial	26
fu9	9	9	3.67	38	First 9 pieces of fu	29
threep3	9	9	3.67	7	Artificial	16
threep3w9	9	9	3.67	9	Artificial	13
glass3	9	9	5.44	100	Artificial	177
fu10	10	10	3.70	38	First 10 pieces of fu	34
dighe2	10	10	4.70	100	Jigsaw puzzle	120
J1-10-10-0	10	10	6.20	10	Random Jakobs1	22
J1-10-10-1	10	10	4.60	10	Random Jakobs1	22
J1-10-10-2	10	10	5.80	10	Random Jakobs1	21
J1-10-10-3	10	10	5.80	10	Random Jakobs1	27
J1-10-10-4	10	10	6.30	10	Random Jakobs1	16
J2-10-35-0	10	10	5.10	35	Random Jakobs2	28
J2-10-35-1	10	10	5.30	35	Random Jakobs2	27
J2-10-35-2	10	10	5.00	35	Random Jakobs2	25
J2-10-35-3	10	10	5.70	35	Random Jakobs2	26
J2-10-35-4	10	10	5.80	35	Random Jakobs2	28
J1-12-20-0	12	12	6.00	20	Random Jakobs1	13
J1-12-20-1	12	12	5.83	20	Random Jakobs1	12
J1-12-20-2	12	12	5.83	20	Random Jakobs1	16
J1-12-20-3	12	12	5.83	20	Random Jakobs1	11
J1-12-20-4	12	12	6.08	20	Random Jakobs1	16
J2-12-35-0	12	12	5.17	35	Random Jakobs2	31
J2-12-35-1	12	12	4.92	35	Random Jakobs2	32
J2-12-35-2	12	12	5.33	35	Random Jakobs2	28
J2-12-35-3	12	12	6.00	35	Random Jakobs2	28
J2-12-35-4	12	12	5.42	35	Random Jakobs2	30
fu12	12	12	3.58	38	Artificial, convex	34
J1-14-20-0	14	14	5.79	20	Random Jakobs1	15
J1-14-20-1	14	14	5.50	20	Random Jakobs1	15
J1-14-20-2	14	14	6.00	20	Random Jakobs1	18
J1-14-20-3	14	14	6.21	20	Random Jakobs1	12
J1-14-20-4	14	14	6.07	20	Random Jakobs1	18
J2-14-35-0	14	14	5.21	35	Random Jakobs2	35
J2-14-35-1	14	14	5.07	35	Random Jakobs2	35
J2-14-35-2	14	14	5.21	35	Random Jakobs2	30
J2-14-35-3	14	14	5.64	35	Random Jakobs2	32
J2-14-35-4	14	14	4.79	35	Random Jakobs2	28
poly1a0	15	15	4.53	40	Artificial	18
dighe1ok	16	16	3.88	100	Jigsaw puzzle	153

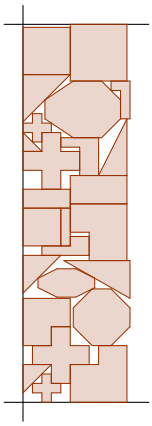

Jakobs1: $L = 11.31$

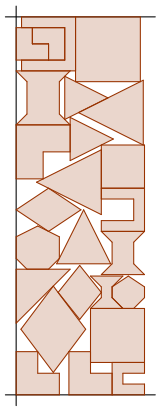

Jakobs2: $L = 23.76$

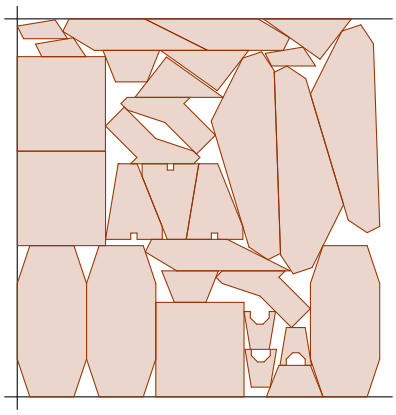

Dagli: $L = 57.54$

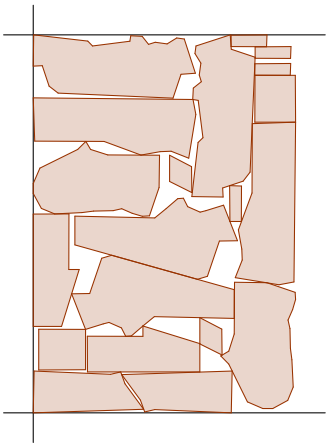

mao: $L = 1769.54$

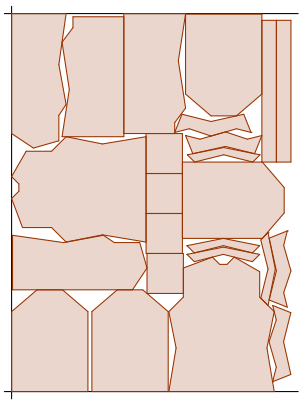

marques: $L_{best} = 76.85$

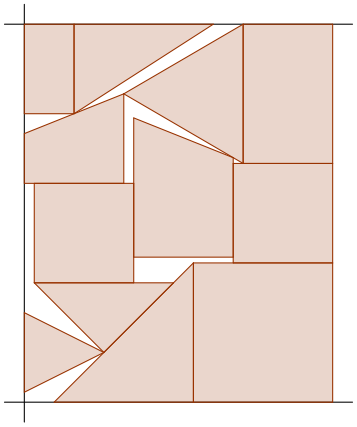

fu: $L = 31.00$

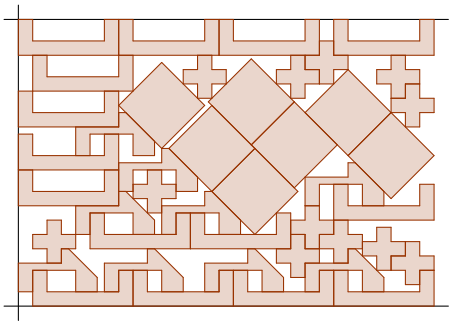

shapes0: $L_{best} = 58.00$

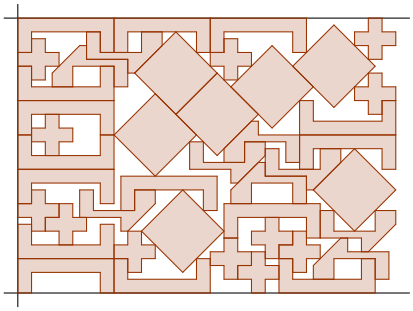

shapes1: $L = 55.00$

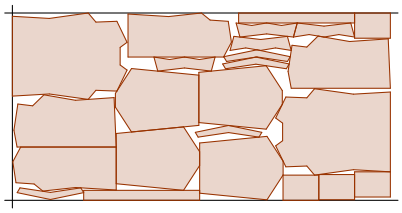

Albano: $L = 9887.62$

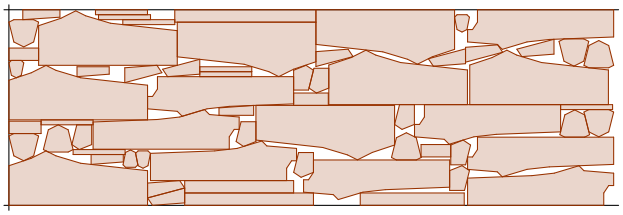

Trousers: $L = 244.25$

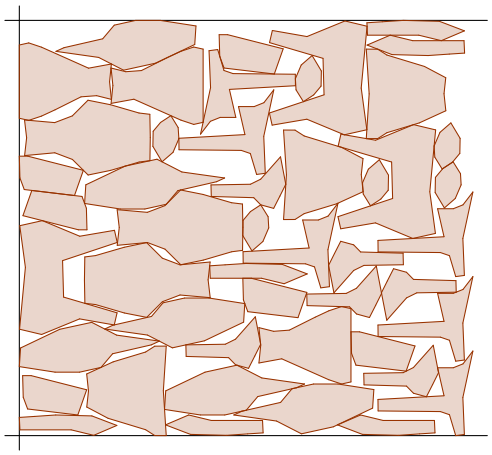

(transformed) *swim*: $L = 6164.40$

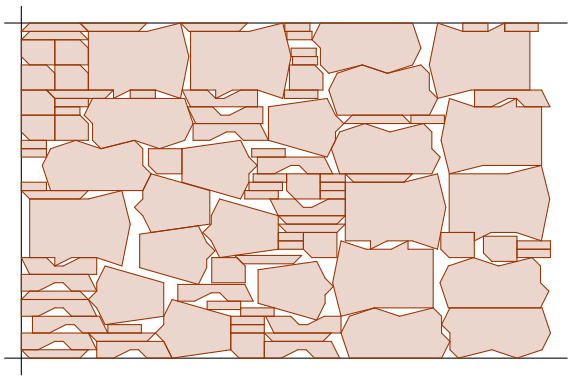

shirts: $L = 63.16$

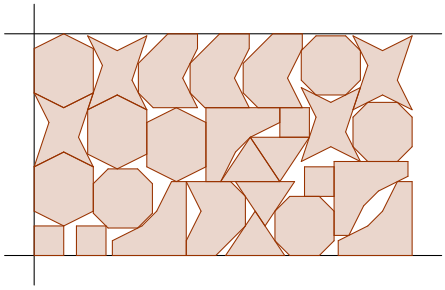

shapes2: $L_{best} = 25.57$

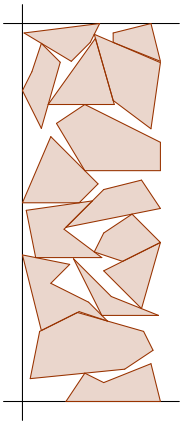

poly1a0: $L_{best} = 14.60$

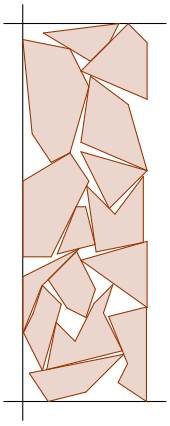

poly1a: $L_{best} = 13.16$

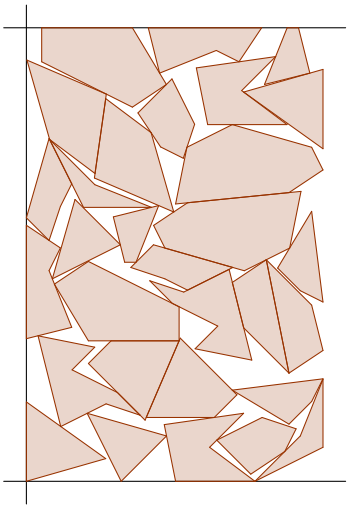

poly2a: $L_{best} = 26.16$

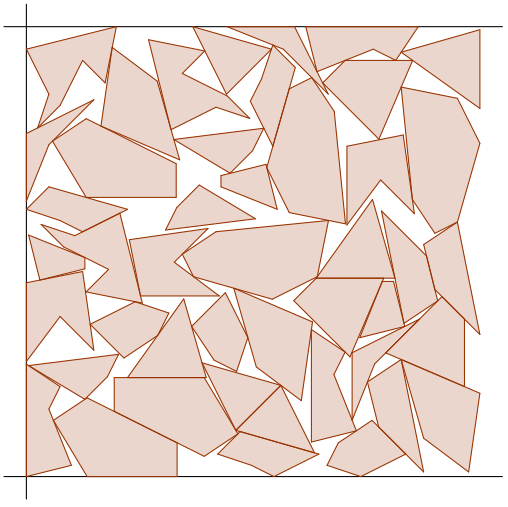

poly3a: $L_{best} = 40.32$

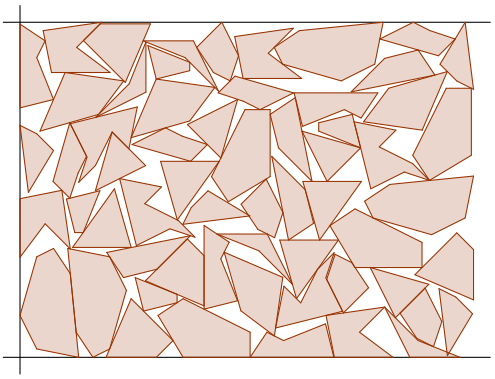

poly4a: L_{best} = 54.14

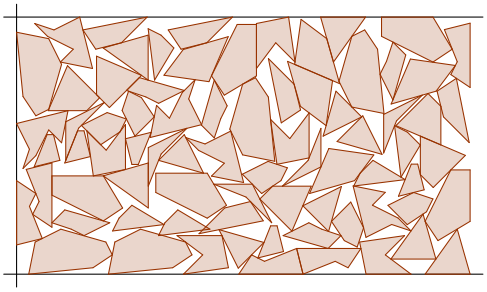

poly5a: L = 70.56

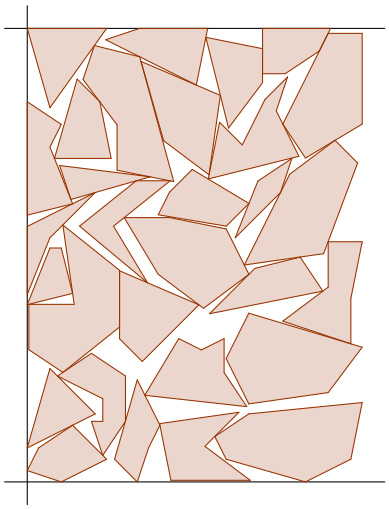

poly2b: L_{best} = 29.54

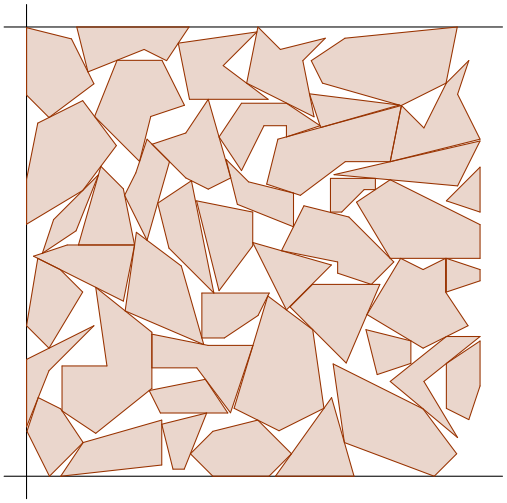

poly3b: L_{best} = 40.38

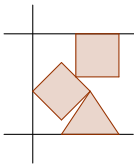

three: $L = 6$

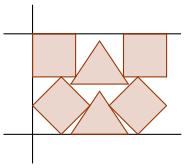

threep2: $L = 9.33$

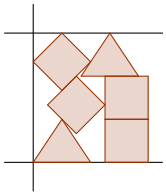

threep2w9: $L = 8$

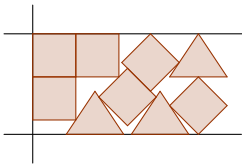

threep3: $L = 13.53$

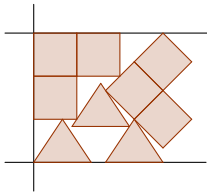

threep3w9: $L = 11$

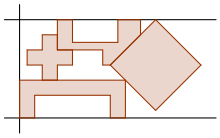

shapes4: $L = 24$

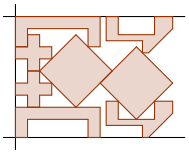

shapes8: $L = 26$

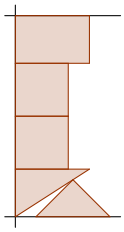

fu5: $L = 17.89$

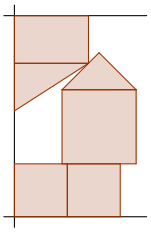

fu6: $L = 23$

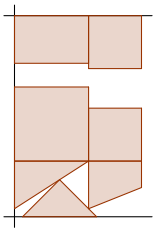

fu7: $L = 24$

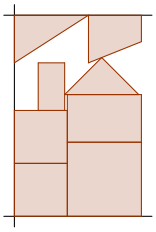

fu8: $L = 24$

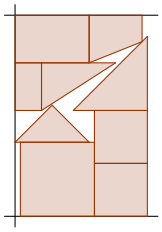

fu9: $L = 25$

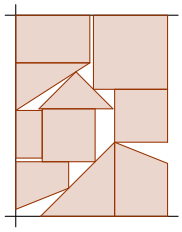

fu10: $L = 28.68$

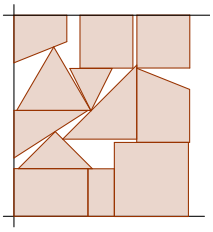

fu: $L = 33.13$

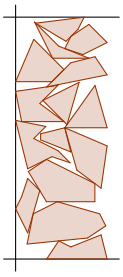

poly1a0: $L_{ub} = 15.13$

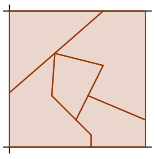

glass1: $L = 45$

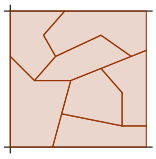

glass2: $L = 45$

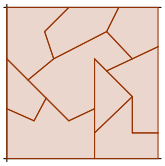

glass3: $L = 100$

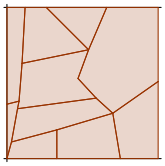

dighe2: $L = 100$

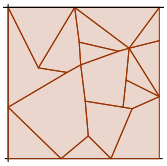

dighe1ok: $L = 100$

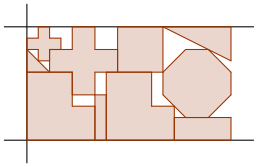

J1-10-20-0: $L = 18$

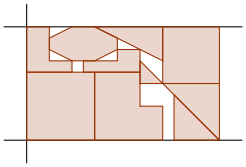

J1-10-20-1: $L = 17$

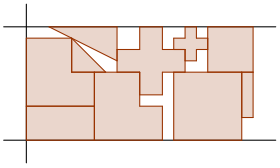

J1-10-20-2: $L = 20$

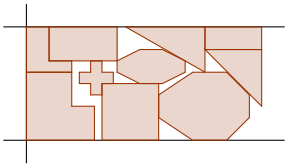

J1-10-20-3: $L = 20.75$

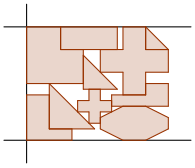

J1-10-20-4: $L = 12.5$

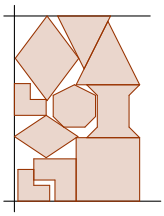

J2-10-35-0: $L = 23.66$

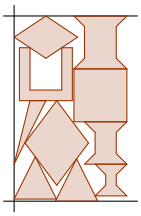

J2-10-35-1: $L = 21.30$

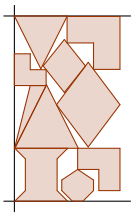

J2-10-35-2: $L = 19.95$

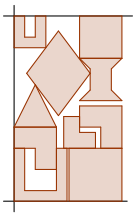

J2-10-35-3: $L = 20.37$

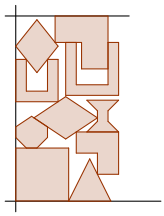

J2-10-35-4: $L = 19.4$

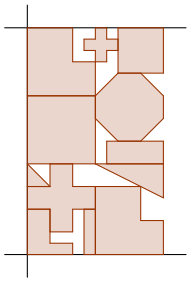

J1-12-20-0: $L = 12$

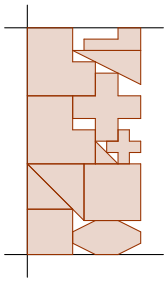

J1-12-20-1: $L = 10$

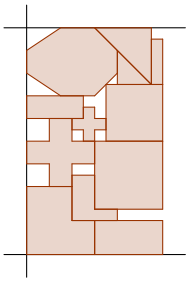

J1-12-20-2: $L = 12$

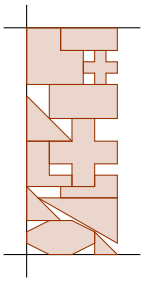

J1-12-20-3: $L = 8$

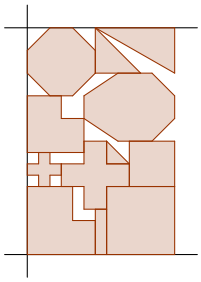

J1-12-20-4: $L = 13$

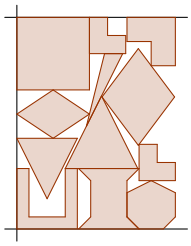

J2-12-35-0: $L = 26.21$

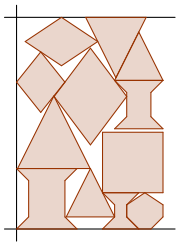

J2-12-35-1: $L = 24.22$

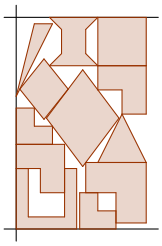

J2-12-35-2: $L = 21.5$

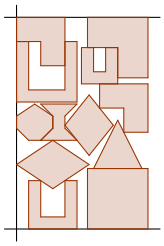

J2-12-35-3: $L = 21.73$

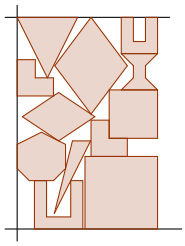

J2-12-35-4: $L = 23.21$

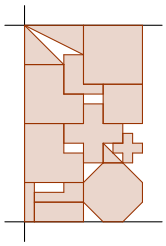

J1-14-20-0: $L = 12$

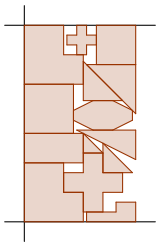

J1-14-20-1: $L = 11.33$

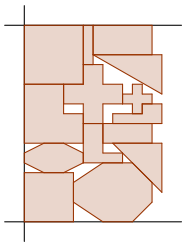

J1-14-20-2: $L = 14$

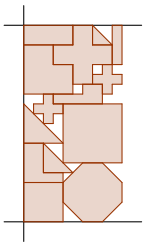

J1-14-20-3: $L = 10$

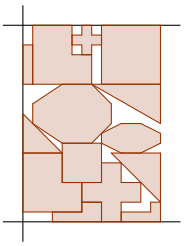

J1-14-20-4: $L = 14$

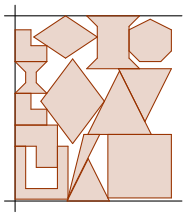

J2-14-35-0: $L_{ub} = 29.53$

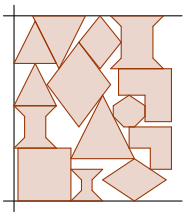

J2-14-35-1: $L_{ub} = 29.75$

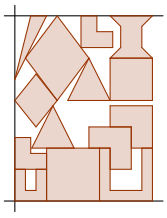

J2-14-35-2: $L_{ub} = 26$

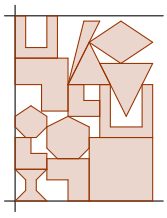

J2-14-35-3: $L_{ub} = 26$

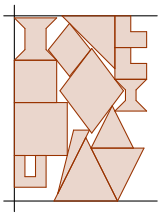

J2-14-35-4: $L_{ub} = 25$

1.6.3 Instances for the two dimensional irregular bin packing problems with guillotine cuts

The two dimensional irregular bin packing problems with guillotine cuts is a recent problem and Bennell et al. [11] is the only paper which has studied it so far. They propose 8 instances, 4 of them corresponding to real data from industry and the other 4 instances generated using properties of the industrial data. The number of pieces ranges between 40 and 149. The instance name is coded by a letter and a number: the letter can be *J* if the data is provided by industry or *H* if the data are generated; the number represents the total number of pieces to be packed into the bins.

Table 1.3 provides details of the test data: the average and standard deviation of the number of edges, the average and the standard deviation of the area. This table has been obtained from [11].

Table 1.3: *Test instances for the problem with guillotine cuts*

Dataset	Ave. no. edges	Stdev. edges	Ave. area	Stdev. area	Irregular degree
*J*40	3.56	0.741	1070889	864460	0.2741
*J*50	3.70	0.647	1104653	825371	0.3416
*J*60	3.73	0.607	1041775	791634	0.2986
*J*70	3.77	0.569	1018279	782675	0.2578
*H*80	3.67	0.508	727813	622035	0.2457
*H*100	3.83	0.493	968581	739522	0.2520
*H*120	3.61	0.562	819777	732018	0.3142
*H*149	3.82	0.695	932110	813401	0.2667

In order to test the constructive algorithm presented in Chapter 9 on other problems, we have also considered rectangular bin packing problems with guillotine cuts. There are 500 benchmark problem instances divided into 10 classes. The first 6 classes were proposed by Berkey and Wang [15] and the last 4 classes by Lodi et al. [42]. We consider two rotations for the insertion of each piece (0^o and 90^o).

In what follows, we present the pictures of the best solution obtained with the constructive algorithms presented in Chapter 9 on these instances.

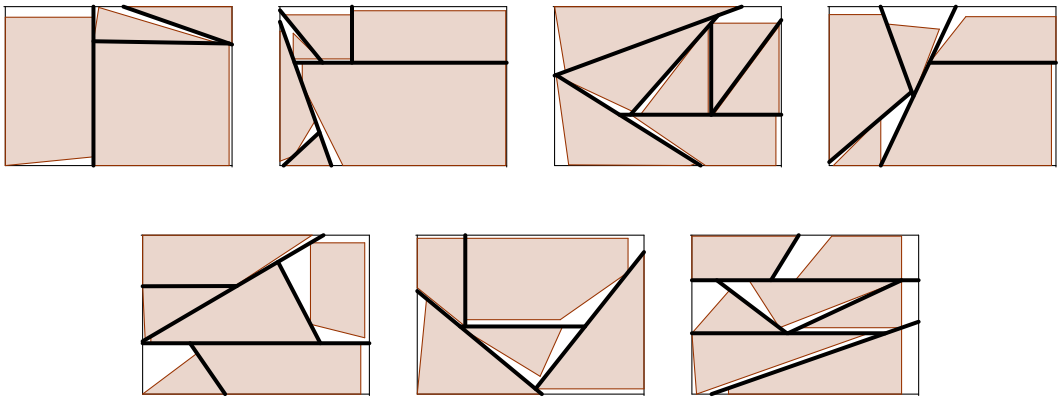

Figure 1.16: *J40*

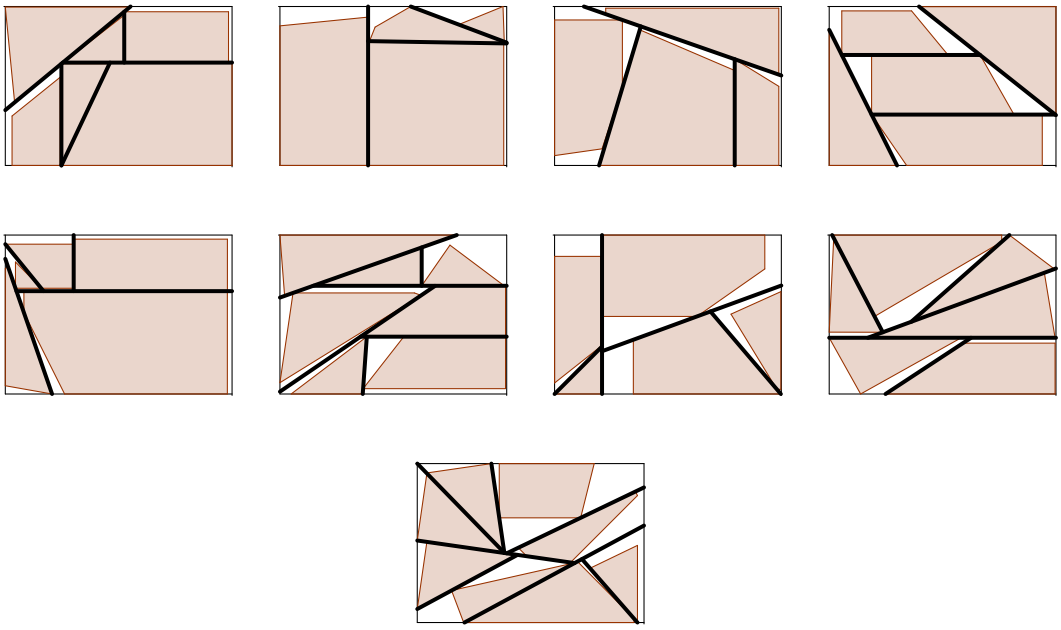

Figure 1.17: *J50*

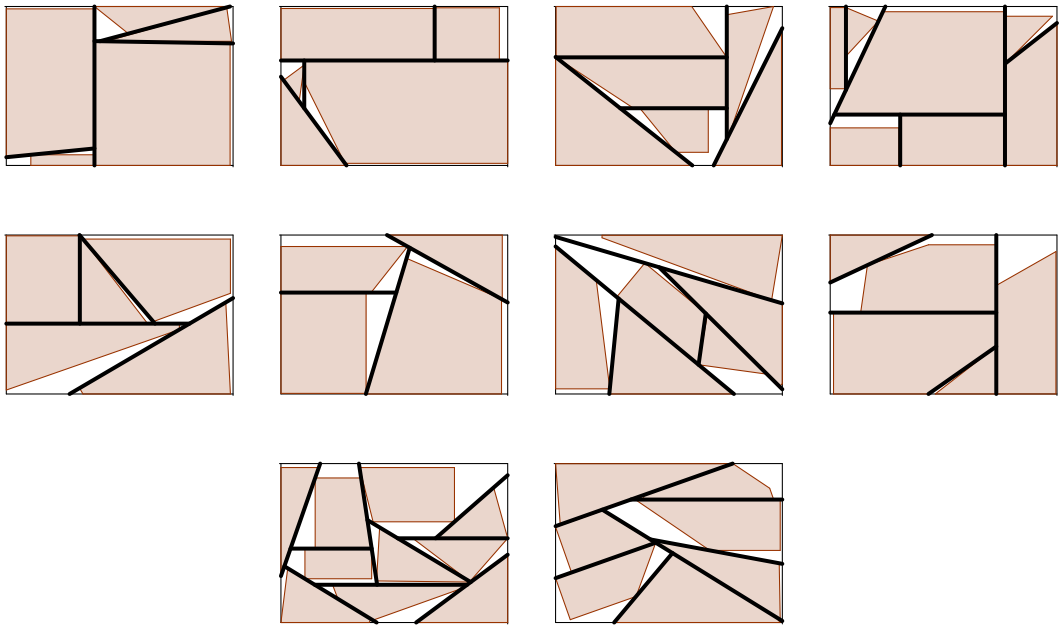

Figure 1.18: *J60*

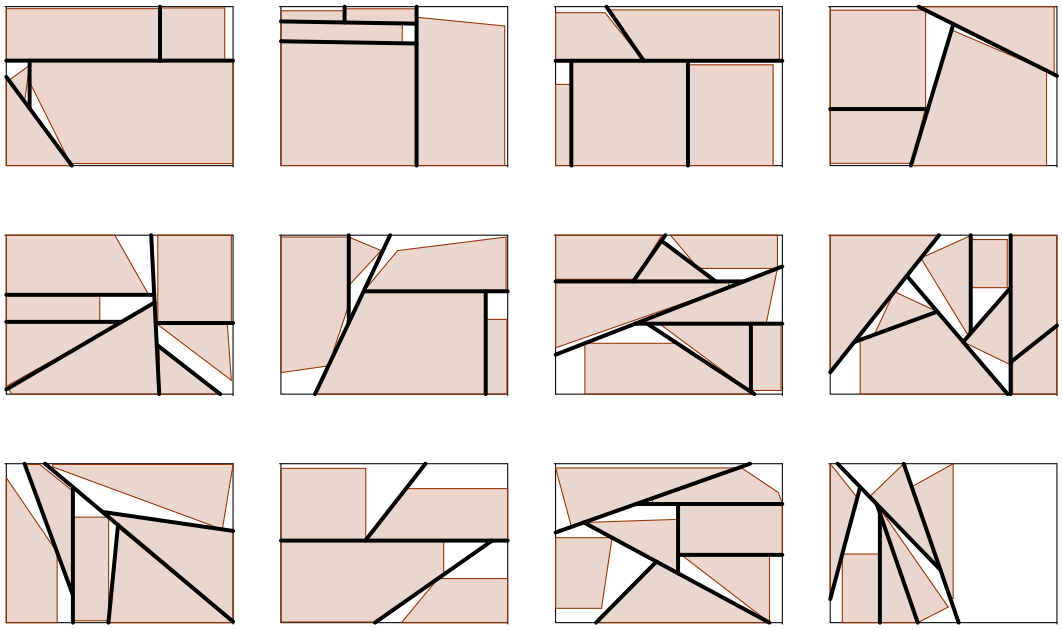

Figure 1.19: *J70*

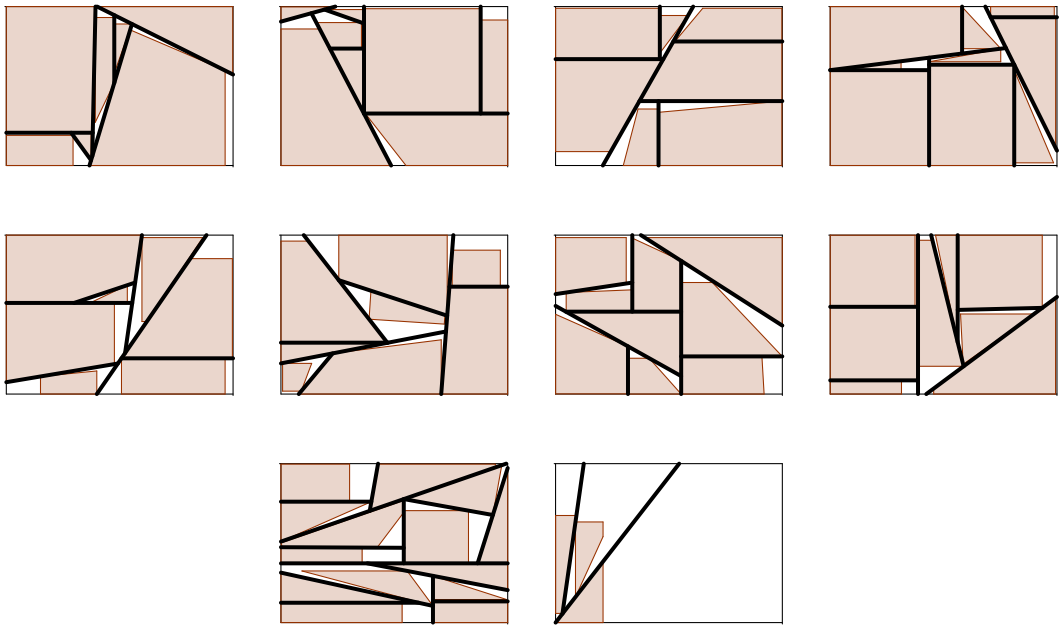

Figure 1.20: *H80*

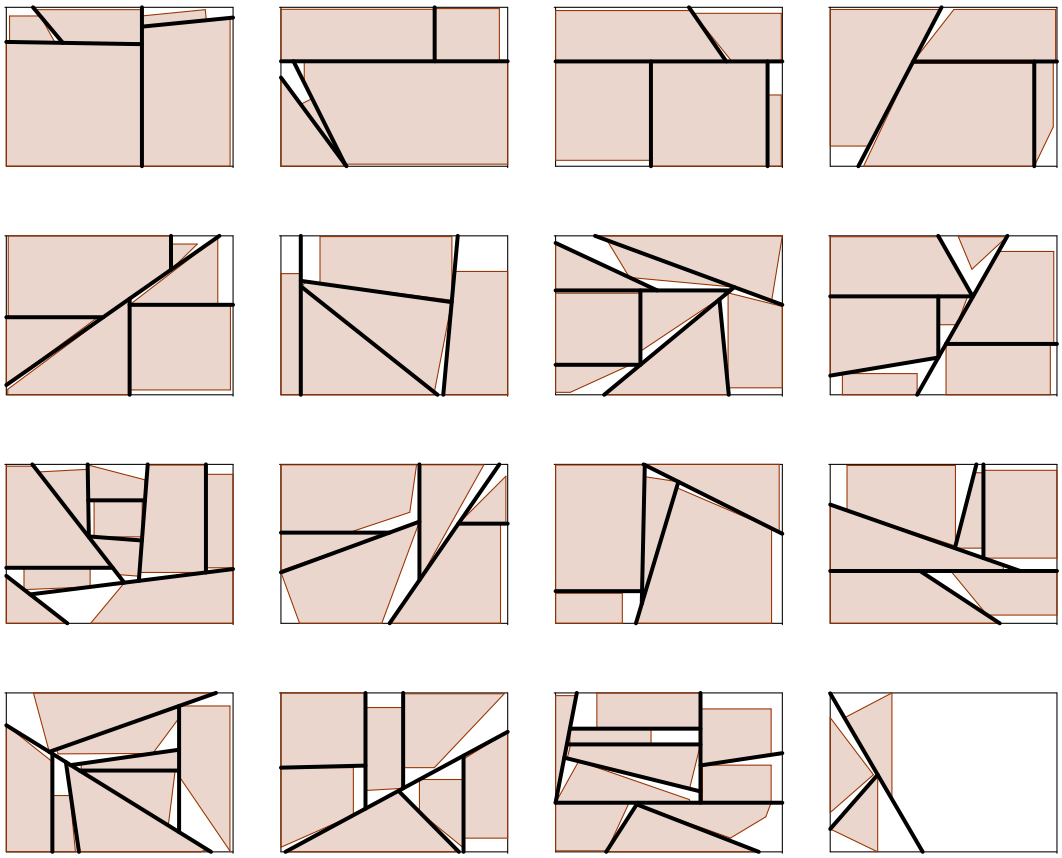

Figure 1.21: *H100*

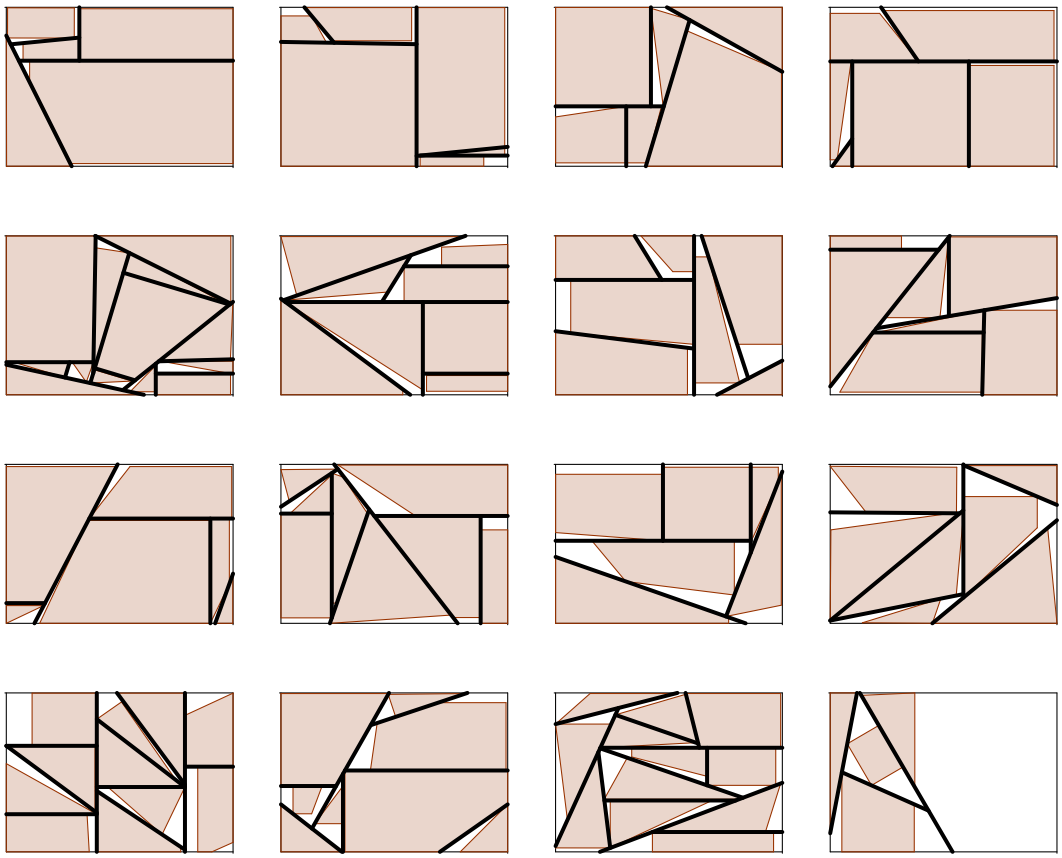

Figure 1.22: *H120*

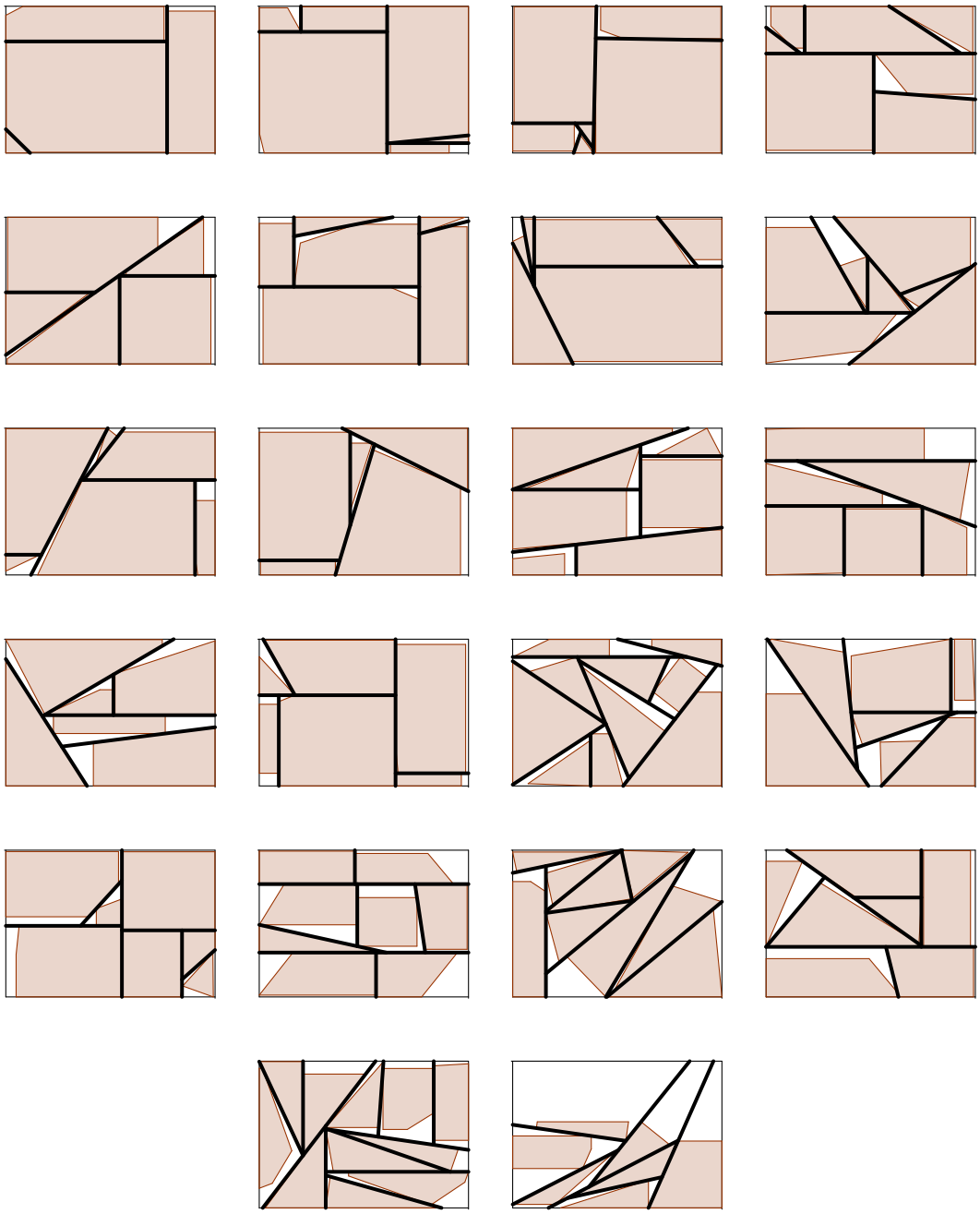

Figure 1.23: *H149*

Chapter 2

Mixed integer formulations for *Nesting problems*

In this chapter we will first describe the formulation used by Gomes and Oliveira [32], and then two new proposals based on the ideas of Fischetti and Luzzi [27]. In all cases the objective function will be the minimization of L, the strip length required to accommodate all the pieces without overlapping. Also, all formulations contain two types of constraints: those preventing the pieces from exceeding the dimensions of the strip and those forbidding the pieces from overlapping. The differences between formulations lie in the way these constraints are defined.

More specifically, the Gomes and Oliveira formulation, *GO*, and our proposals, *HS1* and *HS2*, differ in the way they use the *NFP* to define the non-overlapping constraints. Gomes and Oliveira assign a binary variable to each edge or (convex) concavity of the *NFP* and then use a *big M* constant to activate or deactivate each one of the non-overlapping constraints. In our *HS1* and *HS2* formulations we take the Fischetti and Luzzi idea of partitioning the outer region of each *NFP* into convex polygons, called *slices*, and use it in a particular way, defining horizontal slices. A binary variable is then assigned to each *slice* and all the variables corresponding to the slices of one *NFP* are included in each one of the non-overlapping constraints constructed from this *NFP* in order to eliminate the *big M*. The third formulation proposed, *HS2*, has the same non-overlapping constraints as the *HS1* formulation, but the containment constraints are lifted by considering the interaction between each pair of pieces.

Let $P = \{p_1, \ldots, p_N\}$ be the set of pieces to be arranged into the strip. We denote the length and the width of the strip by L and W, respectively. The bottom-left corner of the strip is placed at the origin. The placement of each piece is given by the coordinates of its reference point, (x_i, y_i), which is the bottom-left corner of the enclosing rectangle, see Figure 2.1. We denote by w_i and l_i the width and length of piece i, respectively. Let i and j be two pieces. The number of binary variables that we define in order to separate pieces i and j is represented by m_{ij}. The binary variables defined over NFP_{ij} are represented by $b_{ijk}, k = 1 \ldots, m_{ij}$. The set of binary variables created from the NFP_{ij} is denoted by $VNFP_{ij}$. The number of inequalities needed to describe the *slice* k of the NFP_{ij} (*slice* defined by variable b_{ijk}) is represented by f_{ij}^k.

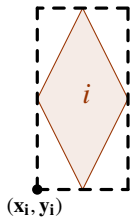

Figure 2.1: *Referent point of piece i*

2.1 Formulation *GO* (Gomes and Oliveira)

Let us consider the simple example in Figure 2.2. Pieces i and j are rectangles, and then NFP_{ij} is a rectangle. Associated with each edge of NFP_{ij}, a binary variable b_{ijk} is defined. Variable b_{ijk} takes value 1 if piece j is separated from piece i by the line defined by the k^{th} edge of NFP_{ij}, otherwise it takes value 0. In Figure 2.2, if $b_{ij1} = 1$, p_j is placed above p_i. Similarly, variables b_{ij2}, b_{ij3}, b_{ij4} place p_j to the left, below, or to the right of p_i, respectively. As at least one of these variables must take value 1 to prevent overlapping, $\sum_{k=1}^{4} b_{ijk} \geq 1$.

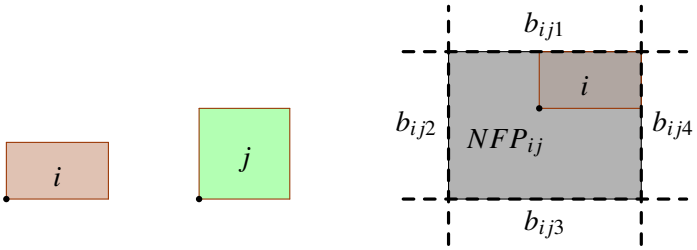

Figure 2.2: *Definition of variables* b_{ijk}

If $b_{ij1} = 1$, one way of expressing that p_j has to be placed above p_i would be:

$$y_j - y_i \geq w_i b_{ij1} \tag{2.1}$$

where w_i is the width of i. However, this inequality is not valid if $b_{ij1} = 0$. In order to transform (2.1) into a valid inequality, Gomes and Oliveira [32] include a *big-M* term (where M is a large positive number). The valid constraint would be:

$$y_j - y_i \geq w_i - (1 - b_{ij1})M \tag{2.2}$$

The general form of the constraints preventing overlapping is:

$$\alpha_{ijk}(x_j - x_i) + \beta_{ijk}(y_j - y_i) \leq q_{ijk} + M(1 - b_{ijk}) \tag{2.3}$$

where $\alpha_{ijk}(x_j - x_i) + \beta_{ijk}(y_j - y_i) = q_{ijk}$ is the equation of the line including the k^{th} of the m_{ij} edges of NFP_{ij}. The complete *GO* formulation is:

$$Min\ L \tag{2.4}$$

$$s.t. \quad x_i \leq L - l_i \qquad i = 1, ..., N \tag{2.5}$$

$$y_i \leq W - w_i \qquad i = 1, ..., N \tag{2.6}$$

$$\alpha_{ijk}(x_j - x_i) + \beta_{ijk}(y_j - y_i) \leq q_{ijk} + M(1 - b_{ijk}) \qquad 1 \leq i < j \leq N,\ k = 1, ..., m_{ij} \tag{2.7}$$

$$\sum_{k=1}^{m_{ij}} b_{ijk} \geq 1 \qquad 1 \leq i < j \leq N \tag{2.8}$$

$$b_{ijk} \in \{0, 1\} \qquad 1 \leq i < j \leq N \tag{2.9}$$

$$x_i,\ y_i \geq 0 \qquad 1 \leq i \leq N \tag{2.10}$$

The objective function (2.4) minimizes the required length of the strip. Constraints (2.5), (2.6) and (2.10) are bound constraints, keeping the pieces inside the strip. Constraints (2.7) prevent overlapping. Variables b_{ijk} are integer (constraints 2.9) and at least one of them must take value 1 for each NFP (constraints 2.8).

One potential disadvantage of this formulation is that the previous definition of non-overlapping constraints does not limit the relative position of the pieces very strictly. Let us consider the more complex situation in Figure 2.3. As NFP_{12} has 8 edges, 8 binary variables are defined. If p_2 is placed into the shaded region on the upper left-hand side, two variables b_{121} and b_{122} can take value 1. In fact, if p_2 is placed well to the left of p_1 in that zone, even variable b_{123} can take value 1. If we use this formulation in a branch and bound procedure, many different branches can contain the same solution and that can slow down the search.

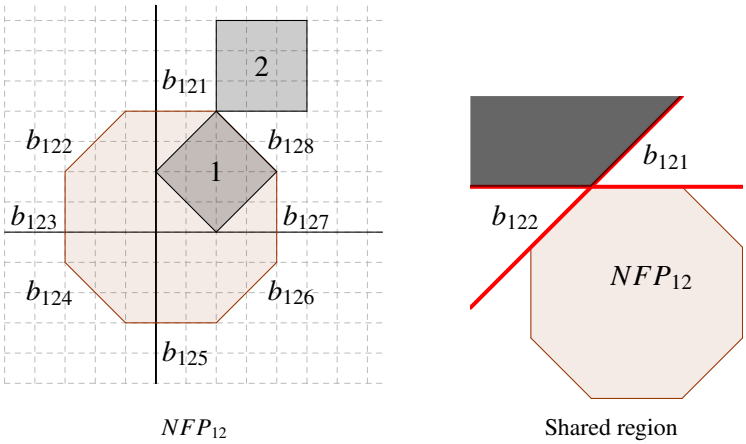

Figure 2.3: *Variables of GO formulation*

2.2 Formulation HS1 (Horizontal Slices 1)

The formulation proposed by Fischetti and Luzzi [27] differs from the Gomes and Oliveira model in their use of NFP for the definition of variables. They consider the region outside each NFP_{ij} partitioned into k convex disjoint regions called *slices*, S_{ij}^k , and define a variable b_{ijk} so that $b_{ijk} = 1$ if the reference point of piece j is placed in S_{ij}^k, and 0 otherwise. In this approach, in order to consider the *slices* as convex polygons

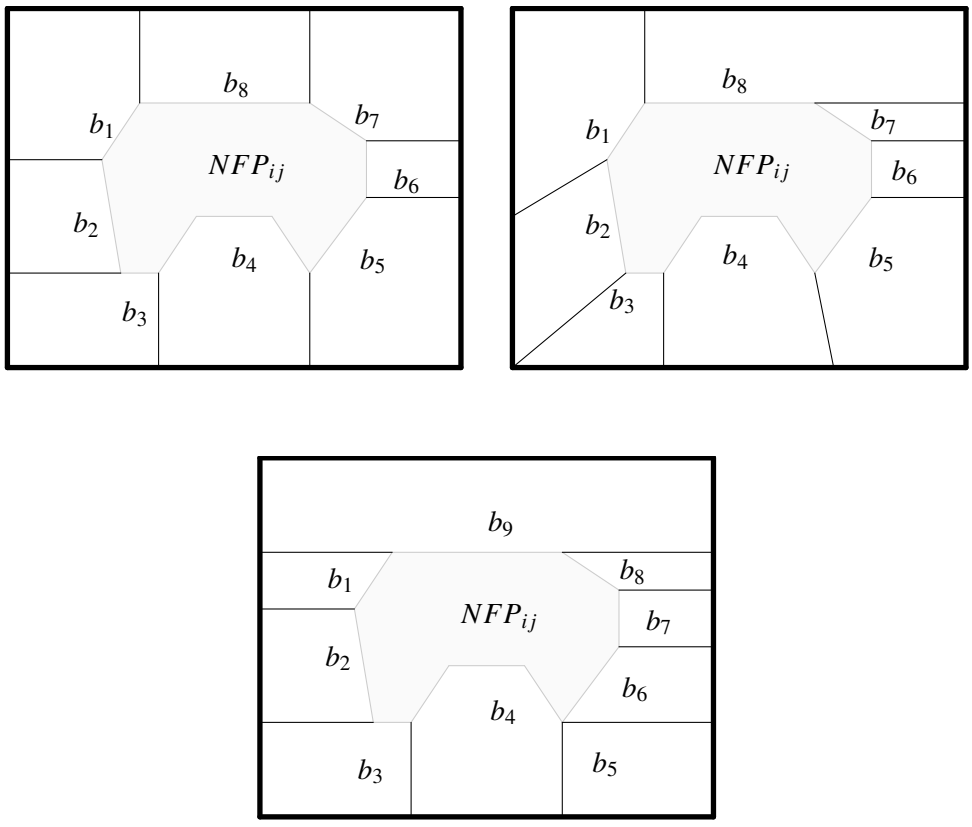

Figure 2.4: *Different ways of defining slices*

or segments or points, an upper bound for the length of the strip is needed. It can be obtained by a simple heuristic algorithm or just by calculating the total length of the pieces. In a vertical way, the maximum separation between each pair of pieces is given by the width of the strip, W.

Fischetti and Luzzi do not specify the way to obtain the *slices*. In Figure 2.4 we can see three different ways to define the *slices*. Note that the way in which the *slices* are defined affects the number of *slices* corresponding to an *NFP*. For instance, the third case in Figure 2.4 requires one *slice* more than the others.

The main idea of our proposal is based on defining the *slices* through horizontal inequalities. In a first step, if necessary, the complexities of the *NFP* are eliminated and one or more binary variables are assigned to each complexity. Figure 1.11 shows the three cases of complexities that we can find in the *NFP*s, and if one of these complexities appears in the *NFP* then it ceases to be a polygon. So, in this step, we transform the *NFP* into a polygon.

In a second step, all the concavities of the *NFP* are going to be *closed*, and each concavity produces one or more binary variables depending on the degree of concavity. After this procedure we transform the *NFP* into a convex polygon.

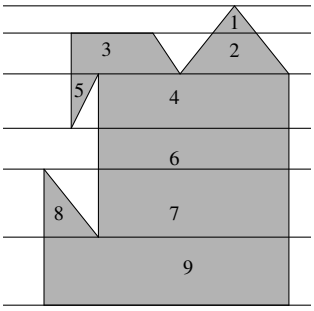

Figure 2.5: *Partition of a inner irregular polygon of the NFP in* 9 *convex polygons.*

Finally, in a third step, the *slices* of the outer region of *NFP* (transformed into a convex polygon) are defined using horizontal inequalities. In this step a binary variable is assigned to each one of the *slices* defined.

The set of binary variables defined in the three steps for each pair of pieces is the set of all the binary variables in the formulation.

Finally, the *non-overlapping constraints* are constructed without using *big M* constants of the *GO* formulation.

2.2.1 Step 1: Complex *slices*

As was shown in Figure 1.11, when building the NFP_{ij} some special elements can appear: points, segments and inner polygons. We define a variable b_{ijk} for each point, for each segment and for each convex inner polygon, so that the variable takes value 1 if the reference point of p_j is placed at this point, segment or polygon. If an inner polygon is non-convex, it is previously decomposed into convex polygons and a variable is associated with each convex polygon. This composition is done by adding a horizontal line through each vertex, see Figure 2.5.

Once these elements have been considered, NFP_{ij} is just a polygon, convex or not. We say that the binary variables defined in this step define a *complex slice*. We denote by B_1 the set of binary variables which define *complex slices*.

These complexities are not common in real-life problems because the pieces have to have very specific forms in order to produce an *NFP* with one of these types of complexities.

2.2.2 Step 2: Closed *slices*

If NFP_{ij} is non-convex, we close its concavities by adding convex polygons in a recursive way until the resulting polygon is convex. We go through the ordered set of vertices counterclockwise, identifying concavities. A concavity starts at vertex v_n when not all the vertices are to the left-hand side of the line defined by v_n and v_{n+1}. The concavity ends when the next vertex v_{n+r} is not to the right-hand side of the line defined by v_{n+r-2} and v_{n+r-1}. In Figure 2.6 there is just one concavity, $C = \{v_4, v_5, v_6, v_7\}$, but in the general case many

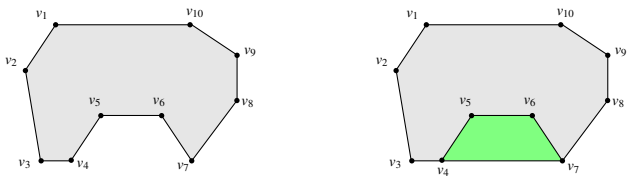

$C_1 = \{v_4, v_5, v_6, v_7\}$ Updated NFP

Figure 2.6: *Closing the concavities of* NFP

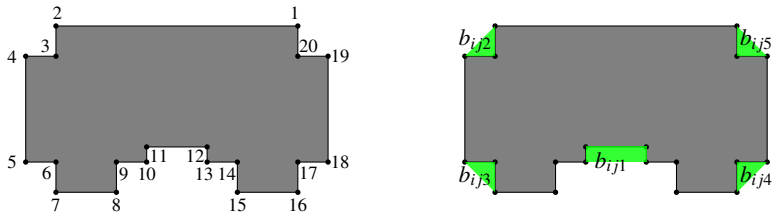

(a) Initial NFP (b) First iteration

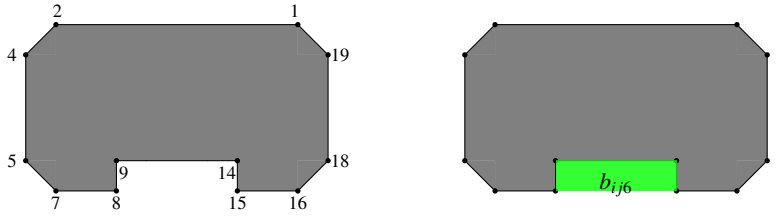

(c) Updated *NFP* after first iteration (d) Second iteration

Figure 2.7: *Transforming* NFP *into a convex set*

concavities can appear.

We say that a given concavity is a *convex concavity* if the polygon defined by the vertices of the concavity is convex. In the general case, from the list of convex concavities of the *NFP*, we choose that with the largest number of vertices and close it by adding a segment from its first to its last vertex. Other convex concavities can also be closed if they are disjoint with those already closed. The list of NFP_{ij} vertices is updated, eliminating the intermediate vertices, and a variable b_{ijk} is associated with each closed concavity. The process is repeated until the resulting polygon NFP^c_{ij} is convex. Figure 2.7 illustrates the process. In a first iteration several convex concavities are found: $C_1 = \{v_2, v_3, v_4\}$, $C_2 = \{v_5, v_6, v_7\}$, $C_3 = \{v_8, v_9, v_{10}\}$, $C_4 = \{v_{10}, v_{11}, v_{12}, v_{13}\}$, $C_5 = \{v_{13}, v_{14}, v_{15}\}$, $C_6 = \{v_{16}, v_{17}, v_{18}\}$ and $C_7 = \{v_{19}, v_{20}, v_1\}$. C_4 with 4 vertices is chosen to be closed, as are C_1, C_2, C_6 and C_7, which are disjoint with C_4 and with each other. Binary variables b_{ij1} to b_{ij5} are associated with these closed regions. The updated NFP appears in Figure 2.7(c). As this polygon is still non-convex, the process is repeated in Figure 2.7(d) until a convex polygon is obtained.

In Figure 2.8 we can see an NFP with one non-convex concavity. In this case, firstly we eliminate the only convex concavity given by $C_1 = \{v_5, v_6, v_7\}$, and then we drop v_6 from the list of vertices. After that, the next convex concavity to eliminate is $C_2 = \{v_5, v_7, v_8\}$, where vertex v_7 is eliminated. Finally we eliminate the resulting convex concavity given by $C_3 = \{v_4, v_5, v_8\}$, where vertex v_5 is eliminated.

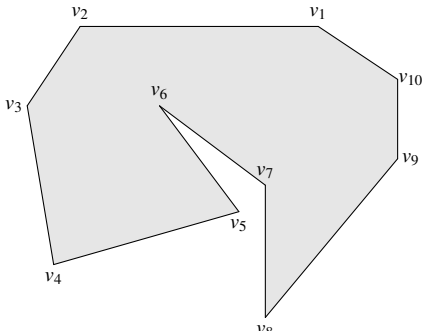

Figure 2.8: *Example of a non-convex concavity*

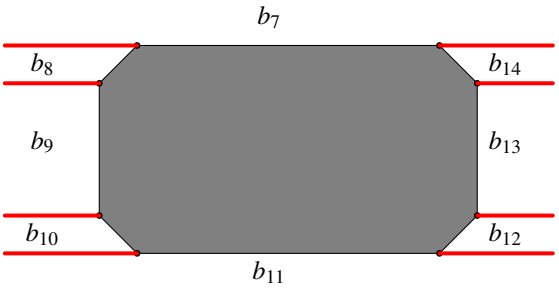

Figure 2.9: *Horizontal slices*

A *closed slice* is defined by a binary variable associated with a concavity of the *NFP*. The set of binary variables defined from a concavity of a *NFP* is denoted by B_2.

2.2.3 Step 3: Horizontal *slices*

This is the core of our approach. For each edge of every NFP^c, we define a horizontal slice by drawing two horizontal lines, one from each vertex, in the opposite direction to NFP^c. If there is a horizontal edge at the bottom (top), the slice goes from the line containing that edge to the bottom (top) edge of the strip. If there is a vertex at the bottom (top), an additional slice is built by drawing a horizontal line at the bottommost (topmost) vertex, stretching the whole length of the strip. An example can be seen in Figure 2.9.

We denote by B_3 the set of binary variables which define horizontal *slices*. Then $VNFP_{ij} := B_1 \cup B_2 \cup B_3$, the set of binary variables defined from NFP_{ij}.

The variables are defined in that way for two main reasons. First, using variables associated with slices overcomes the disadvantages of the Gomes and Oliveira definition. Each feasible position of piece j with respect to piece i corresponds to a unique variable (except for the unavoidable common border between slices). Second, defining the slices in a horizontal way helps us to control the relative vertical position of the pieces. We will take advantage of that when developing the branch and bound algorithm.

2.2.4 Non-overlapping constraints

Each slice S_{ij}^k is a 2-dimensional polyhedron, defined by m_{ij}^k linear inequalities. Initially, one way of writing valid inequalities would be to use *big-M* constants, as in the *GO* formulation:

$$\alpha_{ij}^{kf}(x_j - x_i) + \beta_{ij}^{kf}(y_j - y_i) \leq q_{ij}^{kf} + M(1 - b_{ijk}), \forall f = 1 \dots m_{ij}^k$$

The coefficients of b_{ijk} can be lifted (and the *big-M* avoided) in the following way. First, we substitute M with a set of coefficients:

$$\alpha_{ij}^{kf}(x_j - x_i) + \beta_{ij}^{kf}(y_j - y_i) \leq q_{ij}^{kf} + \sum_{h=1}^{m_{ij}} \theta_{ij}^{kfh} b_{ijh}$$

Then, taking into account that $\sum_{h=1}^{m_{ij}} b_{ijh} = 1$, and substituting q_{ij}^{kf} with $q_{ij}^{kf} \sum_{h=1}^{m_{ij}} b_{ijh} = 1$, we get:

$$\alpha_{ij}^{kf}(x_j - x_i) + \beta_{ij}^{kf}(y_j - y_i) \leq \sum_{h=1}^{m_{ij}} \delta_{ij}^{kfh} b_{ijh}$$

where $\delta_{ij}^{kfh} = q_{ij}^{kf} + \theta_{ij}^{kfh}$.

Finally, in order to have a valid inequality, coefficients δ_{ij}^{kfh} are obtained by computing the maximal value of the left-hand side where each variable b_{ijh} takes value 1:

$$\delta_{ij}^{kfh} := \max_{(v_j - v_i) \in S_{ij}^h \cap C} \alpha_{ij}^{kf}(x_j - x_i) + \beta_{ij}^{kf}(y_j - y_i)$$

where C is a box which is large enough to include all the possible placements of p_i and p_j, of width $2W$ and length $2\overline{L}$, and where $\overline{L}$ is an upper bound on L. This maximization problem can be solved by evaluating the function on the vertices of the closed region $S_{ij}^h \cap C$.

2.2.5 Formulation *HS1*

The complete *HS1* formulation is the following one:

$$\begin{aligned}
& Min\ L && && (2.11)\\
s.t.\quad & x_i \leq L - l_i && i = 1, ..., N && (2.12)\\
& y_i \leq W - w_i && i = 1, ..., N && (2.13)\\
& \alpha_{ij}^{kf}(x_j - x_i) + \beta_{ij}^{kf}(y_j - y_i) \leq \textstyle\sum_{h=1}^{m_{ij}} \delta_{ij}^{kfh} b_{ijh} && && \\
& \qquad 1 \leq i < j \leq N,\ \ k = 1, ..., m_{ij}, && f = 1, ..., t_{ij}^k && (2.14)\\
& \textstyle\sum_{k=1}^{m_{ij}}\ b_{ijk} = 1 && 1 \leq i < j \leq N && (2.15)\\
& b_{ijk} \in \{0, 1\} && 1 \leq i < j \leq N && (2.16)\\
& x_i,\ y_i \geq 0 && 1 \leq i \leq N && (2.17)
\end{aligned}$$

2.3 Formulation *HS2* (Horizontal Slices 2)

The bound constraints (2.12), (2.13), (2.17) of the *HS1* formulation are the same as those of the *GO* formulation (2.5), (2.6), (2.10). In this section we lift these constraints by using the interaction between pairs of pieces.

2.3.1 Relative position of pieces

Let NFP_{ij} be the *Non-Fit Polygon* associated with pieces p_i and p_j. We say we are working in the NFP_{ij}-coordinate system when we fix the reference point of p_i at the origin and let p_j move around in all the possible positions in the strip. We denote by $\overline{Y}^{ij}$ ($\underline{Y}^{ij}$) the maximum (minimum) value of the y-coordinate of NFP_{ij}. In a similar way, $\overline{X}^{ij}$ ($\underline{X}^{ij}$) is the maximum (minimum) value of the X-coordinate of NFP_{ij} (see Figure 2.10).

Let us consider the slice $k \in \{1, \ldots, m_{ij}\}$. We denote by $\overline{x}_{ijk}$ ($\underline{x}_{ijk}$) the maximum (minimum) value x_j can take in the NFP_{ij}-coordinate system when $b_{ijk} = 1$. Analogously, $\overline{y}_{ijk}$ ($\underline{y}_{ijk}$) is the maximum (minimum) value y_j can take in the NFP_{ij}-coordinate system when $b_{ijk} = 1$. In the example in Figure 2.10, these values are represented for *slice* $k = 2$, considering $W = 10$ and an upper bound on L, $\overline{L} = 11$. In this case, if the reference point of p_i is placed at the origin, and as $l_i = 4$ and $\overline{L} = 11$, there is a space of 4 units to the left of NFP_{ij} and 3 units to its right into which the reference point of piece p_j can be placed. Similarly, as $w_i = 4$ and $W = 10$, the space above NFP_{ij} for the reference point of p_i has 3 units and below it also has 3 units. Looking at NFP_{ij}, $\overline{Y}^{ij} = 4$, $\underline{Y}^{ij} = -3$, $\overline{X}^{ij} = 4$ and $\underline{X}^{ij} = -3$. Looking at slice $k = 2$, $\overline{x}_{ij2} = -1$, $\underline{x}_{ij2} = -7$, $\overline{y}_{ij2} = 4$ and $\underline{y}_{ij2} = 2$.

The subset of variables associated with NFP_{ij} which forces the reference point of p_j to be above (below) the reference point of p_i is denoted as U_{ij} (D_{ij}). Analogously, the subset of variables which force the reference point of p_j to be to the right (left) of the reference point of p_i is denoted as R_{ij} (L_{ij}). If $VNFP_{ij}$ is the set of all the variables associated with NFP_{ij}, these sets can be described as follows:

- $U_{ij} := \{b_{ijk} \in VNFP_{ij} \mid \underline{y}_{ijk} \geq 0\}$.
- $D_{ij} := \{b_{ijk} \in VNFP_{ij} \mid \overline{y}_{ijk} \leq 0\}$.
- $R_{ij} := \{b_{ijk} \in VNFP_{ij} \mid \underline{x}_{ijk} \geq 0\}$.
- $L_{ij} := \{b_{ijk} \in VNFP_{ij} \mid \overline{x}_{ijk} \leq 0\}$.

In the example in Figure 2.10, we have: $U_{ij} := \{b_{ij1}, b_{ij2}, b_{ij8}\}$, $D_{ij} := \{b_{ij4}, b_{ij5}, b_{ij6}\}$, $R_{ij} := \{b_{ij6}, b_{ij7}, b_{ij8}\}$, $L_{ij} := \{b_{ij2}, b_{ij3}, b_{ij4}\}$.

2.3.2 Lifted bound constraints

For each piece p_j, the formulations GO and HS1 include four bound constraints, ensuring that the piece does not exceed the left, right, top and bottom limits of the strip. We can lift each of these constraints by considering the variables in sets U_{ij}, D_{ij}, R_{ij}, L_{ij}, for each piece p_i, $i \neq j$.

- *Left-hand side bound*

  In the constraint we include the variables forcing p_j to be to the right of p_i, that is, the variables in R_{ij}. The coefficient of each variable, that is, the forced displacement of p_j to the right of p_i, is given by $\underline{x}_{ijk}$. The lifted constraint will be:

$$x_j \geq \sum_{k \in R_{ij}} \underline{x}_{ijk} b_{ijk} \tag{2.18}$$

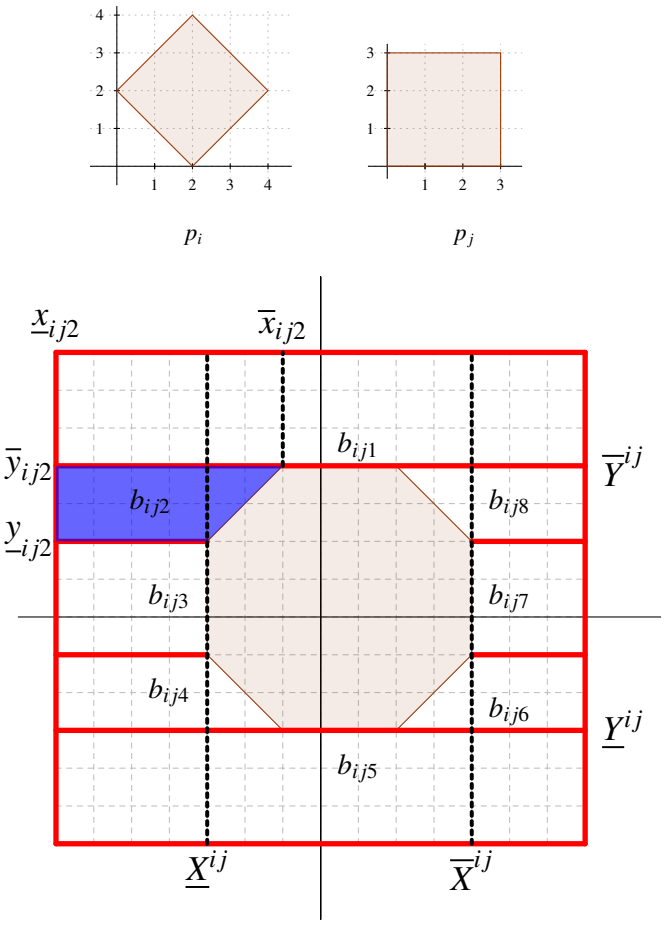

Figure 2.10: *Definitions in the NFP_{ij}-coordinate system*

In Figure 2.10, the constraint will be: $x_j \geq 2b_{ij6} + 4b_{ij7} + 2b_{ij8}$.

- *Right-hand side bound*

  In this case, the variables to be included are those forcing p_j to be to the left of p_i, those in L_{ij}. The corresponding coefficient, the minimum distance from the reference point of p_j to L forced by the variable, is $\lambda_{ijk} = l_i - (\overline{x}_{ijk} - \underline{X}^{ij})$. This value can be seen as the length of piece p_i, l_i, which would be the extra separation if p_j were completely to the right of p_i, minus the maximum amount of parallelism between both pieces which is allowed in slice k, given by $\overline{x}_{ijk} - \underline{X}^{ij}$. Then, the lifted right-hand side bound constraint is:

$$x_j \leq L - l_j - \sum_{k \in LS_{ij}} \underline{\lambda}_{ijk} b_{ijk} \tag{2.19}$$

  where $LS_{ij} := \{k \mid \lambda_{ijk} > 0\}$. In the example in Figure 2.10: $x_j \leq L - 3 - 2b_{ij2} - 4b_{ij3} - 2b_{ij4}$. In slice 3, p_j is completely to the left of p_i and the coefficient of b_{ij3} is 4, corresponding to l_i. In slice 2, 2 units of this initial separation can be eliminated if piece p_j is placed at the rightmost point inside the slice. Then, the coefficient of b_{ij2} is 2.

- Bottom-side bound

  The variables forcing p_j to be above p_i, are those in U_{ij}. The coefficient of each variable, that is, the forced displacement of p_j on top of p_i, is given by $\underline{y}_{ijk}$. The lifted constraint will be:

$$y_j \geq \sum_{k \in U_{ij}} \underline{y}_{ijk} b_{ijk} \tag{2.20}$$

  In the example in Figure 2.10 we have: $y_j \geq 4b_{ij1} + 2b_{ij2} + 2b_{ij8}$.

- Upper-side bound

  The variables to be included are those forcing p_j to be at the bottom of p_i, those of D_{ij}. The corresponding coefficient, the minimum distance from the reference point of p_j to W forced by the variable, is $\mu_{ijk} = w_i - (\overline{y}_{ijk} - \underline{Y}^{ij})$. The constraint will be:

$$y_j \leq W - w_j - \sum_{k \in DS_{ij}} \underline{\mu}_{ijk} b_{ijk} \tag{2.21}$$

  where $DS_{ij} := \{k \mid \mu_{ijk} > 0\}$. In the example in Figure 2.10: $y_j \leq W - w_j - 2b_{ij4} - 4b_{ij5} - 2b_{ij6}$.

2.3.3 Formulation *HS2*

The complete *HS2* formulation is:

$$Min\ L \tag{2.22}$$

$$s.t. \quad \sum_{k\in R_{ij}} \underline{x}_{ijk} b_{ijk} \le x_i \le L - l_i - \sum_{k\in LS_{ij}} \underline{\lambda}_{ijk} b_{ijk} \qquad 1 \le i < j \le N \tag{2.23}$$

$$\sum_{k\in U_{ij}} \underline{y}_{ijk} b_{ijk} \le y_i \le W - w_i - \sum_{k\in DS_{ij}} \underline{\mu}_{ijk} b_{ijk} \qquad 1 \le i < j \le N \tag{2.24}$$

$$\alpha_{ij}^{kf}(x_j - x_i) + \beta_{ij}^{kf}(y_j - y_i) \le \sum_{h=1}^{m_{ij}} \delta_{ij}^{kfh} b_{ijh} \tag{2.25}$$

$$1 \le i < j \le N, \ \ k = 1, ..., m_{ij}, \quad f = 1, ..., t_{ij}^{k} \tag{2.26}$$

$$\sum_{k=1}^{m_{ij}} b_{ijk} = 1 \qquad 1 \le i < j \le N \tag{2.27}$$

$$b_{ijk} \in \{0, 1\} \qquad 1 \le i < j \le N \tag{2.28}$$

$$x_i,\ y_i \ge 0 \qquad 1 \le i \le N \tag{2.29}$$

where constraints (2.23) and (2.24) are the lifted bound constraints which substitute for the initial bound constraints (2.12) and (2.13) of the *HS* 1 formulation.

2.4 Avoiding duplicate solutions

It is quite common in nesting instances that several copies of the same piece type have to be packed or cut. In that case, if these copies are considered as different pieces, the algorithm will have to study partial and complete solutions which are really identical to other solutions already studied elsewhere in the search tree, just changing one piece for another belonging to the same type. In order to partially avoid this unnecessary effort, for each piece type i consisting of n copies of the same piece, we add a set of inequalities to the formulation:

$$x_{i1} \le x_{i2} \le ..... \le x_{in}$$

imposing a left-to-right order in the positioning of these pieces.

2.5 Computational results

In this section we compare the different formulations by solving the instances presented in Section 1.6.2.

For solving the instances, we have used the *Branch & Bound* algorithm given by *CPLEX* 12.2 with 64 *bits*, using just one processor at 3.40 *GHz*. The stopping criterion is the time limit, considering 1 hour of computational time.

In Table 2.1, for each formulation we can see the lower bound (*LB*), the *GAP* calculated as $(UB - LB)/UB$, where UB denotes the upper bound given by *CPLEX*, and the running time in seconds. The last two rows of the table contain the averages and the number of optimal solutions obtained before the time limit.

It can be seen that the formulation *HS2* clearly works better than *GO* and *HS1*, solving 29 instances to optimality and having an average *GAP* of 0.14.

Table 2.1: *Comparing formulations GO, HS1 and HS2*

		GO			*HS1*			*HS2*		
Instance	Pieces	LB	GAP	Time	LB	GAP	Time	LB	GAP	Time
three	3	6.00	0.00	0.02	6.00	0.00	0.22	6.00	0.00	0.75
shapes_4	4	24.00	0.00	0.08	24.00	0.00	0.03	24.00	0.00	0.00
fu_5	5	17.89	0.00	1.40	17.89	0.00	0.94	17.89	0.00	0.14
glass1	5	45.00	0.00	0.02	45.00	0.00	0.05	45.00	0.00	0.06
fu_6	6	23.00	0.00	0.11	23.00	0.00	0.12	23.00	0.00	0.48
threep2	6	9.33	0.00	20	9.33	0.00	3.2	9.33	0.00	3.9
threep2w9	6	8.00	0.00	96.	8.00	0.00	11.4	8.00	0.00	8.5
fu_7	7	24.00	0.00	0.67	24.00	0.00	1.5	24.00	0.00	1.0
glass2	7	45.00	0.00	0.72	45.00	0.00	7.0	45.00	0.00	2.8
fu_8	8	24.00	0.00	0.76	24.00	0.00	2.6	24.00	0.00	1.3
shapes_8	8	25.00	0.04	3600	26.00	0.00	126	26.00	0.00	272
fu_9	9	25.00	0.00	161	25.00	0.00	257	25.00	0.00	70
threep3	9	9.15	0.32	3600	13.53	0.00	2565	13.53	0.00	3394
threep3w9	9	7.00	0.36	3600	8.67	0.22	3600	10.00	0.09	3600
glass3	9	100.00	0.00	2909	100.00	0.00	175	100.00	0.00	324
fu_10	10	28.00	0.02	3600	28.00	0.03	3600	28.68	0.00	3064
dighe2	10	96.27	0.04	3600	100.00	0.00	359	100.00	0.00	177
J1-10-20-0	10	16.00	0.11	3600	18.00	0.00	82	18.00	0.00	45
J1-10-20-1	10	17.00	0.00	442	17.00	0.00	69	17.00	0.00	34
J1-10-20-2	10	20.00	0.00	428	20.00	0.00	124	20.00	0.00	304
J1-10-20-3	10	18.00	0.14	3600	19.00	0.10	3600	20.67	0.00	3600
J1-10-20-4	10	11.00	0.15	3600	12.50	0.00	3413	12.50	0.00	628
J2-10-35-0	10	20.00	0.18	3600	20.25	0.16	3600	23.66	0.00	2858
J2-10-35-1	10	20.00	0.12	3600	20.00	0.11	3600	21.30	0.00	1443
J2-10-35-2	10	18.00	0.10	3600	18.38	0.13	3600	19.95	0.00	452
J2-10-35-3	10	18.00	0.13	3600	20.00	0.03	3600	18.38	0.15	3600
J2-10-35-4	10	18.00	0.08	3600	18.00	0.10	3600	19.43	0.00	2721
J1-12-20-0	12	10.00	0.17	3600	11.56	0.04	3600	12.00	0.00	509
J1-12-20-1	12	9.00	0.18	3600	9.00	0.25	3600	10.00	0.00	2430
J1-12-20-2	12	10.00	0.23	3600	12.00	0.00	22056	12.00	0.00	2332
J1-12-20-3	12	7.00	0.22	3600	7.00	0.22	3600	8.00	0.00	214
J1-12-20-4	12	8.00	0.43	3600	9.01	0.40	3600	12.00	0.14	3600
J2-12-35-0	12	20.25	0.26	3600	20.00	0.35	3600	20.37	0.34	3600
J2-12-35-1	12	17.00	0.35	3600	16.37	0.49	3600	16.91	0.40	3600
J2-12-35-2	12	15.50	0.30	3600	14.00	0.43	3600	15.08	0.34	3600
J2-12-35-3	12	16.00	0.29	3600	16.00	0.30	3600	14.00	0.39	3600
J2-12-35-4	12	18.00	0.26	3600	15.20	0.42	3600	20.00	0.20	3600
fu	12	28.00	0.17	3600	24.00	0.29	3600	24.00	0.29	3600
J1-14-20-0	14	7.00	0.46	3600	10.00	0.33	3600	11.00	0.21	3600
J1-14-20-1	14	6.08	0.49	3600	8.00	0.43	3600	8.00	0.43	3600
J1-14-20-2	14	8.00	0.47	3600	8.30	0.48	3600	10.00	0.36	3600
J1-14-20-3	14	6.25	0.43	3600	7.00	0.42	3600	8.00	0.33	3600
J1-14-20-4	14	8.00	0.47	3600	10.00	0.33	3600	10.00	0.35	3600
J2-14-35-0	14	12.78	0.57	3600	16.67	0.52	3600	19.19	0.45	3600
J2-14-35-1	14	12.00	0.59	3600	14.50	0.59	3600	16.00	0.54	3600
J2-14-35-2	14	13.00	0.48	3600	14.18	0.53	3600	14.00	0.53	3600
J2-14-35-3	14	12.00	0.54	3600	13.00	0.59	3600	15.87	0.50	3600
J2-14-35-4	14	12.00	0.54	3600	14.00	0.50	3600	14.00	0.50	3600
poly1a0	15	13.00	0.21	3600	13.00	0.28	3600	13.00	0.28	3600
dighe1ok	16	56.00	0.58	3600	65.62	0.57	3600	71.00	0.54	3600
Average			**0.21**	2621		**0.19**	2302		**0.14**	1970
#opt			**14**			**20**			**29**	

Table 2.2: *Comparing lower bounds*

	Longest piece	*Area*	*1-CBP*
Average distance (%)	46.08	20.44	9.58

2.6 Lower bounds

There are two obvious lower bounds for the nesting problem. The first one, the length of the longest piece, is already included in the formulation. Another lower bound can be obtained by calculating the area of the pieces, adding them up and dividing this value by W, the strip width. This bound can be easily obtained, but it is usually very loose, except for the artificial *"broken glass"* instances.

A third alternative we have considered is solving a special case of a *1-Contiguous Bin Packing Problem (1-CBPP)*, which was shown to be very effective for the Strip Packing Problem with rectangular pieces (Martello et al. [46] ; Alvarez-Valdes et al. [2]). Each piece is divided into a set of vertical slices of width w. From each slice the maximum embedded rectangle is obtained (see Figure 2.11). The problem is then to pack all these rectangles into the minimum number of levels N, putting the rectangles corresponding to one piece into contiguous levels. The value wN is a lower bound for the original problem. An integer formulation for the *1-CBPP* appears in Alvarez-Valdes et al. [2]. We solve this formulation using CPLEX, with limited time, and obtain the corresponding lower bound.

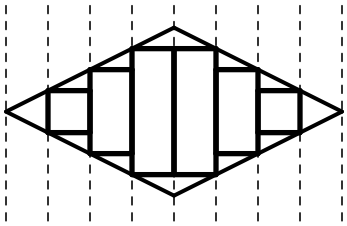

Figure 2.11: *Slicing the piece into rectangles*

Table 2.2 shows the relative performance of the three lower bounds expressed as the average percentage distance from each bound to the optimal or best known solution for each instance in the test set. The *1-CBP* problem associated with each instance has been solved using CPLEX 12.1, with a time limit of 900 seconds. The quality of the area bound is, obviously, much higher than the bound of the longest piece, especially for large instances. The bound based on the 1-CBP problem is much better than the area bound, but its computational cost is sometimes very high and increases with the problem size. Moreover, none of bounds evolve during the search because the integer variables in the formulation do not fix the absolute position of the pieces, but only their relative position. Therefore, we decided not to spend time at the beginning of the algorithm calculating bounds and only the longest piece bound, included in the formulation, is used.

Chapter 3

Branch & Bound algorithms

The *Branch & Bound* algorithm is a well known exact procedure. There are two important elements to analyze in order to build an efficient algorithm: the branching, which studies the way in which we select the binary variables to be set to 0/1 and the order of nodes to be solved; and the cutting, that is, which valid inequalities could be added to the relaxed linear model in order to eliminate unfeasible solutions of the mixed integer model.

The formulations in the previous section can be used in a *Branch & Bound* algorithm in which at each node of the search tree the linear relaxation provides a lower bound and, if the node is not fathomed, branching will consist in building two nodes, one with a variable $b_{ijk} = 1$ and the other with b_{ijk}=0. The initial mixed integer model that we want to solve with a *Branch & Bound* algorithm is the one given by the *HS2* formulation, presented in Section 2.3. In Section 2.5 we saw that the *HS2* formulation provided the best results.

In this chapter we present a study of different ways of branching. We will see that *Branching* is very important because different strategies provide quite different results for a given instance. The study of valid inequalities to be added to the formulation and their corresponding separation procedures are left to chapters 4 and 5 respectively.

The remainder of this chapter is organized in 5 sections. In Section 3.1 different strategies of branching, based on Fischetti and Luzzi priorities [27], are presented. Furthermore, we propose a branching based on giving more priority to the binary variables which define larger *slices*. We also study a dynamic branching scheme in which the decisions of branching are taken depending on the fractional solutions and, finally, a strategy of branching on constraints. In Section 3.1.4 we discuss the computational results obtained by each one of the strategies presented in Section 3.1. As in the previous chapter, we run the *Branch & Bound* algorithm developed by *CPLEX* with a time limit of one hour for each instance.

At each node of the *Branch & Bound* tree there is a subset of binary variables fixed to 1 and another subset fixed to 0. The binary variables fixed to 0 do not guarantee that the pair of pieces which define the corresponding *NFP* do not overlap. On the other hand, if there is a binary variable fixed to 1, we can ensure that the corresponding pair of pieces is completely separated and the relative position is the one defined by the respective *slice*. Then, when a binary variable is fixed to 1, the horizontal and vertical bound constraints of the pieces can be updated because the relative position of the pieces is given by the limits of the *slice* defined by the activated binary variable. In Section 3.2 we propose two different ways of updating the bounds

of the reference points of the pieces.

In an advanced node of the *Branch & Bound* tree there are many pairs of pieces which are separated by fixed binary variables of previous nodes of the same branch. So, it could be that there are non-fixed binary variables which are incompatible with the linear model of the current node. That is, there can be binary variables which, if fixed to 1, make the linear model unfeasible. In Section 3.3 we present two approaches for finding incompatible binary variables. The first approach uses the combination of the bounds on the pieces with the limits of the strip. The idea is to find the binary variables which cannot be activated or otherwise the corresponding *slices* exceed the limits of the strip. The second approach is based on the transitivity of the pieces. If piece i is placed to the left of piece j which, at the same time, is placed to the left of piece k, then all the binary variables of NFP_{ik} which force piece k to be placed to the left of piece i are incompatible binary variables.

Finally, in Section 3.3.3 we discuss the behavior of the previous strategies on the set of test instances and draw some conclusions.

3.1 Branching strategies

One obvious strategy is to leave the integer linear code, in our case CPLEX, to decide the branching variable, using its internal strategy in which some priorities are assigned to the non-integer variables based on the information provided by the linear solution of each node. However, this strategy does not take into account any problem-specific information which could be useful in guiding the search process. Therefore, we study three specific strategies. The first one is based on the branching procedure proposed by Fischetti and Luzzi [27]. Then we consider a dynamic strategy and finally an alternative branching on constraints procedure.

3.1.1 The Fischetti and Luzzi strategy

The strategy followed by Fischetti and Luzzi [27] is first to determine the relative positions of 2 pieces (say A and B), then those of 3 pieces (A, B and, say, C), of 4 pieces (A, B, C and, say, D), and so on. To do that, a simple procedure assigns priorities to the variables in decreasing order, starting from the variables separating A and B, then the variables separating A and C and B and C, then the variables separating A and D, B and D, C and D, and so on. By doing that, they try to avoid the visiting of subtrees that are unfeasible because of inconsistent variable fixings that could have been detected at higher levels in the tree. The procedure is described in Algorithm 1.

Fischetti and Luzzi do not specify any particular order for the pieces. Nevertheless, as their procedure builds an increasingly large clique of non-overlapping pieces (allowing the other pieces to overlap with them and among themselves), it could be interesting to separate large pieces first. If the growing clique is made of large pieces, the lower bound could increase faster than when small pieces are involved. Defining a large piece is not obvious in the case of irregular pieces. Two approximations could be the length and the area of each piece. Therefore, when studying the behavior of the Fischetti and Luzzi branching strategy computationally, we will consider three alternatives:

- ***FL***: Fischetti and Luzzi's priorities without any initial ordering of the pieces
- ***FL_L***: Fischetti and Luzzi's priorities ordering pieces by non-increasing length
- ***FL_A***: Fischetti and Luzzi's priorities ordering pieces by non-increasing area

Algorithm 1 Fischetti and Luzzi's priorities

Require: ψ = number of binary variables;
Require: $S = \emptyset$;
  while $P \neq \emptyset$ **do**
    Select a piece $p_i \in P$;
    for all $p_j \in S$ **do**
      for $k = 1, \ldots, m_{ij}$ **do**
        Assign priority ψ to b_{ijk};
        $\psi = \psi - 1$;
      end for
    end for
    $S = S \cup \{p_i\}$;
    $P = P \backslash \{p_i\}$;
  end while

Even when we specify the order in which the pieces are considered for assigning priorities, there is still a degree of freedom concerning the order in which the variables of the corresponding NFP are considered. One possibility for ordering the variables of an NFP is the area of the corresponding slice, giving more priority to variables associated with larger slices. Then, a fourth strategy to be studied is ***FL_A_SA***, in which we first order the pieces by area and then the variables by the area of the slice. A last strategy in this group could be ***SA***, ordering all the variables according to the area of their slices, but not using Fischetti and Luzzi's priorities.

3.1.2 Dynamic branching (*DB*)

Let us consider the 3-pieces example in Figure 3.1. The pieces are already ordered by some priority criterion and let us suppose that in the first branching level $b_{128} = 1$. That means that p_1 and p_2 are separated and the relative position of p_2 with respect to p_1 is restricted to the corresponding slice. In a static branching strategy, the variable used at the second branching level would be given by a certain predefined criterion. But we can use a dynamic strategy, taking advantage of the information in the solution of the node. In particular, we can take into account the relative position of the pieces and choose a branching variable such that when it is fixed to one, more than two pieces are separated and feasible solutions are obtained faster. In the example, we see that if we branch on variables b_{132}, b_{133}, b_{134}, b_{135} or b_{136} from NFP_{13}, or variables b_{231} y b_{236} from NFP_{23}, the three pieces would be separated and fixing just two variables to value 1 will produce a feasible solution.

We can generalize this idea. Let us consider the pieces ordered by non-increasing value of a given priority criterion. At each node of the search tree, we read the solution and go through the ordered list of pieces until we find a piece p_j overlapping with some of the previous pieces. Let $S = \{p_{i_1}, ..., p_{i_k}\}$ be the set of these pieces, $1 \leq i_1 < .... < i_k$. For each piece $i \in S$, we compute up_i, $down_i$, $left_i$, $right_i$, the number of pieces separated from i from above, from below, from the left and from the right, respectively. We consider that a piece p_k is separated from above piece p_i if there is a variable $b_{ikl} = 1$ for some l, such that $\underline{y}_{ikl} > 0$. Similarly, it is separated from below if $\overline{y}_{ikl} < 0$, to the right if $\underline{x}_{ikl} > 0$ and to the left if $\overline{x}_{ikl} < 0$.

When choosing a variable to separate piece p_j from S, the lower the values of up_i, $down_i$, $left_i$, $right_i$ for some $i \in S$, the more adequate this position is for piece p_j and hence the branching variable should separate p_j from p_i in this direction. For instance, if for some $i \in S$, $up_i = 0$, none of the other pieces in

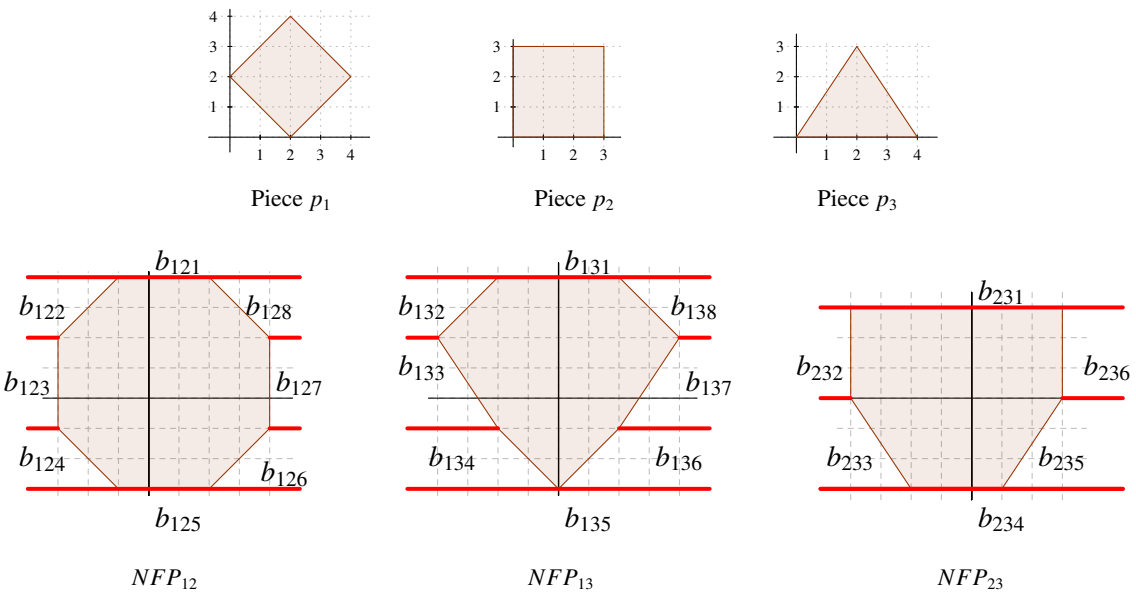

Figure 3.1: *NFP for the example of 3 pieces*

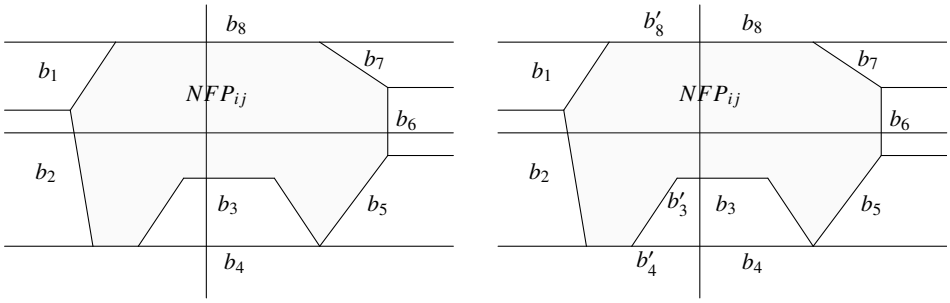

(a) Variables in formulation *HS2*

(b) New variables

Figure 3.2: *Variables for branching on constraints*

S is above p_i and then that would be a good position for p_j. Separating p_j from p_i in this direction could possibly separate p_j from some other pieces in S.

3.1.3 Branching on constraints (*BC*)

An alternative branching strategy is to branch on constraints. In order to do that, we slightly modify the formulation $HS2$ so that all the slices are on one side of the y-axis, which means that some of the slices defined in Section 3.2 are divided into two, as can be seen in Figure 3.2. Associated with the new slices, new variables are defined.

At each node of the search tree we look for a pair of pieces p_i, p_j for which

$$0 < \sum_{k|x_{ijk}\geq 0} b_{ijk} < 1 \tag{3.1}$$

Then, in one of the branches we set $\sum_{k|\underline{x}_{ijk}\geq 0} b_{ijk} = 0$ and in the other $\sum_{k|\underline{x}_{ijk}\geq 0} b_{ijk} = 1$. In the example, one branch would have $b_{ij3}+b_{ij4}+b_{ij5}+b_{ij6}+b_{ij7}+b_{ij8} = 0$ and the other $b_{ij3}+b_{ij4}+b_{ij5}+b_{ij6}+b_{ij7}+b_{ij8} = 1$. If no pair of pieces satisfy (3.1), we branch on variables using strategy ***FL_A***.

One advantage of this branching strategy is that the formulation can be locally enhanced. In the example, if we are in the node in which we have set $b_{ij3} + b_{ij4} + b_{ij5} + b_{ij6} + b_{ij7} + b_{ij8} = 1$, piece p_i must be to the left of piece p_j. Then, constraint $x_i \leq x_j$ is satisfied in all the successor nodes. This constraint can be lifted, considering variables b_{ijk} for which $\underline{x}_{ijk} \geq 0$. The lifted constraint would be:

$$x_i + \sum_{k|\underline{x}_{ijk}\geq 0} \underline{x}_{ijk} b_{ijk} \leq x_j \tag{3.2}$$

In the example, $x_i + 6b_{ij5} + 12b_{ij6} + 6b_{ij7} \leq x_j$.

3.1.4 Computational results for the different branching strategies

In this section we compare the different ways of branching described in the previous section. We have built a *Branch & Cut* algorithm using *CPLEX 12.2* with 64 *bits*, with the default options and just one processor at 3.40 *GHz*. The stopping criterion is the time, considering one hour of computational time.

In Table 3.1 we can find the computational results of the *FL*, *FL_L* and *FL_A* strategies. For each strategy, the columns show the lower bound (LB) obtained for each instance, the GAP=(UB-LB)/UB and the running time. The last two rows show the averages and the number of optimal solutions. There are significant differences between the different methods, so the initial order for the pieces in Fischetti and Luzzi's priorities really matters. We can observe that *FL_A* obtains the best results and the best deviation of the lower bound with respect to the upper bound. The average GAP obtained by *FL_A* is 0.047 and it is able to solve 34 over the 50 instances to optimality.

In Table 3.2 we can observe that if in the *FL_A* strategy we order the *slices* in a non decreasing area, the results are very similar. Furthermore, if we drop Fischetti and Luzzi's priorities but we order the *slices* in a non-decreasing area (*S_A* strategy), we can see that the results are clearly worse, obtaining a deviation average of 0.36.

Table 3.3 presents the comparison between the best strategy at this moment, *FL_A*, with dynamic branching *(DB)* defined in 3.1.2 and the branching on constraints *(BC)*, described in 3.1.3. Note that the results of dynamic branching are slightly worse than the *FL_A* strategy, obtaining an average for the gap of 0.065. On the other hand, branching on constraints obtains bad results.

Finally, Table 3.4 summarizes the comparison between all the branching strategies already described. The performance of each strategy is summarized in three values: the number of optimal solutions, the average GAP and the average CPU time. The strategies compared are:

- CPLEX: the default strategy provided by CPLEX, as shown in the final columns of Table 2.1
- FL: the Fischetti and Luzzi strategy, taking the pieces as they appear in the data file
- FL_L: the Fischetti and Luzzi strategy, ordering the pieces by non-increasing length
- FL_A: the Fischetti and Luzzi strategy, ordering the pieces by non-increasing area

Table 3.1: *Comparing branching strategies **FL**, **FL_L** and **FL_A***

Instances	FL			FL_L			FL_A		
	LB	GAP	Time	LB	GAP	Time	LB	GAP	Time
three	6.00	0.00	0.75	6.00	0.00	0.53	6.00	0.00	0.73
shapes4	24.00	0.00	0.08	24.00	0.00	0.05	24.00	0.00	0.02
fu5	17.89	0.00	0.62	17.89	0.00	0.59	17.89	0.00	0.08
glass1	45.00	0.00	0.06	45.00	0.00	0.02	45.00	0.00	0.02
fu6	23.00	0.00	0.92	23.00	0.00	0.69	23.00	0.00	0.69
threep2	9.33	0.00	1.06	9.33	0.00	1.75	9.33	0.00	1.36
threep2w9	8.00	0.00	5.18	8.00	0.00	4.54	8.00	0.00	7.36
fu7	24.00	0.00	0.86	24.00	0.00	0.66	24.00	0.00	0.62
glass2	45.00	0.00	2.62	45.00	0.00	2.28	45.00	0.00	1.84
fu8	24.00	0.00	0.94	24.00	0.00	0.61	24.00	0.00	0.72
shapes8	26.00	0.00	4.85	26.00	0.00	4.57	26.00	0.00	4.43
fu9	25.00	0.00	124.43	25.00	0.00	12.12	25.00	0.00	32.87
threep3	13.53	0.00	955.26	13.53	0.00	2323.68	13.53	0.00	819.01
threep3w9	11.00	0.00	2344.16	10.33	0.06	3600.00	11.00	0.00	2822.93
glass3	100.00	0.00	1335.54	100.00	0.00	40.05	100.00	0.00	13.74
fu10	28.00	0.02	3600.00	28.69	0.00	2186.18	28.69	0.00	198.59
dighe2	77.82	0.35	3600.00	100.00	0.00	18.02	100.00	0.00	1.64
J1-10-20-0	14.67	0.19	3600.00	18.00	0.00	51.00	18.00	0.00	6.35
J1-10-20-1	11.65	0.35	3600.00	17.00	0.00	36.22	17.00	0.00	3.74
J1-10-20-2	20.00	0.00	2519.21	20.00	0.00	40.47	20.00	0.00	7.71
J1-10-20-3	14.36	0.32	3600.00	20.75	0.00	685.33	20.75	0.00	251.04
J1-10-20-4	9.22	0.29	3600.00	12.50	0.00	257.29	12.50	0.00	89.81
J2-10-35-0	19.80	0.21	3600.00	23.66	0.00	420.81	23.66	0.00	395.12
J2-10-35-1	18.00	0.20	3600.00	21.30	0.00	196.76	21.30	0.00	148.17
J2-10-35-2	19.95	0.00	993.63	19.95	0.00	156.30	19.95	0.00	95.18
J2-10-35-3	17.88	0.16	3600.00	20.38	0.00	1294.96	20.38	0.00	823.05
J2-10-35-4	17.38	0.13	3600.00	19.43	0.00	272.91	19.44	0.00	316.23
J1-12-20-0	10.00	0.17	3600.00	12.00	0.00	115.99	12.00	0.00	32.81
J1-12-20-1	7.00	0.42	3600.00	10.00	0.00	175.94	10.00	0.00	29.73
J1-12-20-2	10.00	0.23	3600.00	12.00	0.00	21.26	12.00	0.00	19.59
J1-12-20-3	7.00	0.22	3600.00	8.00	0.00	16.29	8.00	0.00	28.36
J1-12-20-4	9.00	0.36	3600.00	13.00	0.00	308.35	13.00	0.00	149.06
J2-12-35-0	20.02	0.29	3600.00	25.00	0.11	3600.00	24.50	0.13	3600.00
J2-12-35-1	16.85	0.33	3600.00	22.50	0.08	3600.00	22.00	0.15	3600.00
J2-12-35-2	18.00	0.23	3600.00	18.19	0.20	3600.00	20.00	0.09	3600.00
J2-12-35-3	16.00	0.28	3600.00	19.40	0.17	3600.00	20.00	0.11	3600.00
J2-12-35-4	15.63	0.35	3600.00	22.00	0.08	3600.00	22.00	0.07	3600.00
fu	24.00	0.29	3600.00	28.50	0.16	3600.00	32.11	0.03	3600.00
J1-14-20-0	6.25	0.55	3600.00	12.00	0.08	3600.00	12.00	0.00	446.69
J1-14-20-1	6.00	0.50	3600.00	10.00	0.17	3600.00	11.00	0.06	3600.00
J1-14-20-2	9.00	0.44	3600.00	12.15	0.19	3600.00	13.00	0.13	3600.00
J1-14-20-3	6.00	0.50	3600.00	10.00	0.00	277.20	10.00	0.00	97.81
J1-14-20-4	8.00	0.47	3600.00	13.00	0.10	3600.00	13.50	0.04	3600.00
J2-14-35-0	18.00	0.40	3600.00	24.00	0.21	3600.00	23.70	0.19	3600.00
J2-14-35-1	16.00	0.50	3600.00	21.34	0.31	3600.00	21.88	0.30	3600.00
J2-14-35-2	16.00	0.38	3600.00	18.63	0.31	3600.00	20.00	0.25	3600.00
J2-14-35-3	16.00	0.41	3600.00	20.00	0.23	3600.00	20.12	0.23	3600.00
J2-14-35-4	14.00	0.50	3600.00	19.82	0.24	3600.00	20.00	0.23	3600.00
poly1a0	13.00	0.20	3600.00	13.00	0.21	3600.00	13.00	0.19	3600.00
dighe1ok	74.00	0.48	3600.00	100.00	0.22	3600.00	100.00	0.13	3600.00
Average		**0.21**	**2541.80**		**0.063**	**1474.47**		**0.047**	**1288.94**
#opt	**15**			**32**			**34**		

Table 3.2: *Comparing branching strategies **FL_A**, **FL_A_SA** y **SA***

Instancias	FL_A			FL_A_SA			SA		
	LB	GAP	Time	LB	GAP	Time	LB	GAP	Time
three	6.00	0.00	0.73	6.00	0.00	0.67	6.00	0.00	0.41
shapes4	24.00	0.00	0.02	24.00	0.00	0.05	24.00	0.00	0.31
fu5	17.89	0.00	0.08	17.89	0.00	0.25	17.89	0.00	0.53
glass1	45.00	0.00	0.02	45.00	0.00	0.03	45.00	0.00	0.02
fu6	23.00	0.00	0.69	23.00	0.00	0.28	23.00	0.00	0.69
threep2	9.33	0.00	1.36	9.33	0.00	1.37	9.33	0.00	3.84
threep2w9	8.00	0.00	7.36	8.00	0.00	4.99	8.00	0.00	32.42
fu7	24.00	0.00	0.62	24.00	0.00	1.14	24.00	0.00	2.12
glass2	45.00	0.00	1.84	45.00	0.00	1.93	45.00	0.00	5.80
fu8	24.00	0.00	0.72	24.00	0.00	0.47	24.00	0.00	28.24
shapes8	26.00	0.00	4.43	26.00	0.00	4.87	18.21	0.30	3600.00
fu9	25.00	0.00	32.87	25.00	0.00	33.43	24.00	0.04	3600.00
threep3	13.53	0.00	819.01	13.53	0.00	757.34	9.86	0.34	3600.00
threep3w9	11.00	0.00	2822.93	11.00	0.00	3130.53	7.67	0.32	3600.00
glass3	100.00	0.00	13.74	100.00	0.00	16.36	100.00	0.17	2600.00
fu10	28.69	0.00	198.59	28.69	0.00	209.01	25.45	0.12	3600.00
dighe2	100.00	0.00	1.64	100.00	0.00	7.89	100.00	0.17	3600.00
J1-10-20-0	18.00	0.00	6.35	18.00	0.00	8.88	15.40	0.23	3600.00
J1-10-20-1	17.00	0.00	3.74	17.00	0.00	2.43	15.30	0.10	3600.00
J1-10-20-2	20.00	0.00	7.71	20.00	0.00	7.43	17.20	0.18	3600.00
J1-10-20-3	20.75	0.00	251.04	20.75	0.00	314.83	17.60	0.18	3600.00
J1-10-20-4	12.50	0.00	89.81	12.50	0.00	80.34	10.10	0.28	3600.00
J2-10-35-0	23.66	0.00	395.12	23.67	0.00	368.12	18.06	0.28	3600.00
J2-10-35-1	21.30	0.00	148.17	21.30	0.00	174.83	14.76	0.36	3600.00
J2-10-35-2	19.95	0.00	95.18	19.95	0.00	69.39	14.86	0.32	3600.00
J2-10-35-3	20.38	0.00	823.05	20.38	0.00	785.50	15.29	0.31	3600.00
J2-10-35-4	19.44	0.00	316.23	19.43	0.00	290.88	13.74	0.31	3600.00
J1-12-20-0	12.00	0.00	32.81	12.00	0.00	22.14	10.00	0.23	3600.00
J1-12-20-1	10.00	0.00	29.73	10.00	0.00	21.86	8.90	0.26	3600.00
J1-12-20-2	12.00	0.00	19.59	12.00	0.00	18.89	10.60	0.24	3600.00
J1-12-20-3	8.00	0.00	28.36	8.00	0.00	16.19	7.00	0.18	3600.00
J1-12-20-4	13.00	0.00	149.06	13.00	0.00	169.23	11.10	0.21	3600.00
J2-12-35-0	24.50	0.13	3600.00	24.25	0.13	3600.00	20.06	0.32	3600.00
J2-12-35-1	22.00	0.15	3600.00	22.00	0.15	3600.00	17.83	0.34	3600.00
J2-12-35-2	20.00	0.09	3600.00	20.00	0.09	3600.00	16.20	0.30	3600.00
J2-12-35-3	20.00	0.11	3600.00	20.00	0.13	3600.00	15.91	0.30	3600.00
J2-12-35-4	22.00	0.07	3600.00	22.00	0.07	3600.00	17.54	0.29	3600.00
fu	32.11	0.03	3600.00	32.25	0.04	3600.00	28.50	0.16	3600.00
J1-14-20-0	12.00	0.00	446.69	12.00	0.00	2157.54	10.75	0.28	3600.00
J1-14-20-1	11.00	0.06	3600.00	11.00	0.06	3600.00	10.00	0.23	3600.00
J1-14-20-2	13.00	0.13	3600.00	13.00	0.13	3600.00	12.15	0.29	3600.00
J1-14-20-3	10.00	0.00	97.81	10.00	0.00	420.80	8.80	0.27	3600.00
J1-14-20-4	13.50	0.04	3600.00	13.50	0.07	3600.00	11.95	0.30	3600.00
J2-14-35-0	23.70	0.19	3600.00	23.50	0.22	3600.00	21.54	0.38	3600.00
J2-14-35-1	21.88	0.30	3600.00	21.79	0.26	3600.00	21.34	0.30	3600.00
J2-14-35-2	20.00	0.25	3600.00	20.00	0.23	3600.00	18.63	0.29	3600.00
J2-14-35-3	20.12	0.23	3600.00	20.00	0.24	3600.00	18.83	0.32	3600.00
J2-14-35-4	20.00	0.23	3600.00	20.00	0.23	3600.00	18.97	0.32	3600.00
poly1a0	13.00	0.19	3600.00	13.00	0.19	3600.00	13.00	0.28	3600.00
dighe1ok	100.00	0.13	3600.00	100.00	0.14	3600.00	100.00	0.35	3600.00
Average		**0.047**	**1288.942**		**0.048**	**1333.998**		**0.209**	**2861.487**
#opt	**34**			**34**			**10**		

Table 3.3: *Comparing branching strategies **FL_A**, **DB** y **BC***

Instancias	**FL_A**			**DB**			**BC**		
	LB	GAP	Time	LB	GAP	Time	LB	GAP	Time
three	6.00	0.00	0.73	6.00	0.00	1.00	6.00	0.00	0.42
shapes4	24.00	0.00	0.02	24.00	0.00	0.20	24.00	0.00	0.08
fu5	17.89	0.00	0.08	17.89	0.00	0.51	17.89	0.00	3.62
glass1	45.00	0.00	0.02	45.00	0.00	0.03	45.00	0.00	0.02
fu6	23.00	0.00	0.69	23.00	0.00	0.45	23.00	0.00	1.67
threep2	9.33	0.00	1.36	9.33	0.00	1.70	9.33	0.00	10.00
threep2w9	8.00	0.00	7.36	8.00	0.00	5.44	8.00	0.00	22.79
fu7	24.00	0.00	0.62	24.00	0.00	1.12	24.00	0.00	5.93
glass2	45.00	0.00	1.84	45.00	0.00	3.01	45.00	0.00	42.76
fu8	24.00	0.00	0.72	24.00	0.00	0.67	24.00	0.00	17.94
shapes8	26.00	0.00	4.43	26.00	0.00	4.62	26.00	0.00	817.91
fu9	25.00	0.00	32.87	25.00	0.00	46.47	24.00	0.08	3600.00
threep3	13.53	0.00	819.01	13.53	0.00	852.70	10.87	0.21	3600.00
threep3w9	11.00	0.00	2822.93	11.00	0.00	2834.79	8.00	0.29	3600.00
glass3	100.00	0.00	13.74	100.00	0.00	31.11	100.00	0.26	3600.00
fu10	28.69	0.00	198.59	28.69	0.00	345.54	25.45	0.15	3600.00
dighe2	100.00	0.00	1.64	100.00	0.00	11.47	100.00	0.17	3600.00
J1-10-20-0	18.00	0.00	6.35	18.00	0.00	8.41	15.40	0.19	3600.00
J1-10-20-1	17.00	0.00	3.74	17.00	0.00	6.68	15.30	0.15	3600.00
J1-10-20-2	20.00	0.00	7.71	20.00	0.00	6.86	17.20	0.14	3600.00
J1-10-20-3	20.75	0.00	251.04	20.75	0.00	386.62	17.60	0.20	3600.00
J1-10-20-4	12.50	0.00	89.81	12.50	0.00	128.45	10.10	0.28	3600.00
J2-10-35-0	23.66	0.00	395.12	23.66	0.00	883.76	18.06	0.31	3600.00
J2-10-35-1	21.30	0.00	148.17	21.30	0.00	210.37	16.00	0.31	3600.00
J2-10-35-2	19.95	0.00	95.18	19.95	0.00	175.33	14.90	0.33	3600.00
J2-10-35-3	20.38	0.00	823.05	20.37	0.00	1081.21	15.29	0.31	3600.00
J2-10-35-4	19.44	0.00	316.23	19.43	0.00	389.47	13.74	0.35	3600.00
J1-12-20-0	12.00	0.00	32.81	12.00	0.00	54.40	10.00	0.23	3600.00
J1-12-20-1	10.00	0.00	29.73	10.00	0.00	63.12	8.90	0.26	3600.00
J1-12-20-2	12.00	0.00	19.59	12.00	0.00	53.06	10.60	0.26	3600.00
J1-12-20-3	8.00	0.00	28.36	8.00	0.00	86.63	7.00	0.22	3600.00
J1-12-20-4	13.00	0.00	149.06	13.00	0.00	466.86	11.10	0.28	3600.00
J2-12-35-0	24.50	0.13	3600.00	24.00	0.14	3600.00	20.06	0.35	3600.00
J2-12-35-1	22.00	0.15	3600.00	22.00	0.13	3600.00	17.83	0.41	3600.00
J2-12-35-2	20.00	0.09	3600.00	19.75	0.18	3600.00	16.20	0.38	3600.00
J2-12-35-3	20.00	0.11	3600.00	19.50	0.19	3600.00	15.91	0.39	3600.00
J2-12-35-4	22.00	0.07	3600.00	21.38	0.13	3600.00	17.54	0.36	3600.00
fu	32.11	0.03	3600.00	31.67	0.07	3600.00	28.50	0.16	3600.00
J1-14-20-0	12.00	0.00	446.69	12.00	0.00	949.36	10.75	0.28	3600.00
J1-14-20-1	11.00	0.06	3600.00	11.00	0.08	3600.00	10.00	0.23	3600.00
J1-14-20-2	13.00	0.13	3600.00	12.50	0.18	3600.00	12.15	0.29	3600.00
J1-14-20-3	10.00	0.00	97.81	10.00	0.00	381.16	8.80	0.27	3600.00
J1-14-20-4	13.50	0.04	3600.00	12.33	0.23	3600.00	11.95	0.34	3600.00
J2-14-35-0	23.70	0.19	3600.00	22.47	0.28	3600.00	21.54	0.38	3600.00
J2-14-35-1	21.88	0.30	3600.00	21.34	0.29	3600.00	21.34	0.38	3600.00
J2-14-35-2	20.00	0.25	3600.00	19.25	0.24	3600.00	18.63	0.38	3600.00
J2-14-35-3	20.12	0.23	3600.00	20.00	0.23	3600.00	18.83	0.41	3600.00
J2-14-35-4	20.00	0.23	3600.00	20.00	0.23	3600.00	18.97	0.32	3600.00
poly1a0	13.00	0.19	3600.00	13.00	0.28	3600.00	13.00	0.28	3600.00
dighe1ok	100.00	0.13	3600.00	100.00	0.35	3600.00	100.00	0.35	3600.00
Average		**0.047**	**1288.942**		**0.065**	**1341.452**		**0.219**	**2826.463**
#opt	**34**			**34**			**11**		

Table 3.4: *Comparing branching strategies*

Strategy	Optimal solutions	Average GAP	Average Time
CPLEX	28	0.15	2003
FL	15	0.22	2542
FL_L	31	0.07	1475
FL_A	34	0.05	1289
FL_A_SA	33	0.05	1334
SA	10	0.36	2861
DB	33	0.07	1341
BC	11	0.35	2826

- FL_A_SA: the Fischetti and Luzzi strategy, ordering the pieces by non-increasing area and the variables of each NFP by non-increasing area of the corresponding slice
- SA : ordering the variables by non-increasing area of the corresponding slice
- DB: dynamic branching
- BC: branching on constraints

In summary, we can say that the Fischetti and Luzzi strategy works very well, but only if the pieces have been previously ordered by length or, even better, by area. Doing that, the first pieces to be separated are the largest ones and the lower bounds increase sharply. The table also shows that adding the ordering of variables by slice area to the previous strategy neither harms nor improves the algorithm and it is very poor when used alone. Dynamic branching works quite well. Its slightly worse results are due to the fact that it needs to read the solution at each node, which slows down the search and many fewer nodes are explored. Nevertheless, the strategy seems promising for a more complex algorithm in which the solution at each node has to be read, for instance in a Branch and Cut procedure in which the separation algorithms run at each node require the current solution. Branching on constraints performs quite poorly. It seems clear that only fixing a variable to 1, separating at least two pieces, has a strong effect on the current solution. When branching on constraints, this effect is missing and the results are much worse.

3.2 Updating the bounds on the pieces

When variables are fixed to 1, the relative position of the pieces is constrained and the lower and upper bounds of the pieces can be updated. We have developed two methods: *Method 1* uses the non-overlapping constraints and is an exact and exhaustive approach to updating the bounds on the pieces; *Method 2* uses the concept of *extended slices* in order to make the process of updating the bounds on the pieces easier and faster, but it is not exact, that is, the bounds could be more accurate.

At the beginning, in the root node, the lower and the upper bounds on the reference point of the pieces are given by the width, W, and an upper bound of the length of the strip, L_{ub}. We denote by UX_i (LX_i) to the upper (lower) bound on x_i, and UY_i (LY_i) represents the upper (lower) bound on y_i. In Figure 3.3 we can observe the bounds of piece i at the root node, which are $LX_i = LY_i = 0$, $UY_i = 4$ and $UX_i = 5$. In the root node, the lower bounds always are 0 for all the pieces because of our definition for the reference point.

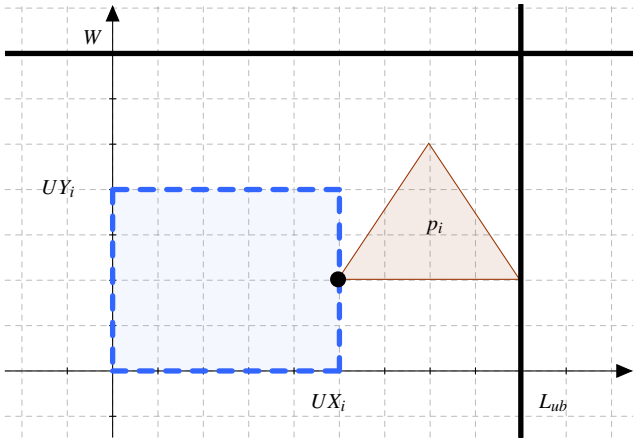

Figure 3.3: *Initial bounds on piece i*

3.2.1 Method I

Let us suppose that a binary variable $b_{ijk} \in NFP_{ij}$ is fixed to 1. This binary variable has f_{ij}^{k} inequalities associated to it corresponding to the non-overlapping constraints defined in the *HS2* formulation used for describing the *slice*. These inequalities have the following structure:

$$\alpha_{ij}^{kf}(x_j - x_i) + \beta_{ij}^{kf}(y_j - y_i) \leq \delta_{ij}^{kfk} b_{ijk} + \sum_{h=1, h\neq k}^{m_{ij}} \delta_{ij}^{kfh} b_{ijh} \tag{3.3}$$

where $\sum_{h=1,h\neq k}^{m_{ij}} \delta_{ij}^{kfh} b_{ijh} = 0$ since $b_{ijk} = 1$.

Let us consider the case in which $\alpha_{ij}^{kf} > 0$ and $\beta_{ij}^{kf} > 0$. The other cases are solved using similar arguments. Constraint (3.3) can be written as:

$$\alpha_{ij}^{kf} x_j \leq \beta_{ij}^{kf} y_i - \beta_{ij}^{kf} y_j + \alpha_{ij}^{kf} x_i + \delta_{ij}^{kfk}. \tag{3.4}$$

The maximum value the right hand side can attain is $\beta_{ij}^{kf} UY_i - \beta_{ij}^{kf} LY_j + \alpha_{ij}^{kf} UX_i + \delta_{ij}^{kfk}$ (where U stands for upper bound and L for lower bound). Then

$$x_j \leq \frac{\beta_{ij}^{kf} UY_i - \beta_{ij}^{kf} LY_j + \alpha_{ij}^{kf} UX_i + \delta_{ij}^{kfk}}{\alpha_{ij}^{kf}}$$

and

$$UX_j = \min\{UX_j, \frac{\beta_{ij}^{kf} UY_i - \beta_{ij}^{kf} LY_j + \alpha_{ij}^{kf} UX_i + \delta_{ij}^{kfk}}{\alpha_{ij}^{kf}}\}$$

In a similar way, the upper bound on y_i can be updated. The lower bounds on x_j and y_j do not need to be updated because they have positive coefficients and the minimum value is 0 in both cases.

On the other hand, it is important to update the lower bounds for the real variables which have a negative coefficient, x_i and y_i. In what follows we explain how we update the lower bound on y_i. Note that x_j and y_j have positive coefficients. Therefore, we substitute these variables with their respective lower bounds, and we assign to variable x_i the maximum value that it can attain, obtaining the following inequality:

$$\beta_{ij}^{kf} y_i \geq \alpha_{ij}^{kf} LX_j + \beta_{ij}^{kf} LY_j - \alpha_{ij}^{kf} UX_i - \delta_{ij}^{kfk},$$

and LY_i can be updated in the following way:

$$LY_i = \max\{LY_i, \frac{\alpha_{ij}^{kf} LX_j + \beta_{ij}^{kf} LY_j - \alpha_{ij}^{kf} UX_i - \delta_{ij}^{kfk}}{\beta_{ij}^{kf}}\}.$$

In Figure 3.4 we can see an example where *slice* defined by b_{ijk} is activated. Piece i is the triangle represented in Figure 3.3 and piece j is a square. This *slice* is the one defined by variable b_{233} in Figure 3.1. When this *slice* is used then piece i has to be placed to the left of piece j, then the lower bounds of piece j, LX_j and LY_j, and the upper bounds of piece i, LX_i and LY_i, can be updated.

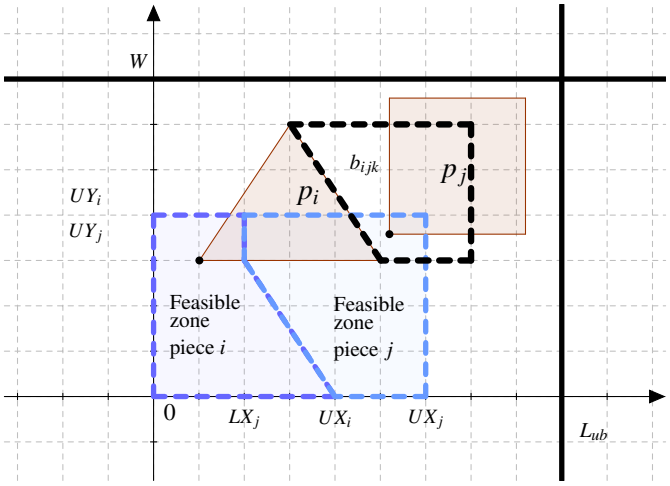

Figure 3.4: *Feasible zone to arrange p_i and p_j when slice defined by b_{ijk} is activated.*

Both methods are used in an iterative way, going through the list of pieces until no bounds are updated. The second method is less accurate, because the extended slice may allow overlapping and the calculated bounds are looser, but it is very fast because the values x_{min}, x_{max}, y_{min}, y_{max} are calculated just once, when NFP_{ij} is built.

3.2.2 Method II

Let us consider a pair of pieces p_i and p_j and one slice S_{ijk} associated with a binary variable b_{ijk}. We define the *extended slice* S^*_{ijk} as the minimum rectangle enclosing S_{ijk}. Let us denote the minimum and maximum coordinates of S^*_{ijk} by x_{min}, x_{max}, y_{min}, y_{max}. Then, if $b_{ijk} = 1$, the bounds for piece p_j can be updated as follows (see Figure 3.5):

- $LX_j = max\{LX_j, LX_i + x_{min}\}$
- $UX_j = min\{UX_j, UX_i + x_{max}\}$
- $LY_j = max\{LY_j, LY_i + y_{min}\}$
- $UY_j = min\{UY_j, UY_i + y_{max}\}$

Analogously, the bounds for piece p_i are:

- $LX_i = max\{LX_i, LX_j - x_{max}\}$
- $UX_i = min\{UX_i, UX_j - x_{min}\}$
- $LY_i = max\{LY_i, LY_j - y_{max}\}$
- $UY_i = min\{UY_i, UY_j - y_{min}\}$

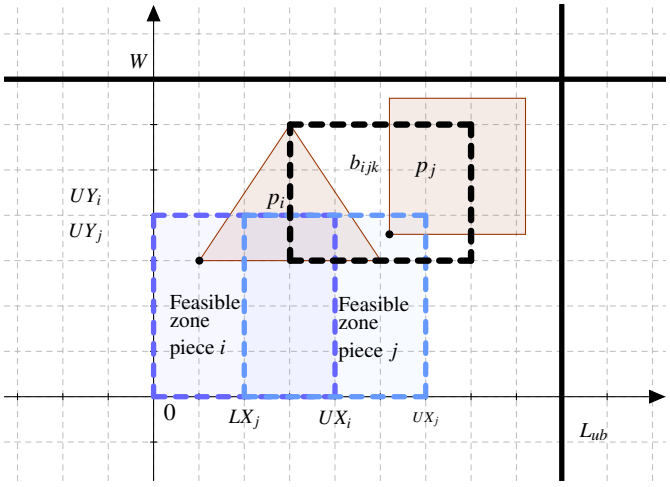

Figure 3.5: *Feasible zones to arrange p_i and p_j using extended slices when slice S_{ijk} is activated.*

3.3 Finding incompatible variables

At each node of the tree we study whether some of the variables not yet fixed cannot take value 1, because that would produce an unfeasible solution. These variables are called *incompatible*. In this case, the variable can be fixed to 0, reducing the size of the problems to be solved in successor nodes and focusing the search on variables which really can take value 1.

In this section we present two approaches to checking if there are incompatible binary variables in a given node created by branching a new variable to 1. The first approach uses the bounds on the pieces and the second approach uses the transitivity of the separated pieces.

3.3.1 Incompatibility using the bounds on the pieces

This way of fixing variables is based on using the *extended slices* defined in the previous section. For each pair of pieces p_i and p_j and each variable b_{ijk}, we suppose $b_{ijk} = 1$ and update the bounds. If an upper bound is lower than the corresponding lower bound, b_{ijk} can be fixed to 0. We use the same notation as the one described in Section 3.2.

Let $S^*_{ijk} = \{(xmin, ymin), (xmax, ymax)\}$ be the *extended slice* defined from b_{ijk}. If one of the following conditions holds, then b_{ijk} is incompatible and can be fixed to 0.

- $xmin + LX_i > UX_j$
- $xmax + UX_i < LX_j$
- $ymin + LY_i > UY_j$
- $ymax + UY_i < LY_j$

Note that the left-hand side of each one of the previous inequalities matches with Method 2 for updating the bounds of piece j (see Section 3.2.2). A similar argument can be applied to obtaining the conditions on piece i.

3.3.2 Incompatibility using the transitivity of the pieces

Let us consider three pieces, p_i, p_j and p_k and let b_{ij1}, b_{ik1}, b_{jk1} be one variable of each non-fit polygon. A sufficient condition for these three variables to be incompatible is that one of these cases is satisfied:

1. $x^{ik1}_{min} > x^{ij1}_{max} + x^{jk1}_{max}$
2. $x^{ik1}_{max} < x^{ij1}_{min} + x^{jk1}_{min}$
3. $y^{ik1}_{min} > y^{ij1}_{max} + y^{jk1}_{max}$
4. $y^{ik1}_{max} < y^{ij1}_{min} + y^{jk1}_{min}$

We consider the extended slices associated with the three variables. One the one hand, if $b_{ij1} = 1$, piece p_j must have its reference point inside $S^*_{ij1} = \{(x^{ij1}_{min}, y^{ij1}_{min}), (x^{ij1}_{max}, y^{ij1}_{max})\}$. If also $b_{jk1} = 1$, in the same coordinate system (with respect to p_i), the possible positions for the reference point of p_k are obtained by considering, for each point in S^*_{ij1}, the points in S^*_{jk1}, that is, all the points in the rectangle $S^*_{ij1,jk1} = \{(x^{ij1}_{min} + x^{jk1}_{min}, y^{ij1}_{min} + y^{jk1}_{min}), (x^{ij1}_{max} + x^{jk1}_{max}, y^{ij1}_{max} + y^{jk1}_{max})\}$. On the other hand, if $b_{ik1} = 1$, the reference point of p_k must be in $S^*_{ik1} = \{(x^{ik1}_{min}, y^{ik1}_{min}), (x^{ik1}_{max}, y^{ik1}_{max})\}$. Therefore, for the 3 variables taking value 1 simultaneously, $S^*_{ij1,jk1}$ and S^*_{ik1} must intersect and none of the above conditions may hold.

Let us consider the following example. In Figure 3.6 we can see three pieces from instance *shapes8*. The respective *NFP*s and the binary variables are represented in Figure 3.7. If we assume that b_{122} is fixed to one in a given node, then the reference point of p_2 must be placed, with respect to p_1, in S^*_{122}, represented in Figure 3.8. Since S_{122} is rectangular, then $S^*_{122} = S_{122}$. Furthermore, let us suppose that b_{236} is fixed to 1. Then, the possible positions for the reference point of p_3 are obtained by considering, for each point in S^*_{122}, the points in S^*_{236}, that is, all the points in the rectangle $S^*_{122,236}$, the green rectangle at the bottom of Figure 3.10.

Let us now consider NFP_{13}. Variables of NFP_{13} can take the value 1 if they allow piece p_3 to be placed in the rectangle defined by $S^*_{122,236}$. In Figure 3.10 we can see the case in which $b_{236} = 1$. The feasible zone to place p_3 with respect to p_1 is given by S_{138}. In this case, $S_{138} \subsetneq S^*_{138}$ because the *slice* is not rectangular. We can observe that S^*_{138} does not intersect with $S^*_{122,236}$. Then, if in a given node of the *Branch & Bound* tree variables, b_{122} and b_{138} are fixed to 1, then b_{236} can be fixed to 0. In a similar way, we can fix variables $b_{231}, b_{232}, b_{233}, b_{234}$ and b_{235} from $VNFP_{23}$ to 0.

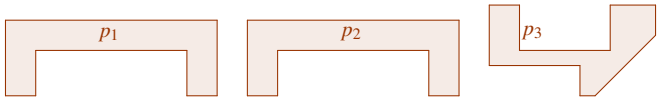

Figure 3.6: *Three pieces from instance shapes8.*

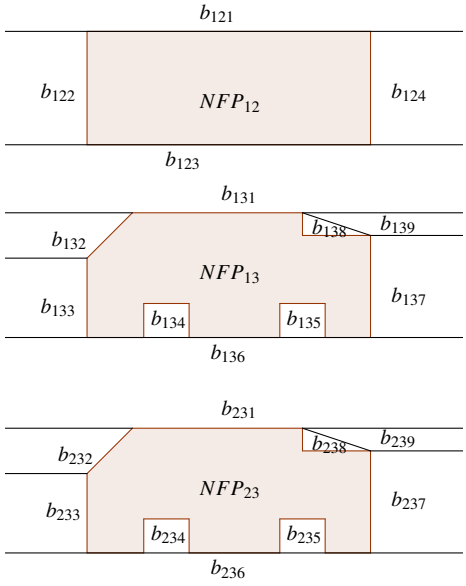

Figure 3.7: *NFPs from pieces represented in Figure 3.6.*

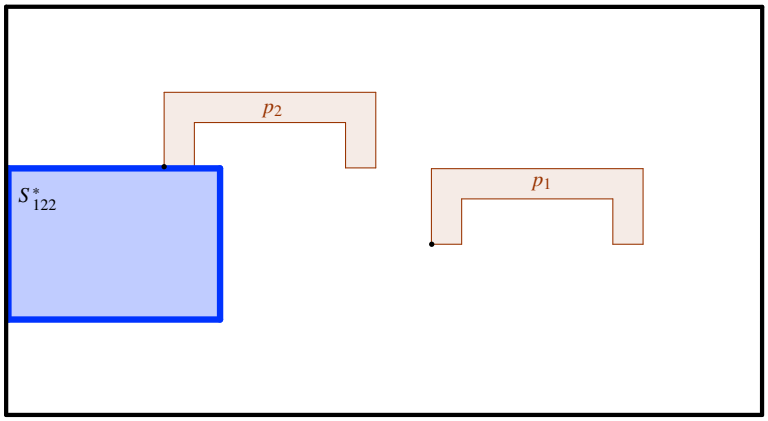

Figure 3.8: *If $b_{122} = 1$ then the reference point of p_2 must be placed in the rectangle.*

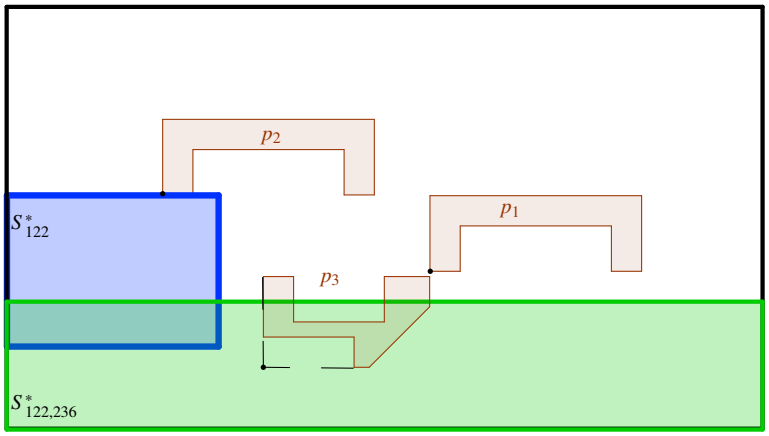

Figure 3.9: *If $b_{122} = 1$ and $b_{238} = 1$, then the reference points of p_2 and p_3 must be placed in their corresponding rectangles.*

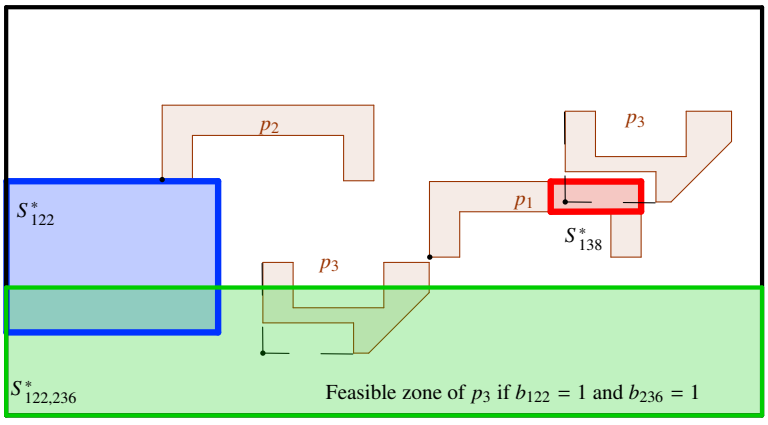

Figure 3.10: *If $b_{122} = b_{138} = b_{236} = 1$, then the reference point of p_3 should be placed in the rectangles defined by variables b_{138} and b_{236}, but it is impossible because they have no intersection.*

Table 3.5: *Comparing strategies for updating bounds and fixing variables: Solved instances*

	Initial	*Strategy 1*	*Strategy 2*	*Strategy 3*	*Strategy 4*
Average Nodes (thousands)	417	345	367	403	353
Average Time (seconds)	131	283	238	140	230

3.3.3 Computational results of the strategies for updating bounds and finding incompatible variables

Tables 3.5 and 3.6 show the effect on the performance of the algorithm of updating bounds and fixing variables as described in Sections 3.2 and 3.3. Table 3.5 focuses on the 34 instances solved to optimality and therefore the information of interest is the number of nodes and the running times. Table 3.6 contains the relevant information for the 16 instances that could not be solved to optimality within the limit of 3600 seconds, the GAP between the lower and the upper bounds and the value of the lower bound. In each table, we compare the results obtained by the Initial strategy (column 2), without updating bounds and fixing variables, with several strategies developed for implementing these procedures.

In Section 3.2 two methods for updating bounds on variables were developed. Method 1, using the non-overlapping constraints, is exact but much slower. Method 2, based on the extended slices, is slightly inexact but faster. A preliminary computational comparison between them clearly showed that the second method performed much better for the same time limit. Therefore, Method 2 is used. The first natural strategy was to update bounds at each node in which a variable had been fixed to 1 and then to try to fix variables for all the variables not yet fixed in the problem. The results of this Strategy 1 appear in column 3. Using these procedures for all the variables in all the nodes in which a variable has been fixed to 1 has a positive effect in reducing the number of nodes to be explored, but the required computational effort slows down the algorithm. In Table 3.5 we observe a significant reduction in the number of nodes, but the running time is more than doubled. In Table 3.6, with a time limit, the results are worse than the initial ones in terms of GAP and lower bound. Therefore, it seemed necessary to modify the strategy to reduce the computational effort of these procedures. Column 4 shows the results of Strategy 2 when not all the variables but only those strictly positive in the solution are considered for fixing. The results improve on those of the previous strategy in terms of computing time, though the reduction of nodes is not so sharp, but they are still worse than the initial ones. A further way of reducing the computational burden is not using the procedures at every node in which one variable is fixed to 1, but only in some nodes, allowing the solution to be changed more profoundly before using them again. That can be done in two ways: calling the procedures after a given number of nodes, n', for instance after every $n' = 5$, $n' = 10$ or $n' = 25$ nodes, or calling them when, in the branch to which the node belongs, a given number of variables has been fixed to 1 from the last call, t', for instance $t' = 3$ or $t' = 5$ variables. Both alternatives have been tested for the values mentioned. In Tables 3.7 and 3.8 we can see the general results of those alternatives, but the results obtained for 10 nodes (Strategy 3 in Table 3.5 and 3.6) and for 3 variables (Strategy 4 in Table 3.5 and 3.6) seem to be the best alternative. For the instances solved, there is a small reduction in the number of nodes and a slight increase in the running time. Therefore, its results are very similar to those of the Initial strategy. For the unsolved instances, the results are slightly better, decreasing the GAP and increasing the lower bound. In summary, updating bounds and fixing variables to 0 have a positive effect only if the computational effort involved is carefully balanced with their advantages in terms of reducing the size of the problem to be solved in successor nodes. According to our results, these procedure should be used every 10 nodes in which a variable has been fixed to 1 and only for variables which are strictly positive.

Table 3.6: *Comparing strategies for updating bounds and fixing variables: Unsolved instances*

	Initial	*Strategy 1*	*Strategy 2*	*Strategy 3*	*Strategy 4*
Average GAP (%)	15.9	19.3	17.5	15.4	19.0
Average LB	25.14	24.42	24.60	25.18	24.48

3.4 Results of the complete algorithm

Summarizing the results obtained in the previous subsections, the best components and strategies for the Branch and Bound algorithm are:

- Formulation: HS2 (horizontal slices, with lifted bound constraints, Section 2.3.3)
- Lower bounds on L: only the trivial bound of the length of the longest piece
- Branching strategy: Fischetti and Luzzi priorities, ordering the pieces by non-decreasing area (Section 3.1.1)
- Updating bounds and fixing variables to 0: every 10 nodes in which a variable has been fixed to 1, and only considering variables with strictly positive values (Sections 3.2.2-3.3.2)

The complete results of the final version of the exact algorithm appear in Tables 3.9 and 3.10, separating its behavior for instances solved to optimality within the initial time limit of 3600 seconds from those not solved in that time. In Table 3.9, for each instance solved to optimality, we show the optimal solution, number of nodes in the tree and running time. In Table 3.10 we allow the algorithm to run much longer in order to study its evolution for harder problems and show the lower and upper bounds obtained at each milestone (1 hour, 2 hours, 5 hours, 10 hours). The last two columns show the total running time if the instance has been solved to optimality, and the optimal solution if it is known. If this not the case, the value corresponds to the best known solution and is marked with an asterisk.

The results of these two tables indicate that our branch and bound procedure is able to solve optimally all the instances with up to 10 pieces, most of those with 12 pieces and some of those with 14 pieces. Even for the solved instances, there are large differences in terms of the number of nodes in the search tree and running times. For example, instances *threep*3 and *threep*3*w*9 have the same pieces and only differ in the strip width, 7 and 9 respectively, but this small increase results in a very large increase in the solution time. Comparing sets $J1$ and $J2$, we can observe that instances derived from $J1$ are much easier than those derived from $J2$. Pieces in $J1$ are more regular and fit together more nicely, while pieces in $J2$ are more irregular and there are always large amounts of waste between them (see Section 1.6). Table 3.10 shows that long runs for instances $J2$ with 12 pieces can obtain if not optimal, then solutions which are at least very close to optimality, while for instances of the same set with 14 instances, even for long runs the gaps between lower and upper bounds do not close.

In summary, even for the moderate number of pieces of the instances tested, our integer formulation, based on assigning variables to regions derived from the edges of the non-fit-polygons, involves a large set of binary variables. Good branching strategies and reduction procedures, plus the power of the latest version of CPLEX, are not enough to speed up the search process and ensure an optimal solution for medium size problems. The optimal solutions for the tested instances appear in Section 1.6.2. When optimality has not been reached, the figure indicates that it corresponds to an upper bound.

Table 3.7: *Comparing the effect of studying every* 5, 10 *and* 25 *nodes in which a variable is fixed to* 1

Instancias	*FL_A II* with $n' = 5$			*FL_A II* with $n' = 10$			*FL_A II* with $n' = 25$		
	LB	GAP	Time	LB	GAP	Time	LB	GAP	Time
three	6.00	0.000	0.61	6.00	0.000	0.92	6.00	0.000	0.45
shapes4	24.00	0.000	0.45	24.00	0.000	0.06	24.00	0.000	0.06
fu5	17.89	0.000	0.36	17.89	0.000	0.47	17.89	0.000	0.23
glass1	45.00	0.000	0.02	45.00	0.000	0.05	45.00	0.000	0.05
fu6	23.00	0.000	0.59	23.00	0.000	0.22	23.00	0.000	0.69
threep2	9.33	0.000	1.40	9.33	0.000	1.75	9.33	0.000	1.70
threep2w9	8.00	0.000	5.58	8.00	0.000	6.19	8.00	0.000	4.41
fu7	24.00	0.000	0.66	24.00	0.000	0.76	24.00	0.000	0.37
glass2	45.00	0.000	2.06	45.00	0.000	1.83	45.00	0.000	2.25
fu8	24.00	0.000	0.94	24.00	0.000	1.40	24.00	0.000	0.30
shapes8	26.00	0.000	4.80	26.00	0.000	4.77	26.00	0.000	5.05
fu9	25.00	0.000	40.65	25.00	0.000	32.28	25.00	0.000	35.26
threep3	13.53	0.000	886.16	13.53	0.000	834.68	13.53	0.000	927.71
threep3w9	11.00	0.000	3500.96	11.00	0.000	3223.73	11.00	0.000	3638.29
glass3	100.00	0.000	15.57	100.00	0.000	29.81	100.00	0.000	28.81
fu10	28.69	0.000	260.04	28.69	0.000	231.43	28.69	0.000	241.44
dighe2	100.00	0.000	1.64	100.00	0.000	1.53	100.00	0.000	1.48
J1-10-20-0	18.00	0.000	6.88	18.00	0.000	6.44	18.00	0.000	5.85
J1-10-20-1	17.00	0.000	5.16	17.00	0.000	4.27	17.00	0.000	6.29
J1-10-20-2	20.00	0.000	7.91	20.00	0.000	9.56	20.00	0.000	8.52
J1-10-20-3	20.75	0.000	301.38	20.75	0.000	299.52	20.75	0.000	308.52
J1-10-20-4	12.50	0.000	89.70	12.50	0.000	67.72	12.50	0.000	96.02
J2-10-35-0	23.66	0.000	421.03	23.66	0.000	554.30	23.66	0.000	522.87
J2-10-35-1	21.30	0.000	170.65	21.30	0.000	112.54	21.30	0.000	175.83
J2-10-35-2	19.95	0.000	114.21	19.95	0.000	107.67	19.95	0.000	118.31
J2-10-35-3	20.38	0.000	988.24	20.37	0.000	971.67	20.37	0.000	1045.52
J2-10-35-4	19.44	0.000	383.28	19.44	0.000	398.21	19.43	0.000	437.40
J1-12-20-0	12.00	0.000	24.30	12.00	0.000	18.72	12.00	0.000	25.88
J1-12-20-1	10.00	0.000	51.57	10.00	0.000	106.31	10.00	0.000	81.14
J1-12-20-2	12.00	0.000	15.91	12.00	0.000	19.19	12.00	0.000	13.32
J1-12-20-3	8.00	0.000	24.21	8.00	0.000	16.41	8.00	0.000	20.65
J1-12-20-4	13.00	0.000	209.91	13.00	0.000	202.91	13.00	0.000	192.18
J2-12-35-0	24.25	0.134	3600.00	24.25	0.134	3600.00	24.00	0.143	3600.00
J2-12-35-1	22.00	0.153	3600.00	22.00	0.112	3600.00	22.00	0.154	3600.00
J2-12-35-2	20.00	0.091	3600.00	20.00	0.103	3600.00	20.00	0.121	3600.00
J2-12-35-3	20.00	0.124	3600.00	20.00	0.111	3600.00	20.00	0.130	3600.00
J2-12-35-4	22.00	0.083	3600.00	21.88	0.098	3600.00	22.00	0.087	3600.00
fu	32.16	0.030	3600.00	32.00	0.055	3600.00	31.67	0.069	3600.00
J1-14-20-0	12.00	0.000	911.87	12.00	0.000	629.95	12.00	0.000	323.81
J1-14-20-1	11.00	0.057	3600.00	11.00	0.057	3600.00	11.00	0.057	3600.00
J1-14-20-2	13.00	0.133	3600.00	13.00	0.133	3600.00	13.00	0.133	3600.00
J1-14-20-3	10.00	0.000	1018.53	10.00	0.000	52.48	10.00	0.000	233.36
J1-14-20-4	13.00	0.133	3600.00	13.33	0.111	3600.00	13.25	0.117	3600.00
J2-14-35-0	23.52	0.231	3600.00	23.50	0.235	3600.00	23.40	0.220	3600.00
J2-14-35-1	21.74	0.313	3600.00	21.50	0.295	3600.00	21.70	0.285	3600.00
J2-14-35-2	20.00	0.231	3600.00	20.00	0.259	3600.00	20.00	0.259	3600.00
J2-14-35-3	20.00	0.231	3600.00	20.00	0.231	3600.00	20.00	0.231	3600.00
J2-14-35-4	20.00	0.230	3600.00	20.00	0.231	3600.00	20.00	0.193	3600.00
poly1a0	13.00	0.235	3600.00	13.00	0.218	3600.00	13.00	0.187	3600.00
dighe1ok	100.00	0.346	3600.00	100.00	0.207	3600.00	100.00	0.222	3600.00
Average		**0.055**	**1341.34**		**0.052**	**1311.00**		**0.052**	**1322.08**
#OPT	**34**			**34**			**34**		

Table 3.8: *Comparing the effect of studying the nodes when the number of variables fixed to* 1 *is a multiple of* 3 *and* 5

Instances	*FL_A II* with $t' = 3$			*FL_A II* with $t' = 5$		
	LB	GAP	Tiempo	LB	GAP	Tiempo
three	6.00	0.000	0.66	6.00	0.000	0.58
shapes4	24.00	0.000	0.03	24.00	0.000	0.05
fu5	17.89	0.000	0.53	17.89	0.000	0.17
glass1	45.00	0.000	0.05	45.00	0.000	0.03
fu6	23.00	0.000	1.12	23.00	0.000	1.00
threep2	9.33	0.000	1.33	9.33	0.000	1.48
threep2w9	8.00	0.000	4.54	8.00	0.000	4.74
fu7	24.00	0.000	0.69	24.00	0.000	0.58
glass2	45.00	0.000	2.28	45.00	0.000	2.32
fu8	24.00	0.000	0.56	24.00	0.000	1.08
shapes8	26.00	0.000	5.15	26.00	0.000	4.51
fu9	25.00	0.000	34.69	25.00	0.000	36.30
threep3	13.53	0.000	957.46	13.53	0.000	991.95
threep3w9	10.90	0.009	3600.00	11.00	0.000	3393.99
glass3	100.00	0.000	20.17	100.00	0.000	16.91
fu10	28.69	0.000	256.04	28.69	0.000	261.10
dighe2	100.00	0.000	1.84	100.00	0.000	1.87
J1-10-20-0	18.00	0.000	6.32	18.00	0.000	6.44
J1-10-20-1	17.00	0.000	5.02	17.00	0.000	5.44
J1-10-20-2	20.00	0.000	7.49	20.00	0.000	7.69
J1-10-20-3	20.75	0.000	293.66	20.75	0.000	278.35
J1-10-20-4	12.50	0.000	98.12	12.50	0.000	70.64
J2-10-35-0	23.66	0.000	612.65	23.66	0.000	494.84
J2-10-35-1	21.30	0.000	202.69	21.30	0.000	191.77
J2-10-35-2	19.95	0.000	120.45	19.95	0.000	116.24
J2-10-35-3	20.38	0.000	1081.23	20.38	0.000	962.18
J2-10-35-4	19.44	0.000	442.26	19.43	0.000	444.96
J1-12-20-0	12.00	0.000	40.25	12.00	0.000	37.91
J1-12-20-1	10.00	0.000	36.86	10.00	0.000	34.76
J1-12-20-2	12.00	0.000	14.79	12.00	0.000	17.44
J1-12-20-3	8.00	0.000	24.71	8.00	0.000	16.04
J1-12-20-4	13.00	0.000	178.50	13.00	0.000	176.47
J2-12-35-0	24.01	0.143	3600.00	24.25	0.134	3600.00
J2-12-35-1	22.00	0.154	3600.00	22.00	0.144	3600.00
J2-12-35-2	20.00	0.119	3600.00	20.00	0.130	3600.00
J2-12-35-3	20.00	0.130	3600.00	20.00	0.130	3600.00
J2-12-35-4	22.00	0.083	3600.00	22.00	0.083	3600.00
fu	31.67	0.063	3600.00	32.00	0.053	3600.00
J1-14-20-0	12.00	0.000	546.47	12.00	0.000	1195.33
J1-14-20-1	11.00	0.057	3600.00	11.00	0.057	3600.00
J1-14-20-2	13.00	0.133	3600.00	13.00	0.133	3600.00
J1-14-20-3	10.00	0.000	740.13	10.00	0.000	81.82
J1-14-20-4	13.23	0.118	3600.00	13.31	0.113	3600.00
J2-14-35-0	23.10	0.241	3600.00	23.33	0.219	3600.00
J2-14-35-1	21.50	0.292	3600.00	21.57	0.281	3600.00
J2-14-35-2	20.00	0.252	3600.00	20.00	0.231	3600.00
J2-14-35-3	20.00	0.231	3600.00	20.00	0.231	3600.00
J2-14-35-4	20.00	0.253	3600.00	20.00	0.238	3600.00
poly1a0	13.00	0.223	3600.00	13.00	0.235	3600.00
dighe1ok	99.98	0.192	3600.00	99.98	0.184	3600.00
Average		**0.054**	**1338.77**		**0.052**	**1329.14**
#OPT	**33**			**34**		

Table 3.9: *Results of the Branch and Bound algorithm: Instances solved in less than 3600 seconds*

Instance	*Pieces*	*Nodes*	*Time*	*Instance*	*Pieces*	*Nodes*	*Time*
three	3	0	0.76	J1_10_20_0	10	8917	10.2
shapes_4	4	10	0.06	J1_10_20_1	10	10627	8.3
fu_5	5	511	0.67	J1_10_20_2	10	12361	8.7
glass1	5	0	0.02	J1_10_20_3	10	957992	469.4
fu_6	6	153	0.16	J1_10_20_4	10	117337	63,5
threep2	6	6536	1.14	J2_10_35_0	10	1691310	630.6
three2w9	6	17772	3.43	J2_10_35_1	10	552708	189.8
fu_7	7	157	0.56	J2_10_35_2	10	269290	101,3
glass2	7	2278	1.95	J2_10_35_3	10	2725640	736,5
fu_8	8	277	0.84	J2_10_35_4	10	1070385	281,5
shapes_8	8	11969	4.76	J1_12_20_0	12	67833	29,9
fu_9	9	203094	37.58	J1_12_20_1	12	106897	46.6
threep3	9	3056101	1107.1	J1_12_20_2	12	24819	15,1
threep3w9	9	11803440	3365.6	J1_12_20_3	12	21502	12.9
glass3	9	25200	21.4	J1_12_20_4	12	564821	282.5
fu_10	10	1133842	272.5	J1_14_20_0	12	1162529	601.8
dighe2	10	3835	7,5	J1_14_20_3	12	219984	120.6

Table 3.10: *Results of the Branch and Bound algorithm: Instances not solved in 3600 seconds*

		1 hour		*2 hours*		*5 hours*		*10 hours*			
Instance	Pieces	LB	UB	LB	UB	LB	UB	LB	UB	Time	Optimum
J2-12-35-0	12	24.3	28.0	25.4	27.9	26.2	26.2			12803	26.21
J2-12-35-1	12	22.0	22.5	22.5	25.6	23.1	24.4	24.0	24.4		24.22
J2-12-35-2	12	20.0	23.0	20.0	23.0	20.0	23.0	20.4	22.0		21.50
J2-12-35-3	12	20.0	22.8	20.0	22.0	20.0	22.0	21.0	21.7		21.73
J2-12-35-4	12	22.0	24.0	22.2	24.0	22.7	23.8	22.9	23.8		23.21
fu	12	32.2	33.5	33.1	33.1					5844	33.1
J1-14-20-1	14	11.0	11.7	11.3	11.3					6004	11.3
J1-14-20-2	14	13.0	15.0	13.0	15.0	14.0	14.0			14996	14.0
J1-14-20-4	14	13.8	14.0	14.0	14.0					3984	14.0
J2-14-35-0	14	23.5	31.3	24.0	30.0	24.4	30.0	24.7	30.0		28.00
J2-14-35-1	14	22.0	30.0	22.0	30.0	23.0	30.0	23.5	30.0		28.00*
J2-14-35-2	14	20.0	27.0	20.0	27.0	20.0	26.0	20.0	26.0		24.75*
J2-14-35-3	14	20.3	26.0	21.6	26.0	22.0	26.0	22.0	26.0		25.00*
J2-14-35-4	14	20.0	26.0	20.7	26.0	21.3	24.7	21.5	24.7		24.00*
poly1a0	15	13.0	17.0	13.0	16.2	13.0	15.9	13.0	15.9		15.07*
dighe1ok	16	95.0	137.4	98.2	137.3	100.0	100.0			11109	100.0

Chapter 4

Valid Inequalities for the *HS2* formulation

In this chapter we present several classes of valid inequalities for the mixed integer formulation *HS2* defined in Section 2.3. We discuss the separation algorithms in the next chapter.

In a branch and cut algorithm additional inequalities are used to cut fractional solutions appearing in the nodes of the tree. Nevertheless, in many different problems there are valid inequalities such that their separation algorithms require a great computational effort and it does not make sense to use these inequalities. Therefore, if the separation algorithms are too complicated, it can be better to branch rather than cut the fractional solution. However, it is interesting to explore ways of improving the cutting process in the *Branch & Cut* algorithm.

When we solve the linear relaxation of the *HS2* formulation, with the binary variables relaxed to real variables and bounded between 0 and 1, in many cases most of the pieces in the resulting solution are placed at the origin, overlapping each other. One possible reason is that the relationship between the real and the binary variables is too weak. In order to strengthen the relation between variables x_i and y_i and variables b_{ijk}, $p_i, p_j \in P$, $k \in \{1, \ldots, m_{ij}\}$, we use ***X-Y inequalties*** defined in Section 4.1, and ***impenetrability inequalities*** defined in Section 4.2. These two types of inequalities use the bounds on the reference point of the pieces, so these inequalities are only valid for the branch created from the current node, because the bounds on the pieces change every time the set of binary variables fixed to 1 is modified (see Section 3.2).

In Sections 4.3 and 4.4 we define **cover** and **LU-cover** inequalities. We propose a classification of the set of binary variables depending on how many pieces are separated in a vertical direction. The idea is to find a set of binary variables in such a way that the total width of the pieces which are being separated exceed the width of the strip. Thus, not all of the variables in this set can take the value 1. *LU-cover* inequalities do not take into account how pieces are sorted in the pile, whereas *cover* inequalities consider a specific ordering of the pieces in the pile.

Finally, in Section 4.5, we present the ***transitivity inequalities***, which are an extension of the idea presented in Section 3.3. The aim of these inequalities, as with *LU-cover* and *cover* inequalities, is to find a set of binary variables which cannot take the value 1 simultaneously. In this case we use the transitivity of the pieces instead of the width of the strip.

4.1 *X-Y inequalities*

These inequalities improve the relation between x_i and y_i variables and variables b_{ijk}, $\forall p_i \in P$, $\forall p_j \in P \backslash p_i$, $\forall k \in \{1, \ldots, m_{ij}\}$. We study two types of *X-Y* inequalities. The first type of inequalities modify the coefficients of the inequalities needed to describe the *slices* of the *NFP*s (Type I). The second type of inequalities study the relation between one of the coordinates of the reference point of one piece and the binary variables created from *NFPs* of the given piece and the rest of the pieces (Type II).

4.1.1 Type I

Let $p_i, p_j \in P$, $i \neq j$ be a pair of pieces. An inequality used for describing a *slice* $k \in \{1, \ldots, m_{ij}\}$ of the NFP_{ij} has the following structure:

$$\alpha(x_j - x_i) + \beta(y_j - y_i) \leq \sum_{t=1}^{m_{ij}} q_t b_{ijt} \tag{4.1}$$

where α, β and q_t, $\forall t \in \{1, \ldots, m_{ij}\}$ are the coefficients described in Section 2.2.

Let us suppose that the corresponding *slice* is being used, i.e. $b_{ijk} = 1$. We use the following notation:

- $\alpha' = \begin{cases} -\alpha & \text{if} \quad \alpha > 0 \\ 0 & \text{otherwise} \end{cases}$
- $\alpha'' = \begin{cases} \alpha & \text{if} \quad \alpha < 0 \\ 0 & \text{otherwise} \end{cases}$
- $\beta' = \begin{cases} -\beta & \text{if} \quad \beta > 0 \\ 0 & \text{otherwise} \end{cases}$
- $\beta'' = \begin{cases} \beta & \text{if} \quad \beta < 0 \\ 0 & \text{otherwise} \end{cases}$

Now we consider the positive terms of the left-hand side of inequality (4.1). The following condition must hold:

$$\alpha' x_i + \alpha'' x_j + \beta' y_i + \beta'' y_j \leq q_k$$

because $\alpha' x_i + \alpha'' x_j + \beta' y_i + \beta'' y_j \leq \alpha(x_j - x_i) + \beta(y_j - y_i)$. Let us consider the case in which $\alpha > 0$ and $\beta > 0$ (the other cases are similar). That implies $\alpha'' = \beta'' = 0$, $\alpha' = -\alpha$ and $\beta' = -\beta$, then $\alpha' x_i + \alpha'' x_j + \beta' y_i + \beta'' y_j = -\alpha x_i - \beta y_i \leq -\alpha x_i - \beta y_i + \alpha x_j + \beta y_j$.

In the case that $b_{ijk} = 0$, the previous inequality may not be valid. However, if we multiply the right-hand side by b_{ijk}, then the resulting inequality is valid because the coordinates of every piece, by definition, must be positive. Therefore, inequality

$$\alpha' x_i + \alpha'' x_j + \beta' y_i + \beta'' y_j \leq q_k b_{ijk}$$

is valid.

This inequality can be improved by adding to its right hand side the binary variables defined from the same *NFP* whose coefficients are negative, i.e.:

$$\alpha' x_i + \alpha'' x_j + \beta' y_i + \beta'' y_j \leq q_k b_{ijk} + \sum_{t \in H} q_t b_{ijt} \tag{4.2}$$

where $H = \{t \in \{1, \ldots, m_{ij}\}, t \neq k \mid q_t < 0\}$.

In the case of there being lower bounds on variables x_i, x_j, y_i, y_j greater than 0, inequalities (4.2) can be improved. Let CX_i, CX_j, CY_i, CY_j be, respectively, the lower bounds. Inequality (4.2) can be lifted as follows:

$$\begin{aligned} \alpha' x_i + \alpha'' x_j + \beta' y_i + \beta'' y_j \quad &\leq \quad (q_k + \alpha'' CX_i + \alpha' CX_j + \beta'' CY_i + \beta' CY_j) b_{ijk} \\ &+ \quad \sum_{t \in H} (q_t + \alpha'' CX_i + \alpha' CX_j + \beta'' CY_i + \beta' CY_j) b_{ijt} \end{aligned} \tag{4.3}$$

We call inequalities (4.3) *X-Y inequalities of type I*. These inequalities are valid because in each solution exactly one *slice* of each *NFP* is used (one binary variable takes the value 1). Let $b_{ijl} = 1$ with $l \in H \cup \{k\}$. At most two terms of the right-hand side in inequality (4.3) take a negative value, the other two taking the value 0. Let us suppose that $\alpha'' = \beta'' = 0$, $\alpha' = -\alpha$ and $\beta' = -\beta$ ($\alpha > 0$ and $\beta > 0$ is satisfied), then the other cases are similar. Inequality (4.3) can thus be rewritten in the following way:

$$\alpha' x_i + \beta' y_i \leq q_l + \alpha' CX_j + \beta' CY_j$$

which is valid $\forall l \in \{1, \ldots, m_{ij}\}$ because if we consider CX_j and CY_j instead of x_j and y_j in equation (4.1), then the resulting inequality coincides with the previous one.

4.1.2 Type II

Let $p_i \in P$. In what follows we are going to study what the binary variables of the entire problem are such that, when they take value 1, coordinates x_i or y_i have to be increased.

Let $p_j \in P \setminus \{p_i\}$ and let $b_{ijk} \in VNFP_{ij}$ ($VNFP_{ij} = \{b_{ijk} | \forall k = 1, \ldots, m_{ij}\}$). The minimum value that x_i or y_i can take when $b_{ijk} = 1$ is defined by the limits of the *slice* in the NFP_{ij}-coordinate system, defined by $\overline{x}_{jik}, \overline{y}_{jik}, \underline{x}_{jik}$ and $\underline{y}_{jik}$. In Figure 4.1 we can see that $\overline{x}_{jik} = -\overline{x}_{ijk}$, $\underline{x}_{jik} = -\underline{x}_{ijk}$, $\overline{y}_{jik} = -\overline{y}_{ijk}$, $\underline{y}_{jik} = -\underline{y}_{ijk}$.

Figure 4.1 shows that the *slice* defined by variable b_{ijk} is placed in the third quadrant. Then when it is used, it forces piece i to be moved $\underline{x}_{jik}$ units in a horizontal direction because piece j protrudes from the left of piece i. Then any inequality with this form, $x_i \geq \underline{x}_{jik} b_{ijk}$, is valid. In the case that $\underline{y}_{jik} > 0$ (*slices* in the first and second quadrant), then inequality $y_i \geq \underline{y}_{jik} b_{ijk}$ is also valid. This idea is the same as the one we used to lift the bound constraints in the *HS2* formulation (see Section 2.3), but in this case we consider the lower bounds on the coordinates of the pieces and we are going to include more binary variables from other *NFPs*.

We denote by CX_t and CY_t, respectively, the lower bounds on x_t and y_t, $\forall p_t \in P$. In Figure 4.1, if we consider $CX_j > 0$, we can see that inequality $x_i \geq \underline{x}_{jik} b_{ijk}$ can be improved in the following way:

$$x_i \geq (\underline{x}_{jik} + CX_j) b_{ijk} \tag{4.4}$$

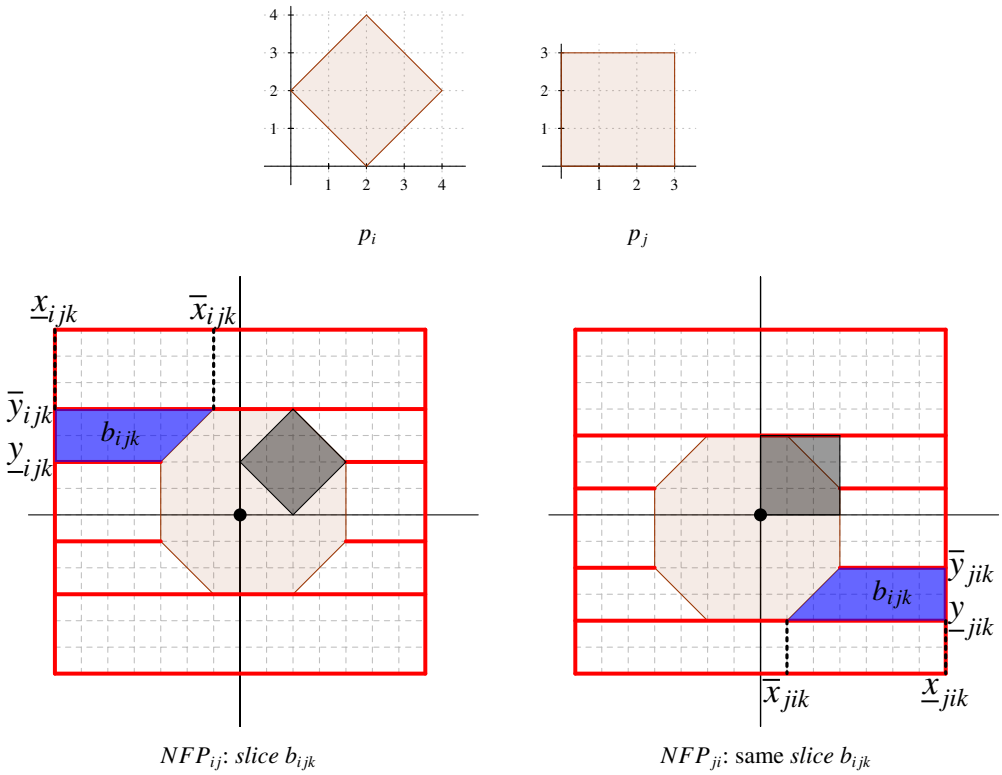

Figure 4.1: *Relation between NFP_{ij} and NFP_{ji}.*

The inequality obtained from y_i can be obtained in a similar way. If we consider NFP_{ji}, we can add any subset of binary variables satisfying $\underline{x}_{jik} > 0$ for each binary variable to equation (4.4). We define $H_{ij} := \{b_{ijk} \mid \underline{x}_{jik} > 0\}$ and $H'_{ij} \subseteq H_{ij}$. Inequality (4.4) can be lifted in the following way:

$$x_i \geq \sum_{b_{ijv} \in H'_{ij}} (\underline{x}_{jiv} + CX_j) b_{ijv} \tag{4.5}$$

Let $p_t \in P \setminus \{i, j\}$ be another piece and let us consider the *slices* whose associated variables $b_{itk'}$, $k' \in \{1, \ldots, m_{it}\}$ satisfy $\underline{x}_{tik'} > 0$. These variables cannot be added to (4.5). It may not be valid because pieces j and t could both be placed to the left of piece i, and one on top of the other, in such a way that $x_i \geq (\underline{x}_{jik} + CX_j) b_{ijk}$ and $x_i \geq (\underline{x}_{tik} + CX_t) b_{itk}$, but $x_i \geq (\underline{x}_{jik} + CX_j) b_{ijk} + (\underline{x}_{tik} + CX_t) b_{itk}$ is not satisfied.

However, if we build an inequality such that

$$x_i \geq \theta_{ijk} b_{ijk} + \theta_{itk} b_{itk} \tag{4.6}$$

and the following conditions hold:

1. $\theta_{ijk} \leq \underline{x}_{jik} + CX_j$ and $\theta_{itk} \leq \underline{x}_{tik} + CX_t$
2. $\theta_{ijk} + \theta_{itk} \leq \max\{\underline{x}_{jik} + CX_j, \underline{x}_{tik} + CX_t\}$

then inequality (4.6) is valid. If both variables take the value 0, then the inequality is valid. In the case that exactly one of them takes the value 1, then by Condition 1 inequality (4.6) it is also valid. Finally, if both binary variables take the value 1, inequality (4.6) is also valid because of Condition 2.

In what follows we generalize inequality (4.6) by considering any number of pieces. We study the coordinate x_i (the inequality for y_i can be obtained in a similar way).

Let b^* be a subset of binary variables of $\bigcup_{p_j \in P \setminus \{p_i\}} H_{ij}$ in such a way that when every variable of b^* takes the value 1 it is possible to build a feasible solution for the problem. The set of all possible subsets of binary variables b^* is denoted by B^*. Note that it is impossible for two binary variables of the same *NFP* to appear in any subset b^* because they cannot take the value 1 simultaneously. Let us consider the following constraints:

$$x_i \geq \sum_{p_j \in P \setminus \{p_i\}} \sum_{b_{ijv} \in H_{ij}} \theta_{ijv} b_{ijv} \tag{4.7}$$

such that the following conditions hold:

1. $\theta_{ijk} \leq \underline{x}_{jik} + CX_j$, $\forall p_j \in P \setminus \{p_i\}$, $\forall b_{ijk} \in H_{ij}$
2. $\forall b^* \in B^*$, $\sum_{b_{ijk} \in b^*} \theta_{ijk} \leq \max_{b_{ijk} \in b^*} \underline{x}_{jik} + CX_j$.

then, we say that inequalities (4.7) are *X-Y inequalities of type II*.

Relation between inequalities *X-Y* of type I and type II

In the case that one coefficient α or β in inequalities *X-Y of type I* takes the value 0, then it would be dominated by inequalities *X-Y of type II*.

Let us suppose that $\beta = 0$ (case $\alpha = 0$ is similar). The corresponding inequality *X-Y of type I* has the following structure:

$$\alpha' x_i + \alpha'' x_j \leq (q_k + \alpha'' CX_i + \alpha' CX_j) b_{ijk} + \sum_{t \in H} (q_t + \alpha'' CX_i + \alpha' CX_j) b_{ijt}$$

where just one of the coefficients α' or α'' takes a value different from 0 and, furthermore, it is negative by definition. Let us suppose that $\alpha' < 0$ and $\alpha'' = 0$. If we divide the previous inequality by α', we obtain the following inequality:

$$x_i \geq \mu_k b_{ijk} + \sum_{t \in H} \mu_t b_{ijt} \tag{4.8}$$

where $\mu_t = (q_t + \alpha' CX_j)/\alpha'$. Inequality (4.8) has the same structure of an *X-Y inequality of type II* for x_i.

In the case that $\alpha \neq 0$ and $\beta \neq 0$, an *X-Y inequality of type I* is not dominated by *X-Y inequalities of type II*. If we look at the *NFP* represented in Figure 4.2, we can see that the *slice* defined by b_{ij8} is not rectangular, so the *extended slice* does not match the original *slice*. The *NFP*-constraint obtained from the segment of the NFP_{ij}, which is necessary to define the limits of the *slice* associated with b_{ij8}, has the following form:

$$x_i - x_j + y_i - y_j \leq 3b_{ij1} + 5b_{ij2} + 8b_{ij3} + 10b_{ij4} + 13b_{ij5} + b_{ij6} - 3b_{ij7} - 6b_{ij8}$$

If we build the corresponding *X-Y inequality of type I* without taking into account the lower bounds greater than 0, we get the following inequality:

$$x_j + y_j \geq 3b_{ij7} + 6b_{ij8}$$

The coefficient of variable b_{ij8} in the inequality is 6. The only way to obtain this inequality using inequalities of *type II* is by considering the sum of two *X-Y inequalities of type II*, one for variable x_j and another one for variable y_j. In both cases, the maximum coefficient of b_{ij8} is 2 because $\underline{x}_{ij8} = \underline{y}_{ij8} = 2$, so the resulting coefficient of b_{ij8} in the sum of these inequalities is at most 4, and it is impossible to obtain the value 6 for the coefficient in the corresponding inequality *X-Y of type I*.

However, if for each binary variable the associated *slice* has the same shape as its *extended slice*, then *X-Y inequalities of type I* would be a particular case of *X-Y inequalities of type II*.

4.2 *Impenetrability* constraints

In the non-overlapping constraints (see Section 2.2), we can see the four variables which represent the coordinates of the reference points for the given pair of pieces. These inequalities have the following structure:

$$\alpha(x_j - x_i) + \beta(y_j - y_i) \leq \sum_{t=1}^{m_{ij}} q_t b_{ijt}$$

where i and j are the two pieces which are being separated, $k \in \{1, \ldots, m_{ij}\}$ is the *slice* of the NFP_{ij} and the inequality defines one of its edges.

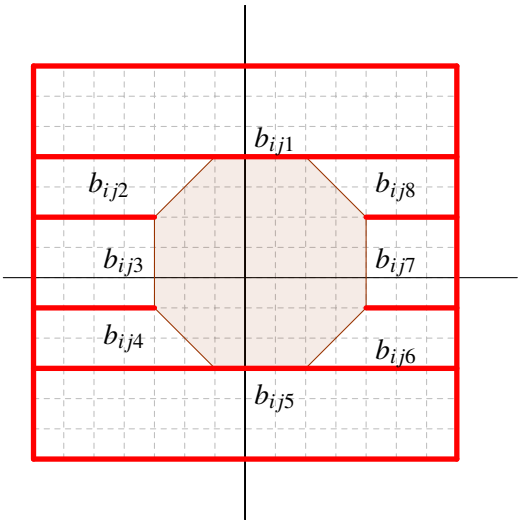

Figure 4.2: NFP_{ij}

Coefficients x_i and x_j have different signs, $-\alpha$ and α, in all the inequalities of the *NFPs* which have $\alpha \neq 0$ and $\beta \neq 0$. The same situation applies to coefficients y_i and y_j, whose signs are, respectively, $-\beta$ and β.

Let i and j be two pieces and let NFP_{ij} be the associated *Non-Fit Polygon*. We are going to study the minimum value of $s := x_i + x_j + y_i + y_j$ in each one of the *slices* of the NFP_{ij}. The core of the *impenetrability constraints* is the separation of one piece from the origin because all the fractional solutions obtained when the initial linear problem is solved place many pieces at the origin or very close to it, with a lot of overlapping.

In Section 4.1 we presented the *X-Y* inequalities. In these inequalities we studied one or the sum of two variables defined from the reference point of one or two pieces. Inequalities *X-Y of type I* study the sum of two of these variables, where each one of the variables could be defined from different pieces. In inequalities *X-Y of type II*, each variable associated with a coordinate of the reference point of any piece is studied separately.

If we calculate the sum of four of the *X-Y inequalities of type II*, we can obtain a lower bound for s. In the *Impenetrability constraints* this lower bound is improved and the resulting inequalities will have better coefficients.

The *Impenetrability constraints* have the following structure:

$$s \geq \sum_{l=1}^{m_{ij}} q_l b_{ijl} \tag{4.9}$$

where $s = x_i + x_j + y_i + y_j$ and coefficients q_l are obtained by solving:

$$q_l := \min_{b_{ijl}=1} s \tag{4.10}$$

In the case that there are lower bounds on x_i, y_i, x_j or y_j greater than 0, these coefficients would have a greater value. These inequalities are then valid just in the corresponding branch defined from the current

node on the branch and cut tree (local constraints).

The difficulty of obtaining an *impenetrability constraint* is given by problem (4.10). We need to solve this problem in order to calculate coefficients q_l, $\forall l \in \{1, \ldots, m_{ij}\}$. Note that $q_l \geq 0 \ \ \forall l \in \{1, \ldots, m_{ij}\}$ because, by definition, none of the coordinates of the pieces can take a negative value.

In what follows we present two approaches to dealing with problem (4.10). The first approach, an exact method, calculates the minimum value of s in such a way that there is a feasible placement for pieces i and j that reaches this value. The second approach, an approximate method, uses a simplification of the *slices* in order to alleviate the computational effort. If we use the second approach, the resulting inequality could be slightly weaker because coefficients q_l could be lower than those in the exact method.

Exact method for calculating coefficients q_l

Let i and j be two pieces and let $k \in \{1, \ldots, m_{ij}\}$ be a *slice* of NFP_{ij}. We are going to calculate the minimum value of $s = x_i + x_j + y_i + y_j$ when $b_{ijk} = 1$.

We use the notation described in Subsection 3.2.2. Let $S_{ijk} = \{(x_1, y_1), \ldots, (x_r, y_r)\}$ be the set of r vertices sorted in an anticlockwise order in the NFP_{ij}-coordinate system. We denote the four quadrants by $Q_t, \ t = 1, \ldots, 4$. The geometric space defined by *slice* k in the NFP_{ij}-coordinate system is given by the convex hull of S_{ijk}, $conv(S_{ijk})$.

First we calculate the coefficient q_k in the case that there are no lower bounds greater than 0. After that we study how the lower bounds can be used to improve the coefficients.

Let us suppose that $CX_i = CY_i = CX_j = CY_j = 0$. A partition of $\mathbb{R}^2$ is defined by quadrants $Q_t, \ t = 1, \ldots, 4$. It is obvious that

$$q_k = \min_{t \in \{1,\ldots,4\}} \{ \min_{(x,y) \in conv(S_{ijk}) \cap Q_t} |x| + |y| \}.$$

We have to minimize $|x| + |y|$ because any coordinate of piece j with a negative value in the NFP_{ij}-coordinate system has the following behavior in the stock sheet coordinate system (the bottom-left corner of the stock sheet is located at the origin):

- If $x < 0$, then piece i has to be moved in a horizontal direction from the origin to the right in order to place piece j in that position, in such a way that $x_j = 0$ and $x_i = |x|$.
- If $y < 0$, then piece i has to be moved in a vertical direction in order to place piece j such that $y_j = 0$ (and $y_i = |y|$).

In the case that the coordinates of piece j are positive in the NFP_{ij}-coordinate system, the behavior in the stock sheet coordinate system will satisfy:

- If $x > 0$, then piece i satisfies $x_i = 0$ and piece j satisfies $x_j = x$.
- If $y > 0$, then piece i satisfies $y_i = 0$ and piece j satisfies $y_j = y$.

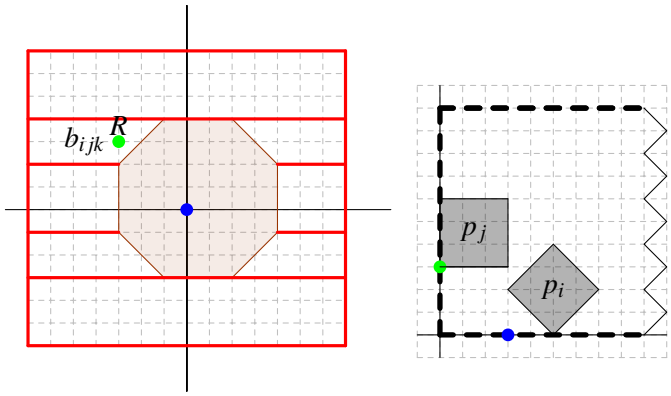

Figure 4.3: *Relative position of both pieces defined by point* $R = (-3, 3)$ *such that* s *is minimized.*

For each point in the NFP_{ij}-coordinate system there is an associated placement for pieces i and j in the stock sheet coordinate system in such a way that s is minimized. The relative position of both pieces is fixed and any other values of the coordinates of the pieces placed in the same *slice* (respecting the relative position) would have a greater value of s.

An example is shown in Figure 4.3. The pair of pieces is drawn in Figure 4.1 and the corresponding NFP_{ij} is drawn in Figure 4.2. Let us suppose that we use the point $R = (-3, 3)$ in order to separate pieces i and j. The reference point of pieces i and j is represented, respectively, in blue and green. In the stock sheet coordinate system we have to place piece i and j as Figure 4.3 shows in order to minimize s, and the relative position described by point R is satisfied. Then, $x_i = 3$ and $x_j = 0$, and coordinates Y remain with the same value as in the NFP_{ij}-coordinate system (NFP_{ij}-CS).

In the case that there is a t such that $conv(S_{ijk}) \cap Q_t = \emptyset$, then we consider $\min_{(x,y)\in conv(S_{ijk})\cap Q_t} |x|+|y| = 0$. If variable b_{ijk} is incompatible, i.e. b_{ijk} cannot take the value 1 because the pieces would exceed the limit of the strip, then we consider that $q_k = 0$. That is, we do not include it in the inequality because it can be dropped from the problem.

Using the intersections of *slice* k with the quadrants, we define, for all $t = 1, \ldots, 4$, the following subsets:

$$S^t_{ijk} := \{(x^t_1, y^t_1), \ldots, (x^t_{r_t}, y^t_{r_t})\},$$

in such a way that the convex hull of points of S^t_{ijk} matches with $conv(S_{ijk}) \cap Q_t$, i.e. $conv(S^t_{ijk}) = conv(S_{ijk}) \cap Q_t$. The intersection of two convex polygons will be a convex polygon, so $conv(S^t_{ijk})$ is the convex polygon which contains the part of the *slice* defined by b_{ijk} placed in Q_t. Figure 4.4 shows a partition of *slice* k into two rectangles, the part corresponding to Q_2 is drawn in green, $conv(S^2_{ijk})$, and the part placed in Q_3, $conv(S^3_{ijk})$ is represented in blue. The sets of points are the following ones:

$$\begin{aligned} S^2_{ijk} &:= \{(-3, 2), (-7, 2), (-7, 0), (-3, 0)\} \\ S^3_{ijk} &:= \{(-3, 0), (-7, 0), (-7, -1), (-3, -1)\} \end{aligned}$$

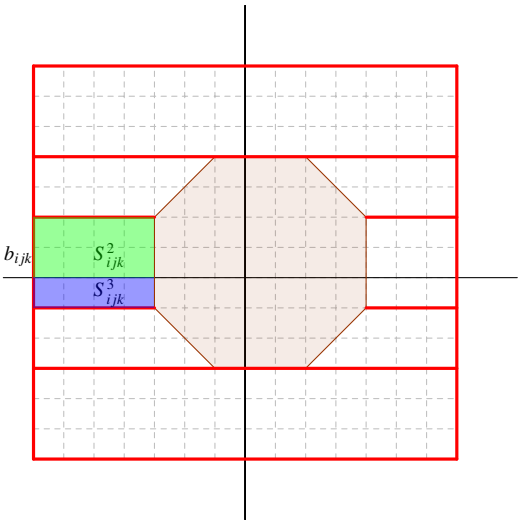

Figure 4.4: *Sets S^2_{ijk} and S^3_{ijk} built from slice k.*

In this case there are no lower bounds on the coordinate of pieces. In order to obtain the coefficient q_k of an *impenetrability constraint*, we have to calculate the sum of the minimum value of each coordinate of i and j in the NFP_{ij}-coordinate system in all the relative positions given by the vertices of $S^t_{ijk}, \forall t \in \{1, \ldots, 4\}$. In the example shown in Figure 4.4 we can see that there are six points which we have to study. These points are defined by S^2_{ijk} and S^3_{ijk}. The minimum value of the sum of the coordinates considering absolute values is given by the point $(-3, 0)$, and then $q_k = 3$.

If the coordinates of both pieces have positive lower bounds, denoted as CX_i, CY_i, CX_j and CY_j, then coefficients q_k of an impenetrability constraint can be improved. In order to modify the coefficients we have to take into account the unfeasible configurations.

The minimum value of q_k is:

$$q_k \geq CX_i + CY_i + CX_j + CY_j$$

In the case that $R = (CX_j - CX_i, CY_j - CY_i)$ belongs to *slice k*, i.e. if $R \in conv(S_{ijk})$, then $q_k = CX_i + CY_i + CX_j + CY_j$.

Using the same idea presented above, quadrants Q_t, $t = 1, \ldots, 4$ define a partition of $\mathbb{R}^2$ such that

$$q_k = \min_{t \in \{1,\ldots,4\}} \{ \min_{(x,y) \in conv(T_{ijk}) \cap Q_t} \omega \}.$$

In this case, instead of $|x|+|y|$, we use ω. The value of ω will be greater than $|x|+|y|$. Let us define $\omega = \omega_1 + \omega_2$ where ω_1 denotes the sum of the X-coordinate of both pieces, which can be calculated in the following way:

- If $x < CX_j - CX_i$ then we have to move piece i in a horizontal direction in order to place piece j in such a way that $x_j = CX_j$ and $x_i = CX_j - x$. In this case, $\omega_1 = 2CX_j - x$.
- If $CX_j \geq x \geq CX_j - CX_i$, then pieces i and j satisfy $x_i = CX_i$ and $x_j = CX_j$. In this case, $\omega_1 = CX_i + CX_j$.
- If $x > CX_j$, the pieces i and j satisfy $x_i = CX_i$ and $x_j = x$. In this case, $\omega_1 = CX_i + x$.

Similarly, ω_2 denotes the sum of the Y-coordinates of both pieces, which can be calculated in the following way:

- If $y < CY_j - CY_i$, then piece i has to be moved in a vertical direction in order to place piece j in such a way that $y_j = CY_j$ and $y_i = CY_j - y$. In this case, $\omega_2 = 2CY_j - y$.
- If $CY_j \geq y \geq CY_j - CY_i$, then pieces i and j satisfy $y_i = CY_i$ and $y_j = CY_j$. In this case, $\omega_2 = CY_i + CY_j$.
- If $y > CY_j$, then pieces i and j satisfy $y_i = CY_i$ and $y_j = y$. In this case, $\omega_1 = CY_i + y$.

Then, for each point in *slice k* in the NFP_{ij}-coordinate system, we can obtain the coordinates of both pieces in the stock sheet coordinate system (x_i, y_i, x_j, y_j), for which $\omega = s$. By definition, lower bounds of pieces are always satisfied and, furthermore, any other placement of both pieces satisfying the relative position given by the point of the *slice* will produce a greater value of s.

The transformation of the relative position of both pieces in order to build a feasible placement for two different points of the *slice* could produce the same value of s. Furthermore, when we represent the point which minimizes s in the NFP_{ij}-coordinate system, it is not necessary to be at any vertex of S^t_{ijk} for a $t = 1, \ldots, 4$. In this case, there is a vertex from S^t_{ijk} such that the transformation will place both pieces in such a way that the value of s is minimum.

To obtain q_k, we calculate $|s|$ in the NFP_{ij}-coordinate system and ω for all the relative positions given by the vertices of $S^t_{ijk}, \forall t \in \{1, \ldots, 4\}$. The minimum value would be q_k. In Figure 4.4 we can see an example. Lower bounds are $CX_i = 2$, $CY_i = 1$, $CX_j = 1$ and $CY_j = 3$. When we consider these lower bounds, then configuration $x_i = 3$, $y_i = 0$, $x_j = 0$ and $y_j = 0$ is not valid because the lower bound would not be satisfied. The minimum coefficient is given by vertex $(-3, 2)$ of S^2_{ijk}, where:

- $x < CX_j - CX_i$, so $\omega_1 = 2CX_j - x = 5$.
- $y = CX_j - CX_i$, so $\omega_2 = CY_i + CY_j = 4$.

As $\omega = \omega_1 + \omega_2 = 9$, then $q_k = 9$. The transformation of point $(-3, 0)$ produces $x_i = 4$, $y_i = 3$, $x_j = 1$ and $y_j = 3$, so at that point $s = 11$. In Figure 4.5, pieces i and j are drawn in the stock sheet coordinate system in such a way that *slice k* is used and s is minimized. The dashed lines in blue represent the lower bounds of piece i and the dashed lines in green represent the lower bounds of piece j.

If we consider $CX_i = 5$, then $q_k = 10$, which is obtained at vertex $(-3, 2)$. Pieces are placed satisfying $x_i = CX_i$, $y_i = CY_i$, $x_j = CX_j$ and $y_j = CY_j$. If we represent the relative position in the NFP_{ij}-coordinate system, we can observe that the point is $(-4, 2)$, which is not a vertex of S^2_{ijk}.

Approximated method to calculate q_l

Let $i, j \in P$. When a *slice* from NFP_{ij} has more than 4 vertices, then it is generated from a concavity of the NFP_{ij}. This kind of *slices* has more complex shapes and we need more effort to calculate the coefficients of an *impenetrability constraint*. Note that there are more vertices to be considered, so we have to study more points in order to calculate the coefficient.

In this case, the idea is to consider the transformation of these complex *slices* (*slices* with more than 4 vertices) into *extended slices*, see Section 3.3.2. If the *slice* is approximated, then we have not guaranteed that the coefficient obtained is the best one, i.e. the coefficient could be lower but the calculation is easier

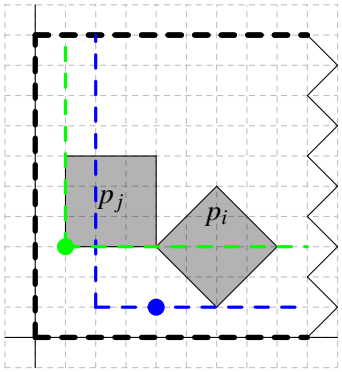

Figure 4.5: *Position of pieces i and j such that s is minimized when slice k is used (see Figure 4.4).*

and faster.

Every *slice* is modified to have at most 4 vertices. We therefore have to study at most $4+h$ points, where $h = 2$ if the *slice* crosses one of the axes in the NFP_{ij}-coordinate system or $h = 4$ if it crosses both axes.

In the following example we can see an NFP_{ij} in which the *impenetrability* inequality obtained by the approximate method, is dominated by the inequality obtained by the exact method.

Let us consider the NFP_{ij} drawn in Figure 4.6. If there are no lower bounds on the pieces, the corresponding *impenetrability constraint* obtained by the exact method is:

$$x_i + y_i + x_j + y_j \geq 4b_{121} + 5b_{122} + 3b_{123} + 4b_{124} + 3b_{125} + 5b_{126} + 4b_{127} + 6b_{128} + 1.5b_{ij9}$$

On the other hand, if we calculate the coefficients using the approximated method, the *extended slice* obtained from *slice* 9 is:

$$S^*_{ij9} := \{(-2.5, -1.5), (-0.5, -0.5)\},$$

where these vertices represent, respectively, the bottom-left corner and the top-right corner of the enclosing rectangle, so $q_9 = 0.5 + 0.5 = 1$. All the other coefficients remain equal, and we obtain an *impenetrability* inequality which is dominated by the previous one.

4.3 *Cliques* and *Covers*

The width (W) of the strip is given and fixed. There are therefore sets of pieces such that their total width is greater than W, so the pieces of each of these sets cannot stacked up one on top of the other. That is, no solution can use all the *slices,* which forces pieces to be placed forming a pile. In order to build a *clique* or *cover* inequality, in a first step we identify one of these sets of pieces and, in a second step, we try to find a

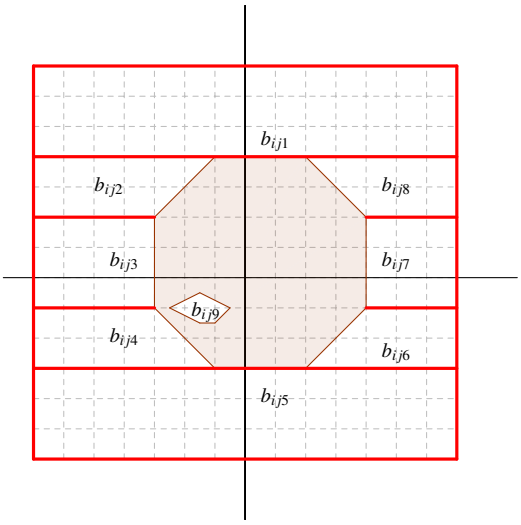

Figure 4.6: *NFP_{ij} with a hole which defines a slice with* 5 *vertices, associated with variable b_{ij9}.*

set of binary variables (*slices*) of each *NFP* between these pieces in such a way that if all the selected binary variables take the value 1, the configuration of the pieces exceeds the width of the strip. *Clique* inequalities are obtained by sets of 3 pieces and *cover* inequalities consider more than 3 pieces.

The inequalities studied in this section consider a specific order for the pieces. That is, it is important to know which piece is placed at the bottom of the pile and in which order the rest of the pieces are placed. If we place all the pieces one completely on top of the other (there is no parallelism between any pair of pieces), then any order of the pieces in the set produces the same width of the pile. In the next section we develop this idea.

If the binary variables that we consider in the inequality allow the pieces to match in a vertical way, that is, when the segments obtained by the projection on the Y-axis of the pieces overlap, then the given order of pieces could affect the total width of the pile, depending on the quantity of overlap in the Y-axis which is allowed for each pair of pieces in the pile.

Let us take a pair of pieces $i, j \in P$ and let b_{ijk} for some $k \in \{1, \ldots, m_{ij}\}$ be a binary variable which takes the value 1. In order to identify if the separation of these two pieces forces one piece to protrude from the other piece in a vertical direction, we are going to use the limits of the *slice* in the Y-axis. If we want the total width of the two pieces to increase, the minimum width of arranging both pieces must be greater than the width of both pieces separately.

Let $\{1, \ldots, l\}$ be a set of l pieces. We call a *stack* a set of ordered pieces $1 - 2 - \cdots - l$, such that piece p_1 (or 1) is placed at the bottom of the pile, piece 2 protrudes from the top of piece 1 in a vertical direction, and so on, with piece l placed on the top of the pile. Let $C(1, \ldots, l)$ be the set of l piles of pieces in such a way that the order $1 - 2 - \cdots - l$ is satisfied but the starting piece can be changed. That is, the pile built by $2 - 3 - \cdots - l - 1$ also belongs to $C(1, \ldots, l)$. We say that $C(p_1, \ldots, p_l)$ is a *chain*.

Let us suppose that $b_{ijk} = 1$ and $\underline{y}_{ijk}$ is strictly positive. That is, piece j is placed satisfying $y_j \geq y_i + \underline{y}_{ijk}$. On the other hand, if $\overline{y}_{ijk} < 0$ and $b_{ijk} = 1$, then piece j is placed satisfying $y_j \leq y_i + \underline{y}_{ijk}$ (see Figure 2.10).

Now we are going to use some notation used in Section 2.3 with some changes. Let i and j be a pair of pieces. $\mathbf{U_{ij}}$ is the set of variables whose associated *slices* separate piece j upwards from piece i and piece i protrudes from below piece j (note that this definition is somewhat different from that used in Section 2.3). In a similar way, $\mathbf{D_{ij}}$ is the set of variables whose associated *slices* separate piece i upwards from piece j and piece j protrudes from below piece i.

$$\begin{aligned} \mathbf{U_{ij}} &:= \{k \mid \underline{y}_{ijk} > 0, \quad \overline{Y}_{ij} - \underline{y}_{ijk} < w_j\} \\ \mathbf{D_{ij}} &:= \{k \mid \overline{y}_{ijk} < 0, \quad |\underline{Y}_{ij} - \overline{y}_{ijk}| < w_j\} \end{aligned}$$

Note that $U_{ij} = D_{ji}$. In Figure 4.7 we can see an example.

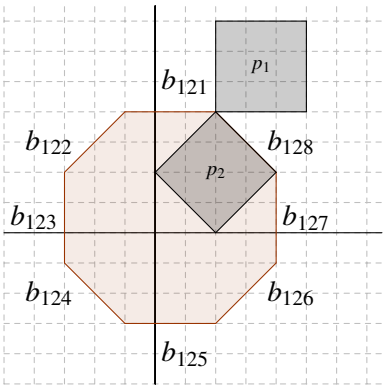

Figure 4.7: $U_{12} = \{1, 2, 8\},\ D_{12} = \{4, 5, 6\}$.

In what follows, we define a partition of $\mathbf{U_{ij}}$ ($\mathbf{D_{ij}}$) for classifying the binary variables, taking into account the amount of overlap allowed in a vertical direction for both pieces.

We denote by U^0_{ij} (D^0_{ij}) the subsets of binary variables which separate piece j entirely on top of i (piece i is separated entirely from on top of piece j).

$$\begin{aligned} \mathbf{U^0_{ij}} &:= \{k \in U_{ij} \mid \overline{Y}_{ij} - \underline{y}_{ijk} = 0\} \\ \mathbf{D^0_{ij}} &:= \{k \in D_{ij} \mid |\underline{Y}_{ij} - \overline{y}_{ijk}| = 0\} \end{aligned}$$

In the example appearing in Figure 4.7, $U^0_{12} = \{1\}$ and $D^0_{12} = \{5\}$.

Let $\upsilon^1_{ij} := \min_{k \in U_{ij} \setminus U^0_{ij}} \overline{Y}_{ij} - \underline{y}_{ijk}$ ($\delta^1_{ij} := \min_{k \in D_{ij} \setminus D^0_{ij}} |\underline{Y}_{ij} - \overline{y}_{ijk}|$). We define the following subsets of

variables:

$$\begin{aligned}\mathbf{U_{ij}^1} &:= \{k \in U_{ij} \quad | \quad \overline{Y}_{ij} - \underline{y}_{ijk} = \upsilon_{ij}^1\} \\ \mathbf{D_{ij}^1} &:= \{k \in D_{ij} \quad | \quad |\underline{Y}_{ij} - \overline{y}_{ijk}| = \delta_{ij}^1\}\end{aligned}$$

In the example represented in Figure 4.7, we can see that $U_{12}^1 = \{2, 8\}$, $D_{12}^1 = \{4, 6\}$, $\upsilon_{12}^1 = 2$ and $\delta_{12}^1 = 2$

.

Iteratively, if we have already defined U_{ij}^{t-1}, D_{ij}^{t-1} and $\upsilon_{ij}^t := \min_{k \in U_{ij} \setminus \bigcup_{s=0}^{t-1} U_{ij}^s} \overline{Y}_{ij} - \underline{y}_{ijk}$ ($\delta_{ij}^t := \min_{k \in D_{ij} \setminus \bigcup_{s=0}^{t-1} D_{ij}^s} |\underline{Y}_{ij} - \overline{y}_{ijk}|$), then we define:

$$\begin{aligned}\mathbf{U_{ij}^t} &:= \{k \in U_{ij} \quad | \quad \overline{Y}_{ij} - \underline{y}_{ijk} = \upsilon_{ij}^t\} \\ \mathbf{D_{ij}^t} &:= \{k \in D_{ij} \quad | \quad |\underline{Y}_{ij} - \overline{y}_{ijk}| = \delta_{ij}^t\}\end{aligned}$$

Let $\upsilon_{ij} \in \mathbb{N}$ ($\delta_{ij} \in \mathbb{N}$) be the integer such that the following condition holds:

- $U_{ij}^{\upsilon_{ij}} \neq \emptyset \qquad (D_{ij}^{\delta_{ij}} \neq \emptyset)$
- $U_{ij}^{\upsilon_{ij}+1} = \emptyset \qquad (D_{ij}^{\delta_{ij}+1} = \emptyset)$

Then we have built a partition for U_{ij} (similarly for D_{ij}),

$$U_{ij} = \bigcup_{s=0}^{\upsilon_{ij}} U_{ij}^s \qquad (D_{ij} = \bigcup_{s=0}^{\delta_{ij}} D_{ij}^s)$$

in such a way that variables in U_{ij}^t (D_{ij}^t) allow pieces i and j to match in a vertical direction less than variables from U_{ij}^s (D_{ij}^s), where $t < s \leq \upsilon_{ij}$ ($t < s \leq \delta_{ij}$).

We say that U_{ij} (D_{ij}) has $\upsilon_{ij} + 1$ ($\delta_{ij} + 1$) *classes*. Variables from $U_{ij}^{\upsilon_{ij}^t}$ ($D_{ij}^{\delta_{ij}^t}$) belong to *class* υ_{ij}^t (δ_{ij}^t).

Now we present a preliminary result. The idea is fix a binary variable to 0 such that, if it was fixed to 1, the relative position of the pieces associated with the corresponding *NFP* would exceed the width of the strip.

Theorem 1
Let $i, j \in P$. If there is a variable b_{ijk} for any k such that $\overline{y}_{ijk} > W - w_j$ or $\overline{y}_{jik} > W - w_i$, then all feasible solutions s of the problem satisfy $b_{ijk} = 0$.

Proof:
If $b_{ijk} = 1$, then $W - w_j \geq y_j \geq \overline{y}_{ijk} > W - w_j$ or $W - w_i \geq y_i \geq \overline{y}_{jik} > W - w_i$. §

Theorem 2
Let $i, j, k \in P$. If there are three subsets $U'_{ij} \subseteq U_{ij}$, $U'_{jk} \subseteq U_{jk}$ and $U'_{ki} \subseteq U_{ki}$ in such a way that the following conditions are satisfied:

1. $U'_{ij} \neq \emptyset$, $U'_{jk} \neq \emptyset$ and $U'_{ki} \neq \emptyset$.

2. For each subset:

   - If $k \in U'_{ij}$, such that k belongs to class v ($k \in U^v_{ij}$), then $\bigcup_{l \leq v} U^l_{ij} \subseteq U'_t$.
   - If $k \in U'_{jk}$, such that k belongs to class v ($k \in U^v_{jk}$), then $\bigcup_{l \leq v} U^l_{jk} \subseteq U'_t$.
   - If $k \in U'_{ki}$, such that k belongs to class v ($k \in U^v_{ki}$), then $\bigcup_{l \leq v} U^l_{ki} \subseteq U'_t$.

   We denote by τ^*_{ij} the highest class given by variables from U'_{ij}. Similarly, we define τ^*_{jk} and τ^*_{ki}, respectively, as the highest classes given by variables from U'_{jk} and U'_{ki}.

3. Let $\varpi_1 \in \mathbb{R}$ and $\varpi_2 \in \mathbb{R}$ be, respectively, the largest and the second largest value of the following real numbers: $\{\upsilon_{ij}^{\tau^*_{ij}}, \upsilon_{jk}^{\tau^*_{jk}}, \upsilon_{ki}^{\tau^*_{ki}}\}$. Then,

$$w_i + w_j + w_k - \varpi_1 - \varpi_2 > W$$

If 1, 2 and 3 are satisfied, then inequality (4.11) is valid.

$$\sum_{s \in U'_{ij}} b_{ijs} + \sum_{s \in U'_{jk}} b_{jks} + \sum_{s \in U'_{ki}} b_{kis} \leq 1. \tag{4.11}$$

We say that the previous inequality is a *vertical clique* (or just a *clique*) inequality *associated with chain* $C(i, j, k)$.

Proof:
The different feasible orderings for stacking three pieces with chain $C(i, j, k)$ are:

(a) $i - j - k$: That implies that piece i is placed below piece j and, simultaneously, piece j is placed below piece k.

(b) $j - k - i$: That implies that piece j is placed below piece k and, at the same time, piece k is placed below piece i.

(c) $k - i - j$: That implies that piece k is placed below piece i and, at the same time, piece i is placed below piece j.

The combination which produces the minimum total width is the one that allows more overlap in a vertical direction between the adjacent pieces. Let us suppose that $\varpi_1 = \upsilon_{ij}^{\tau^*_{ij}}$ and $\varpi_2 = \upsilon_{jk}^{\tau^*_{jk}}$, i.e, $\upsilon_{ij}^{\tau^*_{ij}} \geq \upsilon_{jk}^{\tau^*_{jk}} \geq \upsilon_{ki}^{\tau^*_{ki}}$. The other cases can be proved in a similar way.

As $\upsilon_{ij}^{\tau^*_{ij}} \geq \upsilon_{ij}^{\tau^*_{ki}}$ and $\upsilon_{jk}^{\tau^*_{jk}} \geq \upsilon_{ki}^{\tau^*_{ki}}$, the combination with less width is given by chain (a). The amount of width used is $w_i + w_j + w_k - \varpi_1 - \varpi_2$, which by hypothesis 3 exceeds the width of the strip. So if any variable of $b_{ijs} \in U'_{ij}$ takes the value 1, then it is impossible to build a feasible solution. Thus it is satisfied that:

$$\sum_{s \in U'_{ij}} b_{ijs} + \sum_{s \in U'_{jk}} b_{jks} \leq 1$$

In order to add the term $\sum_{s \in U'_{ki}} b_{kis}$ to the left hand side of the inequality, we have to prove that none of the variables in set U'_{ki} can take the value 1 simultaneously with any variable of sets U'_{ij} or U'_{jk}.

- If both $b_{kis} \in U'_{ki}$, $b_{ijt} \in U'_{ij}$ take the value 1, then we get the combination $k - i - j$ which produces a stack wider than $i - j - k$, so the width of the strip is exceeded.

- If $b_{kis} \in U'_{ki}$ and $b_{jkt} \in U'_{ij}$ take the value 1, then we get combination $j - k - i$ which produces a stack wider than $i - j - k$, so the width of the strip is exceeded.

In conclusion, inequality 4.11 is valid when $\varpi_1 = \upsilon_{ij}^{\tau^*_{ij}}$ and $\varpi_2 = \upsilon_{jk}^{\tau^*_{jk}}$. By applying this argument to the remaining cases, we obtain that inequality 4.11 is valid in all cases. §

Theorem 3
Let $i_1, \ldots, i_r \in P$ be r pieces and let $U'_{s(s+1)} \subseteq U_{s(s+1)}, 1 \leq s \leq r$, where $i_{r+1} = i_1$, in such a way that the following conditions hold:

- $U'_{s(s+1)} \neq \emptyset,\ 1 \leq s \leq r$

- If $k \in U'_{s(s+1)}$ such that $k \in U^v_{s(s+1)}$, then $\bigcup_{l \leq v} U^l_{s(s+1)} \subseteq U'_{s(s+1)}$.

- We denote by $t^*_{s(s+1)}$ the highest class given by variables of $U'_{s(s+1)}$. Then,

$$\sum_{l=1}^{r} w_l - (\sum_{l=1}^{r} \upsilon_{l(l+1)}^{t^*_{l(l+1)}} - \upsilon_{\tau(\tau+1)}^{t^*_{\tau(\tau+1)}}) > W, \tag{4.12}$$

  where $\tau \in \{1, \ldots, r\}$ satisfy: $\upsilon_{\tau(\tau+1)}^{t^*_{\tau(\tau+1)}} \leq \upsilon_{l(l+1)}^{t^*_{l(l+1)}}$, $\forall l \in \{1, \ldots, r\}$.

Therefore, inequality 4.13 is valid.

$$\sum_{l=1}^{r} \sum_{b_{l(l+1)k} \in U'_{l(l+1)}} b_{l(l+1)k} \leq r - 1. \tag{4.13}$$

We say that inequalities 4.13 are *vertical covers*, or just *covers*, *associated with chain* $C(1, 2, \ldots, r-1)$.

Proof:
If $r = 3$, we really have a *clique* inequality because the third condition is the same in both cases.
Let us suppose that the combination with the minimum total width is given by:

$$1 - 2 - \cdots - r$$

that is, this is the combination which allows more overlap between adjacent pieces in a vertical direction.

If a binary variable from $U'_{s(s+1)}, 1 \leq s < r$ takes value 1 then, by the third condition, the stack exceeds the width of the strip and any solution satisfies:

$$\sum_{l=1}^{r-1} \sum_{b_{l(l+1)k} \in U'_{l(l+1)}} b_{l(l+1)k} \leq r - 1$$

because for the left-hand side to take its maximum value r, it would be necessary to fix one binary variable of each subset $U'_{l(l+1)}$ to 1, which is unfeasible.

To get inequality (4.13) we need to add the sum $\sum_{b_{1rk} \in U'_{r1}} b_{1rk}$ to the left-hand side. Note that any combination obtained is such that $\sum_{l=1}^{r} \sum_{b_{l(l+1)k} \in U'_{l(l+1)}} b_{l(l+1)k} = r$ exceeds the width of the strip, because any way of stacking the pieces produces a pile wider than the combination defined by $1 - 2 - \cdots - r$. Then inequality (4.13) is valid. §

All the results presented above can be modified in order to build *cliques* and *covers* in a horizontal direction. In order to build these inequalities we need an upper bound of the length of the strip, L_{ub}. The following definitions are similar to the vertical case.

Let $i, j \in P$ be two pieces. We denote by $\mathbf{R_{ij}}$ the set of variables whose associated *slices* separate piece j to the right of piece i and, furthermore, piece i protrudes from the left of piece j. Similarly, we define by $\mathbf{L_{ij}}$ the set of variables whose associated *slices* separate piece i towards the right of piece j and, furthermore, piece j protrudes from the left of piece i.

$$\begin{aligned} \mathbf{R_{ij}} &:= \{k \mid \underline{y}_{ijk} \geq 0, \quad \overline{X}_{ij} - \underline{x}_{ijk} < l_j\} \\ \mathbf{L_{ij}} &:= \{k \mid \overline{y}_{ijk} \leq 0, \quad |\underline{X}_{ij} - \overline{x}_{ijk}| < l_j\} \end{aligned}$$

Note that $R_{ij} = L_{ji}$. In what follows we define a partition of $\mathbf{R_{ij}}$ ($\mathbf{L_{ij}}$) in order to classify binary variables, taking into account the quantity of overlap allowed between the given pair of pieces in horizontal direction.

Let $i, j \in P$ and let $k \in \{1, \ldots, mij\}$. We define R^0_{ij} (L^0_{ij}) as the subset of variables whose associated *slices* separate piece j towards the right of piece i (piece i towards the left of piece j), described in the following way:

$$\begin{aligned} \mathbf{R^0_{ij}} &:= \{k \in R_{ij} \mid \overline{X}_{ij} - \underline{x}_{ijk} = 0\} \\ \mathbf{L^0_{ij}} &:= \{k \in L_{ij} \mid |\underline{X}_{ij} - \overline{x}_{ijk}| = 0\} \end{aligned}$$

Let $\rho^1_{ij} := \min_{k \in R_{ij} \setminus R^0_{ij}} \overline{X}_{ij} - \underline{x}_{ijk}$ ($\lambda^1_{ij} := \min_{k \in L_{ij} \setminus L^0_{ij}} |\underline{X}_{ij} - \overline{x}_{ijk}|$). We define:

$$\begin{aligned} \mathbf{R^1_{ij}} &:= \{k \in R_{ij} \mid \overline{X}_{ij} - \underline{x}_{ijk} = \rho^1_{ij}\} \\ \mathbf{L^1_{ij}} &:= \{k \in L_{ij} \mid |\underline{X}_{ij} - \overline{x}_{ijk}| = \lambda^1_{ij}\} \end{aligned}$$

Iteratively, let $\rho^t_{ij} := \min_{k \in R_{ij} \setminus \bigcup_{s=0}^{t-1} R^s_{ij}} \overline{X}_{ij} - \underline{x}_{ijk}$ ($\lambda^t_{ij} := \min_{k \in D_{ij} \setminus \bigcup_{s=0}^{t-1} L^s_{ij}} |\underline{X}_{ij} - \overline{x}_{ijk}|$). We define:

$$\begin{aligned} \mathbf{R^t_{ij}} &:= \{k \in R_{ij} \mid \overline{X}_{ij} - \underline{x}_{ijk} = \rho^t_{ij}\} \\ \mathbf{L^t_{ij}} &:= \{k \in L_{ij} \mid |\underline{X}_{ij} - \overline{x}_{ijk}| = \lambda^t_{ij}\} \end{aligned}$$

Let $\rho_{ij} \in \mathbb{N}$ ($\lambda_{ij} \in \mathbb{N}$) be the integer which satisfies:

- $R_{ij}^{\rho_{ij}} \neq \emptyset \qquad (L_{ij}^{\lambda_{ij}} \neq \emptyset)$
- $R_{ij}^{\rho_{ij}+1} = \emptyset \qquad (L_{ij}^{\lambda_{ij}+1} = \emptyset)$

Then, we have built a partition of R_{ij} (L_{ij}),

$$R_{ij} = \bigcup_{s=0}^{\rho_{ij}} R_{ij}^{s} \qquad (L_{ij} = \bigcup_{s=0}^{\lambda_{ij}} L_{ij}^{s})$$

in such a way that variables from R_{ij}^{t} (L_{ij}^{t}) allow pieces i and j to match in the horizontal direction less than variables from R_{ij}^{s} (L_{ij}^{s}) with $t < s \leq \rho_{ij}$ ($t < s \leq \lambda_{ij}$).

We say that R_{ij} (L_{ij}) has $\rho_{ij} + 1$ ($\lambda_{ij} + 1$) *classes*. Variables of $R_{ij}^{\rho_{ij}^{t}}$ ($L_{ij}^{\lambda_{ij}^{t}}$) belong to *class* ρ_{ij}^{t} (λ_{ij}^{t}).

Theorem 4
Let $i, j, k \in P$. If there are three subsets $R'_{ij} \subseteq R_{ij}$, $R'_{jk} \subseteq R_{jk}$ and $R'_{ki} \subseteq R_{ki}$ such that the following conditions hold:

1. $R'_{ij} \neq \emptyset$, $R'_{jk} \neq \emptyset$ and $R'_{ki} \neq \emptyset$.
2. For each subset of variables:
   - If $k \in R'_{ij}$ such that k belongs to class v ($k \in R_{ij}^{v}$), then $\bigcup_{l \leq v} R_{ij}^{l} \subseteq R'_{t}$.
   - If $k \in R'_{jk}$ such that k belongs to class v ($k \in R_{jk}^{v}$), then $\bigcup_{l \leq v} R_{jk}^{l} \subseteq R'_{t}$.
   - If $k \in R'_{ki}$ such that k belongs to class v ($k \in R_{ki}^{v}$), then $\bigcup_{l \leq v} R_{ki}^{l} \subseteq R'_{t}$.

   We denote by τ_{ij}^{*} the higher class given by variables from U'_{ij}. Similarly, τ_{jk}^{*} and τ_{ki}^{*} denote the higher class given by R'_{jk} and R'_{ki} respectively.
3. $$l_i + l_j + l_k - \varpi_1 - \varpi_2 > L_{sup}$$

   where $\varpi_1 \in \mathbb{R}$ and $\varpi_2 \in \mathbb{R}$ are, respectively, the largest and the second largest value of the following real numbers: $\{\rho_{ij}^{\tau_{ij}^{*}}, \rho_{jk}^{\tau_{jk}^{*}}, \rho_{ki}^{\tau_{ki}^{*}}\}$.

Then inequality (4.14) is valid.

$$\sum_{s \in R'_{ij}} b_{ijs} + \sum_{s \in R'_{jk}} b_{jks} + \sum_{s \in R'_{ki}} b_{kis} \leq 1. \tag{4.14}$$

We say that this inequality is a *horizontal clique associated with chain* $C(i, j, k, i)$.

Proof:
Similar to Theorem 2.

Theorem 5
Let $i_1, \ldots, i_r \in P$ be r pieces and let $R'_{s(s+1)} \subseteq R_{s(s+1)}, 1 \leq s \leq r$, where $i_{r+1} = i_1$, such that the following conditions hold:

- $R'_{s(s+1)} \neq \emptyset,\ 1 \leq s \leq r$
- If $k \in R'_{s(s+1)}$ such that $k \in U^v_{s(s+1)}$, then $\bigcup_{l \leq v} U^l_{s(s+1)} \subseteq R'_{s(s+1)}$.
- We denote by $t^*_{s(s+1)}$ the highest class given by variables from $R'_{s(s+1)}$. Then:

$$\sum_{h=1}^{r} l_h - (\sum_{h=1}^{r} \upsilon^{t^*_{h(h+1)}}_{h(h+1)} - \rho^{t^*_{\tau(\tau+1)}}_{\tau(\tau+1)}) > L_{sup},$$

  where $\tau \in \{1, \ldots, r\}$ satisfies: $\rho^{t^*_{\tau(\tau+1)}}_{\tau(\tau+1)} \leq \rho^{t^*_{h(h+1)}}_{h(h+1)}$, $\forall h \in \{1, \ldots, r\}$.

Then inequality (4.15) is valid. We say that this inequality is a *horizontal cover associated with chain* $1 - 2 - \cdots - r - 1$.

$$\sum_{h=1}^{r} \sum_{b_{h(h+1)k} \in U'_{h(h+1)}} b_{h(h+1)k} \leq r - 1. \tag{4.15}$$

Proof:
Similar to Theorem 3.

Let us consider the example with three pieces shown in Figure 3.1 and $W = 7$. We build a *clique* inequality as follows:
First, we identify the following sets of variables:

* $U^0_{12} = \{b_{121}\}$ y $U^1_{12} = \{b_{122}, b_{128}\}$. Furthermore, $\upsilon_{12} = 1$ y $\upsilon^1_{12} = 2$.
* $U^0_{23} = \{b_{231}\}$. Furthermore, $\upsilon_{23} = 0$.
* $U^0_{31} = \{b_{135}\}$ y $U^1_{31} = \{b_{134}, b_{136}\}$. Furthermore, $\upsilon_{31} = 1$ y $\upsilon^1_{31} = 2$.

Then, if we consider the following subsets:

- $U'_{12} = \{b_{121}, b_{122}, b_{128}\}$.
- $U'_{23} = \{b_{231}\}$.
- $U'_{31} = \{b_{135}\}$.

we can see that $w_1 + w_2 + w_3 - \varpi_1 - \varpi_2 = 4 + 3 + 3 - 2 - 0 = 8 > W$, so the corresponding *clique* is:

$$b_{121} + b_{122} + b_{128} + b_{231} + b_{135} \leq 1$$

4.4 *LU-cover* inequalities

LU cover inequalities have a similar idea to *cover* inequalities. The main difference is that in *LU cover* we do not take into account the order of the pieces when building a pile. That is, in the inequality we consider variables of *NFP*s from each pair of pieces of the set of pieces chosen to build the pile.

We denote by $\overline{Y}_{ij}$ ($\underline{Y}_{ij}$) the maximum (minimum) value of coordinate Y of the NFP_{ij} in the NFP_{ij}-coordinate system.

In order to know the extent that piece j protrudes from piece i in the vertical direction when a given *slice* is used, $b_{ijk} = 1$, we need to calculate $\overline{Y}_{ij} - \underline{y}_{ijk}$ if $\underline{y}_{ijk} > 0$, or $(-1)\underline{Y}_{ij} - (-1)\overline{y}_{ijk}$ if $\overline{y}_{ijk} < 0$. This is a measure of the overlap allowed for pieces i and j in the vertical direction, and we have to compare it with the minimum width of pieces i and j. If the difference is less than the minimum width of pieces i and j, then piece j must protrude from piece i. In the case that $\underline{y}_{ijk} < 0$ and $\overline{y}_{ijk} > 0$, the *slice* would allow piece j to be placed such that $y_j = y_i$ and piece j would not protrude from piece i.

Let $i, j \in P$. We define by $\mathbf{U^*_{ij}}$ ($\mathbf{D^*_{ij}}$) the set of binary variables whose associated *slices* separate piece j from on top of piece i (piece i on top of piece j):

$$\begin{aligned} \mathbf{D^*_{ij}} &:= \{B_{ijk} \mid (-1)\underline{Y}_{ij} - (-1)\overline{y}_{ijk} < w_{ij}\} \\ \mathbf{U^*_{ij}} &:= \{B_{ijk} \mid \overline{Y}_{ij} - \underline{y}_{ijk} < w_{ij}\} \end{aligned}$$

where $w_{ij} := \min\{w_i, w_j\}$.

In Figure 4.8 we present an example in which $w_i = 5$ and $w_j = 6$. *Slices* defined from variables $\{b_0, b_1, b_7, b_8\}$ separate piece j from on top of piece i. Variable b_0 forces piece j to be placed entirely on top of piece i, i.e. if $b_0 = 1$, then pieces i and j cannot overlap in the vertical direction. If we look at the *slice* defined by b_1, pieces can be placed in such a way that an overlap of 4 units in a vertical direction is allowed, then piece j would protrude just 2 units from piece i because $w_j = 6$ and piece i would protrude 1 unit below piece j. Note that $U^*_{ji} = \{b_0, b_1, b_7, b_8\}$ and $D^*_{ji} = \{b_3, b_4, b_5\}$.

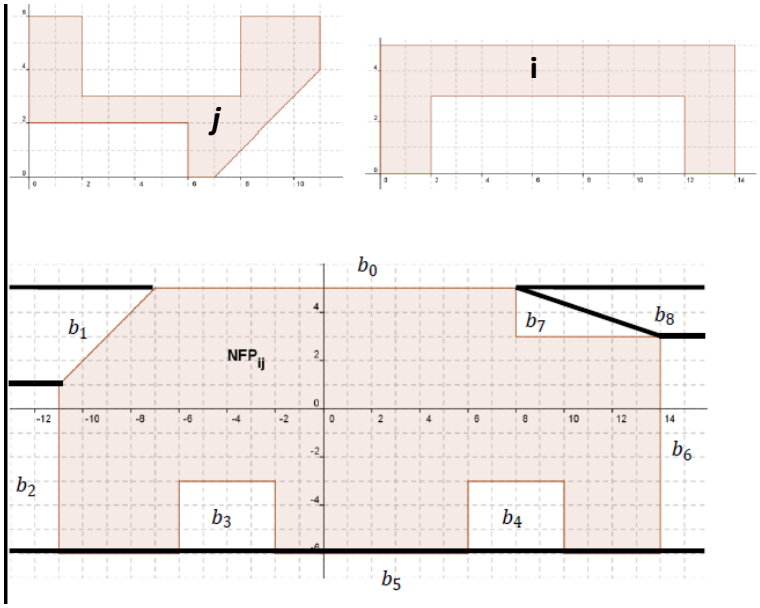

Figure 4.8: $U^*_{ji} = \{b_0, b_1, b_7, b_8\}$ *and* $D^*_{ji} = \{b_3, b_4, b_5\}$.

Let $C = \{i_1, \ldots, i_r\}$, $1 < r \leq N$ r, be a set of r pieces, and let $U'_{i_s i_t} \subseteq U^*_{i_s i_t}$, $U'_{i_s i_t} \neq \emptyset$ and $D'_{i_s i_t} \subseteq D^*_{i_s i_t}$, $D'_{i_s i_t} \neq \emptyset$, $\forall 1 \leq s < t \leq r$. We denote by h the index of a variable $b_{i_s j_t h}$ which satisfies $\underline{y}^h_{ij} = \overline{Y}_{ij}$ and h' the index of a variable $b_{i_s j_t h'}$ which satisfies $\overline{y}^{h'}_{ij} = \underline{Y}_{ij}$. We always consider that $b_{i_s i_t h} \in U'_{i_s i_t}$ and $b_{i_s i_t h'} \in D'_{i_s i_t}$. We denote by $UD'_{i_s i_t} := U'_{i_s i_t} \cup D'_{i_s i_t}$. Note that $U'_{i_s i_l} = D'_{i_l i_s} \forall i_s, i_t \in C$.

Theorem 6
If inequality (4.16) is satisfied, then inequality (4.17) is valid. We say that this inequality is an *LU-cover* inequality.

$$\sum_{s=1}^{r} w_{i_s} - \delta \quad > \quad W \tag{4.16}$$

$$\sum_{s=1}^{r-1} \sum_{l=s+1}^{r} \sum_{k \in UD'_{i_s i_l}} B_{i_s i_l k} \quad \leq \quad \sum_{s=1}^{r-1} (r-s) - 1. \tag{4.17}$$

where

$$\delta := \max_{\tau \in \pi\{C\}} \{ \sum_{t=1}^{r-1} \sum_{l \in U'_{\tau(t)\tau(t+1)}} q_{\tau(t)\tau(t+1)l} B_{\tau(t)\tau(t+1)l} \}$$

$q_{\tau(t)\tau(t+1)l}$ being the amount of overlap over the Y axis of pieces $\tau(t+1)$ and $\tau(t)$ when $b_{\tau(t)\tau(t+1)l} = 1$. $\pi\{C\}$ is the set of all the permutations of the pieces in C. An element $\tau \in \pi\{C\}$ is defined by $\tau = \{\tau(1), \ldots, \tau(r)\}$ where $\forall t, \tau(t) = i_l$ for some $l \in \{1, ..., r\}$.

Proof:
From equations $\sum_{k=1}^{m_{ij}} B_{ijk} = 1$ for each NFP_{ij}, $1 \leq i < j \leq N$ used in *HS2* formulation, we get:

$$\sum_{s=1}^{r-1} \sum_{l=s+1}^{r} \sum_{k \in UD'_{i_s i_l}} B_{i_s i_l k} \leq \sum_{s=1}^{r-1} (r-s).$$

Let us suppose that there is a solution satisfying the previous inequality as an equality. Note that all pieces $i_1, \ldots i_r$ have to be separated using *slices* whose associated binary variables belong to UD'_{ij}.

In order to calculate the minimum width given by any pile built with pieces $i_1, \ldots i_r$, we add up the width of the pieces as if they were placed one on top of the adjacent piece and then for each pair of adjacent pieces we have to subtract the maximum overlap allowed along the Y axis.

The minimum width of the r pieces is given by the left hand side of inequality (4.16), which is greater than W. Then, it is not possible that $\sum_{s=1}^{r-1} \sum_{l=s+1}^{r} \sum_{k \in UD'_{i_s i_l}} B_{i_s i_l k} = \sum_{s=1}^{r-1} (r-s)$, so inequality (4.17) holds. §

In the example appearing in Figure 4.8, the coefficients are:

$$\begin{aligned} q_{ij0} &= 0 \\ q_{ij1} &= 4 \\ q_{ij7} = q_{ij8} &= 2 \\ q_{ji3} = q_{ji4} &= 3 \\ q_{ji5} &= 0 \end{aligned}$$

Note that variables b_3, b_4 and b_5 belong to $U^*_{ji} = D^*_{ij}$ and we have to calculate how much piece j protrudes from piece i.

4.5 *Transitivity* inequalities

The idea of these inequalities is to identify subsets of variables which cannot take the value 1 simultaneously by studying the relative position between more than two pieces. If a given *slice* is used to separate pieces i_1 and i_2, and at the same time another *slice* which separates pieces i_1 from i_3 is used, then there could be some binary variables from $VNFP_{i_2 i_3}$ (the set of variables defined from $NFP_{i_2 i_3}$) that cannot take the value 1 because the problem would become unfeasible. We will use the classification of the binary variables into sets U, D, R and L. defined in Section 4.3.

These inequalities could be more accurate without using the classification of the binary variables but the computational effort would increase considerably. In order to reduce the effort needed to know which *slices* are incompatible, we will use the *extended slices* defined in Section 3.2.2.

In Section 3.3.2 we present an example of incompatibility involving three pieces of instance *shapes8*. In Figure 3.10 we can see that if variables $b_{122} = 1$ and $b_{138} = 1$, the variable b_{236} cannot take the value 1, so inequality $b_{122} + b_{138} + b_{236} \leq 2$ is valid in all the nodes of the branch & cut tree.

Note that we can consider more variables in order to lift the previous inequality. If we look at NFP_{23}, variables $b_{232}, b_{233}, b_{234}, b_{235}, b_{236}, b_{238}$ are also incompatible with $b_{122} = 1$ and $b_{138} = 1$, so the inequality $b_{122} + b_{138} + b_{232} + b_{233} + b_{234} + b_{235} + b_{236} + b_{238} \leq 2$ is also valid.

In the previous inequality we consider more than one binary variable from $VNFP_{23}$. It is possible to add other binary variables from $VNFP_{12}$ and $VNFP_{13}$ instead of these variables from $VNFP_{23}$, but we would have to check that there is no combination of three binary variables taking the value 1 producing a feasible solution. In Section 3.3.1 we presented several conditions to determine whether three binary variables are incompatible.

Chapter 5

Separation algorithms

In this Chapter we present separation algorithms for some of the inequalities presented in Chapter 4 and some computational results.

In Section 5.1 we present the separation algorithms for both types of *X-Y inequalities*. For *X-Y inequalities of type I* we use an exact procedure which is based on studying each one of the inequalities (9.7) used in the *HS2* formulation (non-overlapping inequalities). For *X-Y inequalities of type II* we propose an iterative procedure which builds either the most violated inequality or the inequality which is closest to being violated by the current fractional solution.

Separation for the *Impenetrability* constraints is discussed in Section 5.2. Finally, in Section 5.3 we present an algorithm to add all the *cliques* at the root node and two separation algorithms for the *cover* inequalities. The computational experiments in all the cases show that the separation algorithms require a great computational effort and, despite the fact that we need to explore fewer nodes on the solved instances, the computational time increases and it makes no sense to add the separation algorithms of these inequalities to the *Branch & Bound* algorithm described in Chapter 3.

We do not present any separation algorithm for the *LU-cover* inequalities described in Section 4.4 or the *Transitivity* inequalities defined in Section 4.5 because our computational experience shows that the separation algorithms that we have tried work in a similar way to the cover inequalities and it is not appropriate to add these inequalities to the *Branch & Bound* algorithm.

5.1 *X-Y* inequalities

In Section 4.1 we presented two types of *X-Y* inequalities. *X-Y inequalties of type I* are based on the non-overlapping constraints used in *HS1* and *HS2* formulations. These inequalities have an easy separation, obtaining at most one *X-Y* inequality for each inequality used to describe a *slice* in the *HS2* formulation. On the other hand, *X-Y inequalties of type II* have a more complex separation. We study both coordinates of each piece and binary variables with a greater value are included in the inequality. Note that in this case we study the interaction of one piece with all the other pieces.

In order to separate *X-Y inequalties of type I*, we study each one of the inequalities (9.7) in the *HS2* formulation defined from each *NFP*. These inequalities have the following structure:

$$\alpha_{ij}^{kf}(x_j - x_i) + \beta_{ij}^{kf}(y_j - y_i) \leq \sum_{h=1}^{m_{ij}} \delta_{ij}^{kfh} b_{ijh} \tag{5.1}$$

where $1 \leq i \leq j \leq N$, $k \in \{1, ..., m_{ij}\}$. In the case that $\alpha_{ij}^{kf} \neq 0$ and $\beta_{ij}^{kf} \neq 0$, i.e. the corresponding *X-Y* inequality has on the left-hand side two variables, then we build the *X-Y inequalty of type I* (see Section 4.1). Otherwise, we do not build the inequality because it would be dominated by an *X-Y inequality of type II*.

In order to separate *X-Y inequalties of type II*, we consider each one of the coordinates of each piece and, in each case, we build the most violated (or closest to being violated) by the current solution *X-Y inequality of type II*. Let s' be the solution given by the linear problem of the current node. We denote by $B^+ := \{b_{ijk} \mid b'_{ijk} > 0,\ \forall 1 \leq i < j \leq N, \forall 1 \leq k \leq m_{ij}\}$, where b'_{ijk} denotes the value of variable b_{ijk} in the solution s'. The set of variables B^+ contains the binary variables of the *HS2* formulation whose values in the current solution are positive.

Let $i \in P$. In what follows we build two inequalities, one for each coordinate of piece i. We define the following sets of binary variables:

- $B_{x_i}^+ := \{b_{ijk} \in B^+ \mid p_j \in P \setminus \{p_i\},\ \underline{x}_{jik} > 0\}$
- $B_{y_i}^+ := \{b_{ijk} \in B^+ \mid p_j \in P \setminus \{p_i\},\ \underline{y}_{jik} > 0\}$

The order of the variables in vectors $B_{x_i}^+$ and $B_{y_i}^+$ is given by the value of the given variables in the current solution in non-increasing order, i.e. the first positions are taken by the variables with large values in the current solution (s').

Let $t_x = |B_{x_i}^+|$ y $t_y = |B_{y_i}^+|$. We build the *X-Y inequality of type II* for coordinate x_i in t_x steps. In a similar way, we build the *X-Y inequality of type II* for coordinate y_i in t_y steps.

Let λ_j be the maximum value that the coefficient of any binary variable $b_{ijk} \in B_{x_i}^+$, $j \in \{1, \ldots, N\}$, $j \neq i$, can take. At the beginning we consider that $\lambda_j = 0, \forall p_j \in P \setminus \{p_i\}$.

In a first step we include the first variable of vector $B_{x_i}^+$, $b_{ij_1k_1}^x$, in the inequality. The corresponding coefficient is $\theta_1^x := \underline{x}_{ij_1k_1}^x + CX_{j_1}$, where $\underline{x}_{j_1ik_1}^x$ denotes the minimum value defined by $b_{ij_1k_1}^x$ on the X-axis in the NFP_{j_1i} coordinate system.

The inequality has the following structure:

$$x_i \geq \theta_1^x b_{ij_1k_1}^x$$

When $\theta_1^x b_{ij_1k_1}^x$ is added to the inequality, we update the value of $\lambda_{j_1} = \theta_1^x$. The previous inequality is going to be updated by adding more terms to the right-hand side until all the variables of $B_{x_i}^+$ have been studied. Let $b_{ij_2k_2}^x \in B_{x_i}^+$ ($b_{ij_2k_2}^x \in VNFP_{ij_2}$) be the next variable of $B_{x_i}^+$. The coefficient, θ_2^x, is calculated in the following way:

- If $j_1 = j_2 \Rightarrow \theta_2^x = \underline{x}_{j_2ik_2} + CX_{j_2}$.
- If $j_1 \neq j_2 \Rightarrow \theta_2^x = \underline{x}_{j_2ik_2} + CX_{j_2} - \sum_{r=1, r\neq i, j_2}^{N} \lambda_r$.

If $j_1 = j_2$, then variables $b^x_{ij_1k_1}$ and $b^x_{ij_2k_2}$ belong to the same *NFP* and as it is not possible for both to take the value 1 at once, their coefficients do not interfere. However, if $j_1 \neq j_2$, then it is possible for these two variables to take the value 1 simultaneously, so the sum of both coefficients must be lower than or equal to the maximum value that each coefficient could take individually. Note that $\sum_{r=1,r\neq i,j_2}^{N} \lambda_r = \theta^x_1$. In the case that $\theta^x_2 < 0$, the variable is not included in the inequality. If $\theta^x_2 > \lambda_{j_2}$, we update the value $\lambda_{j_2} = \theta^x_2$.

The inequality is modified in the following way:

$$x_i \geq \theta^x_1 b^x_{ij_1k_1} + \theta^x_2 b^x_{ij_2k_2}$$

Let us suppose that we have already done t iterations, $t < t_x$, there are new variables in the inequality and λ_j, $j \neq i$, has been updated in such a way that the following inequality holds:

$$x_i \geq \sum_{r=1}^{t} \theta^x_r b^x_{ij_rk_r} \tag{5.2}$$

where several coefficients $\theta^x_r, r = 1, \ldots, t$ may have taken the value 0. Let $b^x_{ij_{t+1}k_{t+1}}$ be the next variable of $B^+_{x_i}$ to be studied. The maximum coefficient of $b^x_{ij_{t+1}k_{t+1}}$ to add this variable in constraint (5.2) is given by:

$$\theta^x_{t+1} = \underline{x}_{j_{t+1}ik_{t+1}} + CX_{j_{t+1}} - \sum_{r=1,r\neq i,j_{t+1}}^{N} \lambda_r$$

In the case that $\theta^x_{t+1} < 0$, we consider $\theta^x_{t+1} = 0$ and we do not add variable $b^x_{ij_{t+1}k_{t+1}}$ to the constraint. If $\theta^x_{t+1} > 0$, we add a new term to the inequality, and in the case that $\theta^x_{t+1} > \lambda_{j_{t+1}}$ then the value of $\lambda_{j_{t+1}}$ is updated by $\lambda_{j_{t+1}} = \theta^x_{t+1}$.

Once all the variables of $B^+_{x_i}$ have been studied, a new *X-Y inequality of type II* is built:

$$x_i \geq \sum_{r=1}^{t_x} \theta^x_r b^x_{ij_rk_r}$$

The inequality *X-Y of type II* corresponding to coordinates *Y* can be obtained similarly:

$$y_i \geq \sum_{r=1}^{t_y} \theta^y_r b^y_{ij_rk_r}$$

θ^y_r being the coefficients calculated in a similar way to θ^x_r, and $b^y_{ij_rk_r}$ the variables belonging to $B^+_{y_i}$.

Any *X-Y* inequality is added to the linear problem of the current node and every node created in the same branch when it is violated by more than ϵ_1. Initially we consider $\epsilon_1 = 0.1$. The inequalities which are violated by less than ϵ_1 produce a slight modification of the current solution, so we do not add them to the linear problem.

Table 5.1: *Branch & Cut with XY inequalities*

Problem	XY1 + XY2							XY2							XY1						
	LB	GAP	Nnodes	Time	Separation Time	FV	XY	LB	GAP	Nnodes	Time	Separation Time	FV	XY	LB	GAP	Nnodes	Time	Separation Time	FV	XY
three	6.00	0.00	28	0.09	0.02	0	11	6.00	0.00	29	0.05	0.00	0	4	6.00	0.00	26	0.05	0.00	0	8
shapes4	24.00	0.00	10	0.11	0.00	0	4	24.00	0.00	10	0.09	0.00	0	3	24.00	0.00	16	0.09	0.00	0	1
fu5	17.89	0.00	465	0.25	0.11	9	149	17.89	0.00	474	0.22	0.06	9	126	17.89	0.00	470	0.14	0.00	7	86
glass1	45.00	0.00	0	0.09	0.00	0	0	45.00	0.00	0	0.11	0.00	0	0	45.00	0.00	0	0.11	0.00	0	0
fu6	23.00	0.00	191	0.23	0.09	7	133	23.00	0.00	182	0.20	0.05	6	95	23.00	0.00	212	0.11	0.02	14	60
threep2	9.33	0.00	6062	3.51	1.14	0	1973	9.33	0.00	6107	3.20	0.78	8	1545	9.33	0.00	6991	2.14	0.00	4	745
threep2w9	8.00	0.00	15756	9.86	3.21	1008	11510	8.00	0.00	16342	9.91	3.03	957	10443	8.00	0.00	15596	5.55	0.08	898	6495
fu7	24.00	0.00	265	0.42	0.09	29	400	24.00	0.00	203	0.30	0.12	13	280	24.00	0.00	280	0.22	0.00	24	145
glass2	45.00	0.00	1834	7.07	1.08	117	5979	45.00	0.00	1758	6.15	1.15	93	5276	45.00	0.00	1863	2.31	0.02	102	1478
fu8	24.00	0.00	1001	1.42	0.62	87	1378	24.00	0.00	413	0.62	0.23	26	560	24.00	0.00	908	0.55	0.00	67	550
shapes8	26.00	0.00	11402	12.68	3.00	630	11022	26.00	0.00	10677	11.86	3.20	662	10574	26.00	0.00	12305	7.69	0.03	748	5821
fu9	25.00	0.00	197463	202.57	76.63	13766	193212	25.00	0.00	202416	199.15	74.94	12903	187534	25.00	0.00	166032	82.20	0.90	9051	77885
threep3	13.53	0.00	2876976	2757.35	812.27	19749	1290068	13.53	0.00	3018257	2822.92	816.45	24183	1313935	13.53	0.00	3211906	1776.55	11.12	23613	889705
threep3w9	10.00	0.09	2825666	3565.96	1100.54	139968	3135650	10.00	0.11	2644912	3222.33	997.78	131288	2850692	10.00	0.09	5463455	3566.81	23.42	304902	3371871
fu10	28.69	0.00	976564	1445.32	503.09	76216	1266894	28.68	0.00	953524	1430.33	496.27	74569	1163739	28.69	0.00	906734	609.50	4.18	72063	517532
dighe2	100.00	0.00	4429	28.13	4.77	625	18370	100.00	0.00	3851	26.18	4.70	494	14611	100.00	0.00	4370	13.73	0.05	648	5001
fu	28.00	-1.00	796027	3591.05	1011.29	78982	2356059	28.00	-1.00	842213	3579.05	1017.81	78799	2230902	30.00	-1.00	2837758	3575.36	32.56	324573	2959123
poly1a0	13.00	-1.00	593367	3592.87	757.73	121052	3005951	13.00	0.25	748746	3576.34	880.77	136730	3317781	13.00	0.24	1686120	3582.19	25.72	284436	4328784
dighe1	85.00	-1.00	186955	3595.93	515.80	19888	1121163	85.19	-1.00	201722	3573.86	521.32	22047	1098912	90.33	-1.00	459234	3590.39	19.23	54199	646499
J2-10-35-9	18.62	0.00	877233	1394.71	388.38	100819	1555110	18.62	0.00	928350	1417.16	389.21	109727	1596151	18.62	0.00	890338	762.13	4.48	105693	1014935
J2-10-35-8	22.00	0.00	212680	359.19	129.96	22540	370836	22.00	0.00	185031	300.16	107.28	19097	296039	22.00	0.00	172418	118.79	0.84	15863	117172
J2-10-35-7	18.67	0.00	286026	418.39	126.59	32874	523229	18.67	0.00	344069	493.48	148.20	40556	625905	18.67	0.00	291302	224.25	1.44	35715	382301
J2-10-35-6	18.00	0.00	1988136	2979.57	861.36	227334	3041733	18.00	0.00	1877921	2684.54	766.26	223177	2761875	18.00	0.00	2007734	1599.65	8.02	229381	1915170
J2-10-35-5	20.00	0.00	325264	489.25	148.48	38561	513291	20.00	0.00	383017	559.28	167.47	46709	577987	20.00	0.00	366760	278.59	1.56	45744	349828
J2-10-35-4	19.44	0.00	1185856	2041.83	620.45	185875	2625428	19.43	0.00	1128749	1891.82	570.57	176203	2390953	19.44	0.00	1042240	786.76	4.06	176024	1445922
J2-10-35-3	20.00	0.02	2254313	3576.46	1163.08	200438	3736529	20.00	0.02	2360461	3571.19	1155.00	203082	3613464	20.38	0.00	2218086	1493.43	8.21	184861	1714825
J2-10-35-2	19.95	0.00	224637	427.94	124.97	29470	489019	19.95	0.00	251721	453.06	131.15	32594	515185	19.95	0.00	251027	222.61	1.37	33111	316382
J2-10-35-1	21.30	0.00	517025	870.55	282.69	53870	868337	21.30	0.00	643841	1038.17	330.19	66034	1021907	21.30	0.00	501411	385.49	2.50	49967	429790
J2-10-35-0	23.66	0.00	1208417	2526.53	755.03	157306	2528264	23.66	0.00	1078265	2208.49	656.59	140901	2156474	23.66	0.00	1135719	1011.57	6.94	159046	1264005
J1-12-15-9	12.00	0.00	32208	107.34	34.80	4054	86196	12.00	0.00	42808	130.60	42.79	5377	106936	12.00	0.00	35172	41.79	0.37	4113	38679
J1-12-15-8	17.00	0.00	152684	716.62	181.41	11255	389892	17.00	0.00	155021	696.45	176.69	12303	377710	17.00	0.00	162646	246.09	1.28	12548	117341
J1-12-15-7	13.00	0.00	148905	414.76	118.81	14945	339036	13.00	0.00	171525	470.81	135.44	17271	379013	13.00	0.00	121125	148.33	0.89	12288	110057
J1-12-15-6	14.00	0.07	916930	3586.48	934.66	118156	2823282	14.50	0.01	1019142	3572.73	908.08	129795	2757926	14.71	0.00	1031396	1447.14	7.46	142618	1426214
J1-12-15-5	13.00	0.07	1061438	3585.39	1041.76	110874	2550464	13.00	0.04	924123	3579.44	989.86	98772	2352623	13.55	0.00	1163219	1431.68	10.03	123902	1001055
J1-12-15-4	17.50	0.00	649672	2777.63	632.97	64289	1511026	17.50	0.00	655889	2704.71	616.05	65420	1438674	17.50	0.00	649191	977.07	5.90	63416	427769
J1-12-15-3	10.93	0.00	409258	1021.00	289.35	50144	791198	10.93	0.00	439052	1031.31	293.50	54388	786270	10.93	0.00	408227	529.56	3.35	52957	466977
J1-12-15-2	16.00	0.00	233520	894.57	243.33	23991	580773	16.00	0.00	199703	736.03	200.20	21004	476000	16.00	0.00	174545	244.97	1.28	17669	128764
J1-12-15-1	14.00	0.00	563893	1658.62	481.34	64917	1214376	14.00	0.00	1110920	3262.67	944.15	134133	2518901	14.00	0.00	648886	843.44	5.41	73488	650624
J1-12-15-0	15.00	0.00	67658	301.25	82.74	6631	191259	15.00	0.00	68951	320.24	88.73	6958	203237	15.00	0.00	70929	106.63	0.66	6932	59860

5.1.1 Computational results

In order to study the effect of the *XY* inequalities, we have considered three different versions of the *Branch & Cut* algorithm. The first one separates both types of inequalities (*XY1 + XY2*), the second version separates just the second type of *XY* inequalities and the third version only tries to find *XY* inequalities of type I. In Table 5.1 we can see the computational results obtained by these three versions on instances described in Table 1.2. The time limit on all the algorithms is one hour.

We can see that, in general, the computational effort needed to separate *XY* inequalities of both types is not justified. The first column in each algorithm is the lower bound that the algorithm reaches in one hour. The second column represents the relative GAP ($\frac{UB-LB}{UB}$). A value of -1 represents that the given algorithm is not able to find any feasible solution. Note that in instances *fu* and *dighe1*, no algorithm is able to find a feasible solution, so the gap does not make sense. The first algorithm also fails to find a feasible solution for instance *poly1a0*. If we look at instances for which the gap is positive (unsolved instances), we can see that the best results are obtained with *XY1*, probably because it is faster and the algorithm studies a larger number of nodes.

The third and fourth columns represent, respectively, the computational time used by *CPLEX* and the computational time required by the separation algorithm. We can see that the last algorithm has a lower separation time than the first two, that is, the separation of the *XY inequalities of type 2* is very slow.

Finally, in the two last columns we include the number of binary variables fixed to 0 (incompatible variables, see Section 3.3), and the number of *XY inequalities* added in the whole branch and cut tree.

5.2 *Impenetrability* constraints

In Section 4.2 we defined the *impenetrability constraints*. These inequalities study the sum of the coordinates of two pieces and the relation of this sum and the binary variables belonging to the *NFP*.

We build the *impenetrability constraint* for each pair of pieces $i, j \in P$ only in the following cases:

- There is a variable $b_{ijk} \in VNFPij$ such that the value in the current solution is fractional, between 0 and 1. Note that if there are no variables of $VNFP_{ij}$ with a fractional value in the current solution, then there is a variable with a value of 1, which means that pieces i and j are separated and no *impenetrability* constraint is violated.

- The enclosing rectangles of both pieces have a non-empty intersection. In the case that the intersection is built, then the pieces are separated and no *impenetrability constraint* would be violated.

Once we have decided to build the inequality, its coefficients can be calculated by using either the exact or the approximate methods described in Section 4.2. The exact method requires a very high computational effort and the separation would be very slow.

Every time an inequality is built, it is added to the linear problem in the case of it being violated by more

than ϵ_2, i.e. if:

$$s^* - \sum_{l=1}^{m_{ij}} q_l b^*_{ijl} \leq -\epsilon_2 \tag{5.3}$$

where $s^* = x^*_i + y^*_i + x^*_j + y^*_j$; x^*_i, y^*_i, x^*_j, y^*_j y $b^*_{ijk}, \forall k \in \{1, \ldots, m_{ij}\}$ being the values in the solution of the corresponding variables. Initially we consider that $\epsilon_2 = 0.1$.

5.2.1 Computational results

In Table 5.2 we can see the computational results of the branch and cut algorithm when *XY of type 1* and *impenetrability* inequalities are identified and added. We have used instances described in Table 1.2.
The second column shows the lower bound that the algorithm reaches after one hour. The gap is represented in the third column. The fourth column shows the number of nodes of the branch and cut tree. The total time and the separation time are represented, respectively, in the fifth and sixth columns. The number of fixed binary variables (FV) throughout the tree is represented in the seventh column. The next column, *NRest*, shows the number of inequalities added in all the nodes and the last two columns represent, respectively, the number of inequalities added in the root node and the lower bound obtained after the root node is studied.

We can see that the computational effort needed to separate the impenetrability constraints is not justified. Branching is a better strategy than trying to find these types of inequalities.

5.3 *Cliques* y *Covers*

In Section 4.3 we defined the *clique* and *cover* inequalities. The idea of separating these inequalities is based on finding a set of pieces and a set of binary variables in such a way that the sum of the values of the binary variables is as high as possible and they force the pieces to pile up.

Let $C' = C(1, 2, \ldots, r)$, $3 \leq r \leq N$ be a chain of pieces and let $U'_{s(s+1)} \subseteq U_{s(s+1)}, 1 \leq s < r$, and $U'_{r1} \subseteq U_{r1}$ be the subsets of the chosen binary variables. Let $B^* := \bigcup_{s=1}^{r-1} U'_{s(s+1)} \cup U'_{r1}$. In order to identify violated inequalities, the next two conditions must be satisfied:

(AP) Pieces must be stacked, i.e. the sum of the given binary variables must satisfy:

$$\sum_{b_{ijk} \in B^*} b'_{ijk} \geq r - 2,$$

where b'_{ijk} denotes the value of the variable in the current solution.

(EX) The total width of the given pieces subtracting the maximum overlap of the pieces in a vertical direction must exceed the width of the strip. That is, condition (4.12) must be satisfied.

In the next subsection we present an exact method for the separation of the *clique* inequalities. In Subsections 5.3.2 and 5.3.3 we propose two different heuristic algorithms, a first algorithm with a more exhaustive search and the second algorithm which is simpler and faster.

Table 5.2: *Branch & Cut + IMPENETRABILITY + XY*1

Problem	IMPENETRABILITY + XY1								
	LB	GAP	Nnodes	Time	Separation time	FV	NRest	NR0	LB0
three	6.00	0.00	24	0.09	0.00	0	10	0	4.00
shapes4	24.00	0.00	9	0.08	0.00	0	7	7	21.27
fu5	17.89	0.00	459	0.20	0.00	15	158	4	14.00
glass1	45.00	0.00	0	0.12	0.00	0	5	5	45.00
fu6	23.00	0.00	169	0.16	0.00	3	65	4	14.00
tresp2	9.33	0.00	6854	2.85	0.48	11	962	8	5.00
tresp2w9	8.00	0.00	15792	7.38	1.01	986	7486	8	4.00
fu7	24.00	0.00	171	0.20	0.02	9	72	19	14.00
glass2	45.00	0.00	2060	3.98	0.53	141	2016	22	34.00
fu8	24.00	0.00	700	0.72	0.05	46	559	4	14.00
shapes8	26.00	0.00	10845	8.77	0.87	690	6029	15	16.00
fu9	25.00	0.00	178004	110.37	10.34	13011	105137	31	14.00
tresp3	13.53	0.00	2776978	1860.98	187.83	17520	714015	6	5.00
tresp3w9	10.00	0.09	4448536	3524.59	361.50	251912	2979949	12	4.00
fu10	28.69	0.00	813207	651.57	57.21	63194	531849	24	14.00
dighe2	100.00	0.00	3765	15.80	0.98	401	3834	66	67.00
fu	30.00	0.12	2224684	3405.10	394.93	206344	2296365	25	14.00
poly1a0	13.00	0.22	1228164	3528.90	312.13	237736	4281461	112	13.00
dighe1ok	89.10	0.33	311068	3594.03	209.18	31542	378513	143	56.00
J2-10-35-9	18.62	0.00	789616	794.95	63.32	94169	905585	22	12.00
J2-10-35-8	22.00	0.00	123512	103.02	10.26	9803	86340	11	12.00
J2-10-35-7	18.67	0.00	254364	239.31	20.40	35617	353998	18	12.00
J2-10-35-6	18.00	0.00	1932739	1838.85	131.51	230074	1940402	12	12.00
J2-10-35-5	20.00	0.00	432430	396.26	31.90	50271	405917	10	12.00
J2-10-35-4	19.44	0.00	1030523	932.39	64.18	178838	1532060	14	12.00
J2-10-35-3	20.37	0.00	2149237	1839.77	138.22	182364	1984297	5	12.00
J2-10-35-2	19.95	0.00	195338	223.44	24.55	26882	240879	19	12.00
J2-10-35-1	21.30	0.00	287296	263.94	23.62	27610	236471	19	12.00
J2-10-35-0	23.66	0.00	1093007	1251.19	134.47	155785	1202051	11	12.00
J1-12-15-9	12.00	0.00	13678	23.74	2.40	1794	14828	28	6.00
J1-12-15-8	17.00	0.00	143581	326.67	24.38	9895	89891	21	8.00
J1-12-15-7	13.00	0.00	135682	206.37	19.31	13612	136873	20	6.00
J1-12-15-6	14.71	0.00	1133536	1829.47	136.06	157573	1648729	23	8.00
J1-12-15-5	13.55	0.00	1368169	2039.49	208.98	149769	1323670	26	7.00
J1-12-15-4	17.50	0.00	646391	1155.98	97.42	65418	488509	27	8.00
J1-12-15-3	10.93	0.00	602760	889.94	78.52	74640	675109	34	7.00
J1-12-15-2	16.00	0.00	159673	264.39	21.53	15253	121729	24	8.00
J1-12-15-1	14.00	0.00	978985	1557.73	157.98	109504	1132158	39	6.00
J1-12-15-0	15.00	0.00	64039	123.72	11.19	6111	54182	10	6.00

5.3.1 Finding all the *Cliques*

Clique inequalities consider combinations of 3 pieces. What is needed is a subset of binary variables such that if two variables take the value 1, then the three pieces are stacked and the pile exceeds the width of the stock sheet.

Let us consider the directed graph $G = (V, E)$. The set of vertices V represents all the variables in the problem, i.e. each vertex is associated with a binary variable b_{ijk}, for any $i, j \in P$, $k \in VNFP_{ij}$. We add an arc for each pair of vertices $(b_{ij_1k_1}, b_{ij_2k_2})$, $i, j_1, j_2 \in P$.

Then, by construction, any maximal clique of $G = (V, E)$ involves at most three pieces. Note that it is possible for a clique to involve only two pieces. We do not take into account these cliques. In order to build a *clique* inequality we consider the maximal cliques in graph $G = (V, E)$ which involve exactly three pieces.

Then, all the sets of three pieces and the respective subsets of binary variables needed to build a clique inequality (see theorem 2) are given by all the maximal cliques in graph $G = (V, E)$. We use the Patric and Östergård ([52]) algorithm to obtain all the maximal cliques in the graph.

5.3.2 *SC1* algorithm

SC1 is a heuristic algorithm for separating *clique* and *cover* inequalities. In a first step we choose a promising chain of pieces, i.e. the relative position of the pieces form a pile. In order to obtain the chain of pieces we solve a shortest path problem in a graph. In a second step we select the binary variables that we will consider in the inequality of each *NFP* formed by two pieces of the chain.

We denote by N_{min} the minimum number of pieces needed to exceed the width of the strip. Let P_{min} be an ordered list of pieces in a non-decreasing order of width. Then, we need the first N_{min} pieces of P_{min} to exceed the width of the strip.

Let w_{min} be the minimum width such that, when we add up the width of the $N_{min} - 1$ first pieces of P_{min} and w_{min}, then the width of the strip is exceeded. We denote by p_{min} the piece which satisfies:

- $w_{p_{min}} > w_{min}$
- There is no piece whose width is less than w_{min} and greater than $w_{p_{min}}$.

Let N^* be the number of pieces whose width is greater than w_{min}.

In order to obtain a chain of pieces we build the next graph. Let $G = (V, A)$ be a directed graph represented in Figure (5.1). We denote the set of vertices by V and the set of arcs by A.

The set of vertices is formed by $r + 1$ copies of each of the N^* widest pieces ($r \geq 3$) in such a way that $|V| = (r + 1)N^*$. We represent the different copies of piece i by $i,\ i + N^*,\ i + 2N^*, \ldots,\ i + (r + 1)N^*$. Initially we consider that $r = N_{min}$ because it makes no sense to consider fewer pieces (condition (EX) would not be satisfied). Then, we study the case $r = N_{min} + 1$.

Set A is formed by arcs (i, j) such that $i \in \{tN^* + 1, \ldots, tN^* + N^*\}$, $j \in \{(t + 1)N^* + 1, \ldots, (t + 1)N^* + N^*\}$ and $p_{j-(t+1)N^*} \neq p_{i-tN^*}\ \forall t \in \{0, \ldots, r\}$. That is, i and j make reference, respectively, to the t and $t + 1$ copy of pieces p_{i-tN^*} and $p_{j-(t+1)N^*}$, which are represented in columns t and $t + 1$ of the graph. Note that i and j have to make reference to different pieces. The cost of arc (i, j) is given by:

$$1 - \sum_{k \in U_{i-tN^*, j-(t+1)N^*}} b'_{i-tN^*, j-(t+1)N^*, k}$$

Once the graph G is generated, we calculate the N^* shortest paths between each one of the vertices in the first column and the vertices in the last column (last copy), in such a way that the initial and the final vertices of the path represent the same piece. If there is a path whose length is lower that 2, then the chain of pieces given by the path satisfies condition (AP) and i would be interesting to study it.

Let $\gamma = (i_1, \ldots, i_r, i_1)$ be the shortest path. In order to reduce the notation, we consider now that $i_1, \ldots, i_r$ make reference to the pieces and not to the copies. One of the following conditions hold:

(a) The chain given by path γ does not repeat any pieces with the exception of piece i_1.

(b) There is a piece i_k, $k \neq 1$ such that it appears more than once in path γ, i.e. $\gamma = (i_1, \ldots, i_k, \ldots, i_k, \ldots, i_r, i_1)$.

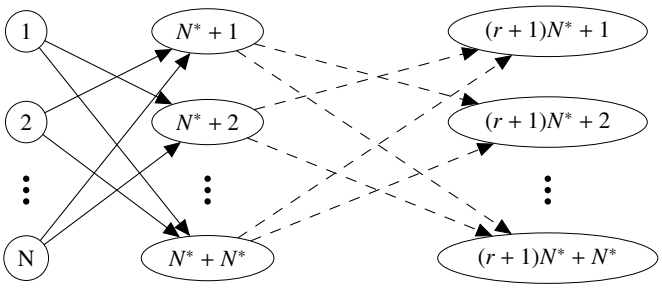

Figure 5.1: *Directed graph used to obtain the set of pieces*

We do not study case (b) because the value of the binary variables is strongly reduced and the given path is not promising to find a violated inequality. We will continue studying the shortest path with other endpoints.

If case (a) holds, then we consider the chain given by the path in order to build a *clique* or a *cover* inequality (condition (AP) holds). Then, we have to check if condition (EX) is satisfied.

Path γ provides the chain $C_\gamma = C(i_1, \ldots, i_r)$. We know that the following condition holds:

1. $\sum_{s=1}^{s=r} w_{i_s} > W$
2. $\sum_{b_{ijk} \in B^T} b_{ijk} > r - 2$, where $B^T := \bigcup_{s=1}^{s<r} U_{s(s+1)} \cup U_{r1}$

Condition 1 shows that pieces exceed the width of the strip if they cannot overlap in the vertical direction. On the other hand, condition 2 shows that pieces form a pile because the sum of variables that we consider is greater than or equal to $r - 2$. Note that we consider all possible matchings of pieces in the vertical direction because we consider all the binary variables whose *slices* separate both pieces in the *NFP* in a vertical direction.

We define $h_{ex} := \sum_{s=1}^{s=r} w_{i_s} - W$ and $h_{ap} := \sum_{b_{ijk} \in B^T} b_{ijk} - (r - 2)$. These two numbers make reference to the slack that conditions 1 and 2 have.

Let $S := (\upsilon_{12}^{t_{12}}, \ldots, \upsilon_{(r-1)r}^{t_{(r-1)r}}, \upsilon_{r1}^{t_{r1}})$ be the vector of allowed overlap. Initially, as we consider all variables of subsets $U_{s(s+1)}$, $s = 1, \ldots, r-1$ and U_{r1}, then $\upsilon_{s(s+1)}^{t_{s(s+1)}} = \upsilon_{s(s+1)}^{\upsilon_{s(s+1)}}$ and $\upsilon_{r1}^{t_{r1}} = \upsilon_{r1}^{\upsilon_{r1}}$.

The chain C_γ defines r feasible orderings of the pieces. Each one of them can be obtained by changing the piece which is situated at the bottom of the pile, and the subsequent pieces are given by the next pieces of C_γ until all the pieces are stacked. In order to obtain the ordering with more overlap in the Y axis, i.e. the ordering of the r pieces in such a way that the width of the pile is minimum, we have to add up all the elements of vector S with the exception of the minimum value, which makes reference to the pair of pieces with less overlap allowed.

Let $s' = \min\{\min_{1 \leq s < r} \upsilon^{t_{s(s+1)}}_{s(s+1)}, \upsilon^{t_{r1}}_{r1}\}$. The width of the ordering with maximum overlap, a_m, is given by:

$$a_m = \sum_{s=1}^{s=r} w_{i_s} - (\sum_{s=1}^{s<r} \upsilon^{t_{s(s+1)}}_{s(s+1)} + \upsilon^{t_{r1}}_{r1} - s')$$

We consider these two cases:

- If $a_m > W$ ($\sum_{s=1}^{s<r} \upsilon^{t_{s(s+1)}}_{s(s+1)} + \upsilon^{t_{r1}}_{r1} - s' < h_{ex}$), then we have found a violated inequality by adding all the variables of B^T to the inequality.
- In the case that $a_m < W$, then the ordering with the minimum width fits on the strip. We then try to eliminate some variables of B^T in order to forbid certain overlaps of pieces in the vertical direction.

When we are in the second, we select one of the subsets $U^* \in U_{s(s+1)} \cup U_{r1}$ and eliminate variables in the following way:

(P1) We select a set $U_* \in U_{s(s+1)} \cup U_{r1}$ which has not been studied yet.

(P2) We calculate the overlap of the class of variables that we are going to eliminate as $sc^* = \max\{s', W - a_m + \epsilon\}$, where $\epsilon > 0$. We denote by c^* the class which allows more overlap in such a way that the overlap is lower than or equal to sc^*. Note that we eliminate the variables which allow placements with an overlap greater than sc^* in order to attain one of the following goals:

- The width of the minimum ordering exceeds W.
- The ordering with minimum width is changed.

(P3) Let $U^*_1 = U^{c^*}_*$. If it is satisfied that $\sum_{b \in U^*_1} b < h_{ap}$, i.e. when variables which allow more overlap are eliminated and pieces are still stacked, then we update the sets $B^T \leftarrow (B^T \setminus U_*) \cup U^*_1$ y $U_* \leftarrow U^*_1$. In the case that condition $\sum_{b \in U^*_1} b < h_{ap}$ holds, we label all the sets as not studied. If the previous condition is not satisfied, then set U_* is labeled as studied.

(P4) If the new chain with minimum width exceeds the width of the strip, we have found a violated inequality. Otherwise, we go back to step (P1).

5.3.3 *SC2* algorithm

For each piece p_i, $i = 1, \ldots, N$ we calculate:

$$U^*_i = \{j \mid j \neq i, u^*_{ij} > \epsilon\}$$

where $u^*_{ij} = \sum_{b_{ijk} \in U_{ij}} b^*_{ijk}$. Note that if $\epsilon > 0.5$, then $j \in U_i \Rightarrow i \notin U_j$.

This algorithm consists in building a tree for each piece. Let $i \in P$. The nodes of the tree represent the pieces. The root node is given by piece i. The successors of a given node k are the pieces of U^*_k such that the chain given by the nodes form the root node to k can generate a violated *clique* or *cover* inequality. Let C be the chain of pieces from the root node (i) to the node defined by piece $k' \in U^*_k$. Let $\alpha_{k'} = \sum_{p_t \in C} w_t$ and let $\delta_{k'}$ be the maximum overlap allowed by chain C. Let $\beta_{k'} = \sum_{t=1}^{|C|-1}(1 - u^*_{C(t),C(t+1)})$. In order to add a successor, the following conditions must be satisfied:

1. $\beta_{k'} < \epsilon_2$

2. $\alpha_{k'} - \delta_{k'} < W$

We consider that $\epsilon = 0.4$ and $\epsilon_2 = 1.7$. In a future study it could be interesting to change these parameters.

In the case that Condition 1 is satisfied and Condition 2 is not, adding the root node to C we obtain a chain that produces a violated *clique* or *cover* inequality. In the case that Condition 1 is not satisfied, we reject chain C and close node k'.

5.3.4 Computational results

In Table 5.3 we can see the effect of adding the *clique* and *cover* inequalities to the *Branch & Cut* algorithm. We have used instances presented in Table 1.2. We present the computational results of three algorithms. The first one, (A), adds all the clique inequalities at the beginning and then there are no separation algorithms for any type of inequality. The second algorithm, (B), separates the *clique* and *cover* inequalities using the *SC1* algorithm. Finally, (C) uses the *SC2* separation algorithm.

The first column in each algorithm shows the lower bound that the algorithm reaches after one hour. The gap is represented in the second column. The third column shows the number of nodes of the branch and cut tree. The total time is represented in the fourth column. The fifth and sixth columns show, respectively, the number of inequalities added at all the nodes and at the root node.

As happened with the previous inequalities, these separation procedures require an excessive computational effort and it does not make sense to use them in the *Branch & Cut* algorithm.

Table 5.3: *(A) Branch & Cut with all cliques added at the root node. (B) Branch & Cut with SC1 algorithm for cliques and covers. (C) Branch & Cut with SC2 algorithm for cliques and covers.*

Problem	(A)						(B)						(C)					
	LB	GAP	Nnodes	Time	NR	NR0	LB	GAP	Nnodes	Time	NR	NR0	LB	GAP	Nnodes	Time	NR	NR0
three	6	0	0	0.78	0	0	6.00	0.00	0	0.51	0	0	6.00	0.00	0	0.61	0	0
shapes4	24.00	0.00	12	0.09	0	0	24.00	0.00	12	0.05	0	0	24.00	0.00	12	0.03	0	0
fu5	17.89	0.00	492	0.41	1	1	17.89	0.00	462	0.09	11	10	17.89	0.00	506	0.11	6	1
glass1	45.00	0.00	0	0.09	0	0	45.00	0.00	0	0.08	0	0	45.00	0.00	0	0.03	0	0
fu6	23.00	0.00	153	0.34	0	0	23.00	0.00	154	0.66	8	7	23.00	0.00	155	0.78	7	7
threep2	9.33	0.00	5852	1.33	1	1	9.33	0.00	6200	3.00	20	11	9.33	0.00	5777	1.01	11	9
threep2w9	8.00	0.00	18181	9.45	153	153	8.00	0.00	16846	10.26	182	53	8.00	0.00	17875	7.00	148	36
fu7	24.00	0.00	171	0.87	0	0	24.00	0.00	155	1.19	16	16	24.00	0.00	211	0.72	8	8
glass2	45.00	0.00	2243	2.48	20	20	45.00	0.00	2043	5.63	49	30	45.00	0.00	2341	2.67	54	36
fu8	24.00	0.00	235	0.64	2	2	24.00	0.00	202	1.83	29	28	24.00	0.00	350	0.89	83	76
shapes8	26.00	0.00	12345	6.21	124	124	26.00	0.00	11255	33.79	250	127	26.00	0.00	11944	5.83	205	108
fu9	25.00	0.00	176826	31.42	2083	2083	25.00	0.00	198719	1766.38	4358	1556	25.00	0.00	228453	60.65	2360	450
threep3	13.53	0.00	2824979	936.65	4436	4436	12.00	0.11	357555	3597.09	646	141	13.53	0.00	2777515	850.99	2885	132
threep3w9	10.71	0.03	11398947	3745.38	113459	113459	9.00	0.20	397973	3608.04	4790	1317	10.00	0.09	7082761	3590.44	64018	1017
fu10	28.69	0.00	1103397	278.90	13881	13881	24.00	0.20	151555	3596.74	4767	2713	28.69	0.00	1062297	807.77	9841	1652
dighe2	100.00	0.00	4483	10.48	75	75	100.00	0.00	4883	127.44	418	353	100.00	0.00	4454	8.55	158	90
J1-10-20-0	18.00	0.00	7280	34.18	43	43	18.00	0.00	5569	123.54	83	44	18.00	0.00	8009	10.31	156	79
J1-10-20-1	17.00	0.00	8380	7.10	32	32	17.00	0.00	9217	182.10	31	2	17.00	0.00	12587	7.10	88	27
J1-10-20-2	20.00	0.00	12433	40.14	71	71	20.00	0.00	17450	313.14	188	50	20.00	0.00	11100	6.16	119	41
J1-10-20-3	20.75	0.00	768432	347.10	4533	4533	19.00	0.10	187520	3597.37	1517	301	20.75	0.00	616733	271.46	3458	282
J1-10-20-4	12.50	0.00	158951	102.01	1925	1925	12.50	0.00	189076	3190.22	3009	493	12.50	0.00	123961	86.02	1962	374
J2-10-35-0	23.66	0.00	1492983	607.84	31663	31663	21.75	0.13	166726	3594.23	8674	5534	22.00	0.12	734730	3594.17	19634	4244
J2-10-35-1	21.30	0.00	579497	206.08	9145	9145	20.00	0.09	184378	3595.40	5662	2930	21.30	0.00	732201	489.36	11114	1246
J2-10-35-2	19.95	0.00	286472	115.08	5991	5991	19.70	0.02	190436	3594.26	8553	5175	19.95	0.00	404291	1140.54	9836	3645
J2-10-35-3	20.37	0.00	2535369	706.93	33234	33234	19.75	0.06	179828	3592.70	6654	4111	20.00	0.02	2667239	3593.19	29351	3503
J2-10-35-4	19.43	0.00	1149119	343.08	25173	25173	18.00	0.10	171418	3628.07	10004	7132	18.50	0.05	790713	3639.67	28357	7599
J1-12-20-0	12.00	0.00	67950	49.56	1320	1320	12.00	0.00	31980	2405.08	4373	3740	12.00	0.00	29060	118.89	4335	3846
J1-12-20-1	10.00	0.00	59193	49.42	1080	1080	10.00	0.09	50874	3592.25	1620	808	10.00	0.00	149688	208.14	5108	3096
J1-12-20-2	12.00	0.00	30249	38.47	390	390	12.00	0.00	42161	3352.31	5044	4439	12.00	0.00	37217	730.77	7644	7095
J1-12-20-3	8.00	0.00	35007	40.06	271	271	8.00	0.00	34017	2622.24	1042	792	8.00	0.00	28290	932.89	18829	18584
J1-12-20-4	13.00	0.00	302181	185.02	5093	5093	12.00	0.20	50233	3594.76	5992	5033	12.46	0.11	205170	3561.25	16036	12450
J2-12-35-0	24.25	0.13	4925214	3574.87	105580	105580	21.30	0.29	36789	3589.10	6729	5879	22.00	0.21	501667	3509.21	15827	6232
J2-12-35-1	22.00	0.15	4935249	3582.19	93123	93123	19.90	0.23	50194	3596.37	7132	6533	20.00	0.23	146181	3639.14	9989	7517
J2-12-35-2	20.00	0.10	5137480	3572.49	119449	119449	18.00	0.27	46399	3591.61	7603	6977	18.00	0.25	185737	3556.45	15203	11374
J2-12-35-3	20.00	0.13	7022615	3566.65	170416	170416	17.00	0.29	40800	3603.94	9795	9090	18.00	0.25	165180	3695.35	19157	15303
J2-12-35-4	22.00	0.09	5805386	3579.22	113488	113488	18.75	0.29	39555	3592.97	8191	7337	19.82	0.23	110763	3579.51	12194	9973
fu	31.66	-1.00	8190820	3565.48	171464	171464	24.00	-1.00	28952	3591.00	5529	4889	25.94	-1.00	724740	3285.90	14409	4232
J1-14-20-0	12.00	0.00	239553	154.05	5205	5205	10.50	0.30	13122	3601.58	1235	1023	12.00	0.08	213500	3578.19	23536	18424
J1-14-20-1	11.00	0.08	5190579	3607.90	106048	106048	10.00	0.33	14452	3601.95	763	631	10.00	0.23	121948	3555.15	24070	21473
J1-14-20-2	13.00	0.13	4979617	3615.48	97156	97156	11.00	0.35	11500	3593.95	3715	3455	11.00	0.35	43760	3568.51	26454	25695
J1-14-20-3	10.00	0.00	174626	153.22	4294	4294	9.42	-1.00	11134	3597.84	1538	1337	10.00	0.09	159460	3581.00	24277	19904
J1-14-20-4	13.33	0.11	4871554	3664.15	103296	103296	12.00	0.28	13606	3597.96	2390	2144	12.00	0.23	110711	3552.21	23198	20747
J2-14-35-0	23.00	0.26	2753150	3585.51	63202	63202	20.00	0.41	9921	3601.97	4401	4110	21.88	0.34	148290	3559.79	15219	11799
J2-14-35-1	22.00	0.29	3181217	3575.76	55764	55764	18.00	-1.00	11794	3604.12	7556	7351	19.62	-1.00	42570	3580.19	14852	13892
J2-14-35-2	20.00	0.22	3406777	3619.97	74663	74663	18.00	-1.00	11452	3595.00	5541	5254	18.00	0.34	148501	3548.96	19983	15888
J2-14-35-3	20.00	0.23	4041754	3626.66	84032	84032	16.00	0.44	13076	3603.61	6176	5868	18.00	0.39	51798	3576.32	19908	18677
J2-14-35-4	20.00	0.21	3049800	4145.76	54661	54661	18.00	-1.00	12452	3599.77	3922	3745	18.85	-1.00	216982	3524.59	15075	12134
poly1a0	13.00	0.14	2866700	4441.72	54431	54431	13.00	-1.00	8358	3597.79	659	299	13.00	-1.00	36022	3573.61	48883	47702
dighe1	85.00	-1.00	238553	3572.00	3499	3499	65.71	-1.00	3734	3609.96	2973	2921	77.20	-1.00	20351	3588.60	8494	8213

Chapter 6

Constructive algorithms

Introduccion

In Chapter 3 we presented an exact algorithm for solving *Nesting* problems. The instances used in the tests were described in Table 1.2. Due to the great difficulty of proving optimality, the number of pieces in these instances was not larger than 16. Furthermore, we did not consider the rotations of the pieces, so the problem was easier than the general case in which some rotations can be allowed.

The *Nesting* instances that can be found in the literature usually have more (up to 99) pieces. With respect to rotation, there are instances for which specific angles of rotation are allowed. These angles are usually $0^o - 180^o$ or $0^o - 90^o - 180^o - 270^o$. The difficulty of solving a nesting instance increases when rotation is allowed. There are very few cases in which free rotation is permitted.

In this chapter we study different constructive algorithms based on the insertion of the pieces one at a time. In order to add a piece, a mixed integer problem is solved. We try to find the optimal insertion of a given piece, keeping the relative position fixed between the pieces already placed.

In Section 6.1 we present the core of the constructive algorithm and we make a comparison between the formulations *GO* and *HS2* described in Chapter 2. In Section 6.2 we do a computational experiment considering the initial insertion of more than one piece.

An interesting approach for the insertion of one piece is the *trunk* insertion, described in Section 6.3. The idea is to allow certain movements on the pieces already placed while a new piece is being inserted.

Finally, we propose two different objective functions for breaking ties when for the current piece there is more than one placement which minimizes L. We add the coordinates of the pieces in the objective function with small coefficients. The computational tests show that the results obtained are slightly better. However, computational time increases when the objective function is more complex.

6.1 Initial models

In Chapter 2 we presented the mixed integer models *GO*, *HS1* and *HS2*. The *GO* formulation does not use Fischetti and Luzzy's *slices*, so when a binary variable takes the value 1 the relative position between the given pair of pieces is less restrictive. That gives more flexibility to the *GO* model compared with *HS2* (or *HS1*). On the other hand, the *GO* model is harder to solve to optimality, and when the set of binary variables is very large the corresponding *MIP* can become impossible to solve.

The core of the constructive algorithms is the optimal insertion of the pieces, one at a time, and the fixing of the relative position between all the pieces already placed. Let us suppose that there are k pieces already placed into the strip and we want to place the next piece from a given list. The relative position of the k pieces is fixed, so the corresponding binary variables are fixed and the number of binary variables in the model is reduced. The only binary variables that we are going to consider in order to add piece $k+1$ to the current solution belong to the *NFP*s defined by piece $k+1$ and all the pieces already placed.

If the *Nesting problem* that we want to solve has a large number of pieces, then insertion of the k^{th} piece requires more computational effort than insertion of the j^{th} piece if $k > j$. In particular, the *MIP*s used for the insertion of the last pieces are much harder to solve because the piece to be inserted must be separated from all the pieces already placed, so we have to consider many *NFP*s and the number of binary variables increases considerably.

The two models that we compare in the constructive algorithm are *GO* and *HS2*, because *HS2* works better than *HS1* and uses the same slices. In both models we eliminate the inequalities defined to avoid symmetrical solutions (see Section 2.4). The objective is to insert the new piece in the optimal position, and if these inequalities are used and a piece with the same shape has already been placed, then the feasible region for the piece may be reduced considerably.

The constructive algorithmic scheme is presented in Algorithm 2, independently of the chosen model. Let $\pi = (i_1, \ldots, i_N)$ be a permutation of the pieces which defines an order for inserting them into the strip. The angle of rotation used for each piece is denoted by $o_i, i \in \{1, \ldots, N\}$. The vector $\theta = (o_1, \ldots, o_N)$ denotes the rotations considered for all the pieces. The set of all allowed rotations is denoted by $O = \{o^1, \ldots, o^{n_o}\}$, where n_o represents the number of allowed rotation angles.

The initial *MIP* takes into account the first n_{ini} pieces and it is solved to optimality. The value of n_{ini} when we use the *HS* model could be greater than in the *GO* model because of the behavior of the models (see 2.5). At the first step we include the pieces $i_1, \ldots, i_{n_{ini}}$.

Then, when we have a solution with the first n_{ini} pieces, we fix the relative position of these pieces by fixing the binary variables of the previous *MIP* and then we add the next piece from π. The set of binary variables considered in the new *MIP* are the ones in relation to the newly added piece. In order to include the new piece in the model we have to modify the bound inequalities (see constraints (2.5), (2.6), (2.23) and (2.24)) and the non-overlapping constraints (see constraints (2.7), (2.8), (9.7) and (2.27)). Iteratively, we add the pieces one by one until piece i_N is placed.

The *MIP*s are becoming harder to solve as they consider more pieces, and the difficulty of finding the optimal solution increases considerably when the instance has a large number of pieces. If at the beginning

Algorithm 2 Constructive algorithm

Require: $\pi = (i_1, \ldots, i_N)$, $\theta = (o_1, \ldots, o_N)$;
  Solve *MIP* with the first n_{ini} pieces of π;
  $B^{n_{ini}} = \{b_{ijk} \mid b_{ijk} = 1$ in the current solution, $i, j \leq n_{ini}, k = 1, .., m_{ij}\}$
  np=n_{ini};
  while $np < N$ **do**
    Fix the binary variables B^{np}.
    $np++$;
    Select i_{np} and add it to the model;
    Solve *MIP*.
    $B^{np} = \{b_{ijk} \mid b_{ijk} = 1$ in the current solution, $i, j \leq np, k = 1, .., m_{ij}\}$
  end while

we consider $n_{ini} = 12$, then the model has 66 active *NFP*s, which means that it has to deal with the binary variables defined in 66 *NFP*s. On the other hand, if we have already placed 66 pieces in a large instance, then the next *MIP* that we have to consider for inserting piece 67 also will have 66 active *NFP*s.

To solve the *MIP*s we use *CPLEX* with a time limit of 100 seconds. If *CPLEX* does not prove optimality within this time, it returns the best feasible solution that it has found, but if no feasible solution is found, then the constructive algorithm fails.

Let $t_1, \ldots, t_\nu$ be the types of pieces, where ν denotes the number of different types of pieces. Each type t_j has a number of copies in order to represent pieces with the same shape. Let n_j, $j = 1, \ldots, \nu$ be the number of pieces of type t_j. The probability of selecting a given piece is

$$P(t_j) = \frac{A(t_j)}{A(T)}$$

where $A(t_j)$ denotes the area of t_j and $A(T)$ denotes the total area of the different types of pieces. The vector π is built iteratively, piece by piece, choosing the pieces by using the previous probability. When all the pieces of a given type are included in π, then the type is eliminated and the probabilities are recalculated.

The first computational test we have done compares the constructive algorithms with both models (*GO* and *HS2*) and the bottom-left corner (*BLC*) on the set of instances presented in Table 6.1. These instances have been obtained from Table 1.1, but we eliminate instance *glass1*, *glass2* and *glass3* because they are easy to solve and we also eliminate instances *poly3b*, *poly4b* and *poly5b* in these preliminary tests. On the other hand, we add other instances by considering a different rotations of the pieces. *Shapes2-0*, *swim0*, *trousers0*, *shirts0* correspond to *shapes2*, *swim*, *trousers* and *shirts* with fixed orientation. With a similar notation we have used instances *poly2a*, *poly2b*, *poly3a* and *poly4a* and *poly5a* without rotation. Instances have been grouped into three sets depending on the rotation of the pieces. The instances of each group appear ordered by a non-decreasing number of pieces.

Instances *swimm0* and *swimm1* have been created by reducing the number of vertices of several pieces of instance *swim* in such a way that a feasible solution for instances *swimm0* and *swimm1* are also feasible for instance *swim*. The average number of vertices is reduced from 21.9 to 12.8. Instance *swimm0* has the same pieces as *swimm1*, but rotation is not allowed.

Table 6.1: *Nesting instances used in the constructive algorithms*

Instances	Types of Pieces	Number of pieces	Average of vertices	Plate width	Problem type
Rotation: 0					
dighe2	10	10	4.7	100	Jigsaw puzzle
poly1a0	15	15	4.6	40	Artificial
dighe1	16	16	3.87	100	Jigsaw puzzle
shapes2-0	4	20	7.5	15	obtained from blaz1
poly2a0	15	30	4.6	40	Artificial
poly2b0	30	30	4.53	40	Artificial
shapes0	4	43	8.75	40	Artificial
poly3a0	15	45	4.6	40	Artificial
swimm0	10	48	12.8	5752	obtained from swim
poly4a0	15	60	4.6	40	Artificial
trousers0	17	64	5.06	79	obtained from trousers
poly5a0	15	75	4.6	40	Artificial
shirts0	8	99	6.63	5752	obtained from shirts
Rotation: 0-180					
albano	8	24	7.25	4900	Garment
shapes2	4	20	7.5	15	Artificial
dagli	10	30	6.3	60	Garment
shapes1	4	43	8.75	40	Artificial
swimm1	10	48	12.8	5752	obtained from swim
trousers	17	64	5.06	79	Garment
shirts	8	99	6.63	5752	Garment
Rotation: 0-90-180-270					
fu	12	12	3.58	38	Artificial, convex
mao	9	20	9.22	2550	Garment
marques	8	24	7.37	104	Garment
jakobs1	25	25	5.6	40	Artificial
jakobs2	25	25	5.36	70	Artificial

In Table 6.2 we have run each algorithm 20 times, building different orders of pieces (π) and choosing the rotation of each piece (θ) randomly. For each order we call three different constructive algorithms: the first one uses the *HS2* formulation, called *CHS2*, the second one uses the *GO* formulation (*CGO*) and the third one is the bottom-left corner (BLC) implemented by A.M. Gomes and J.F. Oliveira (and kindly provided by the authors).

In the constructive algorithms *CGO* and *CHS2* we have considered $n_{ini} = 1$. In Section 6.2 we study the effect of changing this parameter. The objective function considered in both cases is L. In Section 6.4 we propose other objective functions.

We can see that the best results, in general, are obtained with the *CGO* (GO formulation), but the computational time increases considerably when the instances have more than 30 pieces. In 18 out of 28 instances the constructive algorithm *CGO* obtains the best average length and in 13 instances obtains the best solution. On the other hand, *CHS2* is faster than *CGO* and in instances with a large number of pieces such as *swim* it is clearly better than *CGO*. In *CGO* what happens is that *CPLEX* cannot prove optimality in 100 seconds, so it gives an upper bound which can either be very bad or it cannot find a feasible solution at all and then the constructive algorithm fails. For instances *swimm0* and *swimm1*, the constructive algorithm *CGO* only provides a feasible solution in 5 of the 20 runs and the quality is very low.

If we look at constructive algorithm *CHS2*, we can see that the results, on average and for the best solutions, are better than the *BLC* and its computational time is lower than *CGO*. The computational time of the

BLC is not comparable because in many instances the time of one iteration is less than one second. The next computational test that we present consists in increasing the number of *BLC* iterations in order to produce a computational effort similar to *CHS2*. In Table 6.3 we can see the results for the *BLC* in 1000 runs, while the other two constructive algorithms remain equal (20 runs, the same as Table 6.2). The third column in each algorithm represents the total time.

Table 6.2: *Comparing CHS2, CGO and BLC in* 20 *runs*

Set of	*CHS2*			*CGO*			*BLC*		
Instances	Av. L	Best L	Av. Time	Av. L	Best L	Av. Time	Av. L	Best L	Av. Time
Rotation: 0									
dighe2	143.8	130.9	1.0	142.5	130.0	0.9	166.4	135.5	0.1
poly1a0	18.2	16.2	2.7	17.8	16.8	3.8	20.0	17.2	0.1
dighe1	143.6	131.7	2.3	138.0	122.0	4.2	170.6	145.7	0.1
shapes2-0	30.4	28.9	19.2	30.0	28.7	61.1	31.9	29.9	0.1
poly2a0	33.7	30.3	31.5	33.2	31.8	563.2	35.3	33.7	0.2
poly2b0	36.4	34.6	31.0	35.9	33.0	495.8	38.2	36.1	0.6
shapes0	70.6	65.0	36.7	70.4	64.0	37.4	69.8	66.0	0.2
poly3a0	49.1	46.6	156.7	49.1	46.6	1852.9	51.0	48.4	0.3
swimm0	8281.6	7102.0	1414.2	12365.3	9734.7	1894.1	7560.8	7253.9	1.1
poly4a0	63.5	61.4	783.2	66.5	63.0	3058.2	66.1	63.4	0.4
trousers0	296.8	279.4	223.5	283.9	266.6	386.9	286.9	279.8	0.4
poly5a0	79.8	77.0	1643.6	82.0	77.9	4280.5	81.8	78.2	0.5
shirts0	67.4	65.2	830.6	68.9	65.4	2737.5	68.5	65.1	0.3
Rotation: 0-180									
albano	11189.1	10721.1	9.7	11078.6	10337.5	28.6	11785.1	10661.7	0.4
shapes2	30.7	29.4	18.3	30.4	28.7	67.8	32.0	30.0	0.3
dagli	66.9	62.7	11.1	65.4	63.0	63.5	72.2	66.9	0.5
shapes1	65.7	61.0	47.3	68.9	62.0	42.6	67.2	63.0	0.4
swimm1	8033.0	7249.4	1343.7	14370.9	7917.6	1835.1	7453.4	7165.8	2.9
trousers	283.7	267.9	199.9	271.6	261.7	494.0	277.2	254.7	1.2
shirts	67.3	65.0	807.0	69.1	66.4	2549.2	807.0	65.3	0.8
Rotation: 0-90-180-270									
fu	39.1	35.4	1.0	37.8	34.4	0.9	43.0	36.0	0.8
mao	2229.9	2048.7	7.6	2219.1	2061.2	15.5	2352.2	2148.4	0.9
marques	90.8	85.2	8.7	89.0	83.8	29.8	93.4	85.5	1.5
jakobs1	14.3	13.0	4.0	14.2	13.0	3.0	14.6	13.0	0.7
jakobs2	29.7	28.0	4.9	29.5	28.0	6.2	31.2	29.8	0.5

The average length of the 1000 iterations in the *BLC* remains similar, but we can see an improvement in the best results. In Table 6.2 the *BLC* algorithm finds the best solution in 4 instances: *shirts0*, *swimm1* and *trousers*. However, if we look at Table 6.3 we can see that *BLC* provides the best result in 16 instances and the total computational time remains lower than *CHS2*.

Note that *CHS2* algorithm takes more than 100 seconds to build a feasible solution in the following instances:

- No rotation: *poly3a0*, *swimm0*, *poly4a0*, *trousers0*, *poly5a0* and *shirts0*.
- Rotation (0-180): *swimm1*, *trousers* and *shirts*.

We call *hard instances* those instances for which *CHS2* needs more than 100 seconds to build a feasible solution. In general, these instances have a large number of pieces. As the size of the corresponding *MIP*

Table 6.3: *Comparing CHS2, CGO with* 1000 *runs of BLC*

Set of Instances	*CHS2* Av. L	*CHS2* Best L	*CHS2* Total Time	*CGO* Av. L	*CGO* Best L	*CGO* Total Time	*BLC* Av. L	*BLC* Best L	*BLC* Total Time
Rotation: 0									
dighe2	143.8	130.9	20.1	142.5	130.0	18.5	164.7	138.2	39.7
poly1a0	18.2	16.2	53.3	17.8	16.8	76.4	20.4	16.8	72.1
dighe1	143.6	131.7	46.9	138.0	122.0	83.6	171.3	140.2	64.7
shapes2-0	30.4	28.9	384.3	30.0	28.7	1222.2	31.6	29.0	57.0
poly2a0	33.7	30.3	631.0	33.2	31.8	11263.2	35.3	32.2	102.3
poly2b0	36.4	34.6	619.5	35.9	33.0	9916.5	38.4	33.6	310.8
shapes0	70.6	65.0	733.4	70.4	64.0	748.5	70.5	65.5	75.6
poly3a0	49.1	46.6	3133.8	49.1	46.6	37057.3	50.5	46.5	140.8
swimm0	8281.6	7102.0	28284.3	12365.3	9734.7	37882.2	7540.8	6790.4	530.3
poly4a0	63.5	61.4	15664.6	66.5	63.0	61164.7	66.0	61.3	198.2
trousers0	296.8	279.4	4470.9	283.9	266.6	7738.3	295.5	272.0	222.4
poly5a0	79.8	77.0	32872.7	82.0	77.9	85609.9	81.3	76.4	262.2
shirts0	67.4	65.2	16612.2	68.9	65.4	54751.0	68.4	65.0	173.1
Rotation: 0-180									
albano	11189.1	10721.1	193.8	11078.6	10337.5	571.9	11628.7	10545.3	223.9
shapes2	30.7	29.4	365.5	30.4	28.7	1356.0	31.2	28.4	161.9
dagli	66.9	62.7	222.4	65.4	63.0	1270.0	72.2	63.2	239.5
shapes1	65.7	61.0	945.8	68.9	62.0	851.9	65.0	57.0	184.4
swimm1	8033.0	7249.4	26874.3	14370.9	7917.6	36702.7	7311.0	6720.0	1440.7
trousers	283.7	267.9	3997.4	271.6	261.7	9881.0	281.7	253.5	609.9
shirts	67.3	65.0	16140.7	69.1	66.4	50983.2	67.1	63.3	385.8
Rotation: 0-90-180-270									
fu	39.1	35.4	19.5	37.8	34.4	19.0	39.8	33.3	422.7
mao	2229.9	2048.7	152.6	2219.1	2061.2	309.1	2330.4	1921.2	451.2
marques	90.8	85.2	173.2	89.0	83.8	595.5	94.7	83.0	770.6
jakobs1	14.3	13.0	79.8	14.2	13.0	59.6	14.9	13.0	369.7
jakobs2	29.7	28.0	97.6	29.5	28.0	124.8	30.9	27.8	262.1

formulation increases, then *CPLEX* needs more time to solve each one of the corresponding *MIP*s.

In what follows we are going to explore the behavior and possibilities of the *HS2* model. The next sections study different options for the constructive algorithm *CHS2*.

6.2 Studying the initial number of pieces considered (n_{ini})

The next computational test is focused on the n_{ini} parameter. We consider several instances from Table 6.1 and we build 20 solutions for each instance and for each $n_{ini} = 1, \ldots, 12$. We present three tables, one for the average lengths, another one for the length of the best solutions and finally a table for the average computational times.

In Table 6.4 we can see the average length obtained. We can see that if n_{ini} increases, then the average length is reduced, so the quality of the solutions is better.

In Table 6.5 we can see the best solution obtained in each case. In 10 of the 20 instances the best solution is found when $n_{ini} = 12$ and in 7 instances the best solution is found when $n_{ini} = 11$.

Table 6.4: *Average lengths in* 20 *runs*

	$n_{ini}=1$	$n_{ini}=2$	$n_{ini}=3$	$n_{ini}=4$	$n_{ini}=5$	$n_{ini}=6$	$n_{ini}=7$	$n_{ini}=8$	$n_{ini}=9$	$n_{ini}=10$	$n_{ini}=11$	$n_{ini}=12$
Rotation: 0												
poly1a0	17.9	17.9	18.1	18.1	18.1	18.1	18	18.1	18.1	17.5	17.5	17.6
dighe1	142.9	142.9	142.9	141.1	141.7	140.3	140.4	137.7	135.7	132.6	128.9	129.1
shapes2-0	30.5	30.5	30.5	30.4	30.4	30.3	30.2	30	30	30	29.8	29.8
poly2a0	33.4	33.5	33.5	33.5	33.5	33.5	33.8	33.4	33.7	33.6	33.6	32.9
poly2b0	36.7	36.7	36.7	36.7	36.8	36.8	36.6	36	36.2	35.6	35.9	35.6
shapes0	69.5	69.5	69.5	69.4	69.3	69.5	69.3	69.2	69.1	69.2	70.6	69.4
poly3a0	48.8	48.8	48.8	48.9	48.9	48.9	48.6	48.7	48.6	48.9	48.7	48.2
Rotation: 0-180												
albano	11189.1	11189.1	11125.7	11296.2	11255.9	11195.5	11172.6	11123.3	10984.5	11132	10978.2	11031.2
shapes2	30.7	30.7	30.5	30.7	30.7	30.6	30.9	30.1	30.2	29.9	30	30.2
dagli	67.5	67.6	67.6	67.5	67.8	67.3	66.5	66.5	66.7	66.2	66.3	66
shapes1	67.9	67.9	67.5	67.3	67.4	66.4	66.1	66.3	66.4	66.8	65.9	65.7
trousers	283.4	282.8	280.8	282.7	281.2	285.5	283.4	281.9	278.4	278.7	279.7	275.3
shirts	66	66.9	65.8	66.1	66	66.5	66.1	66.2	66.2	66.1	65.9	65.5
Rotation: 0-90-180-270												
fu	39.1	39.1	39.1	39.1	38.3	38.1	37.5	37.6	36.8	37.1	36.6	36.6
mao	2229.9	2229.9	2229.9	2229.9	2229.9	2229.8	2244.3	2327.9	2271.8	2260.1	2264.8	2244.7
marques	90.7	90.7	90.8	91.2	90	89	89.5	88.5	88.9	87.4	88.8	89.6
jakobs1	14.3	14.3	14.3	14.3	14.3	14.3	14.3	14.3	14.3	14.3	14.3	13.9
jakobs2	29.7	29.7	29.7	29.7	29.7	29.7	29.8	29.7	29.6	29.8	29.1	29.3

Table 6.5: *Best solution obtained in* 20 *runs*

	$n_{ini}=1$	$n_{ini}=2$	$n_{ini}=3$	$n_{ini}=4$	$n_{ini}=5$	$n_{ini}=6$	$n_{ini}=7$	$n_{ini}=8$	$n_{ini}=9$	$n_{ini}=10$	$n_{ini}=11$	$n_{ini}=12$
Rotation: 0												
poly1a0	16.1	16.1	16.1	16.1	16.1	16.1	16.1	16.1	16.7	16.4	16.2	15.8
dighe1	131.7	131.7	130.1	128.5	128.5	128.5	127	127.5	117.1	115.1	115	116.7
shapes2-0	28.7	28.7	28.7	28.2	28.2	28.7	28.5	27.9	28.4	28	28.2	28
poly2a0	31.7	31.7	31.7	31.7	31.7	31.7	31.7	31.2	31.1	31.2	31.4	30.4
poly2b0	34.6	34.6	34.6	34.6	34.6	34.6	34.6	33	33.5	33.4	33.2	32.6
shapes0	64.5	64.5	64.5	64.5	64.5	65	65	65	64	64	66	63
poly3a0	47.6	47.6	47.6	47.6	47.6	47.6	46.1	46.9	45.9	46.2	46.9	46.4
Rotation: 0-180												
albano	10721.1	10721.1	10592.5	10721.1	10426.1	10792.8	10772.5	10461.7	10586.8	10641	10205.8	10508.1
shapes2	28.8	28.8	28.8	29.3	29.5	28.8	28.3	29.2	27.8	28.6	28.2	28.1
dagli	63.5	63.5	63.5	63.5	64.2	63.3	62.5	62.9	62.5	63.1	63.3	62.4
shapes1	60	60	60	60	60	60	60	60	61	62	61	61
trousers	263.5	262	264.5	261.5	258.6	259	270.3	262.1	261.9	262	257	256.2
shirts	64	65.1	63.2	64.4	64	64.2	64	63.9	64	63.7	64.5	64
Rotation: 0-90-180-270												
fu	35.4	35.4	35.4	35	35.7	34.9	34.9	35.2	34.1	34.7	33	33
mao	2048.7	2048.7	2048.7	2048.7	2048.7	2066.4	1940.6	2134.8	2018.5	1976	1877	1877
marques	85.2	85.2	85.2	85.2	85	84.4	83.1	82.8	84.8	82	83.3	83.3
jakobs1	13	13	13	13	13	13	13	13	13	13	13	13
jakobs2	28	28	28	28	28	28	28	28	27.5	27.6	26.8	27.2

In Table 6.6 we can see the average computational time needed in each case. The time limit for the first *MIP* is 100 seconds.

In Figure 6.1 we show the relation between quality and computational time. Let us denote by $AvL1$ the average length of the 20 runs with $n_{ini} = 1$. For each instance and for each n_{ini}, we calculate $AvL/AvL1$. The $X - axis$ represents n_{ini}, the left-hand side of the $Y - axis$ represents the average of all the instances of $AvL/AvL1$ and its right-hand side the average time.

We can observe that when n_{ini} increases, the time increases in an exponential way and the quality of the solutions improves slowly. For $n_{ini} = 1, \ldots, 6$ the quality of the solution remains practically at the same level, and when it begins to improve with $n_{ini} = 7, \ldots, 12$, then the computational time increases very sharply.

Table 6.6: *Average time in* 20 *runs*

	$n_{ini}=1$	$n_{ini}=2$	$n_{ini}=3$	$n_{ini}=4$	$n_{ini}=5$	$n_{ini}=6$	$n_{ini}=7$	$n_{ini}=8$	$n_{ini}=9$	$n_{ini}=10$	$n_{ini}=11$	$n_{ini}=12$
Rotation: 0												
poly1a0	2.4	2.5	2.3	2.2	2.4	2.2	2	2	1.9	3	22.1	70.7
dighe1	2.4	2.4	2.5	2.2	2.2	2.4	3.1	6.7	18	47.2	75.9	90.2
shapes2-0	18.6	18.6	18.5	17.2	17.7	17.8	38.5	92.7	112.8	115.7	116.4	115.2
poly2a0	31.9	31.9	31.8	31.6	31.9	32	30	33.8	51.3	59.6	103.9	124.2
poly2b0	37.5	37.4	37.2	38.4	37.6	36	36.2	38.8	49.6	100.4	121.2	132.3
shapes0	37.8	37.6	37.5	37	36.8	36.9	37	49	71	121	131.6	139.7
poly3a0	159.1	159	159.2	157.4	156.9	155.9	162.6	168.7	192.7	227.6	273.4	274.1
Rotation: 0-180												
albano	16.2	15	15.9	14.4	15.4	23.7	53.1	85.9	105.1	113.4	113.5	113.4
shapes2	24.1	24.4	23.8	22.8	23.5	26.8	40.6	94.7	121.3	122.5	122.2	124
dagli	20.9	20.2	20.8	20.3	20.3	21.6	24.9	42.4	65.8	114.1	115.9	113.6
shapes1	62.7	58	59.2	58.7	60.2	59.1	73.5	69.3	113.2	139.6	154.6	158.4
trousers	184	187.7	178.1	183.5	187.8	190.4	185.9	196.6	209.3	211.6	237.4	277.6
shirts	966.4	1028.2	992.3	994.3	1009.1	936	1072.6	1034.9	1060.4	1059.9	1046.3	1066.2
Rotation: 0-90-180-270												
fu	2.4	2.1	2.2	1.9	2	2.1	2.3	12.9	27.4	71.9	100.6	100.3
mao	12.8	12.3	11.5	10.6	11.5	10.7	67.2	85.3	98	113.4	109.9	109.2
marques	15	14.1	15.6	13.6	15.9	13.1	17.9	40	76.7	106.9	110.3	111.2
jakobs1	6.9	7	6.4	7.1	6.5	5.5	5.2	6	5.4	5.3	15.3	38.5
jakobs2	9.7	10.4	10	8.6	7.4	6.6	7	9.3	22.5	51.8	77.1	95.5

The computational time needed to prove optimality in a *Nesting Problem* with 12 pieces is very high. We have considered a time limit of 100 seconds and in several problems there is no guarantee that the solution given by *CPLEX* is optimal. There are instances such as *jakobs1* or *jakobs2* for which *CPLEX* is able to prove optimality in less than 100 seconds, but there are other instances, such as *marques*, where *CPLEX* provides a good solution but it is not usually optimal. Therefore, in the computational tests of the next sections we are going to consider $n_{ini} = 1$.

Instances with large and small pieces

Instances *albano*, *trousers0*, *trousers*, *shirts0* and *shirts* have two definite sets of large and small pieces. We can divide the pieces of these instances into two groups according to their size. If we sort the pieces of these instances by area in a non-decreasing order, then there is a big gap between large and small pieces. The area of the smallest piece in the set of large pieces is more than 1.5 times the area of the larger piece in the set of small pieces.

For these instances we test a slightly different strategy when sorting the pieces. In a first step we are going to place the large pieces and in a second step we add the rest of the pieces. We randomize the order of the pieces within each one of these two sets, as described in the previous section.

The sets of *large* and *small* pieces in the respective instances are the following:

- *albano*: 10 large and 14 small pieces.
- *trouser0* and *trousers*: 16 large and 48 small pieces.
- *shirts0* and *shirts*: 24 large and 75 small pieces.

In Table 6.7 we can see the average lengths obtained. Note that changing parameter n_{ini} does not have any effect, but if we compare these results with those presented in Table 6.4, there is a slight improvement.

In Table 6.8 we present the best results. We can see that there are no improvements when n_{ini} increases. However, these results are slightly better that the ones presented in Table 6.5.

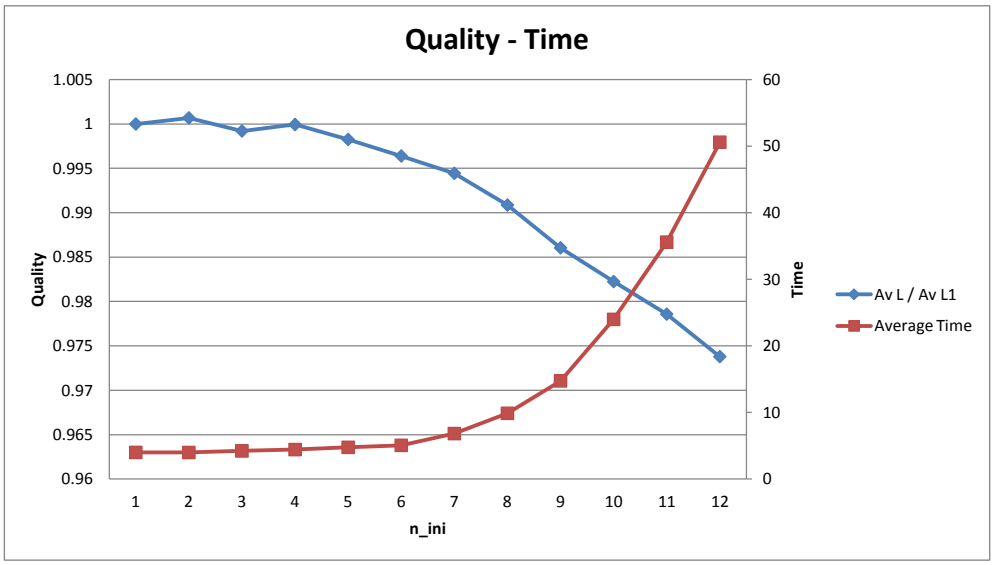

Figure 6.1: *Representation of the quality of the constructed solutions and the computational time required for different values of parameter* n_{ini}.

The average computational time of the 20 runs is presented in Table 6.9. We can see that the algorithm requires a computational effort greater than that required by the previous version, reflected in Table 6.6.

6.3 *Trunk* insertion

In this section we present a constructive algorithm based on the movements that we make in order to arrange the trunk of a car when we slightly move some of the items already placed to make room for the next item. The idea is to select a specific set of binary variables of the pieces already placed and not to fix them, in order to allow some flexibility while a new piece is being inserted.

Let us denote a given solution by $s(X^s, Y^s, B^s, \theta_s)$, where $X^s = \{x_1^s, \ldots, x_N^s\}$ and $Y^S = \{y_1^s, \ldots, y_N^s\}$ are the coordinates of the pieces, $B^s \in (0,1)^{nb}$ gives the values of the binary variables, nb denotes the number of binary variables in the problem and $\theta_s = \{o_s^1, \ldots, o_s^N\}$ gives the rotation angles used by the pieces.

Let us denote by LP_s the linear model that is solved in order to calculate X^s and Y^s when binary variables (b_{ijk}) are eliminated from the model by fixing their values to those in solution s (b_{ijk}^s).

In a given iteration of the constructive algorithm presented above a solution is partially constructed. Let us denote the number of pieces already placed by n' and let $i_{next} \in P$ be the next piece to be placed. Let us

Table 6.7: *Average length in* 20 *runs*

	$n_{ini} = 1$	$n_{ini} = 2$	$n_{ini} = 3$	$n_{ini} = 4$	$n_{ini} = 5$	$n_{ini} = 6$	$n_{ini} = 7$	$n_{ini} = 8$	$n_{ini} = 9$	$n_{ini} = 10$	$n_{ini} = 11$	$n_{ini} = 12$
Rotation: 0												
trousers0	273.15	273.83	274.62	275.89	274.31	279.02	271.69	270.76	271.55	274.56	272.12	270.76
shirts0	67.02	66.73	66.37	66.40	66.33	66.72	66.03	66.22	66.41	67.44	66.95	66.88
Rotation: 0-180												
albano	11139.35	11059.68	11159.11	11082.44	11032.15	10967.87	11238.25	10819.72	11052.70	10977.80		
trousers	264.61	264.36	267.20	261.08	266.12	263.87	266.53	260.55	257.85	258.02	260.34	259.41
shirts	65.60	65.88	66.34	66.18	66.33	66.03	66.03	66.22	66.15	65.76	66.31	65.80

Table 6.8: *Best length in* 20 *runs*

	$n_{ini} = 1$	$n_{ini} = 2$	$n_{ini} = 3$	$n_{ini} = 4$	$n_{ini} = 5$	$n_{ini} = 6$	$n_{ini} = 7$	$n_{ini} = 8$	$n_{ini} = 9$	$n_{ini} = 10$	$n_{ini} = 11$	$n_{ini} = 12$
Rotation: 0												
trousers0	261.56	261.56	265.83	262.38	261.99	267.42	260.37	262.75	259.76	257.18	259.36	262.75
shirts0	64.31	65.17	64.00	64.45	64.17	64.90	63.33	63.99	64.00	66.07	65.50	65.30
Rotation: 0-180												
albano	10544.66	10544.66	10544.66	10544.66	10547.58	10636.70	10948.64	10475.61	10613.88	10606.74		
trousers	250.71	250.71	250.25	251.16	252.33	251.69	249.95	251.93	249.59	248.44	250.32	253.11
shirts	63.81	64.50	64.94	64.35	64.17	63.33	63.33	63.99	65.06	64.08	64.30	64.14

denote the pieces already placed by $i_1, \ldots, i_{n'}$.

The relative position of each pair of pieces already placed is limited by the *slice* used, which is activated by fixing the associated binary variable to 1. In order to make the relative position of a given pair of pieces more flexible we allow the current slice to be changed for an adjacent slice. In what follows, we define the concept of neighborhood of one piece in a given solution and the set of adjacent slices of a given slice.

Let i_r and i_t be two pieces already placed in a given solution s ($1 \leq r < t \leq n'$). We say that piece i_t is a *neighbor by movement* of piece i_r if the distance between the reference point of piece i_t and the limits of the active slice in the $NFP_{i_t i_r}$-coordinate system (defined in section 2.3) is lower than ϵ_s. This distance is defined as follows.

Let $Fr(S^k_{tr})$ be the boundary of *slice* S^k_{tr}. We denote by $\tilde{Fr}(S^k_{tr})$ the boundary $Fr(S^k_{tr})$ when we remove edges which match with the upper bound of the length of the strip ($\overline{L}$). That is, $\tilde{Fr}(S^k_{tr})$ could be not a polygon, but just a set of segments. In Figure 6.2, $\tilde{Fr}(S^k_{tr})$ is represented in blue. The limit drawn in green is given by an upper bound of the length of the strip, so if the reference point of piece i_t is placed in the green zone, we do not consider i_t as a neighbor by movement to piece i_r because the movement of the pieces is being limited by $\overline{L}$.

Then, i_t is a *neighbor by movement* of piece i_r with parameter ϵ_s if

$$\min_{p \in \tilde{Fr}(S^k_{tr})} dist(q_t, p) \leq \epsilon_s$$

where q_t is the placement of the reference point of i_t in the $NFP_{i_t i_r}$-coordinate system.

We denote by NS_{i_r} the set of pieces which are neighbors by movement of i_r. In Figure 6.3 we can see an example, where pieces which belong to NS_{i_r} are drawn in green.

At each step of the constructive algorithm *CHS2* we identify the pairs of pieces which are neighbors by movement. For each pair of neighboring pieces, instead of keeping the variable expressing their relative position fixed in the solution of the previous *MIP*, we consider three or more binary variables defined from

Table 6.9: *Average computational time in 20 runs*

	$n_{ini} = 1$	$n_{ini} = 2$	$n_{ini} = 3$	$n_{ini} = 4$	$n_{ini} = 5$	$n_{ini} = 6$	$n_{ini} = 7$	$n_{ini} = 8$	$n_{ini} = 9$	$n_{ini} = 10$	$n_{ini} = 11$	$n_{ini} = 12$
Rotation: 0												
trousers0	314.96	324.01	285.99	300.31	288.36	257.37	384.46	408.68	440.64	410.73	408.72	480.94
shirts0	1092.22	1150.65	1202.56	1193.52	1131.84	1200.20	1251.41	1200.74	1252.38	1452.36	1417.20	1294.38
Rotation: 0-180												
albano	14.36	14.31	13.38	13.63	15.08	49.57	112.13	112.52	112.23	112.65		
trousers	302.21	313.45	290.50	385.44	315.00	337.06	341.45	461.31	474.67	461.87	453.86	462.99
shirts	1104.09	1132.77	1131.33	1166.95	1131.84	1251.41	1251.41	1200.74	1254.09	1232.15	1258.72	1258.58

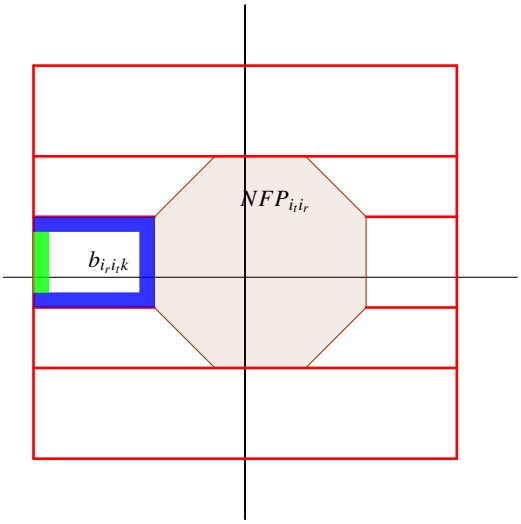

Figure 6.2: *Boundary of slice* $b_{i_r i_t k}$.

the respective NFP, such that their corresponding slices share part of the boundary of the current slice, i.e. we allow their relative position to be changed by an adjacent slice.

In Figure 6.4 we can see an example. Let us consider that pieces i and j are neighbors and let b_{ijk_1} be the binary variable whose associated slice S_{ijk_1} is used. In the next step of the constructive algorithm $CHS2$, instead of fixing variable $b_{ijk_1} = 1$ we add equality $b_{ijk_1} + b_{ijk_2} + b_{ijk_3} = 1$.

We call the combination of the optimal insertion of one piece and the previous relaxation of the relative position of two neighboring pieces *trunk insertion* . The constructive algorithm considering *trunk insertion* is called *CHS2-TI*.

Therefore, in a given iteration of the constructive algorithm *CHS2-TI*, we have more binary variables than in *CHS2* because additionally we allow some of the pieces already placed to be reallocated. Thus the corresponding *MIP*s are harder to solve.

In Figure 6.5 we can see an example of a *trunk insertion* in the third iteration of the constructive algorithm *CHS2-TI* applied on instance *fu*. Initially, 3 pieces are placed. Then, in order to arrange the next piece from the list π, piece 9, we allow certain movements of pieces 4, 6 and 12 that *CHS2* does not contemplate. We can see that the relative position of pieces 4 and 12 has changed while piece 9 is being inserted.

In Table 6.10 we can see the comparison between *CHS2* and *CHS2-TI*. We have chosen 5 instances,

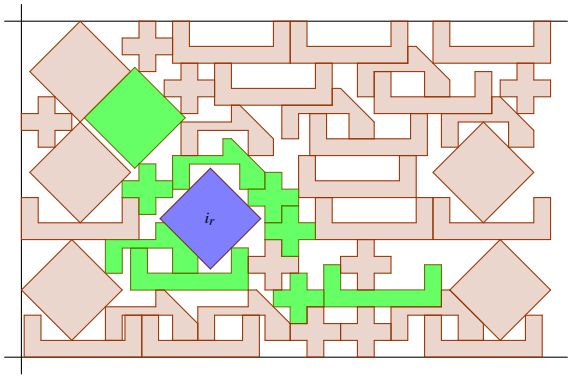

Figure 6.3: *NS_{i_r} considering $\epsilon_s = 0.1$.*

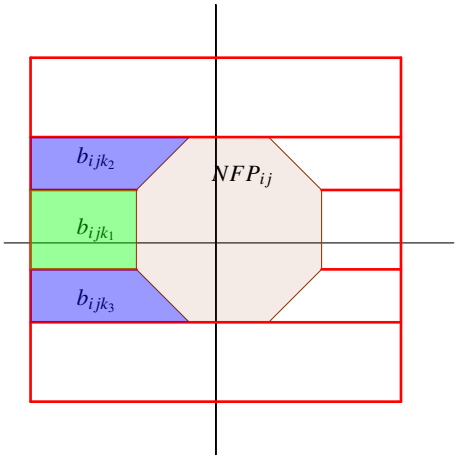

Figure 6.4: *Relaxing the relative position.*

from 12 to 43 pieces, with different types of rotations and with each constructive algorithm we have built 20 solutions.

On the one hand the solutions obtained by *CHS2-TI* are much better, both on average and in the best length, than the results obtained by *CHS2*. On the other hand, the time increases considerably, requiring more than 1000 seconds per iteration in instances with 43 pieces (*shapes0* and *shapes1*).

6.4 Alternative objective functions

The objective function used in constructive algorithms *CHS2* and *CHS2-TI* does not take into account the coordinates of the reference point of the pieces, but only considers the length of the strip (L). There are situations in which there are many places to insert a new piece such that the solution is optimal. In such situations the constructive algorithm allows *CPLEX* to choose one of the optimal solutions. In this section we are going to study different objective functions for placing the pieces, not only considering the length of the strip, but also the coordinates of the pieces.

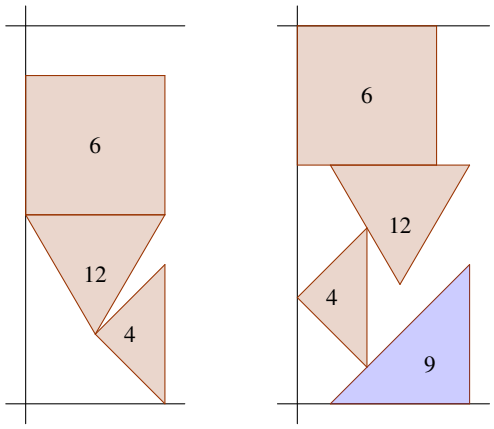

Figure 6.5: *Instance fu: Trunk insertion of piece* 9*. Relative position between pieces* 4 *and* 12 *is modified while piece* 9 *is being inserted.*

Table 6.10: *Comparing CHS2 and CHS2-TI*

Instances	*CHS2* Av. L	Best L	Total Time	*CHS2-TI* Av. L	Best L	Total Time
Rotation: 0						
poly1a	18.2	16.2	2.7	16.5	15.3	30.9
shapes0	70.6	65.0	36.7	64.6	62.0	1183.1
Rotation: 0-180						
albano	11189.1	10721.1	9.7	10642.3	10314.1	128.3
shapes1	65.7	61.0	47.3	59.5	58.0	1100.6
Rotation: 0-90-180-270						
fu	39.2	35.4	1.0	36.7	33.4	1.9

The objective function that we are going to consider has the following form:

$$\min L + \epsilon_1 \sum_{i=1}^{N} x_i + \epsilon_2 \sum_{i=1}^{N} y_i \tag{6.1}$$

where ϵ_1 and ϵ_2 are parameters to be defined.

In order to balance instances which have pieces with a length of more than 100 units (e.g, *albano*, *mao*), we transform the data by dividing the width and all the coordinates of the pieces by a multiple of 10 in such a way that no length is greater than 100.

***FO1*: $\epsilon_1 = 0.001$ and $\epsilon_2 = 0$**

This objective function places the pieces as close as possible to the Y-axis. Note that the main part of the objective function is the minimization of the length of the stock sheet, and only in the case that there are several places to choose for the position of a piece such that the length is not modified, is the model going

to place the piece such that the X coordinate is as low is possible.

FO2: $\epsilon_1 = 0.001$ and $\epsilon_2 = 0.001$

If we consider this objective function, then an attempt is made to place pieces as close as possible to the origin (the bottom-left corner of the strip). In fact, smaller pieces have more preference for being placed closer to the origin than larger ones.

We denote by *FO0* the objective function which considers just the length of the strip ($\epsilon_1 = 0$ and $\epsilon_2 = 0$).

In Table 6.11 we make the comparison of the constructive algorithm *CHS2* with the two objective functions described above, *FO1* and *FO2*. Table 6.2 shows the computational results of *CHS2* with objective function *FO0*. We can observe that objective function *FO2* obtains the best length average in 7 of 14 instances, followed by objective function *FO1* which obtains the best average in 6 instances. Objective function *FO*0 obtains the best average length on instance *dagli*. If we look at the best solution obtained in the 20 runs, objective functions *FO1* and *FO2* find the best solution in 8 instances, in contrast with considering just the length of the strip, *FO0*, which finds the best solution in 2 instances.

Table 6.11: *Comparing objective functions in CHS2*

	CHS2 - FO1			*CHS2* - FO2		
Instances	Av. L	Best L	Av. Time	Av. L	Best L	Av. Time
Rotation: 0						
dighe2	143.3	108.7	1.0	146.0	130.0	1.1
poly1a	18.1	16.0	2.6	17.6	16.3	4.0
dighe1	143.8	129.9	2.8	147.0	130.1	2.8
shapes0	67.9	64.0	70.5	69.0	64.0	67.1
Rotation: 0-180						
albano	11074.4	10434.4	13.8	11133.6	10491.6	13.9
shapes2	30.4	28.2	24.1	30.2	28.2	24.4
dagli	67.0	63.5	16.0	66.7	64.1	17.6
shapes1	65.7	62.0	69.2	65.3	61.0	68.4
Rotation: 0-90-180-270						
fu	38.6	35.1	1.1	38.1	35.0	1.1
mao	2258.4	1939.3	9.6	2190.6	1916.6	13.7
marques	89.3	84.0	12.5	89.7	83.6	14.9
jakobs1	14.1	12.9	4.8	13.9	12.9	5.7
jakobs2	29.2	27.0	5.2	29.3	27.3	6.3

In Table 6.12 we present the comparison of the constructive algorithm *HS2-TI* with the two objective functions *FO1* and *FO2*. Table 6.10 shows the computational results of *HS2-TI* with objective function *FO0*.

We can see that in three instances, *poly1a0*, *albano* and *fu*, the best average length is obtained by objective function *FO2*. However, the computational time increases with respect to *FO0*. In the two remaining instances the best average is obtained with *FO0* (see Table 6.1). The best lengths in instances *poly1a0* and *fu* are obtained with *FO0*, in instance *shapes0* it is obtained with *FO1*, $L = 60.43$, and in instance *albano* the best solution is obtained with *FO2*. The best solution of instance *shapes1*, with $L = 57.33$, is obtained

Table 6.12: *Comparing objective functions in CHS2-TI*

	CHS2-TI - FO1			*CHS2-TI* - FO2		
Instances	Av. L	Best L	Av. Time	Av. L	Best L	Av. Time
Rotation: 0						
poly1a0	16.40	15.44	25.32	16.34	15.60	30.71
shapes0	64.75	60.43	1614.00	68.41	64.00	1519.13
Rotation: 0-180						
albano	10592.49	10317.27	178.74	10582.73	10174.45	196.28
shapes1	60.95	57.33	1527.75	62.16	57.33	1365.80
Rotation: 0-90-180-270						
fu	36.58	35.16	2.1209	36.27	33.68	2.26

with *FO1* and *FO2*.

In general, the computational time of the constructive algorithms when the objective function are *FO1* and *FO2* is greater than the constructive algorithms with *FO0*.

6.5 Conclusions

The constructive algorithms presented in this chapter use a mathematical model which is hard to solve and the required computational time increases considerably if we compare it with the bottom-left corner algorithm (*BLC*).

On the other hand, the results given show that the quality of solutions of the constructive algorithms using model *HS2* is better than the *BLC*. Model *GO* obtains good solutions but the computational time and the complexity of solving the corresponding *MIP*s increases too much in instances with a large number of pieces, and the algorithm could fail.

Trunk Insertion is an interesting approach and the solutions obtained using it are the best ones obtained in all the constructive algorithms. For instance, the best known solution of instance *shapes0* is $L = 58$ and, with this algorithm, a solution of 60.43 is constructed. The problem of *trunk insertion* is the computational time required to build a solution.

Chapter 7

Different approaches to the *Local Search*

In Chapter 6 we studied constructive algorithms using different mathematical models with different objective functions. The computational study showed that the fastest algorithm is the *Bottom-Left Corner* (*BLC*) implemented by Gomes and Oliveira. In this chapter we present different movements with the objective of designing an efficient local search procedure.

Each section of this chapter presents a different local search movement based on the *HS2* model. The initial solution is built with the *BLC* algorithm.
In Section 7.1 we present the *n-insertion* movement. The case in which $n = 1$, *1-insertion*, is similar to the optimal insertion used in the constructive algorithm *CHS2* presented in Chapter 6.

In Section 7.2 we study a *Compaction* procedure. In this movement each piece maintains its position relative to all the other pieces, though it can be modified slightly.

In Section 7.3 we study the *k-compaction*, which is the combination of the *k-insertion* and the *Compaction* movements. There is a strong relation between the *1-compaction* and *trunk insertion* presented in Section 6.3. The *1-compaction* requires a great computational effort, so we propose a simplification of the movement in a two-step procedure. First we do the compaction without the pieces selected for insertion, and then we add the pieces using the *1-insertion* movement.

Finally, in Section 7.4 we study different criteria based on the objective functions described in the previous chapter in order to modify the current solution more frequently.

The set of instances that we are going to consider to test the different types of movements of the local search is presented in Table 7.1. For each one of these instances we build 20 solutions for which the order of the pieces is randomly chosen with probabilities weighted by area. The rotation angles are also randomly chosen. The initial solution is the same in each one of the iterations for each instance.

7.1 *n-insert*

The core of this movement is the optimal re-insertion of a subset of n pieces. We are going to consider the *n-insertion* with $n = 1$, $n = 2$ and $n = 3$. In each one of these cases we consider different objective functions

Table 7.1: *Nesting instances used in the local search study*

Instances	Types of Pieces	Number of pieces	Average of vertices	Plate width	Problem type
Rotation: 0					
dighe2	10	10	4.7	100	Jigsaw puzzle
poly1a	15	15	4.6	40	Artificial
dighe1	16	16	3.87	100	Jigsaw puzzle
shapes0	4	43	8.75	40	Artificial
Rotation: 0-180					
albano	8	24	7.25	4900	Garment
shapes2	4	20	7.5	15	Artificial
dagli	10	30	6.3	60	Garment
shapes1	4	43	8.75	40	Artificial
Rotation: 0-90-180-270					
fu	12	12	3.58	38	Artificial, convex
mao	9	20	9.22	2550	Garment
marques	8	24	7.37	104	Garment
jakobs1	25	25	5.6	40	Artificial
jakobs2	25	25	5.36	70	Artificial

and different strategies for choosing the pieces to be re-inserted.

Let $s(X^s, Y^s, O^s)$ be a solution of a given nesting problem. Vectors $X^s = (x_1^s, \ldots, x_N^s)$ and $Y = (y_1^s, \ldots, y_N^s)$ denote the coordinates of the reference point of the pieces and vector $O = (o_1^s, \ldots, o_N^s)$ denotes the rotation angle used by the pieces.

Each solution $s(X^s, Y^s, O^s)$ is associated with an *HS2* model defined by the vector of rotations O^s. We denote by MIP^s the model defined by the solution s. Furthermore, given s, for each pair of pieces, i, j, we can identify the slice in which the reference point of j lies relative to i and then we can determine which binary variable associated with NFP_{ij} takes the value 1. The identification is not necessarily unique, because the reference point of piece j may lie on the border of more than one slice. We denote this set of binary variables by B_s.

If we solve the corresponding linear problem with the binary variables of B_s set to the value 1, we obtain a solution s' satisfying $L_{s'} \leq L_s$, where L_s and $L_{s'}$ denote the length of solutions s and s', respectively.

We denote by $N_n(i_1, \ldots, i_n; o_1, \ldots, o_n)$ the optimal reinsertion of pieces $i_1, \ldots, i_n$ with angles of rotation $o_1, \ldots, o_n$, respectively. In order to complete $N_n(i_1, \ldots, i_n; o_1, \ldots, o_n)$, we solve an *MIP* model, denoted by $MIP^s(i_1, \ldots, i_n; o_1, \ldots, o_n)$.

In the next subsection we explain the structure of the model $MIP^s(i_1, \ldots, i_n; o_1, \ldots, o_n)$. The relative position between pieces $i_1, \ldots, i_n$ and all the other pieces in the problem has to be free, that is, the model is going to choose the best relative position of pieces $i_1, \ldots, i_n$. However, the relative position between pieces of $P_R = P \backslash \{i_1, \ldots, i_n\}$ is going to be fixed, so binary variables from B_s which separate pieces of P_R are fixed to 1 in the model.

7.1.1 1-insertion

Let $i \in P$ be a given piece and let us denote by $N_1(i)$ the optimal insertion of piece i having studied the different rotations. This movement is done by solving several mixed linear problems *MIP*s, as many as the allowed rotations of piece i. Each one of the *MIP*s considered is denoted by $MIP(i, o_i)$, where o_i denotes the rotation angle of piece i.

In order to complete $N_1(i)$, we have to solve the corresponding $MIP(i, o_i)$ for each $o_i \in O$. The best solution obtained is the optimal insertion of piece i. Note that the placement of piece i after the $N_1(i)$ movement can be its previous position, which means that no change has been made in the solution.

Let us suppose that the rotation of piece i is changed from angle o_i to o_i'. The construction of $MIP(i, o_i')$ is not immediate, because we have to rotate piece i in the current model. Let us denote the previous *MIP* (o_i is the previous rotation of i) by $MIP'(i; o_i)$. All binary variables in the entire problem are considered (no relative position between any pair of pieces is fixed). Then, to build $MIP(i, o_i')$, we have to modify the following components of $MIP(i; o_i)$:

- Non-overlapping constraints (9.7). The *NFP*-constraints to be considered are those formed by the relative position of piece i to the rest of the pieces. Note that NFP_{ij}, $\forall j \in P \backslash \{i\}$ could change when piece i is rotated. For all pairs of pieces $j_1, j_2 \in P \backslash \{i\}$, the non-overlapping constraints do not change.
- The lifted bound constraints (2.23) and (2.24). These constraints also consider the interaction between each pair of pieces and use the *NFP*s. Then, if an *NFP* is modified, the corresponding lifted bound constraints have to be recalculated.
- It is possible that we need more binary variables. The new *NFP*s between piece i and the other pieces can be more complex, their outer regions can have more slices and then more binary variables would be needed for the *MIP* model.

Once piece i is rotated, we have to eliminate binary variables corresponding to NFP_{jk}, $j \neq i$, $k \neq i$ by fixing the corresponding relative position of pieces j and k given in the previous solution.

The first computational experiment that we are going to do consists in applying $N_1(i)$, $\forall i \in P$, stopping when no improvement is found, using the scheme in Algorithm 3.

In Table 7.2 we can see the computational results of the *1-insert* movement with three different objective functions. The first objective function, *FO0*, is the length of the strip (L). The second objective function, *FO1*, also considers the X-coordinate of the pieces and tries to place the pieces as much as possible at the beginning of the strip. The third objective function considers both coordinates of each piece. These objectives functions are defined in Section 6.1, where $\epsilon_1 = 0.001$ and $\epsilon_2 = 0.001$.

The average percentage of improvement obtained using *FO0* is slightly lower (7.91%) than that obtained using objective functions *FO1* and *FO2*, which get very similar results (8.34% and 8.41% respectively). The use of these functions has a positive effect on the performance of the insertion move. However, it increases the computational times, an effect already observed in Chapter 6.

The next computational test consists in checking the linear problem in which the piece to be re-inserted is eliminated from the model. If the solution to this linear problem does not improve the solution for the

Algorithm 3 *1-insertion* movement

Require: $s_c = (X^{s_c}, Y^{s_c}, B^{s_c}, \theta_{s_c})$;
  while s_c improve **do**
    Build π randomly (order of pieces to be re-inserted);
    for $i = 1, \ldots, N$ **do**
      $PIECE = \pi(i)$;
      $N1_1(PIECE)$;
      if Find best solution **then**
        Update solution s_c;
      end if
    end for
  end while

initial complete model, then it is not necessary to re-insert the piece because it cannot produce any improvement and we have to consider other pieces for reinsertion. We call the model without the piece to be re-inserted and with all the binary variables fixed the *reduced linear problem*. The results are presented in Table 7.3. The solutions obtained do not always match the ones given in Table 7.2 because *CPLEX* does not always give the same solutions, because it depends on the *MIP*s solved before the insertion.

We can see that checking the reduced linear problem before re-insertion reduces the computational effort considerably.

Table 7.2: *Performance of 1-insert with different objective functions*

	1-insert-FO0			*1-insert-FO1*			*1-insert-FO2*		
Instances	% Imp	Best L	Av. Time	% Imp	Best L	Av. Time	% Imp	Best L	Av. Time
Rotation: 0									
dighe2	17.91	107.76	1.92	16.78	124.26	2.17	16.83	126.59	2.17
poly1a	12.48	16.37	4.59	14.34	16.23	7.03	13.32	16.27	8.03
dighe1	11.32	129.52	5.92	11.07	128.43	8.83	9.92	128.33	7.31
shapes0	2.64	67.00	22.33	3.19	67.00	99.51	3.11	66.87	120.00
Rotation: 0-180									
albano	5.32	10297.30	85.56	6.12	10297.82	110.94	6.75	10260.16	141.25
shapes2	5.49	29.00	62.09	5.63	28.17	75.81	5.69	28.50	82.70
dagli	9.34	65.04	100.79	10.27	64.17	117.51	10.83	62.79	139.54
shapes1	3.09	61.00	184.63	3.61	60.00	227.19	3.75	60.00	248.90
Rotation: 0-90-180-270									
fu	11.70	33.40	5.53	11.87	33.00	5.48	12.12	33.00	6.31
mao	6.96	1942.06	81.41	7.56	1942.82	94.52	7.66	1942.37	101.23
marques	6.22	82.55	149.42	7.49	82.14	202.20	8.22	80.86	255.83
jakobs1	4.59	13.00	3.30	4.59	13.00	6.29	4.76	13.00	7.21
jakobs2	5.80	28.00	4.61	5.86	28.00	8.97	6.31	27.50	11.01
Average	**7.91**		**54.78**	**8.34**		**74.34**	**8.41**		**87.04**

Table 7.3: *Performance of 1-insert when the reduced linear problem is previously solved*

	1-insert-FO0			*1-insert-FO1*			*1-insert-FO2*		
Instances	% Imp	Best L	Av. Time	% Imp	Best L	Av. Time	% Imp	Best L	Av. Time
Rotation: 0									
dighe2	17.97	107.76	2.49	17.39	124.26	2.80	17.44	123.03	2.58
poly1a	12.84	16.37	5.53	13.92	16.23	6.18	13.20	16.27	6.85
dighe1	11.49	129.43	8.15	10.07	128.43	8.27	9.84	128.06	7.93
shapes0	2.75	67.00	39.46	3.05	67.00	50.26	3.03	67.00	52.42
Rotation: 0-180									
albano	5.22	10358.98	52.20	6.25	10299.48	83.56	5.99	10257.72	76.56
shapes2	5.39	28.83	48.89	6.05	28.17	53.34	6.06	28.50	55.50
dagli	9.16	63.95	64.03	9.39	62.52	66.26	10.24	64.26	81.27
shapes1	3.31	61.00	59.54	3.68	61.00	81.45	3.53	60.00	80.52
Rotation: 0-90-180-270									
fu	11.17	33.40	3.60	11.53	33.00	4.00	12.03	33.00	4.74
mao	6.70	1949.00	43.80	7.96	1942.77	55.61	7.34	1942.52	58.87
marques	6.03	82.55	64.49	7.25	82.60	106.38	7.53	82.14	125.03
jakobs1	4.59	13.00	4.71	4.59	13.00	4.60	4.76	13.00	5.28
jakobs2	5.94	28.00	6.31	6.16	27.50	6.94	6.01	28.00	8.40
Average	**7.89**		**31.01**	**8.25**		**40.74**	**8.23**		**43.54**

7.1.2 2-insertion

The *2-insertion* tries the reallocation of a pair of pieces. We randomly choose a pair of pieces and eliminate the relation of both pieces to all the other pieces. This means that we consider more binary variables than in the *1-insertion* and the corresponding *MIP*s are harder to solve to optimality.

Let us denote by $N_2(i, j; o_i, o_j)$ the optimal insertion of pieces i and j at once with a random rotation. The *MIP*s that we need to solve in order to complete the $N_2(i, j)$ movement are denoted by $MIP(i, j; o_i, o_j)$, $(o_i, o_j) \in OxO$.

In order to rotate a piece in the model we have to modify the constraints described in the *1-insertion*. Since in the *2-insertion* we have to rotate two pieces, we do it iteratively. The rotation angles are obtained randomly.

It could be interesting to choose a promising pair of pieces to be reallocated, but initially we study 10% of all the pairs of pieces using a random selection.

We consider the three different objective functions defined in Section 6.4. In Table 7.4 we can see that the best average results are obtained with the objective function *FO2*. In all cases the improvement percentages are clearly higher than in the *1-insertion*, but we need more computational time to complete the *2-insertion*.

As in the *1-insertion*, we are going to check whether the linear problem considered by dropping the two pieces to be reinserted improves the given objective function. If there is no improvement, we do not complete the *2-insertion* of the given pair of pieces. In Table 7.5 we can see that when checking the linear problems, the total computational time is reduced.

Table 7.4: *Performance of 2-insert with different objective functions*

	2-insert-FO0			*2-insert-FO1*			*2-insert-FO2*		
Instances	% Imp	Best L	Av. Time	% Imp	Best L	Av. Time	% Imp	Best L	Av. Time
Rotation: 0									
dighe2	24.51	100.00	10.78	25.92	100.00	10.72	25.15	100.00	11.13
poly1a	18.83	15.44	33.62	20.05	14.97	51.71	20.70	15.62	67.22
dighe1	16.48	125.22	37.55	16.81	128.33	42.18	17.29	122.72	49.85
shapes0	3.93	65.00	80.44	4.67	64.00	567.72	4.11	66.00	570.35
Rotation: 0-180									
albano	6.72	10413.14	153.56	7.44	10243.85	217.62	7.52	10185.82	230.28
shapes2	9.11	27.16	156.65	10.12	27.62	207.63	9.69	27.77	190.84
dagli	12.64	61.08	222.96	12.85	60.00	262.46	12.99	61.57	302.97
shapes1	4.05	62.00	456.54	3.94	60.00	796.95	3.86	60.00	613.32
Rotation: 0-90-180-270									
fu	16.92	32.69	12.02	18.36	33.00	15.76	17.18	32.87	12.41
mao	9.46	1888.48	204.34	9.65	1946.41	245.86	10.57	1934.83	251.34
marques	7.11	82.55	160.80	8.61	82.56	238.42	8.97	82.00	284.48
jakobs1	8.06	12.00	9.82	6.54	12.44	39.75	7.98	12.50	31.05
jakobs2	8.19	26.50	16.60	8.10	27.00	56.08	8.15	27.00	48.38
Average	**11.23**		**119.67**	**11.77**		**211.76**	**11.86**		**204.89**

Table 7.5: *Performance of 2-insert with FO0 when the reduced linear problem is solved*

Instances	*2-insert-FO0*			*2-insert-FO0* checking LP		
	% Imp	L best	Av. Time	% Imp	L best	Av. Time
Rotation: 0						
dighe2	24.51	100.00	10.78	23.44	100.00	12.88
poly1a	18.83	15.44	33.62	19.73	15.50	40.37
dighe1	16.48	125.22	37.55	18.33	120.82	52.58
shapes0	3.93	65.00	80.44	3.76	66.00	123.88
Rotation: 0-180						
albano	6.72	10413.14	153.56	6.81	10402.15	173.86
shapes2	9.11	27.16	156.65	10.33	27.42	176.39
dagli	12.64	61.08	222.96	11.40	61.65	152.49
shapes1	4.05	62.00	456.54	3.62	61.00	138.66
Rotation: 0-90-180-270						
fu	16.92	32.69	12.02	17.92	33.00	12.37
mao	9.46	1888.48	204.34	9.17	1949.00	129.97
marques	7.11	82.55	160.80	8.16	82.55	113.51
jakobs1	8.06	12.00	9.82	6.73	13.00	10.73
jakobs2	8.19	26.50	16.60	7.72	27.00	22.30
Average	**11.23**		**119.67**	**11.32**		**89.34**

7.1.3 3-insertion

The idea is the same as the previous movements. We denote the optimal reinsertion of three pieces by $N_3(i, j, k)$.

We randomly choose 1% of all the sets of three pieces and we randomly choose the rotation of each piece. In Table 7.6 we can see the computational results of the *3-insertion* movement. The average improvement is increased in relation to the *2-insertion*, but the computational time increases considerably.

Table 7.6: *Performance of 3-insert with different objective functions*

Instances	*3-insert-FO0*			*3-insert-FO1*			*3-insert-FO2*		
	% Imp	Best L	Av. Time	% Imp	Best L	Av. Time	% Imp	Best L	Av. Time
Rotation: 0									
dighe2	28.07	100.00	23.60	29.97	100.00	25.50	27.75	100.00	22.58
poly1a	24.33	15.12	92.18	24.49	14.84	108.18	23.17	15.39	107.13
dighe1	20.48	122.59	84.70	19.82	125.56	76.87	20.16	118.85	78.01
shapes0	6.49	64.00	1215.96	9.24	62.00	4494.49	8.04	61.00	3821.27
Rotation: 0-180									
albano	10.28	9931.25	1827.24	9.51	10131.77	1407.52	7.92	10170.82	1231.73
shapes2	14.18	26.20	5899.70	15.39	26.50	6524.60	14.28	26.50	6396.90
dagli	9.74	59.87	5233.78	9.41	60.20	5592.14	8.83	58.92	5459.56
Rotation: 0-90-180-270									
fu	18.75	32.71	38.72	19.56	32.00	35.84	19.26	32.20	33.41
mao	16.48	1849.12	1500.33	15.57	1853.84	1096.99	14.37	1856.00	1196.17
marques	12.07	79.00	1547.24	12.44	80.33	1563.61	10.97	81.00	1624.10
jakobs1	10.87	12.00	62.40	11.91	12.00	124.31	9.78	12.00	276.01
jakobs2	13.42	26.00	83.16	18.10	25.37	220.95	16.93	26.00	279.65
Average	**15.43**		**1467.42**	**16.28**		**1772.58**	**15.12**		**1710.54**

7.2 *Compaction*

The idea of this movement is to allow certain changes in the position of the pieces by giving them some flexibility to move to adjacent slices but without leaving any piece completely free. This idea is the same as trunk insertion described in Section 6.3.

Let s be a solution. For each NFP_{ij} such that pieces i, j are neighbors, we consider at least three binary variables. We consider the *neighborhood by movement* defined in Section 6.3 and another type of neighborhood, called *neighborhood by placement*, which considers the distance between the pieces. The set of pieces which belongs to the neighborhood by placement of piece i in solution s is given by:

$$NP_i^s = \{j \in P \mid (x_j, y_j) \in R_i\}$$

where R_i is the rectangle whose vertices are: $(x_i - \lambda l_i, y_i - \mu w_i)$,$(x_i + l_i + \lambda l_i, y_i - \mu w_i)$, $(x_i + l_i + \lambda l_i, y_i + w_i + \mu w_i)$ and $(x_i - \lambda l_i, y_i + w_i + \mu w_i)$. Initially, we consider $\lambda = 1$ and $\mu = 1$.

We define the combined neighborhood of a piece i in solution s as $NC_i = NP_i^s \cap NS_i^s$.

Once the combined neighborhood of each piece is calculated, we consider the binary variables whose corresponding *slices* are adjacent to the current *slice* in solution s, as shown in Figure 6.4.

We do the compaction movement until no improvements are obtained. Table 7.7 shows the computational results. We can see that this movement does not produce an important improvement. In fact, it works worse than the *1-insertion* movement.

Table 7.7: *Compaction comparative with different objective functions*

	Compaction-FO0			*Compaction-FO1*			*Compaction-FO2*		
Instances	% Imp	Best L	Av. Time	% Imp	Best L	Av. Time	% Imp	Best L	Av. Time
Rotation: 0									
dighe2	7.91	137.85	0.81	7.38	137.85	0.75	7.41	137.85	0.76
poly1a	12.56	17.06	3.61	10.89	17.06	4.50	11.09	16.60	4.41
dighe1	3.76	140.29	1.22	3.62	140.29	1.56	3.62	140.29	1.57
shapes0	4.10	65.50	221.95	3.72	65.90	228.12	3.59	65.83	250.43
Rotation: 0-180									
albano	4.62	10634.19	10.95	3.30	10634.19	14.99	3.66	10634.19	16.70
shapes2	4.88	29.07	77.59	4.70	29.17	104.35	4.51	29.07	114.26
dagli	4.45	65.39	10.82	4.02	66.13	21.07	3.66	66.13	19.39
shapes1	3.15	62.75	150.66	2.91	63.00	188.21	3.08	62.00	247.92
Rotation: 0-90-180-270									
fu	6.51	34.00	1.46	4.78	34.00	1.46	5.29	34.00	1.59
mao	6.83	1962.78	14.47	6.29	1962.78	31.69	5.98	1962.78	29.19
marques	3.13	86.48	9.31	3.84	86.48	12.65	3.38	86.48	21.42
jakobs1	8.59	12.82	3.63	7.63	12.82	5.47	8.03	12.82	6.22
jakobs2	8.57	27.78	9.27	8.07	27.76	22.67	8.37	27.76	32.75
Average	**6.09**		**39.67**	**5.47**		**49.04**	**5.51**		**57.43**

7.3 *1-Compaction*

In the *compaction* movement there is no piece whose relative position with all the other pieces is completely free. That is, none of the pieces can change its position dramatically.

The idea of the *1-Compaction* movement is a combination of the *1-insertion* with the *compaction*. So, one piece is going to be completely free and not all the variables of the *NFP*s of this piece with all the other pieces are fixed. The remaining pieces can only change their relative positions locally by the *compaction* movement.

We study two ways of performing the *1-compaction*. The first approach is based on solving just one MIP, *1-Compact* in one level, which is harder than the *1-insertion* and the *compaction* because it considers both sets of binary variables at once. The second approach has two phases. The first phase eliminates the selected piece and does the compaction until there is no improvement and then the missing piece is reinserted.

We study all the pieces to be re-inserted in a random order and all the allowed rotations until there is no improvement in the solution.

7.3.1 *1-Compaction* in one level

In Table 7.8 we can see that the computational time is very high and there are instances in which many *MIPs* cannot be solved to optimality and *CPLEX* returns the best upper bound. The time limit for each *MIP* is 50 seconds. This situation is worse when complex objective functions are used because the *MIP*s take longer to solve, which explains the relatively better performance observed when using *FO0*.

Table 7.8: *Performance of 1-Compaction done in one step*

	1-Compaction-FO0			*1-Compaction-FO1*			*1-Compaction-FO2*		
Instances	% Imp	L best	Av. Time	% Imp	L best	Av. Time	% Imp	L best	Av. Time
Rotation: 0									
dighe2	26.06	100.00	7.12	21.13	100.00	7.75	20.71	100.00	7.89
poly1a	27.21	15.16	63.90	19.56	15.85	64.46	16.21	16.15	43.69
dighe1	16.81	128.06	27.12	12.66	129.33	28.40	13.00	128.15	29.11
shapes0	8.02	63.50	3587.68	4.36	65.00	1438.88	3.37	64.83	1184.02
Rotation: 0-180									
albano	9.86	10111.01	1041.28	5.28	10250.08	199.22	5.33	10553.31	141.82
shapes2	15.28	27.03	6463.74	9.58	27.75	2264.51	9.36	27.75	2134.29
dagli	18.35	59.19	608.93	10.97	63.05	644.88	8.05	64.67	269.61
shapes1	7.98	58.50	4343.89	3.56	62.00	2389.22	2.90	61.00	1503.39
Rotation: 0-90-180-270									
fu	20.92	33.00	21.77	15.52	33.00	18.50	16.68	32.47	19.98
mao	15.02	1902.92	329.16	10.44	1890.46	215.00	8.19	1941.28	140.11
marques	12.13	80.00	443.74	8.46	82.55	266.19	6.93	84.23	190.26
jakobs1	14.24	12.00	42.55	11.16	12.07	41.83	8.92	12.89	36.66
jakobs2	16.94	26.00	154.85	12.82	26.45	194.83	9.32	27.01	161.37
Average	**16.06**		**1318.13**	**11.19**		**597.97**	**9.92**		**450.94**

7.3.2 *1-Compaction* into two phases

In Table 7.9 we can see that the computational time is reduced. On average this move is slightly better than the *2-insertion*.

Table 7.9: *Performance of 1-Compaction done in two phases*

Set of Instances	*1-Compaction-2S-FO0*			*1-Compaction-2S-FO1*			*1-Compaction-2S-FO2*		
	% imp	Best L	Av. Time	% imp	Best L	Av. Time	% imp	Best L	Av. Time
Rotation: 0									
dighe2	18.48	123.00	12.17	18.93	100.00	12.28	17.62	118.97	12.02
poly1a	20.62	15.51	59.74	19.72	15.57	55.17	18.85	15.68	44.63
dighe1	13.71	123.63	41.33	13.34	130.45	38.35	13.48	127.19	37.81
shapes0	7.58	63.50	2454.81	6.89	63.50	1953.22	4.64	64.00	1328.72
Rotation: 0-180									
albano	7.49	10242.11	311.16	5.53	10247.19	171.98	5.24	10156.15	182.42
shapes2	11.59	27.52	889.56	11.19	27.54	1095.13	10.55	27.77	814.78
dagli	13.38	61.44	493.97	13.31	61.00	418.01	10.74	62.00	296.87
shapes1	7.39	59.33	1791.13	5.91	61.00	1444.38	5.25	61.00	1303.58
Rotation: 0-90-180-270									
fu	16.01	33.00	16.31	16.12	33.00	14.35	14.74	33.00	14.29
mao	11.71	1935.05	235.14	9.85	1942.15	184.25	7.51	1946.76	187.02
marques	9.44	80.14	206.04	8.30	82.00	194.37	6.92	84.21	182.45
jakobs1	10.32	12.82	44.95	7.93	12.24	49.63	8.30	12.19	78.06
jakobs2	13.48	26.18	94.08	13.21	26.26	132.72	11.86	26.00	121.47
Average	**12.40**		**511.57**	**11.56**		**443.37**	**10.44**		**354.16**

7.4 Crossed objectives

In many of the solutions that we obtain when an *MIP* is solved we do not change the current solution, so much of the computational effort shown in previous tables is unsuccessful. That happens in all the local searches for optimization problems, but it is especially costly in this case because solving the *MIPs* requires very long computing times.

In this section we study alternative objective functions in order for modifying the current solution despite the length of the strip remaining unchanged.

Let us consider the *1-insertion* movement. When a piece is removed from a solution s, a *hole* in the solution is created. To encourage the neighboring pieces to change their positions and cover the hole, we use a *crossed objective function*. Let i be the piece which is going to be reallocated. We denote by NP_i^s the set of pieces which are neighbors of piece i in solution s. We divide NP_i^s into four subsets as follows:

- $NP1(i,s) = \{j \in NP_i^s \mid x_i \leq x_j, y_i \leq y_j\}$
- $NP2(i,s) = \{j \in NP_i^s \mid x_i \geq x_j, y_i \geq y_j\}$
- $NP3(i,s) = \{j \in NP_i^s \mid x_i < x_j, y_i > y_j\}$
- $NP4(i,s) = \{j \in NP_i^s \mid x_i > x_j, y_i < y_j\}$

Note that $NP_i^s = NP1(i,s) \cup NP2(i,s) \cup NP3(i,s) \cup NP4(i,s)$. Then the *crossed objective function*, COF, is defined as follows:

$$COF : \min L + \sum_{j \in NP1(i,s)} \epsilon(x_j + y_j) + \sum_{j \in NP2(i,s)} \epsilon(-x_j - y_j) + \sum_{j \in NP3(i,s)} \epsilon(x_j - y_j) + \sum_{j \in NP4(i,s)} \epsilon(-x_j + y_j)$$

Figure 7.1 shows an example of a *1-insertion* movement using the crossed objective function. In Figure 7.1 (a) we can see a solution of instance *shapes0* with $L = 69$. We randomly select piece 36 to be reinserted. The neighborhood of piece 36 is drawn in blue. In Figure 7.1 (b) piece 36 is removed and the direction

specified in the objective function for each piece of the neighborhood is drawn. After the corresponding *MIP* model is solved, we obtain the solution presented in Figure 7.1 (c), with $L = 68.5$. Note that the hole created when piece 36 is removed is partially covered by piece 28.

We can use these objective functions in the *2-insertion* and *3-insertion*. In these cases it is possible that the coordinates of one piece appear more than once in the objective function because this piece can be a neighbor of the two pieces being reinserted (or the three pieces in the *3-insertion*). In order to forbid this situation we assign a priority to the pieces being reinserted and for a piece which is a neighbor of more than one piece, we consider that it is a neighbor only of the piece which has greater priority.

In Table 7.10 we can see the effect of using the *crossed objective function* in the *1-insertion* and *2-insertion* movements. The results are improved considerably with respect to those obtained with the other objective functions.

Table 7.11 shows the results obtained by the *2-insertion* and *3-insertion* where all the rotations are checked in the reinsertion, and the *crossed objective function* is considered. In the *2-insertion* we can see a strong improvement but in the *3-insertion* the improvement is rather worse and the computational time is reduced. What happens in the *3-insertion* is that *CPLEX* gives upper bounds because it is not able to solve many of the *MIPs* to optimality. Then, when no improvement is detected, the movement stops.

Table 7.10: *Performance of 1-insert and 2-insert with crossed objective functions*

	1-insert-COF			*2-insert-COF*		
Instances	% Imp	Best L	Av. Time	% Imp	Best L	Av. Time
Rotation: 0						
dighe2	19.44	100.00	3.05	23.29	118.97	15.94
poly1a	17.32	15.53	13.93	22.94	15.19	67.12
dighe1	10.26	130.90	12.18	19.41	123.70	82.93
shapes0	2.49	67.00	89.53	7.25	63.00	535.66
Rotation: 0-180						
albano	7.34	10255.62	191.27	10.41	10077.25	514.37
shapes2	7.36	28.02	95.40	12.20	27.10	336.18
dagli	11.86	61.93	210.19	15.87	60.02	633.85
shapes1	3.46	62.00	301.26	10.30	58.00	1385.21
Rotation: 0-90-180-270						
fu	14.41	33.00	10.01	19.42	32.82	26.34
mao	10.75	1907.09	176.48	15.55	1852.82	606.66
marques	10.75	80.67	405.51	11.06	79.56	545.99
jakobs1	5.25	12.94	11.00	8.01	12.00	60.64
jakobs2	6.17	27.00	15.17	10.98	26.00	93.92
Average	**9.76**		**110.99**	**14.36**		**377.29**

Table 7.11: *Performance of 2-insert and 3-insert with crossed objective functions and using the best rotations*

	2-insert-COF-rotation			*3-insert-COF-rotation*		
Instances	% Imp	L best	Av. Time	% Imp	L best	Av. Time
Rotation: 0						
dighe2	26.06	100.00	35.95	26.49	100.00	37.44
poly1a	23.88	15.03	119.81	23.72	14.96	227.36
dighe1	19.84	117.47	114.56	19.48	113.79	113.48
shapes0	6.21	63.00	499.63	3.48	66.00	586.60
Rotation: 0-180						
albano	9.53	10084.08	1025.85	9.29	10201.59	830.49
shapes2	13.71	26.72	981.08	11.96	27.42	1189.40
dagli	16.19	60.02	1388.36	8.71	60.64	1301.64
shapes1	10.15	58.00	2256.27	-	-	-
Rotation: 0-90-180-270						
fu	20.25	32.17	134.63	19.59	31.89	69.56
mao	15.85	1852.73	1331.52	16.07	1844.49	1453.07
marques	13.28	77.37	2132.46	12.40	79.69	1854.55
jakobs1	8.13	12.00	102.40	8.07	12.17	74.81
jakobs2	9.77	26.00	142.68	9.20	26.00	186.31
Average	**14.84**		**789.63**	**14.04**		**660.39**

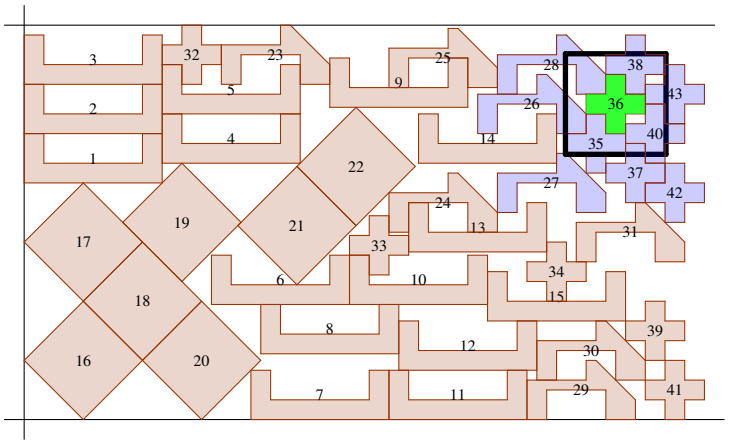

(a)

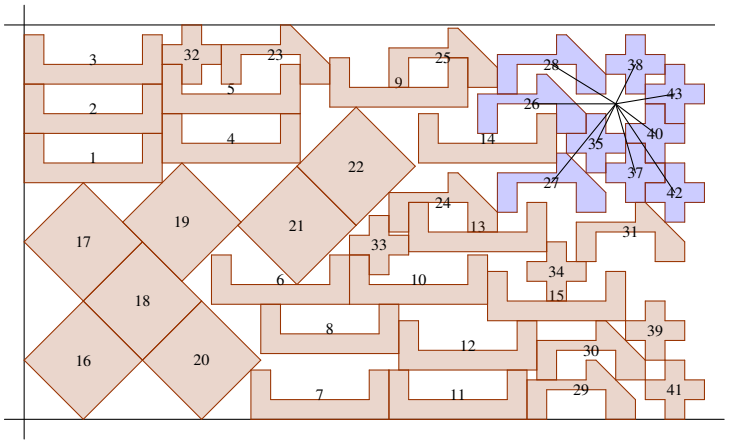

(b)

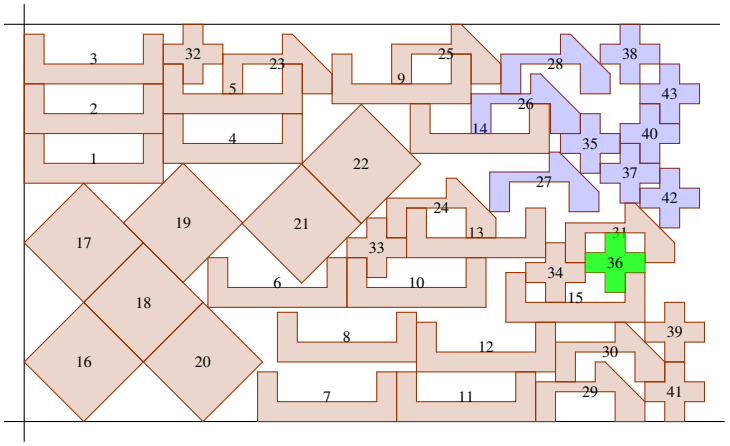

(c)

Figure 7.1: *One iteration of a 1-insertion movement with a crossed objective function*

Chapter 8

Iterated Greedy Algorithm

8.1 Introduction to the *Iterated Greedy* Algorithm

An Iterated Greedy Algorithm (IGA) generates a sequence of solutions by iterating over constructive heuristics using a destruction and a construction phase. It can be improved by a local search after the construction phase. The difference with the Iterated Local Search (ILS) is that the IGA iterates over construction heuristics instead of iterating over a local search procedure.

Iterated Greedy Algorithms have been applied successfully to the Set Covering Problem by Jacobs and Brusco [36] and Marchiori and Steenbeek [44]. Ruiz and Stützle [57] use an IGA for the permutation flowshop problem. However, IGA has not yet been applied to *nesting* problems.

The destruction procedure removes several pieces from either the current solution or the best known solution. The strategy for choosing the number of pieces to be removed and the selection criteria are presented in Section 8.2. As happens in ILS, at an iteration combining destruction, construction and a local search the IGA could produce the same solution from which the iteration started. In this case, the destructive algorithm can change along the IGA iterative process, becoming more aggressive.

The construction phase is based on the insertion of the pieces removed in the destruction phase in a similar way to the constructive algorithm presented in Section 6.3. After this phase we obtain high quality solutions and in many cases the best solution of the algorithm. However, in order to look for even better solutions, after the construction phase we apply a local search procedure based on the movements presented in Chapter 7. In Section 8.2 we present the destructive phase and in Section 8.3 we explain the constructive phase. The local search procedure is defined in Section 8.4. The *Iterated Greedy Algorithm* structure is explained in Section 8.5. Finally, the computational results and conclusions are presented in Section 8.6.

8.2 Destructive phase

The solution obtained after applying the local search procedure described in Chapter 7 is usually tight. To determine the level of tightness of a given solution associated with the current *MIP* model, we solve two linear problems which consist of fixing all the binary variables to their current values and changing the objective function as follows:

FO1: $L + \sum_{i=1}^{n} x_i$

FO2: $L - \sum_{i=1}^{n} x_i$

When we solve the linear model with *FO1*, all the pieces are placed as close as possible to the beginning of the strip. On the other hand, when we consider *FO2*, all the pieces are placed as close as possible to the end of the strip. The total Euclidean distance between the X-coordinates of each piece in both solutions (obtained by *FO1* and *FO2*) is therefore a good indicator of the tightness of the solution.

We divide the pieces into two groups. Let us denote by x_i^1 and x_i^2 the value of the x-coordinate of piece p_i in the solution obtained by considering, respectively, objective functions *FO1* and *FO2*. We divide the pieces into the following two subsets:

- $P^1 = \{i \mid dist(x_i^1, x_i^2) = 0\}$
- $P^2 = \{i \mid dist(x_i^1, x_i^2) > 0\}$

The set of pieces which remains in the same position after the two linear problems are solved, P^1, could be viewed as the *skeleton* of the solution. That is, we have to modify the relative position between a pair of pieces of P^1 in order to improve the current solution. The pieces of P^2 do not determine the current length of the solution directly because they have some slack.

Therefore, we are going to choose pieces from P^1 randomly. At the beginning, the number of pieces to be removed, n', is going to be $n' = 3$, but it could increase by one if the local search procedure or the constructive algorithm reaches the same solution as the previous iteration. If the best solution is found in the current iteration, then n' changes again to 3. We consider $n' \leq 5$ as the upper limit, because the constructive phase allows us to change the relative positions between the pieces already placed and that makes it computationally hard to rebuild the solution if $n' > 5$.

8.3 Constructive phase

In Chapter 6 we developed and studied several strategies for constructive algorithms. The algorithm producing the best results included a special feature, allowing certain flexibility of the pieces already placed in the strip when inserting a new piece ((*trunk insertion*). This algorithm required computing times which were higher than the simpler approaches. If we want to use this strategy in the IGA, we need to control the computational effort at each iteration. We also know from the computational tests in Chapter 6 that since the constructive algorithm inserts the pieces one at a time, the first insertions are easier than the last ones. The number of binary variables can be considered a good indicator of the relative difficulty of the problems, so if there are a lot of binary variables in an *MIP* problem, it is likely to be difficult to solve. Furthermore, we have also seen that when an *MIP* model is solved by *CPLEX* and it stops before optimality because of the time limit, the solution returned by *CPLEX* can be a bad solution.

Bearing in mind all these lessons from Chapter 6, we have to control the computational effort each time an *MIP* is solved. To do that, we use two parameters:

- *nh* : the number of pieces whose relative positions are relaxed in the next insertion. In the constructive algorithm presented in Section 6.3, *nh* is always the number of pieces already placed in the bin,

but here this number will be controlled and adjusted by the dynamic strategy described in the next paragraphs.

- ϵ_s: determines the size of the neighborhood by movement of a piece and thus the number of neighbors whose positions can be relaxed.

The value of these parameters nh and ϵ_s are not fixed beforehand, but adjusted using the information from the *MIPs* being solved, the quality of the solutions obtained and the time spent obtaining them.

Let us denote the number of pieces already placed by n' and let $i_{next} \in P$ be the next piece to be placed. Let us denote the pieces already placed by $i_1, \ldots, i_{n'}$. Initially, nh is going to be the number of pieces already placed in the bin ($nh = n'$). The time limit considered for each insertion is 50 seconds, that is, if *CPLEX* is not able to prove optimality in 50 seconds then it returns the best solution found. We denote by ti the computational time needed by *CPLEX* to solve the *MIP* model.

In the case that $ti \leq 25$, we consider that the *MIP* has been easy to solve and the following parameters are modified:

- nh is incremented by one (in the case that it is less than the number of pieces already placed in the bin). Since i_{next} is placed, then n' has incremented by one and, therefore, nh is increased by one.
- ϵ_s is multiplied by 2. If ϵ_s increases, the neighborhood of a given piece is expanded. If ϵ_s were big enough, all the pairs of pieces in the bin would be considered as neighbors and the structure of the solution could change completely after the new insertion is made.

If $ti > 25$, we consider that the corresponding *MIP* has been hard to solve and the parameters are adjusted in the following way:

- nh is reduced by one
- ϵ_s is divided by 2 in order to reduce the number of binary variables in the next *MIP* model.

Since we use 50 seconds as the time limit for *CPLEX*, in the worst case $ti = 50$. In this case we focus on the *GAP* given by *CPLEX* and compare it with τ.

- If the *GAP* obtained is lower than τ, then the last insertion is accepted, $nh = 0$ and $\epsilon_s = 0.1$ for the next insertion.
- In the case that the *GAP* obtained is greater than τ, then the given solution is not accepted and there is an attempt to reinsert i_{next} with $nh = 0$ and $\epsilon_s = 0.1$.

We are going to consider $\tau = 0.3$, that is, we accept the feasible solution given by *CPLEX* if the *GAP* is lower than 30%.

We denote this constructive algorithm as *DCHS2-TI* (Dynamic *CHS2-TI*). Table 8.1 compares the *DCHS2-TI* with the static version *CHS2-TI*, both with objective function *FO1*. We can see that the *DCHS2-TI* algorithm produces similar results and the computational time is reduced considerably when the instance size increases. In fact, *DCHS2-TI* is able to deal with large instances such as *swim* or *shirts*. Table 8.2 shows the average results of 20 runs for all the instances of *nesting problems* that we can find in the literature (see Section 6.1).

Table 8.1: *Comparing static CHS2-TI and dynamic DCHS2-TI.*

Set of	*CHS2-TI* - FO1			*DCHS2-TI*		
Instances	Av. L	Best L	Av. Time	Av. L	Best L	Av. Time
Rotation: 0						
poly1a0	16.40	15.44	25.32	16.23	15.39	69.19
shapes0	64.75	60.43	1614.00	66.10	62.00	463.69
Rotation: 0-180						
albano	10592.49	10317.27	178.74	10587.49	10128.78	158.99
shapes1	60.95	57.33	1527.75	62.09	58.00	433.88
Rotation: 0-90-180-270						
fu	36.58	35.16	2.1209	35.69	34.10	4.87

The constructive algorithm *DCHS2-TI* is used to build the initial solution for the IGA algorithm and to rebuild the partial solutions given by the destructive phase. When *DCHS2-TI* is used after the destructive phase, we evaluate whether the completed solution is accepted or not for going to the local search phase, depending on the length obtained. The idea is to send only those solutions which are considered promising to the time-consuming local search procedure, that is, those which have possibilities of improving the best known solution. In order to do that, we use a threshold ρ which gives the maximum percentage of deviation with respect to the best known solution a solution can have to be considered for local search. Initially, for each iteration of the IGA algorithm, we consider $\rho = 0.05$ (5%) and it increases 0.01 every two times *DCHS2-TI* fails.

8.4 Local search procedure

In Chapter 7 we described different movements for the local search. The different approaches are the *n-insertion* (see Section 7.1), the *compaction* (see Section 7.2) and the *1-compaction* (see Section 7.3). The *3-insertion* and *1-compaction* require a high computational effort and will not be used here in the design of the local search phase.

On the other hand, we have improved the *1-insertion* and the *2-insertion* in such a way that the local search procedure produces good improvements in a reasonable time. The original *1-insertion* is very rigid and does not produce a good improvement over the constructive algorithm. Therefore we propose a new version of the *1-insertion* which changes dynamically depending on the evolution of the *Iterated Greedy* algorithm. We are going to use a similar idea on the *2-insertion*.

In both movements, *1-insertion* and *2-insertion*, we consider the crossed objective function *COF* defined in Section 7.4. We have shown that this objective function works better than *FO1* or *FO2*.

Table 8.2: *Average results of DCHS2-TI in all the nesting instances.*

Set of Instances	*DCHS2-TI* Av. L	Best L	Av. Time
Rotation: 0			
dighe2	126.17	100.00	2.23
poly1a0	16.23	15.39	69.19
dighe1	133.00	123.68	77.24
shapes2-0	28.48	27.63	255.57
shapes0	66.10	62.00	463.69
trousers0	266.05	256.97	1332.21
shirts0	66.18	63.44	2358.34
Rotation: 0-180			
blaz2	21.56	21.10	74.19
albano	10587.49	10128.78	158.99
shapes2	28.55	27.41	256.31
dagli	63.48	61.27	217.48
shapes1	62.09	58.00	433.88
swimm1	7100.11	6750.09	2232.94
trousers	256.18	248.45	1074.28
shirts	66.07	63.94	1920.12
Rotation: 0-90-180-270			
fu	35.69	34.10	4.87
mao	2042.89	1928.78	98.39
marques	82.25	80.29	91.95
jakobs1	12.47	12.00	147.93
jakobs2	27.08	26.00	222.67
poly1a	15.61	14.71	87.13
poly2a	30.44	28.45	412.24
poly2b	34.03	30.76	447.10
poly3a	45.01	43.19	802.95
poly3b	44.76	42.85	825.39
poly4a	60.47	56.92	1411.32
poly5a	80.06	76.68	2374.67

The local search procedure is based on applying either the *1-insertion* or *2-insertion* while the length is reduced. In the case of the solution changing and the length remaininig equal, then we repeat the same movement one more time. If in the second iteration the length is not reduced, we change to the other movement. The local search finishes when the two movements are performed without changing the current solution, or in two iterations for each movement the length remains equal. The first movement to be applied is chosen randomly.

8.4.1 *1-insertion* modified

We use the notation introduced in Section 7.1. Let $i \in P$. In order to obtain the best re-insertion of piece i with rotation o_i we need to solve the model $MIP(i, o_i)$. In the standard $N_1(i)$ the relative position between the remaining pieces, $P_R = P \setminus \{i\}$, is fixed. We denote by $N_1^{nh,\epsilon_s}(i)$ the $N_1(i)$ where nh pieces of P_R relax their relative positions with respect to their corresponding neighborhood by movement defined by parameter ϵ_s.

To choose the piece to be reinserted, we consider the pieces whose slack in the strip is 0, that is, we are

going to use the strategy presented in Section 8.2 to identify the set of pieces which belongs to the skeleton of the current solution. If there are more than 20 pieces on the skeleton we randomly choose 20 of them to be reinserted, otherwise we try to reinsert all the pieces of the skeleton.

The constructive algorithm presented in Section 8.3 uses a dynamic strategy here to calibrate the values of parameters nh and ϵ_s. When the solution is completely built, the values of nh' and ϵ'_s used in the insertion of the last piece are considered a good starting point for the values of the parameters nh and ϵ_s in the local search procedure. However, in order to intensify the local search movements during the *IG* algorithm, nh could increase.

Initially we consider the values $nh = \min\{5, nh'\}$ and $\epsilon_s = \min\{W/10, \epsilon'_s\}$. If during three iterations of the IG algorithm the best known solution does not change, nh is increased by 1 unit. The upper limit is $nh \leq 15$. If in a given iteration of the local search the best known solution is improved, nh is reset to its initial value.

8.4.2 *2-insertion* modified

Let $i, j \in P$. The *2-insertion* ($N_2(i, j)$) with crossed objective functions presented in Section 7.4 is based on the reinsertion of pieces i and j together, and the objective function encourages neighboring pieces to be placed in the holes produced by removing i and j. However, the position of the neighboring pieces from i and j could be limited by other pieces and the probability of placing both pieces at their initial positions can be very high. So, as in *DCHS2-TI* and in the modified *1-insertion*, some of the pieces are going to relax their relative position within their neighborhood. In *DCHS2-TI* and *1-insertion* these pieces are selected randomly. Here we are going to consider the neighborhood of pieces i and j, that is, we relax the relative position between any piece from the neighborhood of pieces i and j and the pieces from the corresponding neighborhood of the given piece. We call this movement the modified *2-insertion*.

The modified *2-insertion* has the following parameters:

- np: The number of pairs of the skeleton which are attempted to be reinserted.
- ϵ_s: Defines which pieces belong to the neighborhood of a given piece.

The computational test presented in Section 7.4 considered np to be 10% of all the pairs of pieces. In the modified *2-insertion* we consider several values for np, ranging between 5 and 80 without taking into account the total number of pieces. The second parameter, ϵ_s, can take the values 1, $W/10$ and $W/15$. With such values we build different strategies for the *2-insertion*.

L0 : $np = 5$ and $\epsilon_s = 0.1$.

L1 : $np = 20$ and $\epsilon_s = 0.1$.

L2 : $np = 20$ and $\epsilon_s = 1$.

L3 : $np = 20$ and $\epsilon_s = W/10$.

L4 : $np = 40$ and $\epsilon_s = W/10$.

L5 : $np = 60$ and $\epsilon_s = W/10$.

L6 : $np = 80$ and $\epsilon_s = W/10$.

The modified *2-insertion* of level 0 ($L0$) is the fastest. When the IGA does not improve the best solution in three iterations, then the level of the *2-insertion* is incremented. If the best known solution is improved in the current iteration of the IG algorithm, we reset the level of the *2-insertion* to $L0$.

8.5 IG Algorithm

The *Iterated Greedy* (IG) algorithm is based on the constructive algorithm *DCHS2-TI* presented in Section 8.3. The (IG) algorithm is organized as follows:

S.1 Build the solution with the constructive algorithm.

S.2 Apply the local search procedure.

S.3 If the best solution is improved, then it is updated. If the distance between the solution obtained and the best known solution is lower than 1%, we randomly choose the solution to be used in the destruction phase (the best or the current solution). Otherwise, we consider the best known solution in the destructive phase.

S.4 Perform the destructive phase.

S.5 Use the *DCHS2-TI* algorithm to rebuild the partial solution.

S.6 If the threshold (ρ) is satisfied (the distance between the solution obtained and the best solution is lower than ρ), go to (S.2). Otherwise, go to (S.4) with the best known solution.

We denote the best known solution by s^*. The solution obtained in the constructive phase is denoted by s (initially $s = s^*$). In the second step we apply the local search procedure presented in Section 8.4 (S.2). We denote by s' the solution obtained after applying the local search procedure to solution s. Then we differentiate the following cases:

- $L_{s'} \leq L_{s*}$. In that case the best known solution is improved, so $s*$ is updated and the following parameters reset their values:
  - $n' = 3$, where n' denotes the number of pieces to be removed in the destructive phase.
  - $nh = \min\{5, nh'\}$ and $\epsilon_s = \min\{W/10, \epsilon'_s\}$ in the *1-insertion* of the local search (see Subsection 8.4.1).
  - $np = 5$ and $\epsilon_s = 0.1$ in the *2-insertion* (L0) of the local search (Subsection 8.4.2).
- $L_{s'} > L_{s*}$. In that case we update the solution s ($s \leftarrow s'$) (note that by construction $L_{s'} \leq L_s$). The number of iterations without improving the best known solution (*niter*) is incremented by one. In the case that $niter = 3$ and the movements of the local search can increase the parameters (we are not using the most aggressive version of either movements), then we do:
  - If $n' < 10$, then n' increases by one unit.
  - $niter = 0$

– The levels of both movements in the local search procedure are incremented, if possible.

After the local search procedure we use the destructive phase described in Section 8.2 in order to eliminate n' pieces from either the current solution s or the best known solution s^* ((S.3) and (S.4)). In the case that the distance between L_s and L_{s^*} is more than 1%, we consider s^* in the destructive phase. Otherwise, we randomize the selection between s and s^*.

The destructive phase eliminates several pieces randomly chosen from the skeleton of the solution. The partial solution obtained is rebuilt with the constructive algorithm (S.5). As we mention in Section 8.3, we use a threshold (ρ) to eliminate bad solutions obtained in (S.5). If the solution given by (S.5) satisfies that the distance between the best known solution is lower than threshold ρ, we apply the local search (go to S.2). Otherwise, we go to step (S.4) with the best known solution and every two times that happens ρ is incremented by one unit.

The stopping criteria are based on the computational time, the total number of iterations and the number of iterations without improving the best known solution. We consider that one iteration is completed after the local search procedure is used (S.2). The IG algorithm finishes in the following cases:

- Total computational time is greater than 36000 seconds and during 20 iterations the best known solution has not been modified. In difficult instances as *swim*, *trousers*, *poly2a*, *poly2b*, *poly3a*, *poly3b*, *poly4a*, *poly5a* and *shirts*, which one iteration the local search procedure requires more than 1000 seconds we allow only 2 iterations without improve the best known solution.
- The total number of iterations is greater than or equal to 100, and for 20 iterations the best known solution has not been modified.

The next section shows the computational results and a comparison with state of the art algorithms.

8.6 Computational results

The Iterated Greedy Algorithm (IGA) described in the previous section was implemented in C++ using Visual Studio 2008. We used CPLEX 12.5 to solve the Mixed Integer Programming models and the computational tests were performed on a PC with a core i7 2600 processor and a 12 GB memory.

We use the instances presented in Section 1.6.1 with the following exceptions and modifications:

- Instances *glass1*, *glass2*, *glass3*, *dighe2* and *dighe1* are simple to solve. These instances are broken glass instances and the pieces cannot rotate The IGA algorithm obtains the optimal solution in less than 10 seconds in all the instances, with the exception of instance *dighe1* for which it proves optimality in 10567 seconds. Furthermore, all the algorithms that we are going to consider obtain the optimal solution of instances *dighe1* and *dighe2* (instances *glass* are not considered).
- Instances *poly*4*b* and *poly*5*b* have only been used by Burke et al.[18] and with the tools we have available we had problems calculating all the non-fit polygons, as there are too many different types of pieces (60 and 75 respectively).
- For the instance *swim* we have built a version reducing the number of vertices of the pieces in such a way that each solution of the reduced version is a valid solution for the original instance.

We are going to consider the algorithms state of the art algorithms from the literature as follows:

BLFH The Bottom-Left-Fill heuristic algorithm by Burke et al.[18] (2006).

SAHA The hybrid simulated annealing algorithm by Oliveira et al. [32] (2006).

2DNEST The fast neighborhood search for polygon placement using a bottom-left strategy by Egeblad et al. [26] (2007).

ILS The iterated local search by Imamichi et al. [35] (2009).

FITS The local search algorithm by Umetami et al. [69] (2009).

BS The beam search implementation by Song and Bennell [62] (2010).

ELS The extended local search algorithm based on nonlinear programming by Leung et al. [40] (2012).

SA-SMT The two level algorithm by Sato et al. [58] which uses the collision-free region and exact fitting placement. Since the inner level is a simulated annealing algorithm then we refer to this algorithm as *SA-SMT* (Simulated Annealing by Sato, Martins and Tsuzuki, 2012).

In Table 8.3 we compare the minimum length obtained by all the algorithms in all the instances. The table has two parts because some instances have been used by all the authors while others have only been used by Burke et al.[18].

In the first part of the table, we can see that none of the algorithms gets the best solution for all the instances, showing that for this very difficult problem none of the proposed approaches is consistently the best. Our algorithm IGA improves the best solution published in the literature in instances *shapes0* and *shapes2* (in Section 1.6.1 we can see the solutions drawn). In general, the results obtained with *IGA* are competitive with all the other algorithms. However, it seems that our algorithm works slightly worse on instances with a high number of pieces, such as *swim*, *shirts*, *trousers*. Furthermore, in these instances, the computational time increases considerably in order to complete 20 iterations without improvement (see Table 8.4). This behaviour indicates that the corresponding *MIP*s that we solve in each movement of the local search procedure are very hard to solve to optimality.

In the second part of the table, the results obtained with the *IGA* algorithm improve the best know solution in all these instances, with the exception of instance *poly5a*. However, instances *poly2a*, *poly3a*, *poly4a*, *poly5a*, *poly2b* and *poly3b* require a great computational effort although the number of pieces is not too high.

Instance *poly1a0* can only be compared with the result obtained with the exact algorithm presented in chapter 3. We can see that by giving 36000 seconds to both algorithms, the *IGA* obtains a solution of $L = 14.6$, while the exact algorithm gets $L = 15.9$ (see Table 3.10).

Table 8.4 completes the information in Table 8.3 not only for IGA but for all the other algorithms. It can be seen that the good results of *SA-SMT* are obtained at a high computational cost, much higher than those of *ELS*, *ILS* and *FITS*, which attain a very good balance between quality and cost. In our case, we have allowed our algorithm a higher computational time than these three algorithms, but not as high as *SA-SMT*.

Table 8.3: *Best length obtained by each algorithm*

Instances	*BLFH*	*SAHA*	*2DNEST*	*ILS*	*FITS*	*BS*	*ELS*	*SA-SMT*	*IGA*
Albano	9980.86	9957.41	9905.94	9874.48	9942.62	9905.88	9838.70	**9758.70**	9887.62
Dagli	59.94	58.20	58.24	58.08	59.40	57.65	57.56	**57.40**	57.56
Fu	31.57	31.33	**30.97**	31.43	31.24	31.57	31.00	31.00	31.00
Jakobs1	11.50	12.41	**11.00**	11.28	**11.00**	11.40	**11.00**	**11.00**	11.32
Jakobs2	24.70	24.97	23.80	23.39	23.87	24.01	23.00	**22.75**	23.77
Mao	1821.70	1785.73	**1731.26**	1766.43	1760.35	1753.20	1747.80	1749.88	1769.54
Marques	78.00	78.48	77.04	77.70	77.54	77.79	77.09	**76.85**	**76.85**
Shapes0	60.00	60.00	59.52	58.30	60.00	62.00	58.99	59.03	**58.00**
Shapes1	55.00	56.00	54.04	54.04	54.01	55.00	**53.00**	55.02	55.00
Shapes2	26.80	25.84	26.48	25.64	26.44	26.57	25.65	25.93	**25.57**
Shirts	63.40	62.22	61.77	60.83	62.13	**60.21**	61.09	61.65	63.38
Swim	6270.88	5948.37	6097.78	5875.17	5970.52	5892.72	**5864.24**	6162.43	6161.40
Trousers	245.28	242.11	241.23	242.56	243.63	**241.00**	243.01	241.83	244.28
poly1a0									**14.60**
poly1a	13.30								**13.16**
poly2a	27.09								**26.16**
poly3a	41.07								**40.32**
poly4a	54.60								**54.14**
poly5a	**68.84**								70.56
poly2b	29.63								**29.54**
poly3b	40.50								**40.38**

Looking at the results obtained by *IGA* in more detail, we have observed that it obtains good solutions after applying the destructive and constructive phases. In fact, these procedures often obtain the best current solution before applying the local search procedure. Nevertheless, the local search procedure usually improved the current solution. The movements used have been extensively studied. The difficulty of the models that we have to solve each time any movement is done depends on the problem and even on the current solution. For this reason we have chosen a dynamic strategy based on the gap obtained and the computational time needed by CPLEX to solve the corresponding models and we have tried to adjust the parameters in order to build affordable MIP problems.

Despite the fact that instance *shapes1* has 43 pieces and instance *poly2b* only 30, one iteration of the local search procedure requires more time in instance *poly2b*. This difference might be given because the proportion between the width of the strip and the average width of the pieces is greater on instance *shapes1*. That is, generally, pieces are wider in proportion with the strip width on instance *shapes1*.

The computational results show that *IGA* is competitive with the state of the art algorithms and improves the best known solution in several instances.

Table 8.4: *Computational times of algorithms*

Instances	*BLFH*	*SAHA*	*2DNEST*	*ILS*	*FITS*	*BS*	*ELS*	*SA-SMT*	*IGA*
Albano	299	45140	21600	12000	12000	20883	12030	190342	36000
Dagli	252	102200	21600	12000	12000	68601	24100	629047	36000
Fu	139	5920	21600	6000	12000	4435	12000	32497	13605
Jakobs1	29	6640	6000	6000	12000	7543	6030	7497	36000
Jakobs2	51	9080	21600	6000	12000	285	6020	79496	36000
Mao	152	164900	6000	12000	12000	62772	12040	3195538	36000
Marques	28	150140	21600	12000	12000	39508	12040	74614	36000
Shapes0	274	78820	6000	12000	12000	1119	12070	181204	36000
Shapes1	239	206280	6000	12000	12000	1410	12120	491459	36000
Shapes2	281	45140	21600	12000	12000	20784	12050	261004	36000
Shirts	194	207820	21600	12000	12000	32616	12930	2528972	203563
Swim	141	138740	21600	12000	12000	64678	12460	5287061	113981
Trousers	243	171760	21600	12000	12000	28631	12370	1016331	91689
poly1a0									36000
poly1a	254								36000
poly2a	239								67986
poly3a	159								198253
poly4a	224								58931
poly5a	300								108866
poly2b	189								133521
poly3b	114								202277

Chapter 9

Two dimensional irregular bin packing problems with guillotine cuts

9.1 Introduction

The two-dimensional irregular-shape bin packing problem with guillotine cuts arises in the glass cutting industry, where each cut in the cutting process divides the stock sheet, or the given part that is going to be cut, into two different parts. Most of the algorithms that can be found in the literature on two-dimensional irregular-shape packing problems minimize the length of the strip required to accommodate the pieces and do not force a guillotine cut structure. On the other hand, most of the algorithms including guillotine cuts deal with rectangles, so the guillotine cuts are orthogonal with the edges of the stock sheet. Therefore, the problem considered here combines three difficult components: the non-overlapping of the pieces, which with irregular polygons is a hard problem, especially when the pieces are allowed to rotate freely; the bin packing problem in which pieces have to be associated with bins; and the guarantee that the solution can be produced by a set of guillotine cuts. We propose a constructive algorithm which inserts the pieces one at a time by using a mathematical model and two different guillotine cut structures. This constructive algorithm outperforms the previous algorithms designed for this problem.

9.2 Literature review

The problem considered in this chapter is a very special case of nesting problems. As the material to be cut is glass, only guillotine cuts are allowed. That in turn forces the pieces to be convex, but they adopt different geometrical non-rectangular shapes: triangles, trapeziums and other shapes. Another special characteristic is that the raw material cannot be considered a strip of infinite length, because it comes in rectangular sheets of given dimensions. Therefore, the problem is a bin-packing problem in which the number of bins required to accommodate all the pieces has to be minimized. Pieces are allowed to rotate freely. An example of this problem appears in Figure 9.1.

Up to now, the only paper which has dealt with the irregular-pieces bin packing problem with guillotine cuts is presented by Bennell et al. [11]. They propose two different construction heuristics. The first heuristic, a one-stage algorithm, combines two pieces (or two sets of pieces) by matching two of their edges using a dynamic solution evaluation to create a new item which is transformed into its convex hull. Therefore, the guillotine cut structure is always satisfied. This algorithm produces high-quality results in problems with

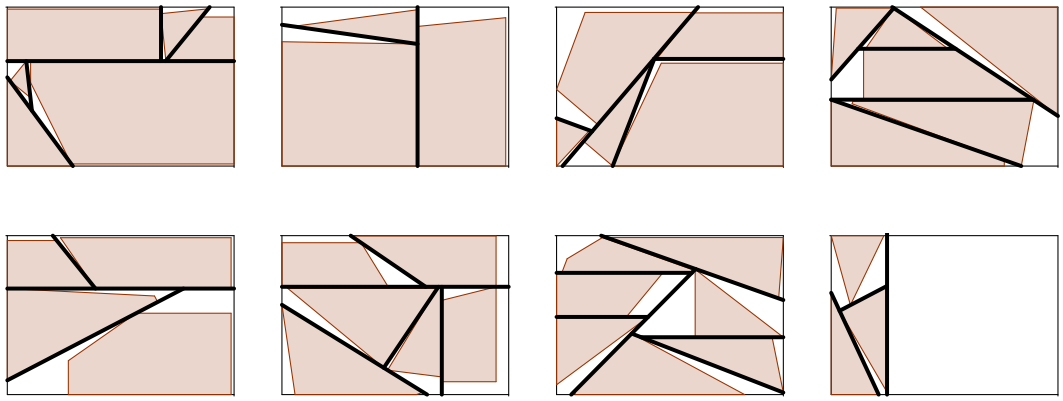

Figure 9.1: *Real example of a bin packing problem with guillotine cuts and non-rectangular pieces*

a low number of pieces per bin. When pieces are small and many pieces fit into one bin, this algorithm requires great computationally effort. The second constructive heuristic, a two-stage algorithm, combines pairs of pieces into rectangles by using the phi-functions presented by Romanova et al. [56], and then uses the guillotine bin packing algorithm developed by Charalambous and Fleszar [19] to pack the rectangles. The combination of the pieces into rectangles using phi-functions requires great computational effort, up to eighteen hours in the largest instance (149 pieces), although the packing algorithm by Charalambous and Fleszar [19] takes less than one second.

In this chapter we propose a constructive algorithm based on the insertion of pieces one at a time. In order to add one piece to a given bin, a mixed integer model is solved to optimality. The model is based on the formulation proposed in Chapter 2 for *nesting problems* but, in order to guarantee a guillotine cut structure, after the insertion of a new piece we identify a new guillotine cut which is going to be associated with one of the pieces already placed. The difference between both constructive algorithms lies in the way the association of guillotine cuts to pieces is done. The first guillotine cut structure associates each new guillotine cut with the latest inserted piece. The second guillotine cut structure does not take into account the insertion order of the pieces. The idea is to associate the new guillotine cut with the piece for which one of the edges is concurrent with the guillotine cut. Note that each guillotine cut is defined in order to separate two pieces, so it is important to associate the guillotine cut with one of those pieces.

The mixed integer formulation (MIP formulation) used here is based on those by Fischetti and Luzzi [27] and by Gomes and Oliveira [32], which use the *Non-Fit polygons* (*NFP*) to obtain the non-overlapping constraints. We use the *horizontal slices* formulation (*HSF*) presented in Chapter 2 to obtain the partition of the outer zone of each *NFP*.

For pieces of irregular shapes, in Bennell and Oliveira [12] we can find an interesting discussion on the different strategies for building the *NFP*s. In our case, as the pieces are convex, it is easy to obtain the *NFP*s. Bennell and Oliveria [12] describe an algorithm which just sorts the edges of both pieces by taking into account the angles and the *NFP* is easily obtained. However, the pieces can be rotated continuously and can also be reflected (a mirror transformation). Each *NFP* corresponds to a fixed rotation and a fixed reflection of two polygons, so each time that a given piece changes its rotation or reflection, the *MIP* model has to be

updated because the *NFP*s of the pieces could be different. In this chapter we also present an algorithm to decide the rotations and reflections of the pieces.

Due to the computational cost of the constructive algorithms it makes no sense to apply a local search procedure like the tabu search presented by Lodi et al [42], which tries to empty less occupied bins by assigning pieces to sub-instances that include pieces from k bins. This tabu search might improve the bin packing component of the problem because the association of the pieces in the bins that we use is completely greedy, but the computational effort would be excessive.

In the next section we give a detailed description of the problem and some notation. Section 9.4 presents the *horizontal slices MIP* model (*HSF*), which is going to be used for the insertion of each piece. The two different guillotine cut structures are presented in Section 9.5. In Section 9.6 we describe the algorithm used to decide the rotations and reflections of the pieces and in Section 9.7 we introduce the constructive algorithm scheme. In Section 9.8 we propose a different way of getting the guillotine cut structure and in Section 9.9 we embed an improvement procedure into the constructive process. Section 9.10 contains the computational study. Finally, in Section 9.11 we draw some conclusions.

9.3 Problem description

The problem consists in cutting a set of required pieces from the minimum number of stock sheets, hence it is an input minimization problem. There are sufficient stock sheets available to meet the demand. The size of the stock sheets is standard, where L denotes the length and W the width. The set of irregular convex pieces is denoted by P, $|P| = n$. Pieces can be rotated continuously, that is, there are no fixed rotation angles. The reflection of the pieces (a mirror transformation) is also allowed. To obtain the reflected polygon of a given piece we calculate the reflection over the Y axis. If the piece has some symmetry, then the mirror transformation is redundant. Only guillotine cuts are allowed and the cutting line is not constrained to being parallel to an edge of the stock sheet. There are no limits on the number of cuts applied to each bin. According to the typology proposed by Waescher et al. [70], this is a single bin size bin packing problem (SBSBPP).

Let B denote the set of bins used. Each bin, $b_i(P_i, X_i, Y_i, R_i, M_i, G_i) \in B$, has a set of pieces associated, $P_i \subseteq P$. Each piece $p \in P_i$ is given by an ordered list of vertices, $p = (v_1, \ldots, v_t)$, and its edges can be expressed by $e_i = (v_i, v_{i+1})$, where $i = 1, \ldots, n-1$ and the n^{th} edge is $e_n = (v_n, v_1)$. The coordinates of the reference points of the pieces are given by vectors $X_i \in \mathbb{R}^{|P_i|}$ and $Y_i \in \mathbb{R}^{|P_i|}$. The rotation angle and the reflection (mirror transformation) of the pieces are given by $R_i \in \mathbb{R}^{|P_i|}$ and $M_i \in \mathbb{B}^{|P_i|}$, where 1 represents that the mirror transformation of the original piece is done. Finally, $G_i = (g_i^1 \ldots g_i^{|P_i|-1})$ is an ordered set of guillotine cuts in such a way that the first guillotine cut, $g_i^1 \in G_i$ divides b_i into two parts. The second guillotine cut, $g_i^2 \in G_i$, is going to divide one of those parts, and so on. Note that the endpoints of a cut can lie on some of the previous cuts instead of on one of the edges of the bin.

Each guillotine cut, $g_i^k(p, v_{ini}, v_{end}) \in G_i$, where $k \in \{1, \ldots, |P_i| - 1\}$, has a piece $p \in P_i$ associated and the endpoints of the cut, v_{ini} and v_{end}, are expressed in a coordinate system in which the reference point of piece p is placed at the origin. This means that we have to know the position of piece p in order to know where g_i is placed in the bin. We say that g_i^k has *order* k if it is the k^{th} guillotine cut. The order in which the guillotine cuts are added is very important because the endpoints of the guillotine cuts are given by the

intersection with either the closest guillotine cut with a lower order or the edges of the bin.

For each $b_i \in B$ we consider that the bottom-left corner of the boundary of b_i is located at the origin, and the position of each piece $p \in P_i$ is given by coordinates of the reference point (x_p, y_p), $x_p \in X_i$ and $y_p \in Y_i$, which corresponds to the bottom-left corner of the enclosing rectangle of the piece, even if p_i changes its rotation or reflection.

Objective

The objective is to minimize the total number of bins (stock sheets) used. The last bin is usually used only fractionally and then if a horizontal or vertical cut is applied, the largest reusable rectangle is not considered as waste. So the objective is to minimize the fractional number of bins (F).

The stock sheet usage (U) is defined as

$$U = \frac{\sum_{i=1}^{n} Area(p_j)}{((N-1)LW) + R^*} \tag{9.1}$$

where N is the total number of bins and R^* is the rectangle of the stock sheet used once the reusable residual part has been removed. In that case, the objective would be to maximize the stock sheet usage.

Either of both measures (U) and (F) is helpful for differentiating the quality of competing methods when they produce solutions with the same number of bins. There is a close relation between (F) and (U). If we consider two different solutions s_1 and s_2 such that $U(s_1) > U(s_2)$, indicating that the usage obtained by solution s_1 is better, then s_1 has a smaller fractional number of bins $F(s_1) < F(s_2)$.

9.4 Mixed integer formulation for the insertion of one piece

Each time a new piece is inserted into a bin, a Mixed Integer Problem (*MIP*) is solved to optimality. In this *MIP* model the position of the pieces already placed is not fixed, though they must respect the guillotine cut structure already defined in previous steps. The solution for the model provides the position of all the pieces involved in such a way that the new piece does not overlap any of the other pieces and does not cross any of the existing guillotine cuts. The *MIPs* become harder to solve when the number of pieces placed into the bin increases. The new piece which is going to be inserted has a fixed rotation and a fixed reflection in order to calculate the *NFPs* between the new piece and the pieces already placed.

Let $P_i \subseteq P$ be the set of pieces already placed and let $p \in P \setminus \{P_i\}$ be the piece which is going to be inserted into bin $b_i \in B$ and let r_p and m_p be, respectively, the rotation and reflection of p. We first write the whole model and then explain each component in detail:

$$
\begin{aligned}
Min \quad & \omega L_c + (1-\omega) W_c && && (9.2)\\
s.t. \quad & L_c \leq L && && (9.3)\\
& W_c \leq W && && (9.4)\\
& x_j \leq L_c - l_j && p_j \in P_i \cup \{p\} && (9.5)\\
& y_j \leq W_c - w_j && p_j \in P_i \cup \{p\} && (9.6)\\
& \alpha_k(x_k - x_p) + \beta_k(y_k - y_p) \leq \sum_{t=1}^{\mu_k} \delta_k^t v_{kt} && 1 \leq k \leq |P_i| && (9.7)\\
& \sum_{t=1}^{\mu_k} v_{kt} = 1 && 1 \leq k \leq |P_i| && (9.8)\\
& \alpha_{kj}(x_k - x_j) + \beta_{kj}(y_k - y_j) \leq \gamma_{kj} && 1 \leq j < k \leq |P_i| && (9.9)\\
& INT(\overline{p}) \cap g_i^k = \emptyset && k = 1, \ldots, |P_i| - 1 && (9.10)\\
& v_{kt} \in \{0, 1\} && 1 \leq k \leq |P_i|, 1 \leq t \leq \mu_k && (9.11)\\
& x_j,\ y_j \geq 0 && p_j \in P_i \cup \{p\} && (9.12)
\end{aligned}
$$

- *Objective function*

  The objective function (9.2) is a weighted combination of the length and width used, represented by L_c and W_c, respectively. With this objective function we try to pack the pieces as tightly as possible. We consider three different alternatives for the relative weight ω:

  - *FO0*: $\omega = \frac{1}{(W/L)+1}$
    In this case, the rectangle (L_c, W_c) grows keeping the proportions of the bin.
  - *FO1*: $\omega = 0.01$
    The objective is to minimize the width, and the length is used as a tie-breaker.
  - *FO2*: $\omega = 0.99$
    The objective is to minimize the length, and the width is used as a tie-breaker.

- *Containment constraints*

  Inequalities (9.3) and (9.4) ensure that the length and width used by the pieces in the bin do not exceed the bin dimensions. Inequalities (9.5) and (9.6) define L_c and W_c, that is, all the pieces are placed into the rectangle whose bottom-left corner is the origin and whose upper-right corner is (L_c, W_c).

- *Non-overlapping constraints*

  Inequalities (9.7) are defined to ensure that the new piece p does not overlap any other piece already included in the bin. These constraints are taken from the *horizontal slices formulation* proposed in Section 2.3. In that case, binary variables associate to *slices* are denoted by v_{ijk}, $i, j \in P$ and $k \in 1, \ldots, m_{ij}$, being m_{ij} the number of *slices* defined from the NFP_{ij}.

- *Guillotine cut constraints*

  The next set of constraints (9.9) is the guillotine cut constraints which separate pieces already placed in the bin. Since the guillotine cuts have to be satisfied by all the pieces and each guillotine cut is defined in order to separate two pieces, it is not necessary to consider non-overlapping constraints for the pieces already placed.

If we consider the piece p which is going to be inserted, besides the non-overlapping constraints already described, we need a set of inequalities (9.10) which ensures that no guillotine cut is going to divide polygon p. These inequalities appear in the formulation in a symbolic way, using the notation $INT(\overline{p})$ to indicate the interior of piece p and g_i^k to indicate the existing guillotine cuts. They will be fully explained in the next section.

- *Lifting the bound constraints*

  The typical containment constraints which are used in Gomes and Oliveira [32] and Fischetti and Luzzi [27] are (9.5) and (9.6). These constraints are going to be used for all pieces already placed in the bin $p_k \in P_i$, but for the new piece p which is going to be inserted we are going to use the *lifted* bound constraints defined in Section 2.3.

Initially, all the pieces are sorted by a certain criterion in order to be inserted into the bins. If one piece does not fit into a given bin, before creating a new bin we try the insertion of the remaining pieces into that bin.

The rotation of the pieces and the reflection are obtained by the algorithm presented in Section 9.6. This algorithm chooses r different rotations of both the original and the reflected polygons, taking into account the pieces and the edges of the bin. Each one of the rotations in the given reflection determined by the algorithm is tried by solving the corresponding *MIP* model. The final position of the pieces is the one which produces a lower value on the current objective function. Note that we solve several *MIP* models in order to make the insertion of one piece, and for each different rotation or reflection (if the piece is not symmetrical) the *NFPs* and the non-overlapping constraints have to be recalculated.

9.5 Guillotine cut structure

In the previous section we mentioned that the *MIP* has to include two types of constraints related to guillotine cuts. On the one hand, when a new piece p is going to be inserted, constraints (9.10) have to ensure that the existing cuts do not cross it. On the other hand, once the model has been solved, we have to identify a new guillotine cut separating the new piece from some piece already placed. This new cut and the cuts from the previous iterations (constraints (9.9)) have to be included in the next models to ensure the separation of the pieces already included.

We consider two different associations between the guillotine cuts and the pieces. A first structure, *associated guillotine cuts* (*AGC*), tries to associate the guillotine cut with the piece which has an edge concurrent with it, in such a way that all the guillotine cuts have at least one piece with one concurrent edge. The second guillotine cut structure, *iterated guillotine cuts* (*IGC*), is based on the association of a new guillotine cut with the latest piece inserted.

AGC

In what follows we are going to use the example presented in Figure 9.2. When the first piece is inserted into the bin, no guillotine cut is needed. So the model defined in Section 9.4 is going to have only the containment constraints (9.3), (9.4), (9.5) and (9.6) because there is no overlapping problem. Once the first piece p_1 is inserted, we try to insert another piece, p_2. The model for the second insertion is going to have

the containment constraints for both pieces and the non-overlapping constraints of both pieces. Note that there are still no guillotine cuts defined. When the model with two pieces is solved, the solution provides the coordinates of both pieces in the bin and we have to identify a guillotine cut.

Since pieces are convex polygons, there is at least one edge of one piece which can be used as a valid guillotine cut. Thus the guillotine cut is associated with the piece for which one of its edges is concurrent with the guillotine cut. In the example in Figure 9.2, the guillotine cut is concurrent with an edge of p_2, so it is associated with p_2. Therefore, the relative position between p_2 and this guillotine cut is fixed throughout the construction process. In other words, wherever piece p_2 is moved after the solution of successive *MIPs*, the guillotine cut will be moved with it.

The first guillotine cut in this example can be denoted as $g^1(p_2, v^1_{ini}, v^1_{end})$, where p_2 is the associated piece and the line defined by points v^1_{ini} and v^1_{end} gives the relative position between p_2 and g^1. That is, in order to know the position of the cut g^1 in the bin, we have to add up the coordinates of p_2 to v^1_{ini} and v^1_{end}. The endpoints of this guillotine cut are determined by the intersection between the cut and the edges of the bin. The inequality defined by g^1 which separates p_1 and p_2 (inequality (9.9)) has the following structure:

$$a_{12}(x_1 - x_2) + b_{12}(y_1 - y_2) \leq c_{12} \tag{9.13}$$

where a_{12}, b_{12} and c_{12} are the coefficients needed to define the inequality. Let p_3 be the third piece to be inserted with a given rotation and reflection. In this case the non-overlapping position between p_1 and p_2 is ensured by an inequality (9.9) defined by the guillotine cut g^1. The non-overlapping constraints (9.7) are included for separating p_3 from p_1 and p_2.

In order to guarantee inequality (9.10) for piece p_3 and g^1, we add the following three inequalities:

$$\alpha_{p_2,p_3,1}(x_{p_3} - x_{p_2}) + \beta_{p_2,p_3,1}(y_{p_3} - y_{p_2}) \leq \gamma^R_{p_2,p_3,1} + (1 - \chi^R_{p_2,p_3,1})M \tag{9.14}$$

$$\alpha_{p_2,p_3,1}(x_{p_3} - x_{p_2}) + \beta_{p_3,p_2,1}(y_{p_3} - y_{p_2}) \leq \gamma^L_{p_2,p_3,1} + (1 - \chi^L_{p_2,p_3,1})M \tag{9.15}$$

$$\chi^R_{p_2,p_3,1} + \chi^L_{p_2,p_3,1} = 1 \tag{9.16}$$

Constraint (9.14) forces p_3 to be placed to the right of g^1 when the corresponding binary variable $\chi^R_{p_2,p_3,1} = 1$. When binary variable $\chi^R_{p_2,p_3,1}$ takes the value 0, then the big-M constant deactivates the inequality. Similarly, in order to place p_3 to the left of g^1, we define a binary variable, $\chi^L_{p_2,p_3,1}$, and inequality (9.15). Equation (9.16) forces p_3 to be placed at one side of the g^1. We consider that the piece which has the guillotine cut associated is always placed to the left of the cut and we maintain that notation in all the cases, irrespective of the slope of the cut.

Coefficients $\alpha_{p_2,p_3,1}$ and $\beta_{p_2,p_3,1}$ are the same in both inequalities (9.14) and (9.15) because the lines are parallel. However, coefficients $\gamma^R_{p_2,p_3,1}$ and $\gamma^L_{p_2,p_3,1}$ are different because the vertex which touches the guillotine cut at each side, maintaining all the vertices on the same side, are different.

Once p_3 is inserted into the bin in Figure 9.2, we have to identify the guillotine cut of order 2 which separates p_3 from either p_1 or p_2. We can observe that the position of pieces p_1 and p_2 and guillotine cut g^1 have changed when piece p_3 is inserted. Since p_3 is placed on the same side of g^1 as p_1, the new guillotine cut is going to separate pieces p_1 and p_3. The thick black edge on the left of piece p_1 is used as the new guillotine cut, g^2, which is associated with p_3. In that case, the top and the bottom limits of g_2 are given by

the intersections with the edges of the bin.

After the third insertion the model becomes somewhat different because of the guillotine cuts. Let p_4 be the piece which is trying to be inserted. Inequalities (9.9) defined by guillotine cuts g^1 and g^2 ensure the non-overlapping configuration of pieces p_1, p_2 and p_3. Note that there are two inequalities (9.9) associated with g^1: one given by (9.13) and another given by fixing $\chi^R_{p_2,p_3,1} = 1$, which reduces equations (9.14), (9.15) and (9.16) to one inequality of type (9.9). Both inequalities are needed for the separation of the pairs $p_1 - p_2$ and $p_2 - p_3$. Finally, there is one inequality which uses the last guillotine cut g^2 to separate p_1 and p_3.

The non-overlapping constraints (9.7) are used to separate p_4 from the rest of the pieces. In order to guarantee that p_4 is going to respect g_1 and g_2, constraints (9.10), we add the following constraints:

$$\alpha_{p_2,p_4,1}(x_{p_4} - x_{p_2}) + \beta_{p_2,p_4,1}(y_{p_4} - y_{p_2}) \leq \gamma^R_{p_2,p_4,1} + (1 - \chi^R_{p_2,p_4,1})M \tag{9.17}$$

$$\alpha_{p_2,p_4,1}(x_{p_4} - x_{p_2}) + \beta_{p_2,p_4,1}(y_{p_4} - y_{p_2}) \leq \gamma^L_{p_2,p_4,1} + (1 - \chi^L_{p_2,p_4,1})M \tag{9.18}$$

$$\chi^R_{p_2,p_4,1} + \chi^L_{p_2,p_4,1} = 1 \tag{9.19}$$

$$\alpha_{p_3,p_4,1}(x_{p_4} - x_{p_3}) + \beta_{p_3,p_4,1}(y_{p_4} - y_{p_3}) \leq \gamma^R_{p_3,p_4,1} + (1 - \chi^R_{p_3,p_4,1})M \tag{9.20}$$

$$\alpha_{p_3,p_4,1}(x_{p_4} - x_{p_3}) + \beta_{p_3,p_4,1}(y_{p_4} - y_{p_3}) \leq \gamma^L_{p_3,p_4,1} + (1 - \chi^L_{p_3,p_4,1})M \tag{9.21}$$

$$\chi^R_{p_2,p_4,1} = \chi^R_{p_3,p_4,1} + \chi^L_{p_3,p_4,1} \tag{9.22}$$

Inequalities (9.17), (9.18) and equality (9.19) have the same structure as constraints (9.14), (9.15), (9.16), corresponding to the insertion of p_3, because the first guillotine cut must always be satisfied, that is, the new inserted piece has to be either to the right or to the left of g^1.

In addition, inequalities (9.20), (9.21) and (9.22) are defined to force p_4 to be placed at one side of g^2, if that is necessary. If $\chi^L_{p_2,p_4,1} = 1$, p_4 and g^2 are placed on opposite sides of g^1, so g^2 and p_4 are separated by g^1 and there is no need for a new constraint to separate them. Equation (9.22) allows the fixing of both binary variables, $\chi^R_{p_3,p_4,1}$ and $\chi^L_{p_3,p_4,1}$, to 0, deactivating inequalities (9.20) and (9.21). If $\chi^R_{p_2,p_4,1} = 1$, then p_4 would be placed on the same side of g_1 as g_2 (also p_1 and p_3), and if we do not add inequality (9.22), then g_2 could cross p_4. In that case, one of both binary variables $\chi^R_{p_3,p_4,1}$ or $\chi^L_{p_3,p_4,1}$ has to take the value 1, activating the corresponding inequality. If, instead of using this conditional structure, we had repeated the structure of constraints (9.17), (9.18) and (9.19), forcing the new inserted piece to satisfy all the guillotine cuts already defined, the model would have become unnecessarily restrictive.

Figure 9.2 shows the insertion of piece p_4. We can see that the endpoints of the new guillotine cut needed to separate pieces p_1 and p_4 are defined by the intersection with previous guillotine cuts instead of with the edges of the bin. It can also be observed that while maintaining their relative positions, pieces p_2 and p_3 have been moved upwards, taking the associated guillotine cuts with them, and making room for piece p_4.

We can add the rest of the pieces iteratively, as shown in the other drawings in Figure 9.2. Let p_l be the next piece to be inserted. The previous solution has already placed $l - 1$ pieces into the bin and there are $l - 2$ guillotine cuts defined. For each guillotine cut g^t, $t = 2, \ldots, l - 2$, we know which of the guillotine cuts with lower order it is associated with, $t' = 1, \ldots, t - 1$. That is, g^t can be placed at one side of $g^{t'}$ or can be separated from $g^{t'}$ by another guillotine cut, having no relation with $g^{t'}$.

We denote the previous guillotine cut with which t is related by $t^* \in \{1, \ldots, t-1\}$.

Then, in a general form, inequalities (9.10) can be written as follows:

$$\alpha_{p_k,p_t,s}(x_{p_t} - x_{p_k}) + \beta_{p_k,p_t,s}(y_{p_t} - y_{p_k}) \leq \gamma^R_{p_k,p_t,s} + (1 - \chi^R_{p_k,p_t,s})M \qquad k = 1, \ldots, t,\ s = 1 \ldots, s_k \tag{9.23}$$

$$\alpha_{p_k,p_t,s}(x_{p_t} - x_{p_k}) + \beta_{p_k,p_t,s}(y_{p_t} - y_{p_k}) \leq \gamma^L_{p_k,p_t,s} + (1 - \chi^L_{p_k,p_t,s})M \qquad k = 1, \ldots, t,\ s = 1 \ldots, s_k \tag{9.24}$$

$$\chi^R_{p^*_k,p_t,1} + \chi^L_{p^*_k,p_t,1} = 1 \tag{9.25}$$

$$\chi^\sigma_{p^*_t,p_t,s} = \chi^R_{p_k,p_t} + \chi^L_{p_k,p_t} \qquad k = 1, \ldots, t,\ s = 1 \ldots, s_k \tag{9.26}$$

Inequalities (9.23) and (9.24) define the guillotine cuts, which are activated by binary variables $\chi^R_{p_k,p_t,s}$ and $\chi^L_{p_k,p_t,s}$, respectively. The number of guillotine cuts associated with piece p_k is denoted by s_k.

Equality (9.25) ensures that the first guillotine cut, i.e. the guillotine cut with order 1, is always satisfied by the new piece to be inserted (p_t). After that guillotine cut is satisfied, the remaining guillotine cuts are going to have a relation with the new inserted piece using equalities (9.26). The value of σ could be L (left) or R (right), depending on what the relation is between the guillotine cuts obtained in the previous steps of the constructive procedure. If the corresponding binary variable which is on the left-hand side of (9.26) takes the value 1, then a relation is needed between the s^{th} guillotine cut associated with p_k and piece p_t.

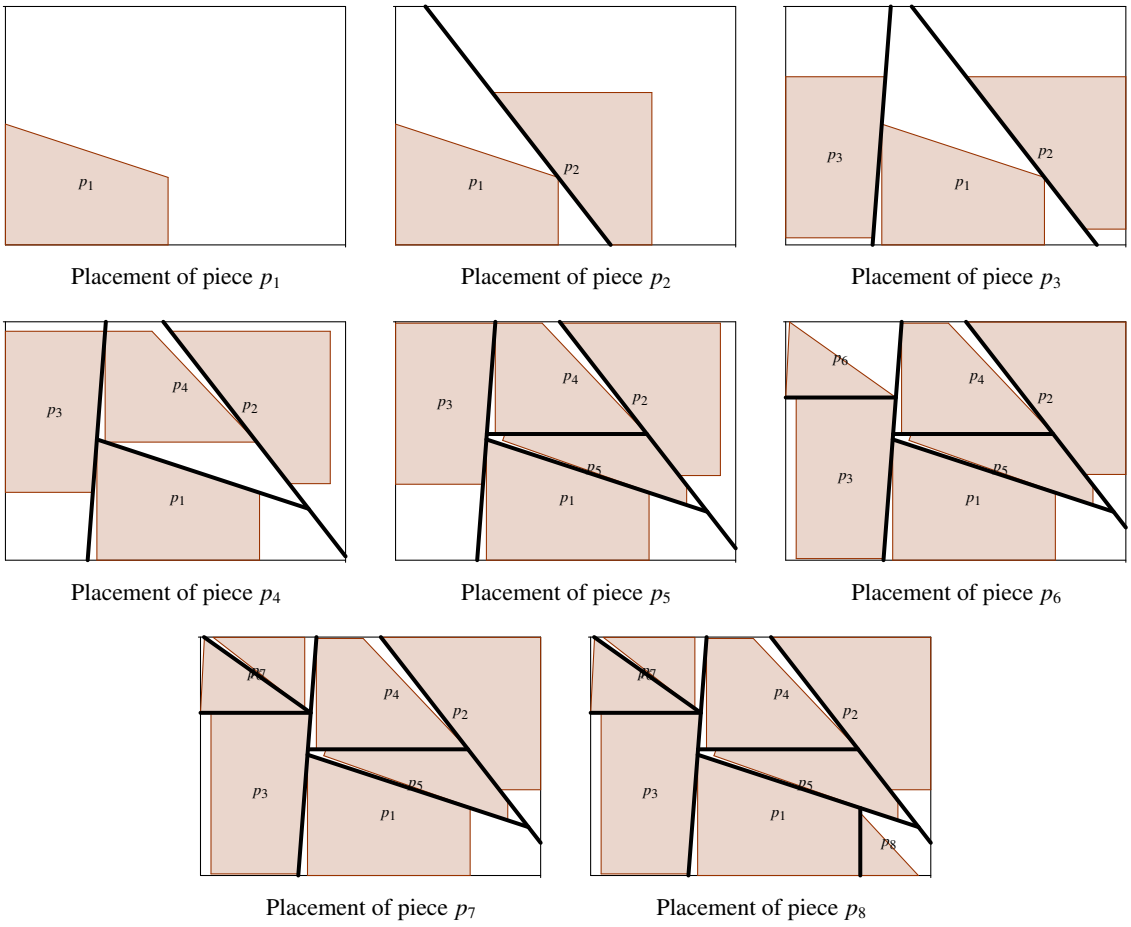

Placement of piece p_1 | Placement of piece p_2 | Placement of piece p_3

Placement of piece p_4 | Placement of piece p_5 | Placement of piece p_6

Placement of piece p_7 | Placement of piece p_8

Figure 9.2: *Example of the packing of a bin with the AGC structure.*

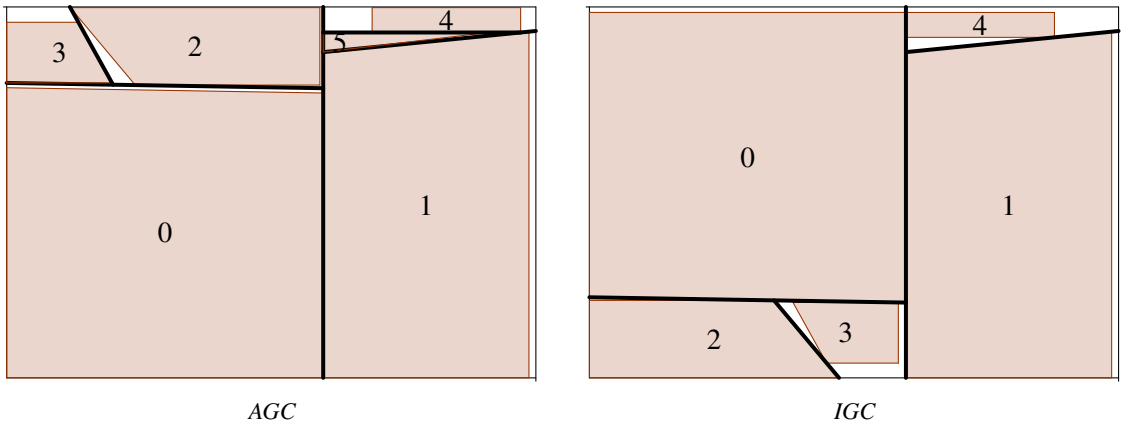

Figure 9.3: *Difference between AGC and IGC (real example on instance han120).*

IGC

The *Iterated Guillotine Cut* structure associates each guillotine cut with the last piece inserted into the bin and does not take into account if any edge of the piece is concurrent with the guillotine cut.

Inequalities (9.9) and (9.10) are the same in both structures. The *IGC* structure is simpler than the *AGC* because each piece, except p_1, has one and only one cut associated ($s_k = 1$ for $k = 2, \ldots, t-1$ and $s_1 = 0$).

Difference between *IGC* and *AGC*

Figure 9.3 shows two different packings of the first bin for instance *H120* (see Section 9.10). With the *AGC* structure the constructive algorithm places 5 pieces instead of the 4 placed when using the *IGC* structure. The algorithm works similarly in both cases until piece 4 is placed. The first two pieces are separated in both cases by a vertical line which is associated with piece 1. The second guillotine cut separates pieces 0 and 2 and is associated with piece 2 in both cases. The third guillotine cut is associated with piece 3 in both cases. When piece 4 is placed, with the *AGC* structure the new guillotine cut is associated with piece 1 with which it has a concurrent edge, while with the *IGC* structure it is associated with piece 4, the last piece placed. Then, piece 5 (a tiny triangle) fits into the packing on the left-hand side of Figure 9.3 because piece 4 can be moved to the top of the bin while the cut stays with piece 1, making room for piece 5. In the packing on the right-hand side of Figure 9.3, if piece 4 is moved to the top of the bin, the guillotine cut has also to be moved upwards and there is no feasible placement for piece 5.

9.6 Rotations and reflections

We define the reflection of a given piece $p \in P$ as the polygon obtained by applying the mirror transformation. The rotation of the pieces is completely free, that is, they can be rotated continuously between 0 and 360 degrees.

In this section we present an algorithm which decides the best rotations of one piece to be inserted into the bin, taking into account the slope of the edges of the pieces already placed and the edges of the bin. Since the model presented in Section 9.4 allows the piece which is going to be inserted to be placed in any part of the bin, it is interesting that the given rotation of the piece produces as many matchings as possible between the new piece and the pieces already placed. That is, the algorithm looks for rotations of the new piece which would allow it to fit better with the pieces already placed.

The algorithm *GR* (Get Rotations) chooses a set of rotations for the piece which is going to be inserted in the next iteration of the constructive algorithm. The number of rotations n_r is an input of the algorithm and the output is a set of n_r rotations.

Let p_i be the piece which is trying to be inserted. The set of rotation angles that we are going to study is obtained by matching each edge of p_i with each edge of the bin and each edge of each piece already placed into the bin. If the number of angles that we obtain is lower than n_r, then algorithm *GR* returns all these angles. In the case that we obtain more than n_r different rotations, we sort the angles by the following criteria:

a) Non-increasing number of matchings between the edges of the polygon obtained by applying the given rotation to the piece and the edges of the bin and the edges of all the pieces already placed in the bin.

b) In order to break ties in *(a)*, we use the total length of the edges of all the matchings.

The first n_r rotations are returned by the *GR* algorithm.

The different strategies that we are going to use in the constructive algorithm are:

- *3R*: We try the three best rotations given by algorithm *GR*.
- *3Rx3R*: We try the three best rotations of the piece given by algorithm *GR* and the three best rotations after applying the mirror movement.
- *6R*: We try the six best rotations given by algorithm *GR*.
- *3R+1x3R+1*: We try the three best rotations given by algorithm *GR* (also in the mirror polygon) for the first piece of each bin and we increase the number of rotations by one every time a new piece is inserted.
- *3R+3x3R+3*: Similar to the previous one, but we increase the number of rotations by three.
- *5R+5x5R+5*: Similar to the two previous strategies, but we increase the number of rotations by five and we begin to study five rotations for the first piece.

- *E30*: Every 30º in both polygons (the original one and after applying the mirror). The first rotation is given by matching the longest edge of the piece with the bottom edge of the bin.
- *E10*: Similar to *E30*, but considering the rotations every 10º.

9.7 Constructive algorithm

In Section 9.4 an *MIP* mixed integer formulation is proposed to insert optimally one piece with a fixed rotation and reflection. The following elements have to be determined in the constructive algorithm:

- The initial permutation of the pieces.
- The rotations of the pieces to be inserted. That implies the number of rotations and the criterion for choosing the rotations. The different criteria are described in Section 9.6.
- The reflections. It would be interesting to know if using reflections produces better solutions or whether with just the rotations it is enough to find good solutions.
- The objective function used in the *MIP* model. We consider the three different objective functions defined in Section 9.4.
- The guillotine cut structure used, *IGC* or *AGC*, described in Section 9.5.

We are going to consider three different criteria for sorting the pieces at the beginning of the process:

- Randomly.
- By non-increasing area. This is very similar to ordering the pieces by a non-increasing perimeter.
- By shape. We are going to pack first the pieces whose shape is similar to a rectangle and then the rest of the pieces. Pieces are therefore divided into two sets: one set is given by pieces whose shape is similar to a rectangle and in the other set we consider the rest of the pieces. In order to identify whether a piece has approximately a rectangular shape, we calculate the minimal enclosing rectangle by matching each edge of the piece with one of the edges of the rectangle and if the usage, define as $U = \frac{Area(Piece)}{Area(Rectangle)}$, is greater than a given threshold μ then the piece is included in the first set of pieces. After all the pieces are classified, we sort both sets by area and we begin with the insertion of the first piece from the first group.

The structure of the constructive algorithm is presented in Algorithm 4. Once a permutation of the pieces is selected, with the given order we try to insert as many pieces as possible into the first bin. When no more pieces fit into the first bin, if there are still some remaining pieces, a new bin is built, and there is an attempt to place the remaining pieces into the new bin. The algorithm ends when all the pieces are placed.

We solve many *MIP* problems along the algorithm. The computational effort of the constructive algorithm depends greatly on the number of rotations to be attempted for each piece and the computational time is duplicated when we consider the reflection. In Section 9.10 the benefit of using the reflection is shown.

The first time the insertion of a new piece into a given bin is tried, we use as an upper bound the value of the objective function when L_c and W_c are substituted for L and W. However, if in a given rotation and

reflection the *MIP* model is feasible, it provides a valid solution whose value can be used as an upper bound for the following insertion of the same piece in the remaining angles of rotation. That is, if we have found a good insertion of a given piece, then we use the objective function value as an upper bound for the remaining polygons obtained by rotating and reflecting the given piece.

Once all pieces are placed into bins, the less occupied bin is rebuilt with the objective functions $FO1$ and $FO2$ in order to find the cut, either horizontal or vertical, which produces a bigger non-used rectangle. This part is not going to be considered as waste (see Section 9.3).

9.8 Constructive algorithm with two phases

In Section 9.7 we presented the constructive algorithm in which each time there is an attempt to insert a new piece, an *MIP* model is solved. The guillotine cuts are guaranteed because there are several constraints in the *MIP* model, described in Section 9.5, which force the piece being inserted to respect all the guillotine cuts previously defined.

Since the guillotine cut inequalities reduce the feasible zone for placing the new piece, we now propose to try first the insertion without taking into account the guillotine cut constraints (inequalities 9.10 in Section 9.4). It may then be that the position of the new piece does not respect the previous guillotine cut structure. In that case, we need to identify a new guillotine cut structure if there is one. A procedure for doing that is presented in this section.

Let $i \in P$ be the piece which is going to be inserted. We denote by MIP^1 the *MIP* model used in the constructive algorithm defined in Section 9.4 without taking into account inequalities (9.10). The complete model is denoted by MIP^2. Then, if MIP^1 is unfeasible, MIP^2 is also unfeasible.

When MIP^1 is feasible we obtain a position of the pieces with no overlap, but we do not know if it could be obtained by guillotine cuts. We use a simple algorithm to find a guillotine cut structure. Each edge of every piece is considered as the possible first guillotine cut. If an edge can be used as the first guillotine cut, because it does not divide any piece and there are pieces on both sides, then the bin is divided into two parts and the same procedure is used on each part until all the pieces are separated. If in any part of the bin there are three or more pieces for which none of the edges of these pieces can be considered a guillotine cut, we consider that the given solution cannot be obtained by guillotine cuts. The algorithm is called *FGCS* (*Finding a Guillotine Cut Structure*).

Then, when MIP^1 is solved and gives a feasible solution, we call *FGCS* to know if there is a feasible guillotine cut structure. If *FGCS* fails, MIP^2 is built and solved. The new guillotine cut structure found is used for the next insertion, building a new *MIP* model.

In the case that MIP^1 is unfeasible, we try the next rotation of the given piece and when there are no rotations left, we consider the next piece to be inserted as in the constructive algorithm (Section 9.7). Then, only in the case that MIP^1 is feasible and *FGCS* fails to find a guillotine cut structure, the MIP^2 is solved.

This algorithm with two phases is more flexible and can produce better solutions. Figure 9.4 shows a

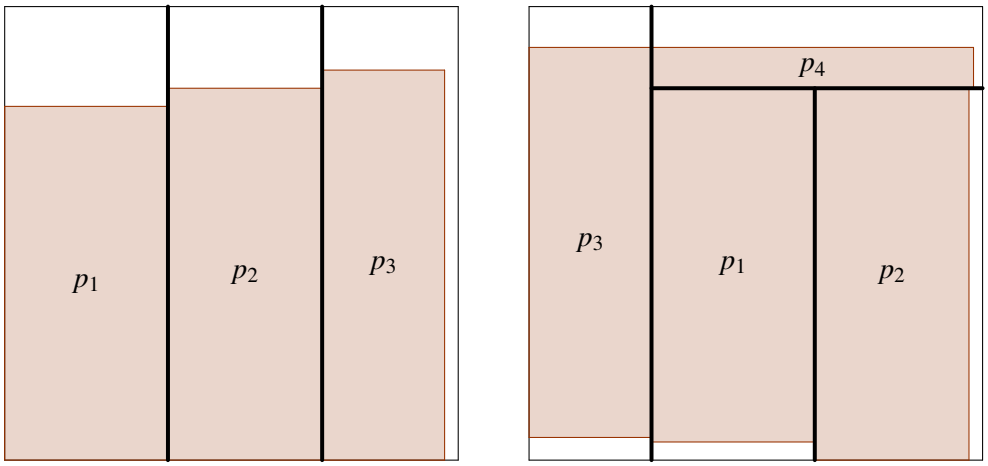

Figure 9.4: *Solutions obtained by a constructive algorithm and a constructive algorithm with two phases.*

simple example with rectangular pieces, applying both constructive algorithms. On the left-hand side we can see that with the initial algorithm the guillotine cuts separating pieces p_1, p_2 and p_3 are too restrictive and it is impossible to place any other rectangle, while on the right-hand side piece p_4 is placed and then a guillotine cut structure is easily found.

9.9 Embedding an improvement procedure into the constructive algorithm

The irregular pieces make the bin packing problem very difficult to deal with. We have tried to adapt several local search procedures which have been reported to work well for the standard bin packing problem with rectangular pieces (Lodi et al. [42] and Charalambous et al. [19]), but we have only obtained marginal improvements at a very high computational cost. Therefore, we have adopted a different strategy. Instead of applying improvement procedures to the complete solutions, we have developed a procedure, embedded into the constructive procedure, which is applied to each bin once no more pieces can be inserted into it and before a new bin is opened.

When a bin is closed, that is, when the constructive algorithm cannot place more pieces into it, if the usage is lower than a given threshold κ, we identify the piece which produces more waste and either the rotation of the piece or even the piece itself is changed. We propose a new criterion to assess the quality of the placement of each piece in a given bin and a new criterion to compare the quality of two different layouts of the bin with the same pieces.

Let n_b be the number of pieces already placed into bin b. The guillotine cuts divide the bin into n_b *containment polygons*. Each one of these polygons contains exactly one piece and the respective waste of each piece in its containment polygon can be calculated. Then, we consider the one which produces more waste as the worst placed piece, taking into account the corresponding containment polygon. Figure 9.5 shows the containment polygon of the worst inserted piece, p_6, in the top-right corner of the bin. In this

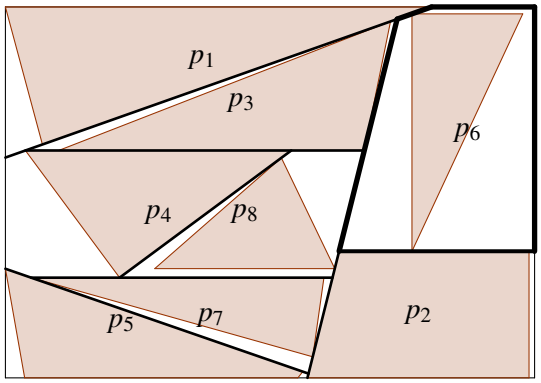

Figure 9.5: *Containment polygon of piece* p_6

example, the usage of the piece in the containment polygon is lower than 0.5.

Once the worst placed piece is identified, the bin is rebuilt in the following way. The bin is emptied, the worst piece is removed from the list and the other pieces are inserted again with their same rotations and reflections. Once all the previous pieces are placed, we try to insert the worst piece considering 10 different rotations for each reflected polygon. These rotations are obtained by using a modified version of algorithm *GR*, in which the edges of the bin are not considered and only the matchings with the previously placed pieces are computed. If we succeed, the remaining pieces in the problem are tested for insertion.

This procedure is applied twice and we accept a new construction of the given bin if the waste has been reduced. In this case we repeat the procedure until no improvements are found in two iterations.

9.10 Computational experiments

In this section we study several strategies to find the best constructive algorithm. All the different versions follow the structure described in Algorithm 4 (page 182).

We have used the test data presented by Bennell et al. [11]. They consider eight instances, four provided by a company in glass cutting for conservatories and another four generated using properties of the industrial data. The number of pieces ranges between 40 and 149. The instance name is coded by a letter and a number: the letter can be *J* or *H* depending on whether the instance is provided by a company (*J*) or is generated (*H*); the number represents the total number of pieces to be packed into the bins.

The first constructive algorithm that we are going to study, $CA1$, considers the one given by sorting the pieces by non-increasing area as the initial permutation. The algorithm to decide the rotation is *3Rx3R*, which considers 3 rotations for both polygons, original and reflected. The guillotine cut structure is *AGC*.

We have considered the following modifications of $CA1$:

CA2: As $CA1$, but initially pieces are sorted randomly.

CA3: As $CA1$, but initially pieces are sorted by shape (see Section 9.7).

CA4: As $CA1$, but the objective function is $FO1$ (see Section 9.4).

CA5: As $CA1$, but the objective function is $FO2$ (see Section 9.4).

CA6: As $CA1$, but the strategy for obtaining the rotation of the pieces is *6R* (see Section 9.6).

CA7: As $CA1$, but the strategy for obtaining the rotation of the pieces is *3R+1x3R+1* (see Section 9.6).

CA8: As $CA1$, but the strategy for obtaining the rotation of the pieces is *3R+3x3R+3* (see Section 9.6).

CA9: As $CA1$, but the strategy for obtaining the rotation of the pieces is *5R+5x5R+5* (see Section 9.6).

CA10: As $CA1$, but the strategy for obtaining the rotation of the pieces is *E30* (see Section 9.6).

CA11: As $CA1$, but the strategy for obtaining the rotation of the pieces is *E10* (see Section 9.6).

CA12: As $CA1$, but the strategy used for the guillotine cuts is *IGC* (see Section 9.5).

Table 9.1 shows the total number of bins used to pack all the pieces using these versions of the constructive algorithm. Tables 9.2 and 9.3 show, respectively, the fractional number of bins used and the usage of the bins, while in Table 9.4 we can see the computational time in seconds.

Table 9.1: *Number of bins used (N)*

Instances	CA1	CA2	CA3	CA4	CA5	CA6	CA7	CA8	CA9	CA10	CA11	CA12
J40	8	9	8	8	8	8	8	8	8	8	8	8
J50	10	11	10	10	10	10	10	10	10	10	10	10
J60	11	12	11	11	11	11	11	11	11	11	11	11
J70	12	14	12	12	12	13	12	12	12	12	12	12
H80	10	11	10	10	10	10	10	10	10	10	10	10
H100	16	18	17	16	16	17	16	16	16	16	16	16
H120	16	18	17	16	17	17	16	16	16	17	16	17
H149	22	25	23	23	23	23	22	22	22	22	22	22

Table 9.2: *Fractional number of bins used (F)*

Instances	CA1	CA2	CA3	CA4	CA5	CA6	CA7	CA8	CA9	CA10	CA11	CA12
J40	7.40	8.42	7.38	7.45	7.43	7.70	7.25	7.21	7.21	7.33	7.25	7.52
J50	9.27	10.51	9.37	9.24	9.31	9.53	9.31	9.16	9.16	9.36	9.25	9.38
J60	10.35	11.67	10.54	10.52	10.40	10.68	10.35	10.21	10.22	10.36	10.28	10.41
J70	11.63	13.60	11.85	11.80	11.78	12.18	11.57	11.66	11.62	11.79	11.74	11.79
H80	9.46	10.35	9.47	9.48	9.46	9.34	9.40	9.30	9.35	9.43	9.33	9.55
H100	15.56	17.48	16.12	15.87	15.82	16.16	15.62	15.43	15.47	15.94	15.54	15.75
H120	15.75	17.26	16.17	15.65	16.24	16.39	15.69	15.65	15.74	16.14	15.95	16.21
H149	21.83	24.53	22.39	22.09	22.24	22.09	21.88	21.72	21.77	21.87	21.75	21.83

The comparison between $CA1$, $CA2$ and $CA3$ in Table 9.1 shows that the best sorting criterion is non-increasing area ($CA1$). We can see that $CA2$ is always worse than $CA1$ and $CA3$ is worse in the last three instances. Furthermore, Table 9.2 shows that $CA1$ obtains better results than $CA3$ in the first five instances with the exception of instance $J40$, in which $CA3$ is slightly better.

In order to decide which objective function produces better results, we compare $CA1$, $CA4$ and $CA5$. Table 9.1 shows that $CA1$ is slightly better than $CA4$ and $CA5$. Only on instances $J50$ and $H120$ is the

Table 9.3: *Usage (U)*

Instances	CA1	CA2	CA3	CA4	CA5	CA6	CA7	CA8	CA9	CA10	CA11	CA12
J40	0.82	0.72	0.82	0.82	0.82	0.79	0.84	0.84	0.84	0.83	0.84	0.81
J50	0.82	0.73	0.82	0.83	0.82	0.80	0.82	0.84	0.84	0.82	0.83	0.81
J60	0.84	0.74	0.82	0.82	0.83	0.81	0.84	0.85	0.85	0.84	0.84	0.83
J70	0.85	0.73	0.83	0.84	0.84	0.81	0.85	0.85	0.85	0.84	0.84	0.84
H80	0.86	0.79	0.86	0.86	0.86	0.87	0.87	0.88	0.87	0.87	0.87	0.85
H100	0.86	0.77	0.83	0.84	0.85	0.83	0.86	0.87	0.87	0.84	0.86	0.85
H120	0.87	0.80	0.85	0.88	0.85	0.84	0.88	0.88	0.87	0.85	0.86	0.85
H149	0.88	0.78	0.86	0.87	0.86	0.87	0.88	0.89	0.88	0.88	0.88	0.88

Table 9.4: *Time in seconds (T)*

Instances	CA1	CA2	CA3	CA4	CA5	CA6	CA7	CA8	CA9	CA10	CA11	CA12
J40	14	24	15	14	16	41	31	83	105	58	177	15
J50	18	36	22	20	19	24	52	89	108	95	237	22
J60	32	50	45	73	36	65	96	204	180	162	440	39
J70	62	84	121	93	129	44	142	334	305	281	609	55
H80	155	231	131	112	158	117	354	610	545	449	1257	99
H100	124	143	97	223	177	92	294	582	587	720	1286	108
H120	326	387	149	288	186	158	771	1198	1424	782	2769	194
H149	624	635	235	225	208	193	1042	1529	1525	1307	3369	250

fractional number of bins used lower with $CA4$. It seems that $CA4$ produces better results than $CA5$ because the length of the bin is greater than the width in all the instances. However, the weighted objective function $FO0$ works better than both $FO1$ and $FO2$.

The advantages of using reflection can be seen by comparing $CA1$ and $CA6$. Each insertion tries 6 different shapes of one piece, $CA1$ considers the best three rotations of both original and reflected polygons and $CA6$ does not take into account the reflection. We can see that the results are clearly better if we consider the reflected polygons.

Algorithm $CA1$ considers 6 different polygons of the piece which is going to be inserted. This means that 6 *MIP* models are solved to optimality in order to decide the relative position between the new inserted piece and the pieces and guillotine cuts already placed. Algorithms $CA7$, $CA8$, $CA9$, $CA10$ and $CA11$ consider more rotations for both polygons, original and reflected, of a given piece. Then, in Table 9.4 we can see that the computational time increases, $CA11$ being the slowest algorithm (note that at each insertion $CA11$ 72 *MIPs* are solved to optimality). Table 9.1 shows that all these algorithms produce results with the same number of bins with the exception of $CA10$ which obtains a worse result on instance $H120$. The best results are given by $CA8$, which produces the best results for 6 of 8 instances. However, the computational time of $CA8$ increases considerably in comparison with $CA1$.

Finally, since $CA1$ works slightly better than $CA12$, it seems that the *AGC* structure produces better solutions than the *IGC*.

Comparison of the constructive algorithms with two phases and the improvement procedure

Table 9.5 shows the comparison between the original $CA1$ and the $CA1$ configuration using the two-phase constructive algorithm. The computational time remains similar and the quality of the solutions is slightly

improved.

On the other hand, when the improvement procedure presented in Section 9.9 is embedded into the constructive algorithm $CA1$ with two phases ($CA1M$), the quality of the solutions is even better. The number of bins in instances $J40$, $J50$ and $J60$ is reduced and in instances $H100$ and $H120$ the fractional number of bins is reduced. That is, on 5 instances this improvement procedure obtains a better solution, though the computational times increase.

Table 9.5: *Comparing the initial and the two-phase constructive algorithms*

	CA1				CA1 two phases				CA1M			
	N	U	F	T	N	U	F	T	N	U	F	T
J40	8	0.82	7.40	14	8	0.83	7.31	21	7	0.88	6.92	168
J50	10	0.82	9.27	18	10	0.83	9.23	26	9	0.85	8.97	344
J60	11	0.84	10.35	32	11	0.83	10.49	68	10	0.87	9.99	445
J70	12	0.85	11.63	62	12	0.88	11.28	99	12	0.86	11.54	703
H80	10	0.86	9.46	155	10	0.89	9.20	121	10	0.89	9.21	1275
H100	16	0.86	15.56	124	16	0.87	15.33	165	16	0.88	15.27	1412
H120	16	0.87	15.75	326	16	0.87	15.74	488	16	0.89	15.37	2406
H149	22	0.88	21.83	624	22	0.89	21.57	524	22	0.89	21.59	3314
Total	**105**		**101.27**		**105**		**100.13**		**102**		**98.87**	

Lower bounds for the total number of bins

In order to assess the quality of the solutions obtained, we have computed a simple lower bound for N by solving a 1-dimensional bin packing model. This model uses an upper bound for N, N_{ub}, given by the constructive algorithm. In order to indicate that bin i is open we use a binary variable y_i, which takes the value 1 if the bin is used in the solution. We consider binary variables x_{ij} which take the value 1 if piece j is placed on bin i, and 0 otherwise. The model can be written as follows:

$$Min \ \sum_{i=1}^{N_{ub}} y_i \tag{9.27}$$

$$s.t. \quad \sum_{j=1}^{n} a_j x_{ij} \leq a_b y_i \qquad i = 1, ..., N_{ub} \tag{9.28}$$

$$\sum_{i=1}^{N_{ub}} x_{ij} = 1 \qquad j = 1, ..., n \tag{9.29}$$

$$x_{ij} \in \{0, 1\}, y_i \in \{0, 1\}, \quad 1 \leq j \leq n, 1 \leq i \leq N_{ub} \tag{9.30}$$

where n denotes the total number of pieces, N_{ub} is an upper bound for the total number of bins, a_j is the area of piece $j \in \{1, \ldots, n\}$ and a_b the area of one bin. In the objective function we try to minimize the total number of bins used. Inequalities (9.28) ensure that the total area of pieces placed in bin $i \in \{1, \ldots, N_{ub}\}$ must be less than or equal to the area of the bin. Finally, equalities (9.29) force each piece to be placed exactly in one used bin.

In Table 9.6 we can see that the number of bins used in every feasible solution is never more than two bins away for the simple 1-dimensional lower bound. That gives an idea of the difficulty of reducing the number of required bins even more.

Table 9.6: *Comparison with lower bound for N*

Instances	Lower Bound	CA1 two phases (N)
J40	7	7
J50	8	9
J60	9	10
J70	10	12
H80	9	10
H100	14	16
H120	14	16
H149	20	22

Comparison with the best known algorithms

Bennell et al. [11] propose several versions for the one step algorithm depending on two parameters: θ is the threshold for accepting matches of blocks and K controls the linearity of the dynamic weighting scheme. The best two algorithms using the one-step approach are given by the following combinations:

- *1S-0.94-5*: with $\theta = 0.94$ and $K = 5$.

- *1S-0.97-3*: with $\theta = 0.97$ and $K = 3$

The two-step algorithm (*2S*) also proposed by Bennell et al. [11] works slightly worse than the one-step algorithms, but there is one instance (see *J70* in Table 9.7) where the two-step algorithm found a better solution with fewer bins than all the one-step algorithms.

Table 9.7 shows the computational results obtained by the two-step algorithm *2S* and the one-step algorithms *1S-0.94-5* and *1S-0.97-3*. The two last columns correspond to *CA*1 and *CA*1*M* (*CA*1 with two phases and the improvement procedure). Algorithm *CA*1*M* produces the best known results for five of the eight instances (the best known solution of instance *J*70 is given by *CA1 two phases* in Table 9.5). The behavior of algorithm *CA*1 is also interesting because on average it works better than the algorithms proposed by Bennell et al. [11], and it is faster. In fact, we can see that *CA*1 reduces the number of bins used in *1S-0.94-5* and *1S-0.97-3* in 4 instances. Algorithm *1S-0.97-3* produces the best result for instance *J50*.

Comparison with the state of the art algorithms in rectangular bin packing problems

The constructive algorithms proposed in this paper deal with irregular pieces and use a mathematical model which is hard to solve to optimality in each step. Nevertheless, they can be applied to standard bin packing problems with rectangular pieces to assess their performance for this problem.

For the bin packing problem with rectangular pieces, there is a standard benchmark set composed of 500 instances divided into 10 classes. The first 6 classes were proposed by Berkey and Wang [15] and the last 4 classes by Lodi et al. [42]. We consider two rotations for the insertion of each piece (0^o and 90^o) and therefore we are solving the $2DBP|R|G$ problem.

Table 9.7: *Comparison with the algorithms proposed by Bennell et al. [11]*

		2S	1S-0.94-5	1S-0.97-3	CA1	CA1M
J40	N	8	8	8	8	7
	F	7.72	7.39	7.32	7.40	6.92
	T	$> 1h$	110	47	14	168
J50	N	10	9	9	10	9
	F	9.66	8.55	8.45	9.27	8.97
	T	$> 1h$	130	74	18	344
J60	N	11	11	11	11	10
	F	10.90	10.23	10.51	10.35	9.99
	T	$> 1h$	170	60	32	204
J70	N	12	13	13	12	12
	F	11.95	12.75	12.65	11.63	11.54
	T	$> 1h$	200	98	62	703
H80	N	10	10	10	10	10
	F	9.63	9.25	9.45	9.46	9.21
	T	$> 1h$	405	187	155	1275
H100	N	17	17	17	16	16
	F	16.40	16.31	16.35	15.56	15.27
	T	$> 1h$	700	201	124	1412
H120	N	17	17	17	16	16
	F	16.14	16.25	16.58	15.75	15.37
	T	$> 1h$	714	247	326	2406
H149	N	23	23	23	22	22
	F	22.29	22.33	22.41	21.83	21.59
	T	$> 1h$	947	389	624	3314
TOTAL	N	108	108	108	105	102
	F	104.69	103.06	103.72	101.27	98.87

Table 9.8 compares the total number of bins used by the constructive algorithm *CA*1 with fast heuristic algorithms: the Knapsack-Problem-based heuristics of Lodi et al. [42] (KP), the Guillotine Bottom-Left heuristic of Polyakovsky and M'Hallah [53] (GBL) and the Constructive Heuristic of Charalambous and Fleszar [19] (CH).

We can observe that the constructive algorithm *CA*1 is competitive, working better than *GBL*, slightly worse than *KP* and clearly worse than *CH*. Algorithm *CA*1 with two phases produces better results than any other constructive algorithm. However, the state of the art procedure on rectangular bin packing problems with guillotine cuts is the CHBP algorithm proposed by Charalambous and Fleszar [19], in which their constructive algorithm (CH) is followed by a postoptimization phase. CHBP requires only 7064 bins.

Table 9.9 shows the total number of bins used by algorithms *CH*, *CA*1, *CA*1 with two phases and *CHBP* for each class of instances. The main differences between algorithms *CH* and *CA*1 appear in classes 7 and 8, the behavior in the rest of the classes being similar. The differences disappear if we consider algorithm *CA*1 with two phases, which seems especially well fitted for these types of instances. Note that *CA*1 and the other constructive algorithms presented in this paper are carefully designed to decide the position of the pieces in a given bin and do not focus on the assignment of pieces to bins. Nevertheless, they work well on rectangular bin packing problems.

Table 9.8: *Total number of bins in the* 10 *classes.*

	Total number of bins
KP	7297
GBL	7367
CH	7191
CA1	7303
CA1(2 phases)	7146
CHBP	7064

Table 9.9: *Total number of bins in each class.*

Class	1	2	3	4	5	6	7	8	9	10
CH	997	127	705	126	894	115	792	792	2131	512
CA1	994	130	718	127	896	116	844	843	2124	511
CA1(2 phases)	984	128	695	126	878	116	792	795	2124	508
CHBP	975	124	687	125	872	113	770	776	2119	503

9.11 Conclusions

A new approach to ensuring a guillotine cut structure is proposed by using a mathematical model. To our knowledge, in the literature of guillotine cut problems we cannot find any mathematical model which considers guillotine cuts.

The rotations and reflections of the pieces make the mathematical model harder to define. A new algorithm (*GR*) for deciding rotations is proposed and it is demonstrated that it produces good results. In order to deal with reflection, we double the computational effort if pieces are not symmetric, trying the insertion of each piece for each reflected polygon.

The constructive algorithm proposed obtains high quality results on the bin packing problem with guillotine cuts and irregular convex pieces, improving the best known solutions in 6 of 8 instances and it is competitive with the rectangular bin packing problem with guillotine cuts.

Algorithm 4 Constructive algorithm structure

Require: P, L, W;
  Set P' (initial permutation);
  Set n_r (number of rotations);
  Set OF (objective function);
  Set guillotine cut structure;
  $B = \emptyset$, $cont = 0$;
  while $P' \neq \emptyset$ **do**
    Create a new bin b_{cont}.
    for $i = 0, \ldots, |P'| - 1$ **do**
      Set $bestOFvalue = \omega L + (1 - \omega)W$ (ω is given by OF);
      $IN = false$;
      P^* is the set of all polygons obtained by the different rotations of $p'_i = P'[i]$;
      if p'_i has no symmetries and reflection is allowed **then**
        P^*_m is the set of all polygons obtained by the different rotations of $m(p'_i)$ (reflected polygon);
      end if
      for each polygon $p \in P^* \cup P^*_m$ **do**
        Add p to the *MIP* model;
        Solve the *MIP* model using as upper bound $bestOFvalue$;
        if model is feasible **then**
          $IN = true$;
          Update best rotation (and reflection) of p'_i.
          $bestOFvalue$ =current objective function value;
        end if
        Remove p from the model.
      end for
      if $IN = true$ **then**
        Add p'_i to b_{cont}
        Insert the piece into the *MIP* model with the best rotation (and reflection).
        Identify the new guillotine cut and update the guillotine cut constraints of the model.
        $P' = P' \setminus \{p'_i\}$
      end if
    end for
    $B = B \cup \{b_{cont}\}$;
    $cont = cont + 1$;
  end while
  Sort bins B by non-decreasing waste;
  Rebuild last bin of B with objectives functions $FO1$ and $FO2$ and choose the best configuration.
  return B;

Chapter 10

Conclusions and future work

This thesis can be divided into three parts. The first part is formed by Chapters 2, 3, 4 and 5. The second part includes Chapters 6, 7 and 8. Finally, the third part is included in Chapter 9.

First of all we have developed an exact algorithm, a Branch & Bound algorithm, for the two-dimensional irregular strip packing problem (*Nesting* Problem) where pieces have a fixed rotation. This algorithm improves the algorithm proposed by Fischetti and Luzzi [27] and is able to solve instances with up to 16 pieces to optimality. In order to add a cutting process to the Branch & Bound we propose several new kinds of valid inequalities. The computational results show that the separation algorithms require too much, time making the cutting process inefficient.

Secondly we have designed an Iterated Greedy algorithm to solve the two-dimensional irregular strip packing problem where pieces can be rotated at several angles. This algorithm can be classified as a *math-heuristic* algorithm because we solve many *MIP* problems to optimality. The computational results show that this algorithm obtains good results and it is competitive with the state of the art procedures.

Thirdly we have proposed an efficient constructive algorithm for the two-dimensional irregular bin packing problem with guillotine cuts appearing in the glass cutting industry. This algorithm outperforms the previous algorithms proposed by Bennell et al. [11] and it is even competitive for the rectangular bin packing problem with guillotine cuts. A new and efficient approach is used to guarantee the guillotine cut structure.

In Chapter 1 we introduce a literature review of the different versions of *Nesting Problems*. Since the exact algorithm and the Iterated Greedy algorithm deal with the two-dimension strip packing problem, the most studied version of *Nesting* Problems, we added two sections with a literature review for both cases, exact and heuristic algorithms. Another section includes the properties of the instances used along the thesis and the pictures of the best solutions obtained by the algorithms that we have developed.

Chapter 2 contains the *MIP* formulations. We have improved the Gomes and Oliveira model proposed in [32] by modifying the Fischetti and Luzzi [27] model. We propose two formulations based on defining the Fischetti and Luzzi *slices* in a horizontal way. The computational results show that *HS2* model works better than all the other formulations.

The exact procedure is based on a *Branch & Bound* algorithm. Chapter 3 studies different strategies

for branching. We have improved the Fischetti and Luzzi strategy and the computational results show that different branching strategies obtain a wide range of quality results.

In order to add a cutting process into the *Branch & Bound* algorithm, we have found different valid inequalities which are presented in Chapter 4. Some of the inequalities combine real and binary variables, *X-Y inequalities* and *Impenetrability constraints*, and other inequalities try to find a set of binary variables which produce an unfeasible solution if all variables take the value 1, *cliques*, *covers*, *LU-covers* and *Transitivity inequalities*. In Chapter 5 we propose separation algorithms for several of those inequalities. The computational results show that we have failed to design good separation algorithms because the computational effort used on the separation algorithms is too high and it is preferable to branch rather than add inequalities.

In Chapter 6 we have designed Constructive Algorithms using the previous models based on the insertion of the pieces one at a time. A new and interesting idea for the insertion of one piece is *trunk* insertion, which allows certain movements of the pieces already placed in order to place the new piece better. Despite the high computational effort needed on these algorithms, the computational results show that they produce high quality results.

In Chapter 7 we have studied different movements separately in order to design an efficient local search procedure. These movements are based on the optimal insertion of *n* pieces (*n-insert*); the *compaction* of the pieces which allows small changes on the relative position of neighboring pieces; and the *1-compaction* with is a combination of the previous two movements. We also propose different objective functions and the computational results show that the *Crossed Objective Function*, presented in Section 7.4, produces the best results.

The *Iterated Greedy* Algorithm is described in Chapter 8. This algorithm is based on a constructive algorithm with *trunk* insertion, but we add a dynamic procedure to calibrate the different parameters along the process. This idea arises because different *MIP*s that we need to solve in order to obtain a solution have different degrees of difficulty. This dynamic procedure is based on the number of binary variables. It seems that *MIP*s with a high number of binary variables are usually more difficult to solve to optimality. We define the *skeleton* of a given solution as the set of pieces which, to improve the current solution, have to modify their relative position. The destructive algorithm removes some of the pieces from the skeleton of the current solution. The local search procedure considers two movements, the *1-insertion* and the *2-insertion*. Both movements, as in the constructive phase, have a dynamic procedure for changing the parameters, making the movements more aggressive in some cases. The computational results show that this algorithm is competitive, providing the best known results in several instances.

In Chapter 9 we propose a constructive algorithm for the two-dimensional irregular bin packing problem with guillotine cuts. In that problem, pieces can rotate freely and can be reflected. Since we use a similar model to the *HS2* model, we have designed an algorithm to decide the rotations and reflections of the pieces to be inserted by taking into account the pieces already placed. As the computational results show, this algorithm decides good rotations to be tested. Furthermore, a new approach to guaranteeing the guillotine cut structure by using linear inequalities is presented. We have also designed a strategy to find a guillotine cut structure for a given solution and a criterion to identify pieces whose placement produces too much waste. Taking into account these two elements, we have designed an improvement procedure embedded into the constructive algorithm which produces good results. The computational results show that this algorithm

produces the best results and it is competitive with algorithms designed specifically for the rectangular bin packing problem with guillotine cuts.

As future work, it could be interesting to combine the algorithm which decides the rotations of the pieces presented in Chapter 9 with the *Iterated Greedy* algorithm presented in Chapter 8, providing an algorithm for general *Nesting Problems*, allowing pieces to be freely rotated.

Since we have failed to design an efficient cutting process in the *Branch & Bound* algorithm, it could be interesting to improve the separation algorithms presented in Chapter 5 and to try to find new valid inequalities. Furthermore, if the formulation were improved, then the constructive algorithms presented in Chapter 6 and the heuristic algorithm presented in Chapter 8 might also improve their computational results.

Bibliography

[1] ALBANO, A., AND SAPUPPO, G. Optimal allocation of two-dimensional irregular shapes using heuristic search methods. *IEEE Transactions on Systems, Man and Cybernetics 10* (1980), 242–248.

[2] ALVAREZ-VALDES, R., PARREÑO, F., AND TAMARIT, J. A branch and bound algorithm for the strip packing problem. *OR Spectrum 31* (2009), 431–459.

[3] ALVES, C., BRÁS, P., DE CARVALHO, J. V., AND PINTO, T. New constructive algorithms for leather nesting in the automotive industry. *Computers & Operations Research 39(7)* (2012), 1487–1505.

[4] ALVES, J., FERREIRA, J., ALBUQUERQUE, C., OLIVEIRA, J., FERREIRA, J., AND MATOS, J. A flexible custom computing machine for nesting problems. *Proceedings of XIII DCIS*.

[5] ART, J. An approach to the two-dimensional, irregular cutting stock problem. Tech. Rep. 36.Y08, IBM Cambridge Scientific Centre, 1966.

[6] BABU, A., AND BABU, N. A generic approach for nesting of 2-d parts in 2-d sheets using genetic and heuristic algorithms. *Computer-Aided Design 33* (2001), 879–891.

[7] BALDACCI, R., BOSCHETTI, M., GANOVELLI, M., AND MANIEZZO, V. Algorithms for nesting with defects. *Discrete Applied Mahtematics doi:10.1016/j.dam.2012.03.026*.

[8] BENNELL, J. *Incorporating problem specific knowledge into a local search framework for the irregular shape packing problem*. PhD thesis, University of Wales, UK, 1998.

[9] BENNELL, J., AND DOWSLAND, K. A tabu search thresholding implementation for the irregular stock cutting problem. *International Journal of Porduction Research 37* (1999), 4259–4275.

[10] BENNELL, J., AND DOWSLAND, K. Hybridising tabu search with optimisation techniques for irregular stock cutting. *Management Science 47* (2001), 1160–1172.

[11] BENNELL, J., HAN, W., ZHAO, X., AND SONG, X. Construction heuristics for two dimensional irregular shape bin packing with guillotine constraints. *Technical Report. University of Southampton. Http://eprints.soton.ac.uk/208137*.

[12] BENNELL, J., AND OLIVEIRA, J. The geometry of nesting problems: A tutorial. *European Journal of Operational Research 184* (2008), 397–415.

[13] BENNELL, J., AND OLIVEIRA, J. A tutorial in irregular shape packing problems. *Journal of the Operational Research Society 60* (2009), S93–S105.

[14] BENNELL, J., STOYAN, Y., SCHEITHAUER, G., GIL, N., AND ROMANOVA, T. Tools of mathematical modeling of arbitrary object packing problems. *Annals of Operations Research 179* (2010), 343–368.

[15] BERKEY, J., AND WANG, P. Two-dimensional finite bin-packing algorithms. *Journal of Operational Research Society 38* (1987), 423–429.

[16] BLAZEWICZ, J., HAWRYLUK, P., AND WALKOWIAK, R. Using a tabu search approach for solving the two-dimensional irregular cutting problem. *Annals of Operations Research 41* (1993), 313–325.

[17] BOUNSAYTHIP, C., AND MAOUCHE, S. Irregular shape nesting and placing with evolutionary approach. In *Proceedings of the IEEE International Conference On Systems, Man and Cybernetics* (1997), vol. 4, pp. 3425–3430.

[18] BURKE, E., HELLIER, R., KENDALL, G., AND WHITWELL, G. A new bottom-left-fill heuristic algorithm for the two-dimensional irregular cutting problem. *Operations Research 54* (2006), 587–601.

[19] CHARALAMBOUS, C., AND K.FLESZAR. A constructive bin-oriented heuristic for the two-dimensional bin packing problem with guillotine cuts. *Computers and Operational Research 38* (2011), 1443–1451.

[20] COSTA, M., GOMES, A., AND OLIVEIRA, J. Heuristic approaches to large-scale periodic packing of irregular shapes on a rectangular sheet. *European Journal of Operational Research 192* (2009), 29–40.

[21] CRISPIN, A., CLAY, P., TAYLOR, G., AND REEDMAN, D. Genetic algorithm coding methods for leather nesting. *Applied Intelligence 5238(1)* (2005), 9–20.

[22] CUNINGHAME-GREEN, R. Geometry, shoemaking and the milk tray problem. *New Scientist 1677* (1989), 50–53.

[23] DIGHE, R., AND JAKIELA, M. Solving pattern nesting problems with genetic algorithms eploying task decomposition and contact detection. *Evolutionary Computation 3* (1996), 239–266.

[24] DOWSLAND, K., AND DOWSLAND, W. An algorithm for polygon placement using a bottom-left strategy. *European Journal of Operational Research 141* (2002), 371–381.

[25] DOWSLAND, K., DOWSLAND, W., AND BENNELL, J. Jostling for position: Local improvement for irregular cutting patterns. *Journal of the Operational Research Society 49* (1998), 647–658.

[26] EGEBLAD, J., NIELSEN, B., AND ODGAARD, A. Fast neighborhood search for polygon placement using a bottom-left strategy. *European Journal of Opeartional Research 183* (2007), 1249–1266.

[27] FISCHETTI, M., AND LUZZI, I. Mixed-integer programming models for nesting problems. *J Heuristics 15* (2008), 201–226.

[28] FOWLER, R., AND TANIMOTO, S. Optimal packing and covering in the plane are np-complete. *Inform Process Lett 12(3)* (1981), 133–137.

[29] FUJITA, K., AKAGJI, S., AND KIROKAWA, N. Hybrid approach for optimal nesting using a genetic algorithm and a local minimisation algorithm. *Proceedings of the 19th Annual ASME Design Automation Conference 65* (1993), 477–484.

[30] GHOSH, P. An algebra of polygons through the notion of negative shapes. *CVGIP: Image Understanding 54 (1)* (1991), 119–144.

[31] GOMES, A., AND OLIVEIRA, J. A 2-exchange heuristic for nesting problems. *European Journal of Operational Research 171* (2002), 811–829.

[32] GOMES, A., AND OLIVEIRA, J. Solving irregular strip packing problems by hybridising simulated annealing and linear programming. *European Journal of Operational Research 171* (2006), 811–829.

[33] HEISTERMANN, J., AND LENGAUER, T. The nesting problem in the leather manufacturing industry. *Annals of Operations Research 57* (1995), 147–173.

[34] HOPPER, E. *Two-dimensional packing utilising evolutionary algorithms and other meta-heuristic methods*. PhD thesis, University of Wales, ardiff, UK, 2000.

[35] IMAMICHI, T., YAGIURA, M., AND NAGAMOCHI, H. An iterated local search algorithm based on nonlinear programming for the irregular strip packing problem. *Discrete Optimization 6* (2009), 346–361.

[36] JACOBS, L., AND BRUSCO, M. A local search heuristic for large set-covering problems. *Naval Research Logistics Quarterly 42 (7)* (1995), 1129–1140.

[37] JAKOBS, S. On genetic algorithms for the packing of polygons. *European Journal of Operations Research 88* (1996), 165–181.

[38] KONOPASEK, M. Mathematical treatments of some apparel marking and cutting problems. Tech. Rep. 99-26-90857-10, Department of Commerce Report, U.S, 1985.

[39] LEE, W., MA, H., AND CHENG, B. A heuristic for nesting problems of irregular shapes. *Computer-Aided Design 40* (2008), 625–633.

[40] LEUNG, S., LIN, Y., AND ZHANG, D. Extended local search algortihm based on nonlinear programming for two-dimensional irregular strip packing problem. *Computers & Operations Research 39* (2012), 678–686.

[41] LIU, X., AND JIA-WEI. Heuristic algorithm based on the principle of minimum total potential energy (hape): a new algorithm for nesting problems. *Journal of Zhejiang University-SCIENCE A (Applied Physics & Engineering) 12(11)* (2011), 860–872.

[42] LODI, A., MARTELLO, S., AND VIGO, D. Heuristic and metaheuristic approaches for a class of two-dimensional bin packing problems. *INFORMS Journal on Computing 11* (1999), 345–357.

[43] MAHADEVAN, A. *Optimisation in computer aided pattern packing*. PhD thesis, North Carolina State University, 1984.

[44] MARCHIORI, E., AND STEENBEEK, A. An evolutionary algorithm for large set covering problems with applications to airline crew scheduling. *Lecture notes in Computer Science 1803* (2000), 367–381.

[45] MARQUES, V., BISPO, C., AND SENTIEIRO, J. A system for the compaction of two-dimensional irregular shapes based on simulated annelaing. In *Proceedings of the 1991 International Conference On Industrial Electronics, Control and Instrumentation - IECON'91* (1991), vol. 99, pp. 1911–1916.

[46] MARTELLO, S., MONACI, M., AND VIGO, D. An exact approach to the strip packing problem. *INFORMS Journal on Computing 15* (2003), 310–319.

[47] MASCARENHAS, W., AND BIRGIN, E. Using sentinels to detect intersections of convex and nonconvex polygons. *Computational & Applied Mathematics 29* (2010), 247–267.

[48] MILENKOVIC, V., DANIELS, K., AND LI, Z. Automatic marker making. In *Proceedings of the Third Canadian Conference on Computational Geometry*. Simon Frase University, Vancouver, BC, 1991, pp. 243–246.

[49] MILENKOVIC, V., AND LI, Z. Compaction and separation algorithms for non-convex polygons and their applications. *European Journal of Operational Research 84(3)* (1995), 539–561.

[50] OLIVEIRA, J., AND FERREIRA, J. Algorithms for nesting problems, Applied Simulated Annealing. In *Lecture Notes in Economics and Maths Systems*, R. Vidal, Ed., vol. 396. Springer-Verlag, 1993, pp. 255–274.

[51] OLIVEIRA, J., GOMES, A., AND FERREIRA, J. TOPOS - A new constructive algorithm for nesting problems. *OR Spectrum 22* (2000), 263–284.

[52] PATRIC, R., AND ÖSTERGÅRD, A. A fast algorithm for the maximum clique problem. *Discrete Applied Mathematics 120* (2002), 197–207.

[53] POLYAKOVSKY, S., AND MHALLAH, R. An agent-based approach to the two-dimensional guillotine bin packing problem. *European Journal of Operational Research 192* (2009), 767–781.

[54] PREPARATA, F., AND SHAMOS, M. *Computational Geometry: An Introduction*. Springer-Verlag, 1985.

[55] RATANAPAN, K., AND DAGLI, C. An object-based evolutionary algorithm for solving irregular nesting problems. In *Proceedings for Artificial Neural Networks in Engineering Conference (ANNIE'97)* (1997), vol. 7, pp. 383–388.

[56] ROMANOVA, T., STOYAN, Y., AND A.PANKRATOV. Mathematical models and solution algorithm for nesting problem of arbitrary shaped objects. *8th Conference of the special interest group on cutting and packing (ESICUP), Copenhagen, Denmark* (2011).

[57] RUIZ, R., AND STÜTZLE, T. A simple and effective iterated greedy algorithm for the permutation flowshop shceduling problem. *European Journal of Operational Research 177* (2007), 2033–2049.

[58] SATO, A., MARTINS, T., AND TSUZUKI, M. An algorithm for the strip packing problem using collision free region and exact fitting placement. *Computer-Aided Design 44* (2012), 766–777.

[59] SCHEITHAUER, G., STOYAN, Y., GIL, N., AND ROMANOVA, T. Phi-functions for circular segments. Tech. Rep. MATH-NM-7-2003, Technische Univarsitat Dresden, Dresden, 2003.

[60] SEGENREICH, S., AND BRAGA, M. Optimal nesting of general plane figures: a Monte Carlo heuristical approach. *Computers & Graphics 10* (1986), 229–237.

[61] SONG, X., AND BENNELL, J. A comprehensive and robust procedure for obtaining the no-fit polygon using Minkowski sums. *Computers & Operations Research 35* (2008), 267–281.

[62] SONG, X., AND BENNELL, J. A beam search implementation for the irregukar shape packing problem. *Journal of Heuristics 16* (2010), 167–188.

[63] STOYAN, Y., NOVOZHILOVA, M., AND KARTASHOV, A. Mathematical model and method of searching for local extremum for the non-convex oriented polygons allocation problem. *European Journal of Operational Research 92* (1996), 193–210.

[64] STOYAN, Y., AND PONOMARENKO, L. Minkowski sum and hodograph of the dense placement vector function. Tech. Rep. SER. A 10, SSR Academy of Science, 1977.

[65] STOYAN, Y., SCHEITHAUER, G., GIL, N., AND ROMANOVA, T. ϕ-functions for complex 2d-objects. *4OR 2* (2004), 69–84.

[66] STOYAN, Y., SCHEITHAUER, G., PANKRATOV, A., AND MAGDALINA, I. Packing of convex polytopes into parallelepiped. *Optimization 54(2)* (2005), 215–235.

[67] STOYAN, Y., SCHEITHAUER, G., AND ROMANOVA, T. Mathematical modeling of interaction of primary geometric 3d objects. *Cybernetics and Systems Analysis 41(3)* (2005), 332–342.

[68] STOYAN, Y., TERNO, J., SCHEITHAUER, G., GIL, N., AND ROMANOVA, T. Phi-functions for primary 2d-objects. *Studia Informatica Universalis 2(1)* (2002), 1–32.

[69] UMETANI, S., YAGIURA, M., IMAHORI, S., IMAMICHI, T., NONOBE, K., AND IBARAKI, T. Solving the irregular strip packing problem via guided local search for overlap minimization. *International Transactions in Operational Research 16* (2009), 661–683.

[70] WÄSCHER, G., HAUSSNER, H., AND SCHUMANN, H. An improved typology of cutting and packing problems. *European Journal of Operational Research 183* (2007), 1109–1130.

[71] WHITWELL, G. PhD thesis, School of Computer Sciences. University of Nottingham, UK, 2005.

[72] YUPINS, Z., AND CAIJUN, Y. A generic approach for leather nesting. *Fifth international conference on natural computing 5* (2009), 303–307.